

30th Panhellenic Conference
on
Solid-State Physics and Materials Science

September 21-24, 2014
Heraklion, Crete



Book of Abstracts

About the Conference

The 30th Pan-hellenic conference on Solid-State Physics and Materials Science will be held from the 21st to the 24th of September, 2014 at the premises of the Foundation for Research and Technology, Hellas at Heraklion, Crete.

The Pan-Hellenic Conference on Solid-State Physics and Materials Science is an annual conference aimed to bring together all researchers in Greece and Cyprus who are working in this field. Previous conferences were held in [Athens](#), [Patras](#), [Limassol](#), [Ioannina](#), [Thessaloniki](#) and [Heraklion](#); the first conference of the series was organized in Thessaloniki in 1982.

The organizing committee of the conference includes Drs. [N. T. Pelekanos](#) (chair), [N. Katsarakis](#), [G. Kopidakis](#), [A. Lappas](#), [I. Perakis](#), [I. N. Remediakis](#) and [M. Vamvakaki](#).

The Conference is sponsored by the [University of Crete](#), the [Institute for Electronic Structure and Laser](#) of [FORTH](#) and the [Technological Educational Institute of Crete](#).

Conference Topics

1. Photonics and optoelectronics.
2. Structural-dynamical and mechanical properties of condensed matter.
3. Strongly correlated electronic systems, magnetism and superconductivity.
4. Surfaces, nanomaterials, and low-dimensional systems.
5. Polymers, organic materials, biomaterials.
6. Ceramics, composites, minerals and metals.
7. Interdisciplinary applications.

Sponsors



Program with links to abstracts

Oral presentations:

Sunday

- 16:00 Registration
- 17:30 S. H. Anastasiadis, director of IESL/FORTH.
- 17:35 N. T. Pelekanos, Conference chairman.
- 17:40 [Samuelson](#) (K)
- 18:20 [Kronik](#) (K)

Monday

Photonics/Plasmonics

- 09:00 [Abajo](#) (K)
- 09:40 [Almpanis](#)
- 09:55 [Droulias](#)
- 10:10 [Kandyla](#)
- 10:25 [Tserkezis](#)
- 10:40 [Kabouraki](#)
- 10:55 [Kenanakis](#)
- 11:10 Coffee

Nanomaterials

- 11:40 [Couris](#)
- 11:55 [Fyta](#)
- 12:10 [Fthenakis](#)
- 12:25 [Chatzakis](#)
- 12:40 [Leontiou](#)
- 12:55 [Florini](#)
- 13:10 Lunch

Strongly Correlated I

- 14:30 [Fischer](#) (K)
- 15:10 [Angelakeris](#) (I)
- 15:35 [Brintakis](#)
- 15:50 [Gjoka](#)
- 16:05 [Litsardakis](#)
- 16:20 Coffee

Strongly Correlated II

- 16:40 [Tasiopoulos](#) (I)

- 17:05 [Galanakis](#) (I)

17:30 [Kavoulakis](#)

17:45 [Bessas](#)

18:00 [Speliotis](#)

18:15 **Poster Session 1**
(Posters 1 to 72)

Tuesday

Graphene and beyond

- 09:00 [Dimoulas](#) (I)
- 09:25 [Papagelis](#) (I)
- 09:50 [Lidorikis](#)
- 10:05 [Economopoulos](#)
- 10:20 [Paradisanos](#)
- 10:35 [Maniadaki](#)
- 10:50 [Michail](#)
- 11:05 Coffee

Optoelectronics

- 11:35 [Kehagias](#) (I)
- 12:00 [Angeli](#)
- 12:15 [Melissinaki](#)
- 12:30 [Eftychis](#)
- 12:45 [Papadomanolaki](#)
- 13:00 [Moratis](#)
- 13:15 Lunch

Composite materials

- 14:35 [Lekka](#) (I)
- 15:00 [Papadogiannis](#)
- 15:15 [Vekinis](#)
- 15:30 [Balliou](#)
- 15:45 [Hadjisavvas](#)
- 16:00 Coffee

Surface science

- 16:30 [Tritsaris](#)
- 16:45 [Klontzas](#)
- 17:00 [Kostoglou](#)
- 17:15 [Loukakos](#)
- 17:30 [Hourdakis](#)
- 17:45 [Panagopoulou](#)
- 18:00 [Karageorgopoulos](#)
- 18:15 **Poster Session 2**

(Posters 73 and up)

21:00 Conference Dinner

Wednesday

Biomaterials

- 09:00 [Pispas](#) (I)
- 09:25 [Manouras](#)
- 09:40 [Daskalaki](#)
- 09:55 [Bakandritsos](#)
- 10:10 [Papaphilippou](#)
- 10:25 [Siafaka](#)
- 10:40 [Lambropoulos](#)
- 10:55 Coffee

Nanocomposites

- 11:25 [Omastova](#) (K)

12:05 [Gegitsidis](#)

12:20 [Androulaki](#)

12:35 [Rissanou](#)

12:50 [Kapetanakis](#)

13:05 Lunch

HSSTCM workshop

14:30 [Workshop](#)

Poster presentations:

[Alexaki](#) [Alexandri](#) [Alexandris](#) [Anastasopoulos](#) [Andrikaki](#) [Angelopoulou](#) [Antonaropoulos](#) [Arvanitidis](#) [Asimakopoulos](#) [Avgeropoulos](#) [Avgouropoulos](#) [Aza](#) [Bairamis](#) [Balliou2](#) [Bessas2](#) [Biniskos](#) [Botzakaki](#) [Boutsioukou](#) [Chousidis](#) [Christofilos](#) [Davelou](#) [Delikoukos](#) [Falireas](#) [Flouraki](#) [Fountoulakis](#) [Frysalis2](#) [Frysalis3](#) [Frysalis](#) [Galanakis](#) [Galata](#) [Gavalas](#) [Georgakopoulos](#) [Georgalas](#) [Georgopoulou](#) [Germanis2](#) [Germanis](#) [Gherca](#) [Giakoumaki](#) [Giannopoulos2](#) [Giannopoulos](#) [Gkanatsiou2](#) [Gkanatsiou](#) [Gkrana](#) [Gryparis](#) [Ioannidou](#) [Jayaprakash](#) [Kaidatzis](#) [Kaliva](#) [Kandyla](#) [Karagiannis](#) [Karakostas](#) [Kavouras](#) [Kazazis](#) [Kechrakos](#) [Kehagias](#) [Kolozoff](#) [Komninou](#) [Kotsina](#) [Kotzabasaki](#) [Koufakis](#) [Koukoula2](#) [Koukoula](#) [Krasanakis](#) [Lazaridou](#) [Liaros](#) [Lotsari](#) [Loukakos](#) [Louloudakis](#) [Makridis](#) [Manouras2](#) [Manousidaki](#) [Mantela](#) [Marinou](#) [Mathioudakis2](#) [Mathioudakis](#) [Mavidis](#) [Mavrikakis](#) [Michail](#) [Michalak](#) [Michelakaki](#) [Moratis](#) [Mygdali](#) [Myrovali](#) [Nika](#) [Orfanou](#) [Papadimitropoulos](#) [Papadopoulos](#) [Papagiannouli](#) [Papamichail](#) [Papananou](#) [Papaphilippou](#) [Papazoglou2](#) [Papazoglou](#) [Paragkamian](#) [Patsidis](#) [Patsiouras](#) [Paxinou](#) [Petrakis](#) [Polymeris](#) [Polyzos](#) [Polyzos2](#) [Power](#) [Psarras](#) [Psifis](#) [Rousalis](#) [Sakkopoulos](#) [Saltas2](#) [Saltas](#) [Samartzis](#) [Senis](#) [Seremetis](#) [Sigelou](#) [Skoufaris](#) [Spanopoulos](#) [Sta2](#) [Sta](#) [Stergiannakos](#) [Stimoniaris1](#) [Stimoniaris2](#) [Sygletou](#) [Talarou](#) [Tamiolakis](#) [G Tamiolakis](#) [I Tasolamprou](#) [Terzakis](#) [Theodosiou](#) [Tiflidou](#) [Tomara](#) [Triantou](#) [Tzagkarakis](#) [Tsididis](#) [Tsolakis](#) [Tsouti](#) [Tzagkarakis](#) [Tzeli](#) [Varitis](#) [Vasilaki](#) [Vasilakis](#) [Velasco](#) [Vrionis](#) [Xanthopoulou2](#) [Xanthopoulou](#) [Xomalis](#) [Xydias](#)

Information for presenters of oral contributions

1. We prefer that you use the computer of the amphitheater for your presentation. Please transfer your pdf or powerpoint file to the computer at least ten minutes before the beginning of the session.
2. If you would like to use your own computer, it might be a good idea to check that your computer connects properly to the projector before the session begins.
3. Technical assistance will be available before the beginning of each session.
4. Please make sure that you conclude your talk early enough so that there is room for questions and discussion within your time slot.

Information for presenters of poster contributions

1. Please find the number of your poster by looking at the program.
2. Authors with poster numbers 1 to 72, please place your poster on Sunday afternoon on the board with the same number. Please remove your poster by Monday evening.
3. Authors with poster numbers 73 and higher, please place your poster on Tuesday morning on the board with the same number. Please remove your poster by Wednesday noon.

About this Book of Abstracts

Abstracts are sorted into eight categories which are oral presentations and one for each topic areas described above. Within each category, abstracts are sorted alphabetically according to the last name of the presenting author.

Extreme plasmonics in atomically thin materials

F. Javier García de Abajo^{1,2,*}

¹ICFO - The Institute of Photonic Sciences, Mediterranean Technology Park,
08860 Castelldefels (Barcelona), Spain

²ICREA - Institució Catalana de Reserca i Estudis Avançats, Passeig Lluís
Comanys 23, 08010 (Barcelona), Spain

The recent observation¹⁻⁴ and extensive theoretical understanding⁵⁻⁷ of plasmons in graphene has triggered the search for similar phenomena in other atomically thin materials, such as noble-metal monolayers⁸ and molecular versions of graphene.⁹ The number of valence electrons that are engaged in the plasmon excitations of such thin layers is much smaller than in conventional 3D metallic particles, so that the addition or removal of a comparatively small number of electrons produces sizeable changes in their oscillation frequencies. This can be realized using gating technology, thus resulting in fast optical modulation at high microelectronic speeds. However, plasmons in graphene have only been observed at mid-infrared and lower frequencies,¹⁻⁴ and therefore, small molecular structures⁹ and atomically thin metals⁹ constitute attractive alternatives to achieve fast electro-optical modulation in the visible and near-infrared (vis-NIR) parts of the spectrum. We will discuss several approaches towards optical modulation using atomically thin structures, as well as the challenges and opportunities introduced by these types of materials, including their application to a new generation of quantum-optics and electro-optical devices.

References

- [1] J. Chen *et al.*, "Optical nano-imaging of gate-tunable graphene plasmons," *Nature*, vol. 487, pp. 77-81, 2012.
- [2] Fei *et al.*, "Gate-tuning of graphene plasmons revealed by infrared nano-imaging," *Nature*, vol. 487, pp. 82-85, 2012.
- [3] Fang *et al.*, "Gated tunability and hybridization of localized plasmons in nanostructured graphene," *ACS Nano*, vol. 7, pp. 2388-2395, 2013.
- [4] Brar *et al.*, "Highly confined tunable mid-infrared plasmonics in graphene nanoresonators," *Nano Lett.*, vol. 13, pp. 2541-2547, 2013.
- [5] A. Vakil and N. Engheta, "Transformation optics using graphene," *Science*, vol. 332, pp. 1291-1294, 2011.
- [6] F. H. L. Koppens, D. E. Chang and García de Abajo, "Graphene plasmonics: A platform for strong light-matter interactions," *Nano Lett.*, vol. 11, pp. 3370-3377, 2011.
- [7] F. J. García de Abajo, "Graphene plasmonics: Challenges and opportunities", *ACS Photonics*, vol. 1, pp. 135-152, 2014.
- [8] A. Manjavacas and F. J. García de Abajo, "Tunable plasmons in atomically thin gold nanodisks", *Nat. Commun.*, vol. 5, p. 3548, 2014.
- [9] A. Manjavacas *et al.*, "Tunable molecular plasmons in polycyclic aromatic hydrocarbons," *ACS Nano*, vol. 7, pp. 3635-3643, 2013.

* javier.garciadeabajo@icfo.es

Light-sound interaction and spontaneous emission control in dual photonic-phononic microcavities

E. Almpanis*[†], N. Papanikolaou

*Institute of Nanoscience and Nanotechnology, NCSR "Demokritos",
Ag. Paraskevi, GR- 153 10 Athens, Greece*

N. Stefanou

*Section of Solid State Physics, University of Athens,
Panepistimioupolis, GR-157 84 Athens, Greece*

The modulation of the optical response of photonic structures in the presence of elastic vibrations is a field of extensive research from the point of view of photoelasticity, Raman and Brillouin spectroscopy, and acousto-optics (AO) in general. In a typical AO experiment, a piezoelectric transducer produces an acoustic wave that changes the optical response of the photonic device [1]. On the other hand, increased popularity gain pump-probe techniques, which employ an ultrafast laser to generate and detect very short strain pulses by monitoring the optical reflectivity of the sample in the time domain [2]. Elastic vibrations can also be used to efficiently manipulate light in structures that simultaneously sustain acoustic and optical resonances in the same volume and enhanced AO effects are expected if such dual resonant modes interact with each other.

In this study we report on appropriately designed microcavities that simultaneously localize light and acoustic waves [3]. We address the problem of the AO interaction in such structures and discuss the consequences of this simultaneous confinement. An extensive analysis is presented for multilayer stacks supporting resonances for both electromagnetic and acoustic fields, resulting in multi-phonon exchange processes and dynamical optical frequency shift. Furthermore, we investigate the influence of a dual photonic-phononic resonant excitation on the spontaneous light emission by active centers [4]. Our calculations are based on the classical approach for light emission, solving the problem of an oscillating point dipole inside the multilayer structure by multiple scattering Green's function techniques. Our results indicate that an acoustic wave can strongly modulate light emission through a resonant AO interaction.

References

- [1] A. Yariv and P. Yeh, *Optical Waves in Crystals* (Wiley, New York, 1984).
- [2] O. Matsuda and O. B. Wright, *J. Opt. Soc. Am. B* **19**, 3028 (2002).
- [3] I. E. Psarobas, N. Papanikolaou, N. Stefanou, B. Djafari-Rouhani, B. Bonello, and V. Laude, *Phys. Rev. B* **82**, 174303 (2010).
- [4] E. Almpanis, N. Papanikolaou, G. Gantzounis, and N. Stefanou, *J. Opt. Soc. Am. B* **29**, 2567 (2012).

*almpanis@imel.demokritos.gr

[†]We acknowledge the European Union (European Social Fund) and the Greek State for financial support under the "ARISTEIA II" Action.

Dynamics of Hyperbranched polymers in the bulk and close to surfaces

K. Androulaki,^{1,2*} K. Chrissopoulou,¹ S. H. Anastasiadis^{1,2}

¹ *Institute of Electronic Structure and Laser, Foundation for Research and Technology–Hellas, Heraklion Crete, Greece*

² *Department of Chemistry, University of Crete, Heraklion Crete, Greece*

M. Labardi, D. Prevosto,

CNR–IPCF, Department of Physics, University of Pisa, Pisa, Italy

Hyperbranched polymers have received much attention lately due to their multiple functionality, their nanosized dimensions, their cost-effective synthesis as compared to dendrimers, as well as their potential applications. Nevertheless, full understanding of the microscopic mechanisms that are responsible for the manifestation of their macroscopic properties is still missing. [1] On the other hand, polymer / layered silicate nanocomposites (PLSN) are considered as a new generation of composite materials due to their unique properties; especially intercalated nanohybrids, where polymer chains form a 1–2nm film within the inorganic galleries provide the opportunity to investigate polymer structure and dynamics close to surfaces. [2]

The dynamics of three different generations of a hyperbranched polyester polyol (Figure 1) was investigated, utilizing Broadband Dielectric Spectroscopy, for temperatures covering the regimes of both sub- T_g local processes and segmental (alpha-process) relaxation and the effects of the dendritic structure and of the generation were studied. Moreover, the three polymers were mixed with natural hydrophilic sodium montmorillonite, Na⁺-MMT, to synthesize nanohybrids in a broad range of compositions between pure polymer and pure clay. In all cases, X-ray diffraction (XRD) measurements show that all hybrids exhibit intercalated structure whereas only excess polymer outside the galleries undergoes a glass transition. The dynamics of nanocomposites, with all chains confined in completely filled galleries, was investigated as well, showing both similarities and differences between the bulk and the confined polymers.

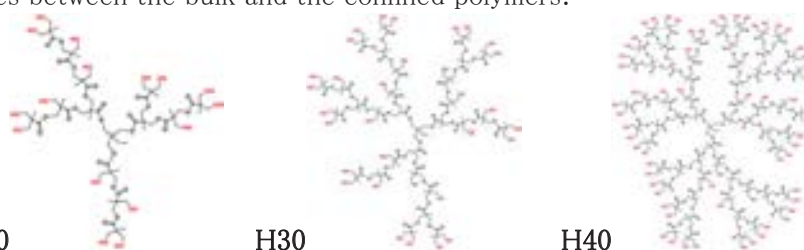


Figure 1: Three generations of the hyperbranched polyester polyol, Boltorn

References

- [1] S. Fotiadou, C. Karageorgaki, K. Chrissopoulou, K. Karatasos, I. Tanis, D. Tragoudaras, S. H. Anastasiadis, *Macromolecules* **46**, 2842 (2013).
 [2] K. Chrissopoulou, K. S. Andrikopoulos, S. Fotiadou, S. Bollas, C. Karageorgaki, D. Christofilos, G. A. Voyiatzis, S. H. Anastasiadis *Macromolecules* **44**, 9710 (2011).

This research has been co-financed by the European Union (ESF) and Greek national funds through the Operational Program "Education and Lifelong Learning" of the NSRF – Research Funding Program: THALES – Investing in knowledge society through the European Social Fund (MIS 377278) and the COST Action MP0902-COINAPO (STSM-MP0902-14971).

* krysand@iesl.forth.gr

Nanoscale magnetism and its biomedical applicability

M. Angelakeris

Department of Physics, Aristotle University, 54124 Thessaloniki, Greece

Magnetic nanomaterials to be used in biomedicine cover a significant part of the market for several tens of €billions. Biomedical nanomagnetism is a multidisciplinary area of research in science, engineering and medicine with broad applications in imaging, diagnostics and therapy (Figure 1). In this field, magnetic nanoparticles with several well-defined and reproducible structural, physical, and chemical properties are required. Eventually, magnetic nanoparticles are proven to be highly effective carrier platforms for both diagnostic and therapeutic purposes by carrying various bioactive molecules such as imaging probes and genes. Recent developments offer exciting possibilities in personalized medicine providing a truly integrated approach, since chemistry, materials science, physics, engineering, biology and medicine are incorporated.

In this talk, I will focus on the magnetic behavior at the nanoscale with emphasis on the relaxation dynamics, synthesis and surface functionalization of magnetic nanoparticles, concluding eventually on the biological constraints and opportunities for in vitro and in vivo applications. More specifically, I will discuss the physics of self-assembly and nanomagnetism in an effort to provide enhanced multifunctional magnetic nanoparticles.



Figure 1: Biomedical applicability schemes of multifunctional magnetic nanoparticles.

Advanced Hybrid Semiconductors for Energy Applications

Giasemi K. Angeli^{1,*} Polykarpos Falaras² and Pantelis N. Trikalitis¹

¹*Department of Chemistry University of Crete, Heraklion 71003, Greece*

²*Division of Physical Chemistry, IAMPNNM NCSR "Demokritos", 15310 Aghia Paraskevi, Attiki, Greece*

Recently layered perovskite materials of the $(R-NH_3)_2MX_4$ ($M = Ge, Sn, Pb, X = Cl, Br, I$) family have resurfaced due to their unique optical and electrical properties, (photoluminescence, electroluminescence, third order optical nonlinearity etc.) which make them promising candidates as light harvesters and/or hole conductors for all solid state solar cells[1-4]. The in depth investigation that has been made as far as the organic-inorganic perovskites are concerned shed light on the effects of the organic counterions on the structural and electronic properties of these compounds. It has been shown that the stability against the distortion of the perovskitic cage strongly depends on the embedded cation. Also, the electronic properties and especially the band gap can be tuned by a suitable choice of the organic molecule [5]. Taking into account these facts, we have developed novel hybrid perovskites with tunable band gap that could lead to the preparation of new solid state solar cells with improved efficiency. Important details will be presented and discussed.

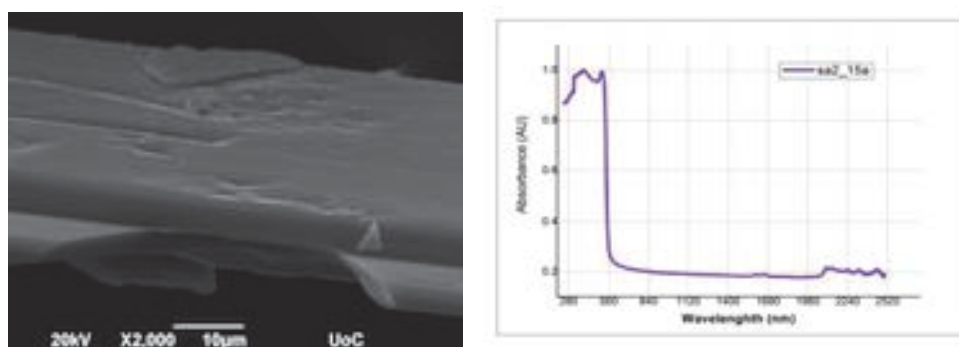


Figure 1. (a) Representative SEM image of the organic inorganic $(C_6H_5CH_3NH_3)PbI_3$ perovskite and (b) the corresponding UV-Vis spectrum.

References

- [1] Chung, I., Lee, B., He, J., Chang, R. P. H. & Kanatzidis *Nature* 485, 486–489 (2012).
- [2] Hui-Seon Kim, Chang-Ryul Lee, Jeong-Hyeok Im, Ki-Beom Lee, Thomas Moehl, Arianna Marchioro, Soo-Jin Moon, Robin Humphry-Baker, Jun-Ho Yum, Jacques E. Moser, Michael Grätzel & Nam-Gyu Park. *Nature Scientific Reports* 2:591 (2012).
- [3] Akihiro Kojima, Kenjiro Teshima, Yasuo Shirai, and Tsutomu Miyasaka *J. Am. Chem. Soc.* 131, 6050–6051 (2009).
- [4] Michael M. Lee, Joël Teuscher, Tsutomu Miyasaka, Takuro N. Murakami, Henry J. Snaith, *Science*, 338, 643–646 (2012).
- [5] Ivo Borriello, Giovanni Cantele, and Domenico Ninno, *PHYSICAL REVIEW B* 77, 235214 (2008)

* s.aggelh@gmail.com

PEGylation of condensed colloidal magnetite nanocrystal clusters for imaging and drug delivery

A. Kolokithas–Ntoukas¹, Y. Sarigiannis¹, A. Bakandritsos^{1*}, R. Zboril³, S. Pispas², G., Mountrichas², Zoppellaro³, C. Diwoy⁴

¹University of Patras, Materials Science Dept. ²Theoretical and Physical Chemistry Institute N.H.R.F., Athens, Greece; ³RCPTM, Olomouc, Czech Republic; ⁴Graz University of Technology, Medical Engineering, Austria

Condensed magnetite colloidal nanocrystal clusters (co–CNCs) have received particular interest due to their application as theranostics. Their development requires solvothermal conditions and/or high temperature.[1] Herein, co–CNCs were synthesized for the first time through one–step soft chemical route in presence of alginate. Co–MNCs, including the present product (MagAlg), display excellent attributes with regard to magnetic manipulation, contrast enhancement in MRI and remotely triggered release.[2] However, they lack colloidal stability upon drug loading and dispersion in blood–isotonic media.

In order to overcome this, installation of a poly(ethylene glycol) (PEG) canopy was pursued through covalent conjugation and, alternatively, through self–assembly with double hydrophilic poly(cationic–b–elthylene glycol) copolymers.

The as–prepared co–MNCs rapidly flocculate at 0.3M NaCl and in presence of doxorubicin. After several trials the appropriate reaction conditions and conjugation reagents were determined, as manifested by the unchanged absorbance in salt–stability assays and light scattering results. In the second PEGylation approach, co–CNCs were incubated with quaternized poly[3,5–bis(dimethylaminomethylene) hydroxystyrene]–b–PEG (QNPHOS–PEG) and poly(L–lysine–b–PEG) (PLL–PEG). After determination of the optimum feeds, PLL–PEG appears to impart excellent entropic stabilization at high salt concentrations. Following the effective PEGylation, doxorubicin loading (10 % wt) was successful without any aggregation ($D_h \sim 100$ nm). Drug release was sustained and could be triggered with magnetic hyperthermia.

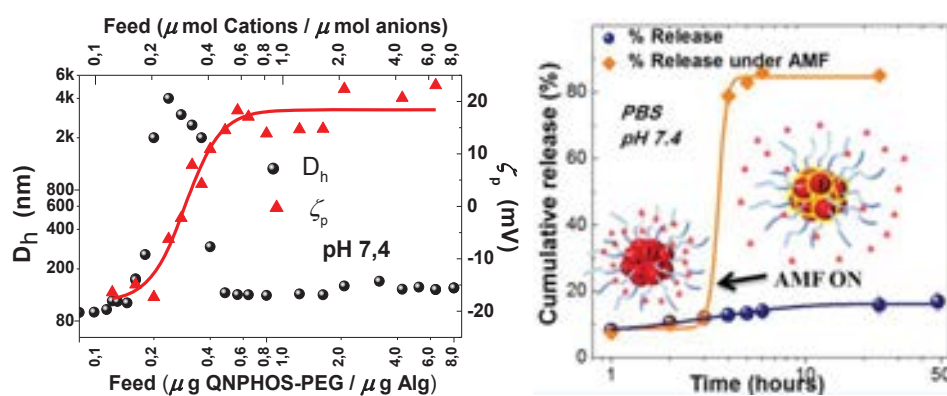


Figure 1. Left: Hydrodynamic diameter and ζ variation at different block–copolymer feeds. Right: Drug release kinetics with and without of magnetic hyperthermia.

References

- [1] Z. Lu, Y. Yin, Chem. Soc. Rev., **41**, 687, (2012).
 [2] Zoppellaro, G.; Kolokithas–Ntoukas, A.; Polakova, K.; Tucek, J.; Zboril, R.; Loudos, G.; Fragogeorgi, E.; Diwoy, C.; Tomankova, K.; Avgoustakis, C.; Kouzoudis, D.; Bakandritsos, A. Chem. Mater. **26**, 2062, (2014).

Hybrid networks based on the interplay of Au nano-particles and CuPcSu ligands-Electronic transport in mesoscopic scale

A. Balliou*, N.Glezos

*Institute of Microelectronics, NCSR Demokritos,
Agia Paraskevi Attikis, 153 10 Athens, Greece*

S. Kazim, J.Pfleger

*Institute of Macromolecular Chemistry, AS CR,
Heyrovsky Square 2, 162 06 Prague 6, Czech Republic*

J. Rakusan

COC Ltd., 533 54 Rybitví, Czech Republic

S.Kennou, G.Skoulatakis

Institute of Chemical Engineering, 26504 Patra, Greece

We report on the fabrication and study of the electronic transport properties of planar devices based on nano-dimensional components, namely semiconducting conjugated oligomers and metal nanoparticles (NPs). Spherical gold (Au) NPs were linked by means of copper 3-diethylamino-1-propylsulphonamide sulfonic acid substituted phthalocyanine (CuPcSu) molecules to form a network confined between Au nanodistant electrodes. Fabrication of these devices was realized via three different approaches: (a) liquid phase approach: Au NPs (av. diameter 17 nm) prepared as hydrosol with chemical reduction were functionalized with CuPcSu and drop cast on the substrate, (b) self-assembling technique: The SiO_2 surface was chemically modified with a stable, positively charged template molecule (3-aminopropyl triethoxysilane, APTES)[1] and the CuPcSu surface-functionalized Au NPs were subsequently adsorbed on the surface driven by electrostatic-type forces and (c) solid state approach: Ultra-fine (av. diam. 4.5 nm) Au NPs were prepared by thermal evaporation and inter-particle gaps were filled with CuPcSu ligands in a subsequent step. The above systems were confined between Au nano-electrodes with inter-electrode distances of 25 and 50nm fabricated on $n-Si/SiO_2$ substrate via e-beam lithography. The conduction mechanisms of these 2D systems were studied using quasi-static and dynamic voltage-current measurements in the 78K-300K temperature range. It was possible to discriminate between various transport mechanisms typical for such structures (i.e. tunneling and hopping), to evaluate conduction thresholds and to reveal charging effects involving few electrons, at lower temperatures. The interpretation was assisted by AFM, FE-SEM and TEM imaging techniques. The system of evaporated NPs (case c) resulted in formation of closely-packed linked NP networks and yielded the best stability and results' reproducibility.

References

- [1] Decher, G. Fuzzy, Science, **277**, 1232–1237 (1997).

*aballiou@imel.demokritos.gr

Pressure mediated structural transition in EuTiO_3

D. Bessas*, I. Kantor, D. G. Merkel, A. Chumakov, R. Ruffer
European Synchrotron Radiation Facility, F-38043 Grenoble, France

K. Glazyrin, I. Sergueev
Deutsches Elektronen-Synchrotron, D-22607 Hamburg, Germany

R. P. Hermann
*Jülich Centre for Neutron Science, JCNS, and Peter Grünberg Institut PGI,
JARA-FIT, Forschungszentrum Jülich GmbH, D-52425 Jülich, Germany
Faculté des Sciences, Université de Liège, B-4000, Liège, Belgium*

The phase competition in compounds with perovskite structure leads to phenomena related with a broad range of applications [1]. EuTiO_3 is an incipient ferroelectric with magnetic cations, thus it can potentially be used in information technology.

The phase purity and the lattice dynamics in bulk EuTiO_3 were investigated both microscopically, using X-ray and neutron diffraction, ^{151}Eu -Mössbauer spectroscopy, and ^{151}Eu nuclear inelastic scattering, and macroscopically using calorimetry, resonant ultrasound spectroscopy, and magnetometry at ambient pressure [2]. Lately, we carried out X-ray diffraction and ^{151}Eu nuclear forward scattering under externally applied pressure, up to 30 GPa. Our investigations were corroborated by *ab-initio* theoretical studies [3].

The perovskite symmetry, $Pm\bar{3}m$, is unstable at the M - and R -points of the Brillouin zone. The lattice instabilities are lifted when the structure relaxes in one of the symmetries: $I4/mcm$, $Imma$, $R\bar{3}c$ with relative relaxation energy around -25 meV. A stiffening on heating around room temperature is indicative of a phase transition similar to the one observed in SrTiO_3 , however, although previous studies reported the structural phase transition to the tetragonal $I4/mcm$ phase [4] our detailed sample purity analysis and thorough structural studies using complementary techniques did not confirm a direct phase transition. Instead, in the same temperature range, Eu delocalization is observed in line with our theoretical calculations. Furthermore, a pressure mediated structural transition to the $Imma$ symmetry was found under 12 GPa applied pressure.

References

- [1] M. E. Lines and A. M. Glass, Principles and Applications of Ferroelectrics and related Materials (Clarendon Press, 1977).
- [2] D. Bessas, K. Z. Rushchanskii, M. Kachlik, S. Disch, O. Gourdon, J. Bednarcik, K. Maca, I. Sergueev, S. Kamba, M. Ležaić, *et al.*, Phys. Rev. B 88, 144308 (2013).
- [3] K. Z. Rushchanskii, N. A. Spaldin, and M. Ležaić, Phys. Rev. B 85, 104109 (2012).
- [4] M. Allieta, M. Scavini, L. J. Spalek, V. Scagnoli, H. C. Walker, C. Panagopoulos, S. S. Saxena, T. Katsufuji, and C. Mazzoli, Phys. Rev. B 85, 184107 (2012); A. Busmann-Holder, J. Köhler, R. K. Kremer, and J. M. Law, Phys. Rev. B 83, 212102 (2011); J.-W. Kim, P. Thompson, S. Brown, P. S. Normile, J. A. Schlueter, A. Shkabko, A. Weidenkaff, and P. J. Ryan, Phys. Rev. Lett. 110, 027201 (2013).

* bessas@esrf.fr

Maghemite nanoclusters: A promising multifunctional material for biomedicine

K. Brintakis^{*,1,2}, A. Kostopoulou¹, S. Psycharakis¹, A. Ranella¹, M. Vasilakaki³, K. N. Trohidou³, A. P. Douvalis⁴, S. K. P. Velu⁵, L. Bordonali⁵, A. Lascialfari⁵, D. Sakellari², K. Simeonidis², M. Angelakeris², I. Athanassakis⁶ and A. Lappas¹

¹*Institute of Electronic Structure and Laser, Foundation for Research and Technology-Hellas, Vassilika Vouton, 71110, Heraklion, Greece*

²*Department of Physics, Aristotle University of Thessaloniki, 54124 Thessaloniki, Greece*

³*IAMPPNM, Department of Materials Science, NCSR "Demokritos", Aghia Paraskevi, 15310, Athens, Greece*

⁴*Department of Physics, University of Ioannina, 45110 Ioannina, Greece*

⁵*Dipartimento di Fisica, Università degli studi di Milano and INSTM, Via Celoria 16, I-20133 Milano, Italy*

⁶*Department of Biology, University of Crete, Vassilika Vouton, 71003 Heraklion, Greece*

Researchers' efforts have been stimulated by the use of nanocrystals (NCs) as multifunctional vehicles for diagnosis (MRI contrast agents) and therapy (targeted drug delivery or/and hyperthermia treatment). The designing of these vehicles named "theranostic agents", takes into account the physical, chemical properties as well as the contingent interactions with the human environment.

We present an iron oxide-based system, which is an assembly of maghemite NCs giving rise to water-dispersible colloidal nanoclusters (CNCs) (Fig. 1a). The high-temperature synthesis has the advantages of size-controlling, good stability and cost-efficiency. The system is ferrimagnetic (Mössbauer spectroscopy) due to the clustering process and the associated interplay of the dipolar interactions among the composing NCs and the intra-particle exchange interactions (SQUID magnetometry & Monte Carlo Simulations) [1].

The potentiality of the CNCs is demonstrated by relaxometric studies which revealed CNCs' 4-times enhanced transverse ¹H-NMR relaxivity against that of superparamagnetic (SPM) contrast agents, like Endorem[®], (r_2 ; Fig. 1b) [2]. CNCs' thermal response in hyperthermia (Specific Loss Power; Fig. 1b inset) compared against the individual SPM NCs, points the role of ferrimagnetism and the corresponding intra-cluster interactions to generate an additional heating response mechanism (hysteresis losses). Preliminary incubation experiments with mice spleen cells indicate CNCs' low cytotoxicity and biocompatibility (Fig. 1c). The tailored physical properties render the CNCs a multifunctional material, which is likely to serve as a modular theranostic agent.

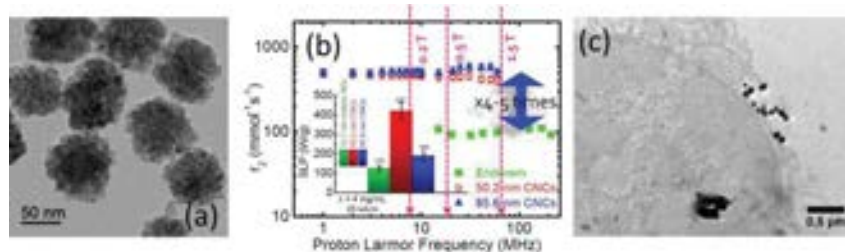


Figure 1: (a) TEM image of nanoclusters. (b) relaxivity (r_2) and specific-loss power (SLP) (as inset). (c) TEM after the incubation of CNCs with mice spleen cells.

References

- [1] A. Kostopoulou, K. Brintakis, M. Vasilakaki, K. N. Trohidou, A. P. Douvalis, A. Lascialfari, L. Manna and A. Lappas, *Nanoscale* **6**, 3764, (2014).
 [2] A. Kostopoulou, S. K. P. Velu, K. Thangavel, F. Orsini, K. Brintakis, S. Psycharakis, A. Ranella, A. Lappas, and A. Lascialfari, *Dalton Trans.*, **43**, 839, (2014).

Ultrafast terahertz probes of interacting dark excitons in
chirality-specific semiconducting single-wall carbon nanotubes

Ioannis Chatzakis^{1,2}, Liang Luo¹, Aaron Patz¹ and Jigang Wang¹,

¹*Department of Physics and Astronomy & Ames Laboratory—U.S. DOE, Iowa State University, Ames, IA
50011, USA*

²*Department of Electrical Engineering, University of Southern California, Los Angeles, CA 90089, USA*

Abstract

Ultrafast terahertz (THz) spectroscopy accesses the dark excitonic ground state in resonantly excited (6,5) single-wall carbon nanotubes (SWNTs). This is feasible via internal, direct dipole-allowed transitions between the lowest lying dark-bright pair states around 6 meV. An analytical model reproduces the response, thus enabling a quantitative analysis of the transient densities of dark excitons and the unbound e - h plasma, the oscillator strength, the transition energy renormalization and the dynamics. Stable quasi-1D multi-exciton states emerge rapidly even with increasing off-resonance photoexcitation. They evolve uniquely from a predominant dark exciton population to complex phase-space filling of both dark and bright pair states. These are distinctly different from dense 2D and 3D excitons, which are characterized by the ionization of free carriers and slow formation.

Nonlinear optics of carbon nanostructures: graphenes, nano-diamonds, carbon-dots and carbon-onions

S. Couris*, N. Liaros, I. Papagiannouli, P. Aloukos

Department of Physics, University of Patras, 26504 Patras, Greece

Institute of Chemical Engineering Sciences (ICE-HT), Foundation for Research and Technology, Hellas, 26504 Patras, Greece

During the last years, the nonlinear optical properties of various carbon allotropes such as fullerenes, carbon nanotubes, graphenes and derivatives, nanodiamonds, carbon-dots and other carbon-based nanostructures have greatly attracted the attention of the scientific community. [1–4] This research interest has been boosted by the very interesting physics exhibited by these nano-entities and also by the various potential applications envisaged for these systems, in photonic and optoelectronic technologies, ranging from optical limiters and optical data storage to optical computing, solar cells and several others. [5–9] In this work we will present results from our recent research activities concerning the systematic study of the nonlinear optical response of different carbon allotropes under nanosecond and picosecond laser excitation. In particular, the nonlinear optical response of some organophilic and hydrophilic C-dots, some nano-diamonds and nano-onions carbon based nanostructures and of graphene oxide and fluoride derivatives will be presented and will be compared between them and with other literature reports. [11-15]

References

- [1] S. Tatsuura *et al.*, *Adv. Mater.* 15(6), 534 (2003).
- [2] L. Dai *et al.*, *Small*, 8(8), 1130, 2012.
- [3] F. Kazjar *et al.*, *Synth. Met.* 77(1–3), 257 (1996).
- [4] V. Georgakilas *et al.*, *Chem. Rev.* 112 (11), 6156, (2012).
- [5] Y. P. Sun and J. E. Riggs, *Int. Rev. Phys. Chem.* 18(1), 43 (1999).
- [6] V. Yong and J. M. Tour, *Small* 6(2), 313 (2010).
- [7] J. Wang, *et al.*, *Adv. Mater.* 21(23), 2430 (2009).
- [8] F. Bonaccorso *et al.*, *Nat. Photonics* 4(9), 611 (2010).
- [9] K. P. Loh *et al.*, *Nat. Chem.* 2(12), 1015 (2010).
- [11] N. Liaros *et al.*, *Appl. Phys. Lett.* 104, 191112 (2014).
- [12] P. Aloukos *et al.*, *Opt. Express* 22(10), 12013, (2014).
- [13] A. B. Bourlinos *et al.*, *Carbon*, 61, 640, (2013).
- [14] N. Liaros *et al.*, *Opt. Materials* 36(1), 112, (2013).
- [15] N. Liaros *et al.*, *J. Phys. Chem. C*, 117(13), 6842, (2013).

* couris@iceht.forth.gr

The authors acknowledge support by the European Union (European Social Fund-ESF) and Greek national funds through the Operational Program "Education and Lifelong Learning" of the National Strategic Reference Framework (NSRF)-Research Funding Programs: THALIS (ISEPUMA): Investing in knowledge society through the European Social Fund.

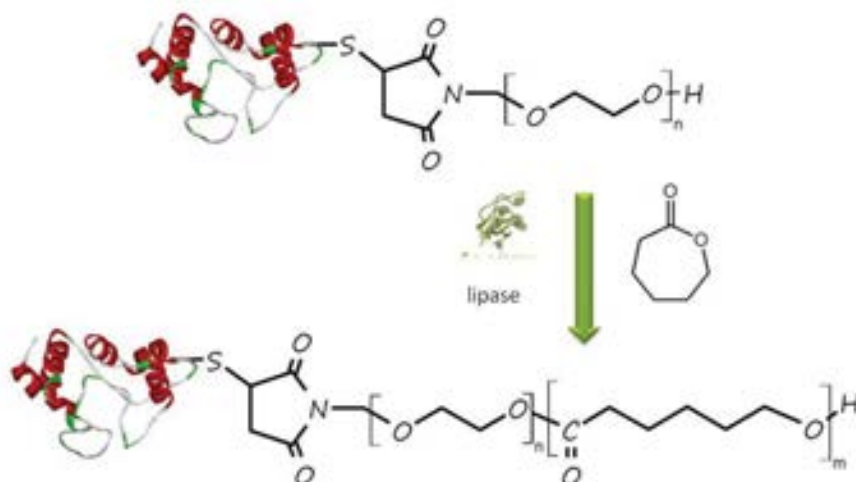
Synthesis of Giant Amphiphiles by Enzyme Catalyzed Ring Opening Polymerization

E.Daskalaki,¹ K. Velonia.²

Department of Chemistry, University of Crete, Voutes, Heraklion Crete

Department of Materials Science and Technology, University of Crete, Voutes, Heraklion Crete

Amphiphilic protein-polymer chimeras -the so-called *Giant Amphiphiles*- are designed to mimic the hierarchical self-assembly displayed in biological and synthetic material systems over a range of lengths. During the last years we synthesized several such protein-polymer amphiphilic bioconjugates using different synthetic approaches varying from the direct coupling of end-functionalized polymers to proteins, to the *grafting* of polymers *from* protein macroinitiators.^{1,2,3} Interestingly, *Giant Amphiphiles* have shown to assemble into well-defined, functional superstructures suitable for a variety of materials applications.



Scheme 1. Synthesis of Giant Amphiphiles by Enzyme Catalyzed ROP.

Herein we present a novel synthetic approach involving the Ring Opening Polymerization (ROP) *grafting* of ϵ -caprolactone *from* protein biomacoinitiators (*Scheme 1*). It will be shown that this method proceeds under mild reaction conditions with the high yields and reaction rates and is characterized by the absence of toxic monomers/catalysts/by-products that are intrinsic to enzymatic catalysis. This the first report of the “*grafting from*”, *in situ*, formation of biocompatible and biodegradable giant soaps with interesting assembling properties that will be comparatively discussed.

References

¹ K. Velonia, A.E. Rowan, R.J.M. Nolte *J. Am. Chem. Soc.* **2002**, *124*, 4224-4225.

² B. Le Droumaguet, G. Mantovani, D.M. Haddleton, K. Velonia *J. Mater. Chem.*, **2007**, *17*, 1916-1922.

³ Le Droumaguet, K.Velonia *Angew. Chem., Int. Ed.* **2008**, *47*, 6263-6266.

Atomically thin 2D materials for nanoelectronics

A. Dimoulas*,

*Institute of Nanoscience and Nanotechnology, NCSR DEMOKRITOS 15310,
Athens, Greece*

As nanoelectronic devices and integrated circuits become smaller and denser, performance degradation and excess heat dissipation on the chip become big issues. Atomically thin, inherently 2D semiconductors such as transition metal dichalcogenides (MX_2 , $\text{M}=\text{Mo}, \text{W}$, $\text{X}=\text{S}, \text{Se}, \text{Te}$) offer excellent thickness scaling capabilities to improve electrostatic control. In addition, at the limit of a single layer, MX_2 become direct gap semiconductors with excellent response in the near IR and visible part of the solar spectrum making it suitable for light emitting devices and energy harvesting. Besides, these materials have high mechanical strength and because they are atomically thin they are bendable and stretchable so they can be used for transparent flexible displays and a number of low power versatile applications. It is quite impressive that advanced devices and integrated circuits have already been realized showing that they can impact nanoelectronics [1]. However, most of the device work worldwide has been performed on small (micron size) flakes exfoliated from bulk. For real world applications, large area synthesis of these materials is required. In this work, we demonstrate that high quality epitaxial single and few-layer MoSe_2 can be obtained by MBE on large area $\text{AlN}(0001)/\text{Si}(111)$ substrates. The electronic band structure imaged by *in-situ* ARPES indicates a direct gap material verified by intense room temperature photoluminescence signals and well defined Raman shifts. The layer is uniform over the entire wafer and has an excellent stability upon exposure to air for several days, allowing transistor processing. In future novel device implementations, 2D semiconductors need to be combined with other 2D layered materials (e.g. dielectrics like BN, AlN) which could be preferably bonded by weak van der Waals forces. A short review will be given with an emphasis on our recent results [2] showing high quality epitaxial growth on $\text{Ag}(111)$ substrates of hexagonal graphite-like few layer AlN, which can be considered as a precursor of the more stable AlN bulk wurtzite phase. Moreover, we will show that MoSe_2 semiconductor can be combined with other selenides such as Bi_2Se_3 to form multilayer structures with novel properties. Bi_2Se_3 belongs to new class of 2D layered materials known as topological insulators (TI). TIs present non-trivial insulator properties since they possess an excitation gap in the bulk co-existing with surface metallic states in the form of spin-polarized (helical) Dirac cones. Our newest data [3] will be presented showing the thinnest Bi_2Se_3 (3 quintuple layers) ever reported with gapless surface metallic states which is epitaxially grown on $\text{AlN}(0001)$ by MBE. This means that Bi_2Se_3 can be scaled down to very small thickness which allows integration in the gate of Si MOSFETs to exploit the quantum capacitance of the surface 2D metallic states in novel steep slope switches aimed for low power/high performance applications.

This work is supported by the ERC Advanced Grant SMARTGATE-291260 and the Greek Program of EXCELLENCE (ΑΡΙΣΤΕΙΑ)-TOP ELECTRONICS -745

References: [1] B. Radisavljevic et al., ACS Nano 5, 9934 (11); [2] P. Tsipas et al., Appl. Phys. Lett. 103, 251605 (2013); [3] P. Tsipas et al., ACS Nano (2014), DOI: 10.1021/nn502397x ;

* dimoulas@ims.demokritos.gr

Band-edge operation of two-dimensional photonic crystals with gain

S. Droulias^{1*}, C. Fietz², T. Koschny² and C. Soukoulis^{1,2}

¹*Institute of Electronic Structure and Laser, FORTH, 71110 Heraklion, Crete, Greece*

²*Ames Laboratory and Department of Physics and Astronomy, Iowa State University, Ames, Iowa 50011, USA*

We present calculations of lasing action in microstructured systems embedded with a four-level gain medium. The Maxwell equations are coupled with the semi-classical laser equations and are self-consistently solved under a finite-difference time-domain scheme [1]. Our simulations show that a two dimensional photonic crystal (2DPC) operating near the band-edge can, in principal, lead to strong reduction of the lasing threshold with respect to a uniform gain slab of the same dimensions, in spite of the lower gain density. We demonstrate this fact with a 2DPC of as few as 10 layers and show how the lasing threshold is further reduced as the number of layers is increased. We also examine how the lasing threshold is affected by the band-edge proximity.

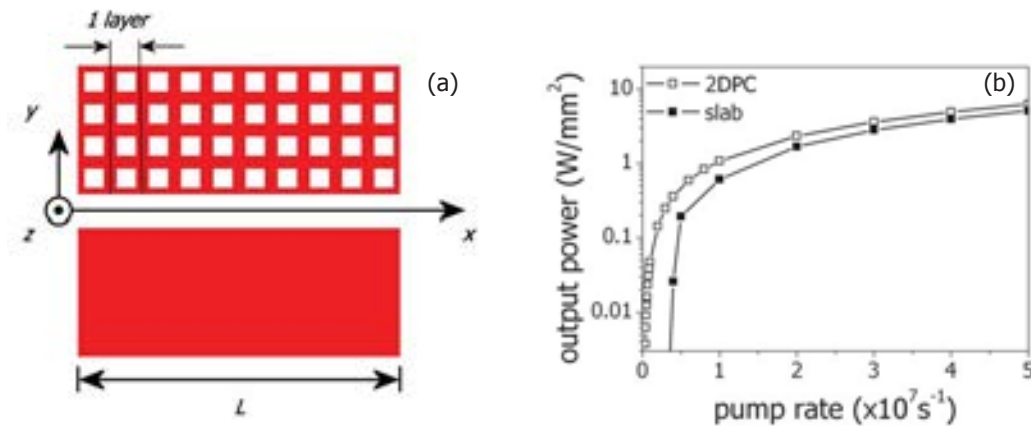


Figure 1: (a) Schematic of the 2DPC consisting of 10 layers (top) and the respective slab of uniform gain and same length (bottom). The red areas denote the host dielectric which is homogeneously embedded with the four-level gain material. Both systems are infinite in the yz plane and confined in the x direction, along which the emitted wave propagates. (b) Lasing power in log scale of the 2DPC (open squares) and gain slab (filled squares) as depicted in Figure 1(a) for different pump rates. Both systems operate at the frequency which corresponds to the bottom of the 2nd band of the 2DPC. The lasing threshold of the photonic crystal is 1 order of magnitude lower than that of the gain slab.

References

- [1] A. Fang, T. Koschny and C.M. Soukoulis, *J. Opt.* **12**, 024013 (2010).

* sdroulias@iesl.forth.gr

Water-Soluble graphene nanoensembles with dual porphyrin donor moieties.

S. P. Economopoulos*, N. Tagmatarchis

Theoretical and Physical Chemistry Institute, National Hellenic Research Foundation, 48 Vassileos Constantinou Avenue, 11635 Athens, Greece

Hybrid materials based on graphene have the potential to cater to a variety of nanotechnological applications ranging from optoelectronics, to biomedical as well as, industrial.[1] We would like to present an array of novel graphene-based materials targeted for energy conversion systems that incorporate multichromophore systems, anchored onto graphene through non-covalent interactions.

The graphene itself has been prepared through ultrasonication processes, introducing minimal defects onto the graphitic backbone.[2] The non-covalent hybrid graphene materials comprise of multiple porphyrin systems stabilized through electrostatic interactions. The porphyrin moieties are negatively and positively charged, respectively and water soluble, forming a multi-chromophore water-soluble graphene trimer. Time-resolved photoluminescence experiments verify the promotion of electronic communication of the second porphyrin with the graphene through a formed porphyrin/graphene antennae dimer system.[3]

The introduction of these organic and aqueous soluble materials opens up a wide array of artificial photosynthesis applications in both solid state and electrochemical organic photovoltaic cells, while allowing more importantly for low-temperature deposition and precise optoelectronic chemical tailoring.

Financial support from GSRT/NSRF 2007–2013 through action “Supporting Postdoctoral Researchers” project GRAPHCELL PE5(2126) is acknowledged.

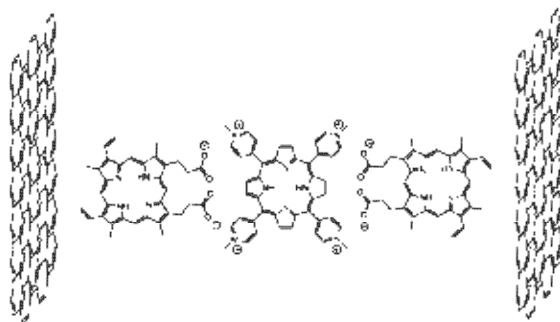


Figure 1: Schematic representation of exfoliated graphene-porphyrin-porphyrin supramolecular structure.

References

- [1] Novoselov, Falko, Colombo, Gellert, Schwab, and Kim, *Nature* **490**, 192 (2012).
- [2] Economopoulos and Tagmatarchis, *Chem. Eur. J.* **19**, 12930 (2013).
- [3] Economopoulos and Tagmatarchis, Manuscript in preparation, (2014).

* economop@eie.gr

Nucleation and growth of GaN nanowires by plasma-assisted molecular beam epitaxy

S. Eftychis^{1*}, J. Kruse^{1,2}, K. Tsagaraki², M. Androulidaki², and A. Georgakilas^{1,2}

1. Physics Department, University of Crete, P.O. Box 2208, 71003 Heraklion, Greece

2. Microelectronics Research Group, IESL/FORTH, P.O. Box 1385, 71110 Heraklion, Greece

T. Koukoula, Th. Kehagias, Ph. Komninou

Physics Department, Aristotle University of Thessaloniki, GR-54124 Thessaloniki, Greece

The last decades, nanowires (NWs) have been under intense research because of their unique characteristics, their high crystal quality and their promising applications. In this work, the spontaneous nucleation and growth of GaN nanowires on Si(111) by plasma assisted molecular beam epitaxy have been investigated.

The height, diameter and density of GaN NWs were determined by field emission scanning electron microscopy (FE-SEM). X-ray diffraction rocking curves (XRD RCs) were obtained to compare the crystallographic alignment of the NWs. Their optoelectronic properties and structural quality were evaluated by photoluminescence spectroscopy. High resolution transmission electron microscopy (HR-TEM) was used to study the GaN/substrate interface and to identify the nucleation sites and the epitaxial relationship of the GaN (0001) NWs and the Si (111) substrate.

Samples of GaN NWs were grown either after intentional nitridation of the Si surface by the active nitrogen beam or after initial growth of an AlN interlayer (IL), with thickness varied between 1 monolayer and 15 nm. The results highlight the competing formation of AlN and SixNy interlayers at the GaN NW/Si interface. A ~1.5nm AlN IL, probably with significant residual strain at the end of its growth, facilitates the nucleation of GaN NWs on top of it while it simultaneously prevents the formation of amorphous silicon nitride at the interface. A thicker AlN IL, which should be closer to a strain free condition, favors the nucleation and lateral growth of 3D GaN islands which coalesce into a continuous GaN film.

To study the effect of the substrate temperature, NWs were grown at temperatures in the range between 730°C-780°C, either keeping the temperature constant throughout the growth or following a two-step growth process with NW nucleation at lower temperature than the final one. For those samples that were grown at a constant temperature, the highest studied substrate temperatures revealed a significant suppression of NW nucleation and growth. The NW nucleation at low temperature is mandatory for growing NWs at substrate temperatures higher than 790°C.

The results highlight the critical role of the nucleation step for the overall spontaneous GaN NW growth.

Acknowledgments: This research has been co-financed by the European Union (European Social Fund – ESF) and Greek national funds through the Operational Program "Education and Lifelong Learning" of the National Strategic Reference Framework (NSRF) - Research Funding Program: THALES.

* eftychis@physics.uoc.gr

Magnetic soft X-ray spectromicroscopy: From nanoscale behavior to mesoscale phenomena

Peter Fischer¹

*Center for X-ray Optics, Lawrence Berkeley National Lab., Berkeley CA 94720, USA
and
Physics Department, University of California, Santa Cruz CA 95064, USA*

Over the last decade magnetism research focused on a fundamental understanding and controlling spins on a nanoscale. Recently, it has been recognized, that the next step beyond the nanoscale will be governed by mesoscale phenomena [1], since those are supposed to add complexity and functionality, which are essential parameters to meet future challenges in terms of speed, size and energy efficiency of spin driven devices. The development and application of multidimensional visualization techniques, such as tomographic magnetic imaging and investigations of fast and ultrafast spin dynamics down to fundamental magnetic length and time scales with elemental sensitivity in emerging multi-component materials will be crucial to achieve mesoscience goals.

Magnetic soft X-ray spectromicroscopy is a unique analytical technique combining X-ray magnetic circular dichroism (X-MCD) as element specific magnetic contrast mechanism with a spatial (2D and 3D) resolution down to currently about 20nm. In addition, utilizing the inherent time structure of current synchrotron sources fast magnetization dynamics in ferromagnetic elements can be performed with a stroboscopic pump-probe scheme with 70ps time resolution [2,3].

To demonstrate the capabilities of magnetic soft x-ray spectromicroscopy I will review in this talk recent achievements with full-field magnetic soft x-ray transmission microscopy (MTXM). In studies of magnetic vortex structures we found a stochastic character in the nucleation process, which can be described within a symmetry breaking DM interaction [4]. With time resolved MTXM of dipolar coupled magnetic vortices an efficient energy transfer mechanism was identified, which can be used for novel magnetic logic elements [5]. Spectroscopic MTXM images allowed us to apply sum rules down to almost the current spatial resolution limit [6]. First attempts to image the 3dim magnetic domain structures in rolled-up Ni nanotubes are very promising [7].

This work was supported by the Director, Office of Science, Office of Basic Energy Sciences, Materials Sciences and Engineering Division, of the U.S. Department of Energy under Contract No. DE-AC02-05-CH1123 and by the Leading Foreign Research Institute Recruitment Program (Grant No. 2012K1A4A3053565) through the National Research Foundation of Korea (NRF) funded by the Ministry of Education, Science and Technology (MEST).

References

- [1] R. Service, *Science* **335**, 1167 (2012).
- [2] P. Fischer, *Materials Science & Engineering* **R72**, 81 (2011).
- [3] W. Chao, et al., *Optics Express* **20(9)**, 9777 (2012).
- [4] M.-Y. Im, et al., *Nature Communications* **3**, 983 (2012).
- [5] H. Jung, et al., *Scientific Reports* **1**, 59 (2011).
- [6] M.J. Robertson, A.T. N'Diaye, G. Chen, M.-Y. Im, P. Fischer, in preparation (2014).
- [7] R. Streubel, *Adv. Mater* **26**, 316 (2014).

¹ PJFischer@lbl.gov; URL: <http://pjfischer.lbl.gov>

Lattice registration and allocation of strain in (211)B InAs/GaAs quantum dot superlattices

N. Florini*, G. P. Dimitrakopoulos, J. Kioseoglou, Th. Kehagias
Physics Department, Aristotle University of Thessaloniki, 54124 Thessaloniki, Greece

S. Germanis, Z. Hatzopoulos, N. T. Pelekanos
Materials Science & Technology and Physics Departments, University of Crete and IESL/FORTH, GR-71003 Heraklion, Greece

Transmission electron microscopy (TEM) techniques were employed to shed light to the structural features and strain properties of piezoelectric InAs quantum dots (QDs), showing extensive potential for single photon emission and photon entanglement. QDs were grown by plasma-assisted molecular beam epitaxy, either on the surface or buried in (211)B GaAs, over a 40x period (1.5 nm AlAs)/(2.3 nm GaAs) superlattice. Regardless their location, QDs exhibit a pyramidal anisotropic shape, elongated along the [-111] direction, with a base-aspect-ratio ranging from 1.2 to 1.4.

Lattice registration and allocation of strain in the InAs/GaAs QDs superlattice were explored by Moiré fringe analysis, fast Fourier transform (FFT) of high-resolution TEM (HRTEM) images, Bragg filtering of the interfacial area and geometrical phase analysis (GPA). Uncapped QDs were almost relaxed due to the introduction of misfit dislocations at the InAs/GaAs interface. Residual elastic strain decreased from the base to the apex area of the QDs that exhibited the strain-free lattice values. Conversely, HRTEM imaging showed full in-plane registration of the buried QDs without any associated line defects, implying fully strained nanostructures. Indium chemical composition maps of the buried QDs, constructed assuming a plane-stress condition and Vegard's law validity, showed possible Ga segregation in the initial stages of growth and a gradual increase of the In content from the base of the QDs towards pure InAs at their apex region (Figure 1).

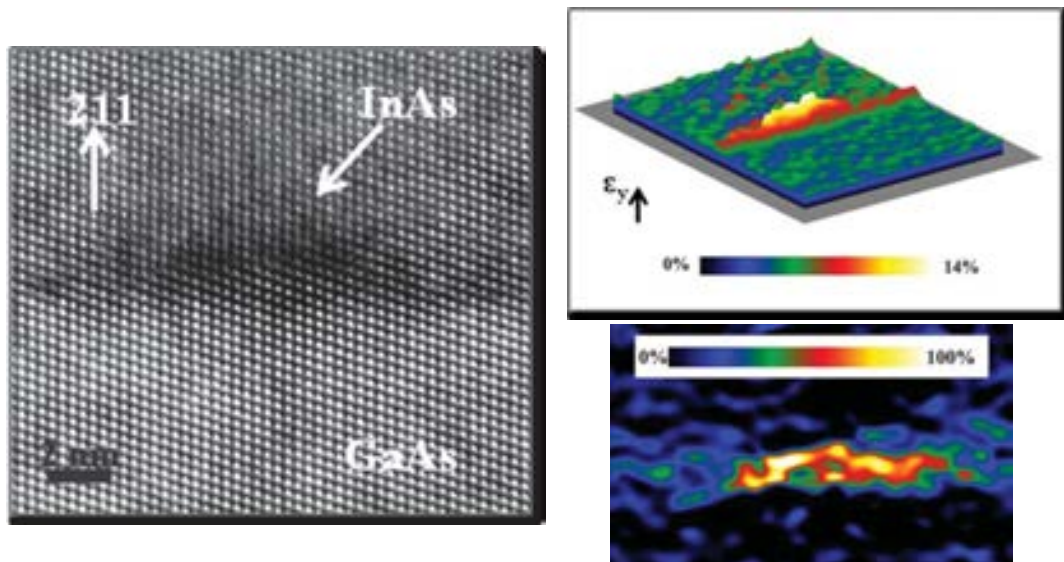


Figure 1. HRTEM image of a buried InAs QD in the [0-11] projection, and the corresponding GPA strain and In chemical composition maps along the growth direction.

Acknowledgement

Research co-financed by the European Union (European Social Fund–ESF) and Greek national funds - Research Funding Program: THALES, project NANOPHOS.

* nflori@physics.auth.gr

Understanding the conduction mechanism of carbon foam surfaces

Z.G. Fthenakis^{†*}, Z. Zhu, J. Guan and D. Tománek

Physics and Astronomy Department, Michigan State University, USA

[†] *Currently at Institute of Electronic Structure and Laser, FORTH, Greece*

Carbon foams are periodic structures containing graphene ribbons which are connected with each other along their edges with sp^3 bonds. Cleavage of the bulk structure normal to the connected graphene ribbon edges, leads to either an sp^3 - or sp^2 -terminated surface, (i.e. terminated by C atoms that were either sp^3 or sp^2 in the bulk, respectively), which are shown in Fig. 1(a) and 1(b).

We performed *ab-initio* calculations using SIESTA and TRAN-SIESTA codes to study the stability, and the electronic and transport properties of foam slabs with either sp^2 or sp^3 terminated surfaces, with and without Hydrogen termination[1]. We find that sp^2 and sp^3 terminated surfaces exhibit metallic and semiconducting behavior, respectively, which occur either with or without Hydrogen termination. Consequently, such behaviors are not related to the surface dangling bonds.

Using Tight Binding calculations in order to understand those different behaviors, we find that the conducting behavior of carbon foam surfaces derives from first- and second-nearest neighbor interactions (f.n.n.i. and s.n.n.i.) between $p_{||}$ orbitals, located at sp^2 sites, which are shown schematically in Fig. 1(c) - 1(e) with solid red and dashed green lines, respectively. Due to the foam topology, f.n.n.i. (see Fig. 1(c)) split the atomic eigenstates E_p to $E_p \pm V_{pp\pi}(1)$, producing a band gap, which turns both sp^3 terminated slabs and the bulk foam to semiconductors. However, $p_{||}$ orbitals located at the sp^2 sites of the sp^2 terminated surfaces, interact only through s.n.n.i. (see Fig. 1(d)), and therefore the atomic eigenstates $E_p = E_F$ do not split, but just broaden around E_p , leading to a metallic system.

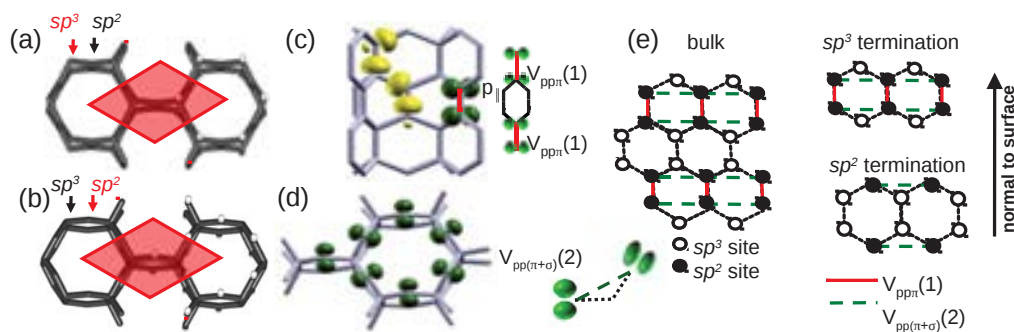


Figure 1: (a) Structure of sp^3 and (b) sp^2 terminated slab. (c) Side and (d) top view with $p_{||}$ orbitals (green). (e) Schematic representation of f.n.n.i. and s.n.n.i.

References

- [1] Z. Zhu, Z. G.Fthenakis, J. Guan and D. Tománek, Phys. Rev. Lett. **112**, 026803 (2014)

*fthenak@iesl.forth.gr

Modified diamondoids for sensing applications

Ganesh Sivaraman, Bibek Adhikari, Frank C. Maier, and Maria Fyta *

Diamondoids are tiny diamond-like cages which are hydrogen terminated and can occur in various sizes and with a diverse type of modifications giving rise to novel biotechnological applications [1, 2, 3]. In this work, based on quantum-mechanical calculations we study the effect of doping and functionalization of diamondoids on their structural characteristics and electronic properties [4]. For this, we use different dopants and atomic groups and focus on the band-gap variations and the influence of the molecular orbitals in the case of the lower diamondoids, adamantane up to heptamantane (Fig. 1(a)). At a second step, we turn to the functionalized diamondoids and use these as probes to sense DNA molecules. Modified diamondoids can form hydrogen bonded complexes to DNA nucleobases tuning their electronic properties [5] (Fig. 1(b)). Accordingly, we have observed that these small modified diamondoid-like cages are able to distinguish between small and large DNA nucleobases based on a difference up to 1 eV in the electronic band-gaps of the respective complexes [6]. In the end, we discuss the possibility to sequence DNA through diamondoid-functionalized nanopores using quantum transport measurements.

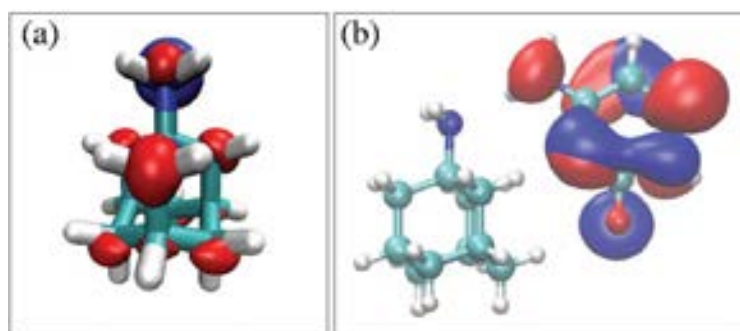


Figure 1: (a) A NH_2 -modified diamondoid. (b) The same diamondoid is probing a DNA nucleobase. The frontier (highest occupied in blue and lowest unoccupied in red) molecular orbitals are shown in both panels.

References

- [1] J. E. Dahl, S. G. Liu, and R. M. K. Carlson, *Science* **299**, 96 (2003).
- [2] W.L. Yang *et al*, *Science*, **316**, 1460 (2007).
- [3] H. Schwertfeger, A. A. Fokin, and P. R. Schreiner, *Angew. Chem. Int. Ed.* **47**, 1022-1036 (2008).
- [4] B. Adhikari and M. Fyta, under review (2014).
- [5] G. Sivaraman and M. Fyta, *Nanoscale* **6**, 4225 (2014).
- [6] F.C. Maier and M. Fyta, under review (2014).

*mfyta@icp.uni-stuttgart.de

Heusler compounds in Spintronics: Theory and Perspectives

Iosif Galanakis

Department of Materials Science, School of Natural Sciences, University of Patras

The developments in nanoelectronics, combining the magnetic and semiconducting materials (known as spintronics)¹ or using exclusively magnetic elements (known as magnetoelectronics)¹ have brought the half-metallic magnets,² initially predicted by de Groot and collaborators in 1983, to the center of scientific research. In these materials the two spin bands show a completely different behavior. While the spin-up electronic band structure is metallic, in the spin-down band the Fermi level falls within an energy gap as in semiconductors. Such half-metallic compounds exhibit, ideally, a 100% spin polarization at the Fermi level and therefore they should have a fully spin-polarized current and be ideal spin injectors into a semiconductor, thus maximizing the efficiency of spintronic and magnetoelectronic devices.³

Heusler compounds are a promising family to achieve half-metallicity since they encompass a large number of members, they crystallize mostly in cubic structures similar to the zincblende structure of semiconductors and several have very high Curie temperatures.⁴ Several among them have been predicted to be half-metals and in case of half-metallicity the total spin magnetic moment in the unit cell is intrinsically connected to the total number of valence electrons. This behavior is usually referred to as "Slater-Pauling rules" in literature.⁵ Most of them are metals exhibiting diverse magnetic phenomena.

A review on the state-of-the-art of the theoretical description of the half-metallic Heusler compounds will be provided based on first-principles density-functional calculations. Several aspects of their magnetic behavior will be discussed. Particular emphasis will be given to novel functionalities like spin-filtering and magnetic semiconductors. The perspectives of their future use in spintronics devices will be summarized, and preliminary results on novel devices based on Heusler compounds such as superlattices combining half-metallicity of Heusler compounds with perpendicular magnetic anisotropy of binary ferromagnets will be presented.

This research has been co-financed by the European Union (European Social Fund - ESF) and Greek national funds through the Operational Program "Education and Lifelong Learning" of the National Strategic Reference Framework (NSRF) - Research Funding Program: ARISTEIA II. Investing in knowledge society through the European Social Fund.



*email: galanakis@upatras.gr

References

- ¹ I. Zutic, J. Fabian, and S. Das Sarma, *Rev. Mod. Phys.* **76**, 323 (2004).
- ² M. I. Katsnelson, V.Yu. Irkhin, L. Chioncel, A.I. Lichtenstein, and R.A. de Groot, *Rev. Mod. Phys.* **80**, 315 (2008).
- ³ A. Hirohata and K. Takanashi, *J. Phys. D: Appl. Phys.* **47**, 193001 (2014).
- ⁴ T. Graf, C. Felser, and S. S. P. Parkin, *Prog. Solid State Chem.* **39**, 1 (2011).
- ⁵ S. Skaftouros, K. Ozdogan, E. Sasioglu, and I. Galanakis, *Phys. Rev. B* **87**, 024420 (2013).

The effect of multi-wall carbon nanotubes addition on the performance of P84 co-polyimide hollow fiber membranes

F.D. Gegitsidis*, N.D. Alexopoulos

Department of Financial Engineering, University of the Aegean, Chios, Greece

E.P. Favvas

Institute of Nanoscience and Nanomaterials, NCSR "Demokritos", Ag. Paraskevi, Attica, Greece

S.K. Kourkoulis

Laboratory of Testing and Materials, National Technical University of Athens, Athens, Greece

The present work investigates the effect of the addition of Multi-Wall Carbon Nanotubes (MWCNTs) of various concentrations in polymeric hollow fiber membranes for gas separation; their performance and their mechanical properties will be analyzed. Polymeric BTDA-TDI/MDI (P84) co-polyimide hollow fiber membranes were prepared using the dry/wet spinning technique, a method which is based on a phase-inversion process [1, 2]. The concept of the present work is based on the use of MWCNTs as filler material. The purpose is to study the effect of these carbon additives (MWCNTs) on the gas permeances as well as in thermal and mechanical stability compared to pure polymer (single phase) [3]. The photos of all prepared HFMs (single and mixed matrix) as well as a characteristic SEM picture which depicts one of them can be seen in Figure 1. Four different types of hollow fibers were produced with different MWCNTs concentration on the polyimide matrix, namely 1, 2, 4 wp% and without nano-reinforcement. The mixed matrix hollow fiber membranes exhibit satisfactory gas selectivities and good gas permeances as well as increased mechanical and thermal properties.



Figure 1: (a) Macro-photograph of the produced hollow fibers with different MWCNTs concentration (from left to right: MMHFM with 0, 1, 2 and 4 % fillers' concentration) and (b) SEM of the cross-section of the 0% MWCNTs hollow fiber [2]

Tensile and three-point bending tests were performed in an MTS-Insight 10 kN loading frame at a 0.005 mm/sec displacement rate. During the tests, time, force and displacement were continuously monitored and recorded. It was found that the addition of MWCNTs essentially increased the tensile and flexural modulus of elasticity; the enhancement in strength properties was not obvious and the results are discussed by taking into account the gas separation performance of the fibers, where at ambient temperature, the increase in permeance coefficients follows the increase in the filler concentration in a linear way.

Acknowledgements

E.P. Favvas would like to thank the "NANOSKAI" project (*Archimedes Framework*) of the Eastern Macedonia and Thrace Institute of Technology which is co-financed by Greece and the European Union in the frame of operational program "Education and Lifelong Learning Investing in Knowledge Society". Ministry of Education and Religious Affairs, Culture and Sports/NSRF 2007–2013.

References

- [1] McKelvey, Clausi and Koros. *Journal of Membrane Science* **124**, 223-232 (1997).
- [2] Favvas, Nitodas, Stefopoulos, Papageorgiou, Stefanopoulos and Mitropoulos, *Separation and Purification Technology* **122**, 262-269 (2013).
- [3] Xuezhong and Hägg, *Chemical Engineering Journal* **215**, 440-448 (2013).

* Filippos Gegitsidis, email: filipgegi@gmail.com

Prospect of MnBi permanent magnets for traction motors and generators

M.Gjoka^{1,*}, C. Sarafidis¹, D. Niarchos¹
¹INN, NCSR Demokritos, Athens 15310, Greece

MnBi has recently attracted large attention due to its potential for permanent magnetic applications. Although it does not present high saturation magnetization, it has large coercivity, above 1 T, which results in a theoretical BH_{\max} value above 17 MGOe. It is also very interesting that the coercivity increases with temperature, up to 2.6 T at 523 K, while for higher temperatures the structure is unstable [1-2].

MnBi ingot was prepared by arc-melting the constituent elements (purity better than 99.9%) in argon atmosphere. The ingot was annealed at 573K for 24 h in vacuum to obtain the low-temperature phase (LTP) MnBi. The annealed alloy ingots were manually crushed and ground down to less than 150 μ m. Low-energy ball milling (LEBM) of 5 g crushed ingot powder was carried out for different milling times up to 4 h in a hardened stainless steel vial using rotary mill with rotation speed of 400 rpm. The milling was performed in hexane with hardened-steel balls 2–4 mm in diameter. The ball-to-powder weight ratio was about 10 : 1. The milled powders were compacted at room temperature in the presence of a 1.0 T magnetic field. The structural characterization of the as-milled powders and hot compacted samples were carried out using x-ray diffraction (XRD) with a Cu- $K\alpha$ radiation. Microstructural characterization of the powders as well as the hot compacted magnet was carried out using scanning electron microscopy (SEM) equipped with energy dispersive x-ray spectroscopy (EDX). Magnetic properties of the field aligned powders samples were measured using a vibrating sample magnetometer (VSM) and SQUID.

The magnetic properties depend heavily on the quality of the basic material. Microstructure plays also a dominant role, the best magnetic properties were obtained after ball milling for three hours, which resulted in a narrow grain size distribution from 0.7 to 4 μ m. We have managed to achieve coercivity near 1.5 T at RT in epoxy oriented powder samples while saturation magnetization was 61 Am²/kg. The production of high-density bulk pieces from MnBi and exchange spring improved magnets could be an alternative for some technological applications, which will be shown.

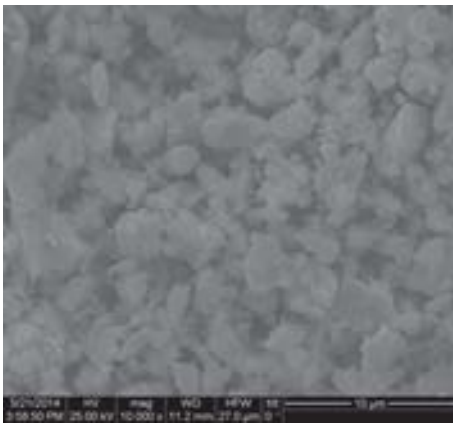


Fig. 1 SEM image of LEBM MnBi powder, milling time 3 h.

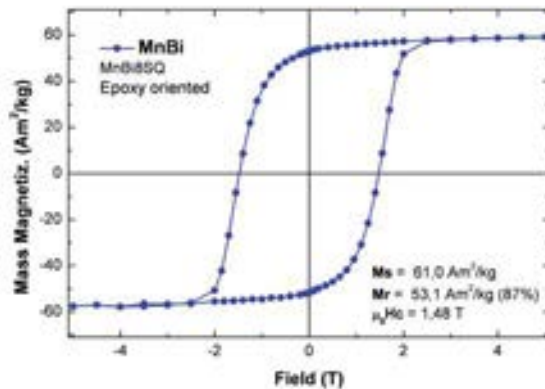


Fig. 2. RT isothermal magnetic loop of MnBi epoxy oriented sample exhibiting high coercivity and rectangular shape.

Acknowledgements. This work is partially supported by European Commission (REFREEPERMAG project) – GA-NMP3-SL-2012-280670.

References

- [1] N. V. Rama Rao, A. M. Gabay, G. C. Hadjipanayis, J. Phys. D: Appl. Phys. **46** (2013) 062001
- [2] J. Cui, J P Choi, G Li, E Polikarpov, J Darsell, N Overman, M Olszta, D Schreiber, M Bowden, T Droubay, M J Kramer, N A Zarkevich, L L Wang, D D Johnson, M Marinescu, I Takeuchi, Q Z Huang, H Wu, H Reeve, N V Vuong, J P Liu, J. Phys.: Condens. Matter **26** (2014) 064212

* gjoka@ims.demokritos.gr

Optical Absorption of Carbon-Metal Nanocomposites

G. Hadjisavvas¹, G. Tritsarlis², C. Mathioudakis¹, E. Kaxiras², and P. C. Kelires^{2*}
¹*Research Unit for Nanostructured Materials Systems, Department of Mechanical and Materials Science Engineering, Cyprus University of Technology, P.O. Box 50329, 3603 Lemesos, Cyprus,*

²*Department of Physics, Harvard University, Cambridge, Massachusetts 02138, USA*

Carbon-based materials, including diamond-like carbon (DLC), have been suggested as promising materials for solar energy harvesting. The properties of DLC may be tuned by the incorporation of transition metal atoms, either dispersed or forming nanoparticles. In a recent work [1], we studied DLC/metal nanocomposites, with metal atoms (Ag, Cu) dispersed in the matrix at substitutional sites. We used 64-atom computational cells and density functional theory (DFT) calculations. We found that metal inclusions enhance the optical absorption in the visible, but lower the sp³ fraction and thus the strength and hardness of the DLC matrix. Here, we extend these studies to the nanoparticle case. We start with metal atoms inserted in the DLC matrix interstitially, which eventually grow into larger nanocrystals. We use larger cells of 512 atoms. The initial DLC networks are generated with tight-binding calculations. The final structures with metals are relaxed with DFT and then properties are calculated. The first results indicate that the reduction of sp³ fraction is less drastic than in the dispersed case, which is beneficial for the mechanical properties. Also, the optical absorption is enhanced. By decomposing the absorption coefficient into site contributions, we aim to identify the strong absorbing atoms in the system, especially in the metal nanocrystals.

References

[1] G. Tritsarlis, C. Mathioudakis, P. C. Kelires, and E. Kaxiras, *J. Appl. Phys.* 112, 103503 (2012).

* pantelis.kelires@cut.ac.cy

High performance MIM capacitors with nanomodulated electrode and dielectric surfaces

E. Hourdakis^{*L}, A.G. Nassiopoulou

*NCSR Demokritos / Institute of Nanoscience and Nanotechnology
Terma Patriarchou Gregoriou, 15310, Athens, Greece*

The development of MIM capacitors has attracted a great deal of attention in recent years due to their use in analog, mixed signal and radiofrequency (RF) circuit applications. The need for more compact circuits has created a need for the engineering of high capacitance density capacitors since they, along with other passives, take up most of the silicon die space in such applications. High-k materials have therefore been investigated in order to meet the requirements posed by the practical applications [1]. According to ITRS (international roadmap for semiconductors), there are four main requirements for MIM capacitors: a capacitance density larger than $10\text{fF}/\mu\text{m}^2$, a leakage current less than $10^{-8}\text{A}/\text{cm}^2$, a non-linearity factor less than $100\text{ppm}/\text{V}^2$ and process temperatures that do not exceed 300 to 400°C , as these are back-end devices. Almost all reports in the literature fail to meet all of the above requirements.

We demonstrated that anodic alumina is an interesting choice as the dielectric material of MIM capacitors [2, 3]. Its advantages include high performance and an easy and cost effective fabrication of the capacitors at room temperature. Low leakage current, as well as high capacitance densities with good stability in terms of frequency were demonstrated.

In this work, we present a novel fabrication scheme for MIM capacitors using bulk anodic alumina as the dielectric. These capacitors have capacitance density and leakage current that both satisfy the posed requirements by ITRS. The non-linearity factor requirement, although not satisfied as in all cases in the literature of a single high-k dielectric layer, is greatly reduced without significant loss to either the value of the capacitance density or the stability of the capacitor with respect to frequency. This is achieved by nanostructuring the bottom electrode surface before the formation of the dielectric layer, using electrochemistry. This nanostructuring leads to reduced leakage current and greatly reduced non-linearity co-efficient.

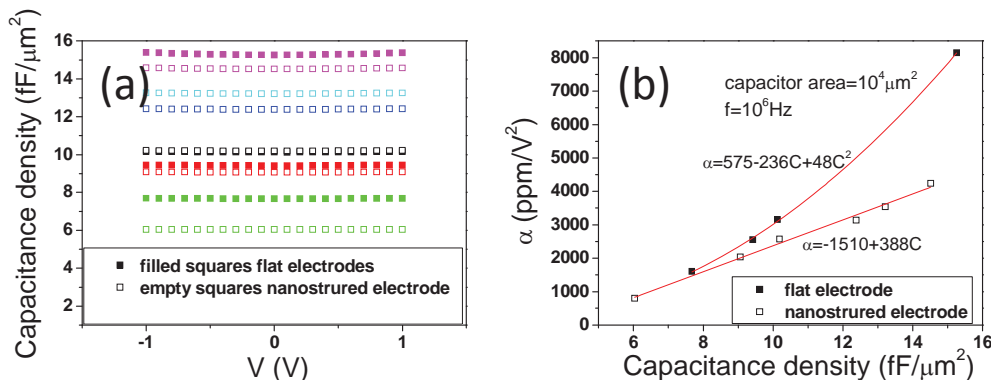


Figure 1: (a) Capacitance density vs. voltage for various MIM capacitors with flat and with nanomodulated electrode and dielectric surfaces. The different colours represent different anodic alumina thicknesses (from 12nm (green) down to 5nm (magenta)). (b) Non-linearity factor α vs. capacitance density for flat (full squares) and nanomodulated (open squares) electrode and dielectric surfaces.

References

- [1] ITRS roadmap 2013 edition (<http://www.itrs.net/Links/2013ITRS/Home2013.htm>)
- [2] Hourdakis and Nassiopoulou, IEEE Trans. on Electr. Devices **57**, 2679 (2010).
- [3] Hourdakis and Nassiopoulou, Microelectron. Engineering **90**, 12 (2012).

* mhour@imel.demokritos.gr

Quantum Dot Based 3D Photonic Devices

E. Kabouraki,^{1,2,*} I. Sakellari,¹ D. Gray,¹ M. Farsari,¹ M. Vamvakaki^{1,2}

¹*Institute of Electronic Structure and Laser (IESL), Foundation for Research and Technology-Hellas (FORTH)*

²*Department of Materials Science and Technology, University of Crete, Greece.*

In this study, we present our recent results on the fabrication of 3D high-resolution photonic nanostructures containing Cadmium Sulfide (CdS) quantum dots (QDs) that exhibit 3rd order non-linear effects and stop-gaps at visible wavelengths. These structures are fabricated using direct laser writing (DLW) and novel, organic-inorganic hybrid materials.

DLW by multi-photon polymerization is a nonlinear optical technique which allows the fabrication of 3D structures with a resolution beyond the diffraction limit. The polymerization process is initiated when the beam of an ultra-fast laser is focused in the volume of a transparent, photopolymerizable material. Multi-photon absorption takes place within the focal volume, where polymerization occurs. By moving the focused laser beam in a three-dimensional manner within the material, 3D structures can be fabricated.

The materials used in this work are photostructurable organic-inorganic hybrid materials, prepared using the sol-gel process. This versatile technique has been exploited for the incorporation of inorganic networks into polymer matrices, using as monomers molecules that carry an inorganic part (which serves as the precursor to the inorganic network) and a polymerizable organic group (which acts as the precursor to the organic polymer). Moreover, a polymerizable quencher has been incorporated within the material, allowing the fabrication of features well below the diffraction limit, as well as cadmium based quantum dot precursor moieties. Next, the microstructures were reacted with Na₂S, leading to the *in situ* synthesis of CdS quantum dots within the volume of the 3D structures that provide to the material intensity dependent refractive index which was measured using the z-scan technique. The z-scan results reveal the characteristic peak-valley graph of a 3rd order non-linear material. Microstructures with spatial resolution below 100 nm and minimal shrinkage distortion were developed [1].

Excellent quality photonic crystal woodpile structures with period as low as 400 nm have been fabricated and we show for the first time the existence of third order nonlinear effects as well as diffraction patterns and higher order stop-gaps at visible wavelengths.



Figure 1: A 500 nm period photonic crystal structure (left) and the diffraction pattern of the same structure (right)

References

- [1] I. Sakellari et al., ACS Nano, **6**, 2302 (2012).

* elmina@iesl.forth.gr

Plasmonic nanotweezers based on femtosecond-laser nanostructured substrates

D.G. Kotsifaki, M. Kandyla*

Theoretical and Physical Chemistry Institute, National Hellenic Research Foundation, 48 Vasileos Constantinou Avenue, 11635 Athens, Greece

P.G. Lagoudakis

School of Physics and Astronomy, University of Southampton, Southampton, SO17 1BJ, UK

Optical tweezers are widely employed for various applications, however the efficiency of conventional optical tweezers is limited when trapping nanoparticles. Following recent advances in nanophotonics, optical manipulation by evanescent plasmonic fields instead of conventional propagating fields has been successfully demonstrated for nanoparticles with promising results. [1]

In this work, we report on the enhancement of optical trapping forces induced by the plasmonic field of femtosecond-laser nanostructured substrates. We employed a home-built optical trapping setup, using either a CW infrared (1070 nm) N-light fiber laser or a femtosecond Ti:sapphire laser system with a tunable emission wavelength of 750 nm – 1080 nm, followed by an optical parametric oscillator with an output wavelength of 1000 nm – 1300 nm. We trapped and measured the optical forces on polystyrene nanobeads (400 nm diameter), suspended on top of femtosecond-laser nanostructured silicon substrates with quasi-periodic sharp spikes (height ~200 nm), coated by thin metallic layers (Ag or Cu/Au), as shown in Fig. 1. Upon coating, the formation of metallic nanoparticles instead of a smooth metallic film is favoured on the substrates, due to the nanometric roughness of the surface of laser-structured silicon. The nanobead solution was imaged by fluorescence excitation with a blue laser diode that was focused on the solution through the trapping objective lens, forming an inverted fluorescence microscope.

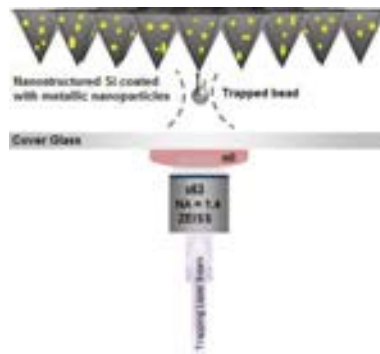


Figure 1: Optical trapping setup.

The optical trapping force is enhanced by a factor of 12 near the substrate surface and the quality factor of the trap presents an exponential decay with the distance from the substrate, which follows the decay of the near field of the coated nanospikes. The quality factor increases for wavelengths approaching the plasmon resonance of the substrate. The combination of quasi-periodic silicon nanostructures with metallic nanoparticles results in electromagnetic near-field enhancement of the trapping force, due to the excitation of localized surface plasmons on the substrate.

References

- [1] M.L. Juan, M. Righini, and R. Quidant, *Nature Photonics* **5**, 349 (2011).

* kandyla@eie.gr

Radiation sensors based on the generation of protons in polymeric gate dielectrics

E. Kapetanakis*, J. Kaliakatsos

Dept of Electronics, TEI of Crete, 73133 Chania, Greece

C. Katsogridakis, A. M. Douvas, S. Koliopoulou, A. Speliotis, V. Psycharis,
P. Argitis, P. Normand

IAPPNM, NCSR 'Demokritos', 15310 Aghia Paraskevi, Athens, Greece

V. Saltas

Dept of Natural Resources & Environment, TEI of Crete, 73133 Chania, Greece

D. Dimotikali

School of Chemical Engineering, NTUA, 15780 Athens, Greece

Ionizing radiation (IonR) has practical uses in many areas such as nuclear science, medicine, food industry and environment. For most applications and personal safety concerns, accurate monitoring and control of the radiation dose is necessary. Depending on the radiation type and dose level to be detected, a wide variety of radiation detection and measurement devices have been developed [1]. Recently, a new sensing scheme based on mobile protons generated by radiation, including IonR, in organic gate dielectrics has been proposed for the development of metal-insulator-semiconductor (MIS)-type dosimeters [2] (Fig.1).

In the present work we explore triphenylsulfonium nonaflate (TPSNF) and triphenylsulfonium hexafluoroantimonate (TPS-SbF₆) photoacid generator PAG-containing polymeric materials as the radiation-sensitive gate dielectric of organic MIS dosimeters using P3HT, as organic semiconductor material (see Fig. 2). The effect of UV and X-ray irradiation on the high-frequency (HF, 1 MHz) capacitance versus the gate voltage ($C-V_G$) curves characteristics of the MIS devices was investigated for different total dose values. The bistable behavior of a MIS device using a TPSNF-PMMA layer as gate dielectric after UV exposure is evidenced by the $C-V_G$ hysteresis loops shown in Figures 2. The presence of mobile ions in the PMMA matrix has been ruled-out, as the reference devices using a spin-coated PMMA layer do not exhibit any proton-related shift in the $C-V_G$ characteristics. Additional features such as the UV-Vis monitoring of photoacid generation through the use of an acid indicator and preliminary results of the drain current vs. gate voltage of hybrid Si-based MISFET and organic FET transistors with radiation-sensitive gate dielectrics will be presented at the conference.

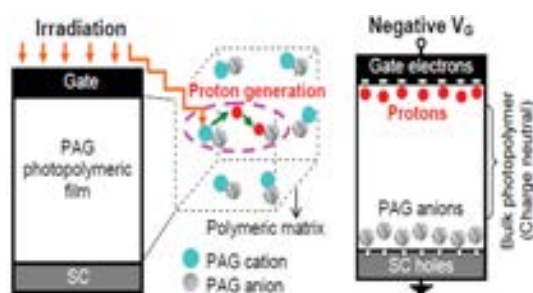


Figure 1: Radiation sensor MIS capacitor made by sandwiching a PAG embedded photopolymeric layer between two electrodes made of semiconductor, SC, and metal materials. Operation principle upon application of negative gate voltage.

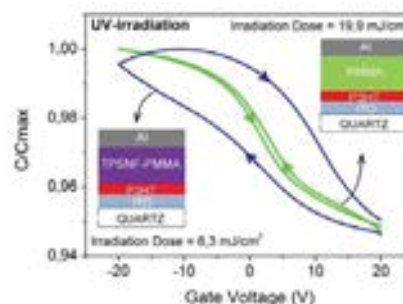


Figure 2: $C-V_G$ curves of organic MIS capacitors after exposure to UV light with a cross-section structure shown in the inset.

[1] Knoll G. F. In *Radiation Detection and Measurement*; Wiley: New York, 2000.

[2] Kapetanakis E. *et al.*, *ACS Appl. Mater. Interfaces* **5**, 5667 (2013).

This research has been cofinanced by the European Union (ESF) and Greek national funds through the Operational Program "Education and Lifelong Learning" of the National Strategic Reference Framework (NSRF)-Research Funding Program: ARCHIMEDES III.

Sol-gel prepared ZnO nanostructured films for dye-sensitized solar cells.

D. Karageorgopoulos^{1,2}, A. Apostolopoulou^{1,2}, E. Vitoratos¹, E. Stathatos^{2,*}
¹Department of Physics, University of Patras, 26504 Patras, Greece. ²Department of Electrical Engineering, Technological-Educational Institute of Western Greece, 26334 Patras, Greece.

Zinc Oxide is a II-VI group semiconductor which is well known for being one of the best alternatives of TiO₂ in several applications such as photocatalysis, solar cells etc. ZnO has attracted special attention as it has similar to TiO₂ band gap energy level and it possesses enhanced electron mobility, large surface area and good transparency. In addition, the low toxicity and cost makes it an ideal material for applications such as dye sensitized solar cells (DSSCs). In this work, DSSCs have been developed based on crystalline ZnO film via a simple aqueous solution process. According to this novel facile method, we fabricated ZnO photoelectrodes using Zinc Nitrate as a precursor of Zinc which reacted with polypropylene glycol-bis(2-aminopropyl) ether oligomer (BPPG). For the deposition of the oxide on conductive glass substrate, the sol-gel method was used. The formation of the ZnO nanocrystals was defined by the polypropylene oligomers which were used as template. Extensive studies of the structural and morphological properties of the prepared electrodes were conducted using various precursor formulations and characterization techniques.

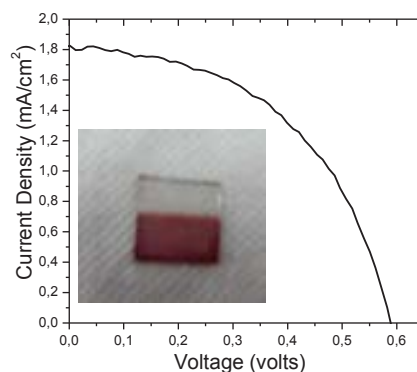


Figure 1: *J-V* characteristic curve for a ZnO based DSSC. A sensitized ZnO photoelectrode with N-719 dye is presented as an inset.

Acknowledgement: The present research has been co-financed by the European Union (European Social Fund – ESF) and Greek national funds through the Operational Program "Education and Lifelong Learning" of the National Strategic Reference Framework (NSRF) - Research Funding Program: Thales MIS: 377756.

Rotational properties of trapped superfluid gases of atoms

G.M. Kavoulakis

TEI of Crete, P.O. Box 1939, GR-71004, Heraklion, Greece

Trapped atomic gases of atoms provide an ideal system for the study of the collection of phenomena that are associated with the more general effect of superfluidity. In particular, the tunability of these systems, and the presence of a trapping potential both introduce novel effects. In my talk I will give a brief description of some of these effects, both within the mean-field approximation, as well as beyond that, where correlations play an important role.



Figure 1: Vortex states in a rotating, harmonically-trapped Bose-Einstein condensed cloud of atoms.

References

- [1] K. W. Madison, F. Chevy, W. Wohlleben, and J. Dalibard, *Phys. Rev. Lett.* **84**, 806 (2000).
- [2] J. R. Abo-Shaer, C. Raman, J. M. Vogels, and W. Ketterle, *Science* **292**, 476 (2001).
- [3] G. M. Kavoulakis, B. Mottelson, and C. J. Pethick, *Phys. Rev. A* **62**, 063605 (2000).
- [4] A. D. Jackson and G. M. Kavoulakis, *Phys. Rev. Lett.* **85**, 2854 (2000).
- [5] A. D. Jackson, G. M. Kavoulakis, B. Mottelson, and S. M. Reimann, *Phys. Rev. Lett.* **86**, 945 (2001).
- [6] A. D. Jackson, G. M. Kavoulakis, and E. Lundh, *Phys. Rev. A* **69**, 053619 (2004).
- [7] G. M. Kavoulakis, A. D. Jackson, and G. Baym, *Phys. Rev. A* **70**, 043603 (2004).
- [8] J. Smyrnakis, S. Bargi, G. M. Kavoulakis, M. Magiropoulos, K. Kärkkäinen, and S. M. Reimann, *Phys. Rev. Lett.* **103**, 100404 (2009).
- [9] T. Papenbrock, S. M. Reimann, and G. M. Kavoulakis, *Phys. Rev. Lett.* **108**, 075304 (2012).
- [10] J. C. Cremon, G. M. Kavoulakis, B. Mottelson, and S. M. Reimann, *Phys. Rev. A* **87**, 053615 (2013).
- [11] J. C. Cremon, A. D. Jackson, E. Karabulut, G. M. Kavoulakis, B. Mottelson, and S. M. Reimann, to be submitted.

Nanostructures and interfaces in III-V compound semiconductors

Thomas Kehagias*

Physics Department, Aristotle University of Thessaloniki, 54124 Thessaloniki, Greece

Nanostructures such as quantum dots (QDs) and nanowires (NWs) are highly attractive in the construction of advanced optoelectronic devices, photovoltaics and sensors. By integrating the unique physical properties of III-V compound semiconductors into quantum-sized structures, a substantial enhancement of quantum confinement is anticipated, leading to high internal quantum efficiency miniature devices.

However, the heteroepitaxial growth of nanostructures on large lattice-mismatch foreign substrates stimulates interfacial phenomena that can severely influence their structural and electronic properties and thus, their optical response. Furthermore, the quantum-confinement Stark effect (QCSE), induced by the spontaneous internal piezoelectric field in polar-grown strained nanostructures, can lead to a strong charge separation. On the other hand, spatial fluctuations of the active element mole fraction within a nanostructure results in the localization of carriers, increasing the exciton radiative recombinations. Hence, a consistent realization of the strain state of nanostructures is absolutely essential. To resolve such complicated issues, Transmission Electron Microscopy (TEM) based techniques are among the most suitable means not only to investigate their nanostructural properties, but also to determine the strain allocation along heteroepitaxial interfaces and the local chemistry of nanostructures, due to their high spatial resolution and the ability for direct observation and accurate determination of structural and crystallographic characteristics at the nanoscale.

* kehagias@auth.gr

Optically controllable THz chiral metamaterials

G. Kenanakis^{*,1,2}, N. Katsarakis^{1,2}, M. Kafesaki^{1,3},
C. M. Soukoulis^{1,4} and E. N. Economou¹

¹*Institute of Electronic Structure and Laser, Foundation for Research & Technology-Hellas, Heraklion, Crete 71110, Greece*

²*Technological Educational Institute of Crete, Heraklion, Crete 71004, Greece*

³*Materials Science and Technology Department, University of Crete, Heraklion, Crete 71003, Greece*

⁴*Ames Laboratory-USDOE, and Department of Physics and Astronomy, Iowa State University, Ames, 50011 Iowa, USA*

Metamaterials are tailored man-made composite materials, made of sub-wavelength building structures, possessing different properties from those of their constituent materials. A very interesting and particularly useful category of metamaterials is the chiral metamaterials, as they offer great possibilities in the control of the light polarization, such as optical activity (i.e. polarization rotation of a linearly polarized wave) and circular dichroism (i.e. the absorption difference between left- and right-handed circularly polarized light).

Very few attempts to realize and demonstrate THz chiral metamaterials have been made up to now [1,2]. The majority of these designs are based on the bi-layer configuration, i.e. are composed of two layers of metallic structures that are not electrically connected but the chiral response comes from their electromagnetic coupling. Here we follow this approach, of the bi-layer conductor configuration, and numerically demonstrate very large tunable optical activity and switchable ellipticity response in different chiral metamaterial structures operating in the THz regime (1-12 THz), by properly inserting into the structures photoconducting silicon, which can be transformed from an insulating to a conducting state by photoexcitation [3].

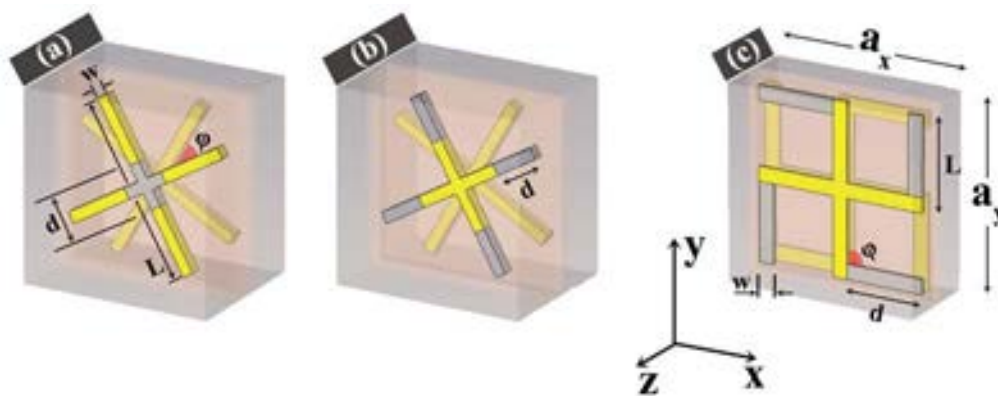


Figure 1: Schematic of the unit cell of the chiral metamaterials under consideration: (a), (b) cross-wires and (c) Z-type crosses with $\phi=90^\circ$, respectively. Grey color corresponds to photoconductive silicon and yellow corresponds to metal (silver).

References

- [1] Zh. Li, M. Mutlu and E. Ozbay, *J. Opt.* **15**, 023001 (2013).
 [2] G. Kenanakis, R. Zhao, A. Stavrinidis, G. Konstantinidis, N. Katsarakis, M. Kafesaki, C. M. Soukoulis, E. N. Economou, *Opt. Mat. Express* **2**, 1702 (2012).
 [3] G. Kenanakis, M. Kafesaki, C. M. Soukoulis, E. N. Economou, *Opt. Express* **22**, 12149 (2014).

* gkenanak@iesl.forth.gr

Effect of Magnesium alkoxide group on the CO₂ adsorption in Metal-Organic Frameworks.

E. Klontzas, T. Stergiannakos, G. E. Froudakis

Department of Chemistry, University of Crete, P.O. Box 2208, 71003 Heraklion, Crete, Greece

E. Tylanakis

Department of Materials Science and Technology, University of Crete, P.O. Box 2208, 71003 Heraklion, Crete, Greece

Ab-initio calculations and Grand Canonical Monte Carlo (GCMC) simulations were performed in order to study the CO₂ adsorption in Mg modified Isorecticular Metal-Organic Framework-10 (IRMOF-10). Mg cations were introduced in the linker of IRMOF-10 by creating Mg alkoxide groups on the linker of IRMOF-10. MP2 calculations on the Mg alkoxide linker showed that up to 4 CO₂ molecules were able to interact simultaneously with the Mg alkoxide group on the linker. The corresponding binding energies of the CO₂ molecules ranged from -13,6 kcal/mol to -8,9 kcal/mol. GCMC simulations were also performed with a modified 12-6 Lennard-Jones potential in order to predict the CO₂ adsorption isotherms at 300K and up to 40 bar. The predicted isotherms showed a clear enhancement of the CO₂ uptake up introduction of one and two Mg alkoxide groups on the linker with respect to the unmodified IRMOF-10, which is more pronounced at low pressures. The calculated isosteric heat of adsorption also showed that the introduction of Mg alkoxide groups on the linker greatly enhances the fluid – solid interactions between CO₂ and modified IRMOF-10.

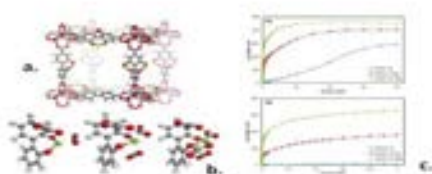


Figure 1: a. Mg alkoxide IRMOF-10 cell; b. stationary points of multiple CO₂ addition on Mg alkoxide group; c. excess volumetric adsorption isotherms of CO₂ adsorption in Mg alkoxide IRMOF-10 at room temperature.

This research has been co-financed by the European Union (European Social Fund – ESF) and Greek national funds through the Operational Program "Education and Lifelong Learning" of the National Strategic Reference Framework (NSRF) - Research Funding Program: THALES



Hydrogen storage capacity of different nanoporous carbon adsorbents

N.K. Kostoglou^{*}, C. Rebholz

*Department of Mechanical & Manufacturing Engineering, University of Cyprus,
1678 Nicosia, Cyprus*

V. Tzitzios, C. Tampaxis, T.A. Steriotis, K. Giannakopoulos
*Institute of Nanoscience & Nanotechnology, National Center for Scientific
Research "Demokritos", Agia Paraskevi Attikis, 15310 Athens, Greece*

G.C. Charalambopoulou
*Institute of Nuclear & Radiological Science & Technology, Energy & Safety,
National Center for Scientific Research "Demokritos", Agia Paraskevi Attikis,
15310 Athens, Greece*

K. Polychronopoulou, Y. Li, K. Liao
*Department of Mechanical Engineering & Department of Aerospace Engineering,
Khalifa University of Science, Technology & Research, Abu Dhabi, UAE*

In this experimental research an extensive series of carbonaceous sorbents with different structural and porous characteristics were investigated for their solid-state H₂ storage gravimetric capacity (wt%) through physical adsorption processes, in an attempt to address the main classes of carbon nanostructures that are currently receiving attention as potential H₂ stores [1-3]. In this respect, both commercially available (carbon nanotubes, few-layer graphenes) and newly synthesized (graphene sponge, microwave-exfoliated graphene oxide) graphene-based and other carbon nanomaterials were examined. Their textural properties were determined by N₂ adsorption at 77K; important parameters were extracted such as BET specific surface area, micropore volume and pore size distribution. Additional characterization techniques were employed in order to elucidate further their structural properties, such as X-Ray Powder Diffraction (XRPD), Fourier-Transform Infrared Spectroscopy (FT-IR), Field-Emission Scanning Electron Microscopy (FE-SEM) and High-Resolution Transmission Electron Microscopy (HR-TEM). The H₂ sorption behavior was studied by systematic adsorption/desorption measurements at different pressures (0-20bar) and temperatures (77K-298K) using specialized volumetric systems [4,5]. All the examined materials were compared for their H₂ storage performance under the same operating conditions, while the H₂ uptake was correlated with specific textural features. The highest capacity of 1,7wt% at 77K and 20bar was demonstrated by a commercial few-layer graphene.

References

- [1] D.P Broom, Hydrogen storage Materials, Green Energy and Technology, Springer-Verlag London Limited, 2011
- [2] Th. A. Steriotis, G.C. Charalambopoulou, A.K. Stubos, "Advanced Materials for Hydrogen Storage" in *Nanoporous Materials: Advanced Techniques for Characterization, Modeling and Processing*, CRC Press-Taylor & Francis, 2011
- [3] Y. Xia, Z. Yang, Zhu Y, "Porous carbon-based materials for hydrogen storage: advancement and challenges", *J. Mater. Ch. A* 1 (2013) 9365-81
- [4] L. Wang, A.J. Lachawiec, R.T. Yang, "Nanostructured adsorbents for hydrogen storage at ambient temperature: high-pressure measurements and factors influencing hydrogen spillover", *RSC Advances* 3 (2013) 23935-52
- [5] K.J Gross, K.R. Carrington, C. Berkeley, J. Purewal et al, *Recommended Best Practices for the Characterization of Storage Properties of Hydrogen Storage Materials*, H2 Technology Consulting LLC V3.35: US DOE; 2012

* me07kn3@ucy.ac.cy

Fundamental and optical gaps from Density Functional Theory

Leeor Kronik*

Department of Materials and Interfaces,

Weizmann Institute of Science, Rehovoth 76100, Israel

E-mail: leeor.kronik@weizmann.ac.il

Accurate prediction of both fundamental gaps and optical gaps, including charge transfer excitation energies is essential for rational theoretical design of novel materials and structures for photovoltaic applications. Preferably, we would like to predict such quantities using density functional theory (DFT) - an approach to the many-electron problem in which the electron density, rather than the many-electron wave function, plays the central role. This is because the relative computational simplicity afforded by DFT allows us to attack realistic problems. Unfortunately, despite many other successes, DFT has traditionally struggled with prediction of the above quantities. Specifically, research has been fraught with very difficult questions as to the extent to which spectroscopic conclusions can be drawn from DFT even in principle, followed by serious concerns as to the reliability of typical DFT approximations in practice.

Here, we present an approach that overcomes these difficulties quantitatively for *finite* systems, based on a range-split hybrid functional that uses exact long-range exchange. Its main novel feature is that the range-splitting parameter is not a universal constant but rather is determined from first principles, per system, based on satisfaction of the ionization potential theorem. A first generalization to molecular solids will also be presented. This DFT approach mimics successfully, to the best of our knowledge for the first time, the quasi-particle picture of many-body theory. In particular, it allows for the extraction of both single- and two-particle excitations from ground-state DFT and linear-response time-dependent DFT calculation, respectively.

Much of this research has been performed in collaboration with Roi Baer (Hebrew University). It has benefited from collaborative work with Sivan Refaely-Abramson, Shira Weismann, David Egger, Natalia Kuritz, Piyush Agrawal, and Eli Kraissler (Weizmann Institute), Tamar Stein, Helen Eisenberg (Hebrew University), Sahar Sharifzadeh, Isaac Tamblyn, and Jeff Neaton (Berkeley Lab), Mathias Dauth, Andreas Karolewski, and Stephan K ummel (Bayreuth University), Alexandre Tkatchenko (Fritz-Haber-Institut), Manish Jain (IISc Bangalore), Jochen Autschbach (U Buffalo), and Niranjana Govind (PNNL).

THz charge oscillations and charge transfer in DNA

K. Lambropoulos, K. Kaklamanis, G. Georgiadis, C. Simserides*[□]

National and Kapodistrian University of Athens, Faculty of Physics, Department of Solid State Physics, Panepistimiopolis, GR-15784 Zografos, Athens, Greece

We investigate [1, 2] charge transfer in DNA dimers, trimers and polymers (monomer is one base-pair) with a tight binding approach at the base-pair level, using the relevant on-site energies of the base-pairs and the hopping parameters between successive base-pairs [3]. A system of N coupled differential equations is solved numerically with the eigenvalue method, allowing the temporal and spatial evolution of electrons or holes along a N base-pair DNA segment to be determined [1, 2]. We predict electron or hole oscillations in DNA dimers [1, 2] with frequency in the range $f \approx 0.25\text{--}100$ THz (period $T \approx 10\text{--}4000$ fs) i.e. mainly in the mid- and far-infrared with wavelengths $\lambda \approx 3\text{--}1200$ μm [2]. The efficiency of charge transfer between the two monomers which constitute the dimer is described with the maximum transfer percentage p and the pure maximum transfer rate pf . For dimers made of identical monomers $p = 1$, but for dimers made of different monomers $p < 1$. For trimers made of identical monomers the carrier oscillates periodically with $f \approx 0.5\text{--}33$ THz ($T \approx 30\text{--}2000$ fs) [2]; for 0 times crosswise purines $p = 1$, for 1 or 2 times crosswise purines $p < 1$. For trimers made of different monomers the carrier movement may be non-periodic [1, 2]. Generally, increasing the number of monomers above three, the system becomes more complex and periodicity is lost; even for the simplest tetramer the carrier movement is not periodic. The inverse decay length β used for the exponential fit of the pure mean carrier transfer rate $k = k_0 \exp(-\beta d)$, where d is the carrier transfer distance and the exponent η used for the power law fit $k = k_0 N^{-\eta}$ are computed [1]. For polymers β falls in the range $\approx 0.2 - 2$ \AA^{-1} , k_0 is usually $10^{-2}\text{--}10^{-1}$ PHz although, generally, it falls in the wider range $10^{-4}\text{--}10$ PHz. η falls in the range $\approx 1.7 - 17$, k_0 is usually $\approx 10^{-2}\text{--}10^{-1}$ PHz, although generally, it falls in the wider range $\approx 10^{-4}\text{--}10^3$ PHz. The results are compared with theoretical and experimental works of other colleagues. This method allows assess the extent at which a specific DNA segment can serve as an efficient medium for charge transfer.

References

- [1] C. Simserides, Chemical Physics (2014) in press
- [2] K. Lambropoulos, K. Kaklamanis, G. Georgiadis, C. Simserides, Annalen der Physik (2014) in press
- [3] L.G.D. Hawke, G. Kalosakas, C. Simserides, Eur. Phys. J. E **32** (2010) 291; *ibid.* **34** (2011) 118

* csimseri@phys.uoa.gr

Biocompatible Titanium-based alloys for orthopaedics

Ch.E. Lekka

Department of Materials Science & Engineering, University of Ioannina, Greece

Medical implants require low Young moduli (E), high corrosion resistance and minimal cytotoxicity. BCC Ti-based alloys are promising candidates for replacing the TiAl6V4, which is currently in use. This β -phase can be achieved by the presence of stabilizers (Nb, Mo, Ta, V) resulting in lower E values (in the range 55 to 85GPa). Nevertheless, these values are still far from the desirable one for bone replacing material that should not exceed 30GPa. The E reduction, e.g. the β -Ti-xNb, ($x < 40\text{w}\%$ above which the E increases) could be further improved by suitable additional non-toxic elements (e.g. In, Sn, Hf). Unfortunately, although at high temperatures, the β -TiNb is favoured, upon quenching and below 40w% several phases may coexist (α , β , α'' and ω), thus impeding E lowering. Aiming in a fundamental understanding of the relationship between structural and mechanical properties of Ti-Nb phases, we performed a detailed theoretical analysis seeking for the electronic origin of structural instabilities. We found that upon Nb enrichment the unit cell increases, a result that is associated with an enhancement of the number of d-electrons, especially around -1eV, and the depletion of the occupied electronic states at the Fermi level, which characterize the β -phase of Ti, thus leading in stable β structure. Moreover, we revealed correlations between the β -phase electronic band structure characteristics at specific k-points that are related to the well known Ti soft phonon modes.

The presence of low content (<6.25at%) In or Sn p-electron dopant in the Ti-25at%Nb introduces low energy states (around -8eV) with anti-bonding characteristics with the first and second neighbouring atoms, thus weakening the chemical bonds, in line with experimental findings that suggest lowering of the Young modulus. At high Sn (or In) concentration (>12.5at%), first or second neighbourhood may include Sn-Sn pairs that exhibit strong direction bonds at even lower energy states, thus increasing the Young modulus.

These results could be of use for the design of low stiffness biocompatible alloys.

Acknowledgments: This work was supported by the BioTiNet ITN (No. 264635) FP7 Marie Curie project

References

- [1] T. Ozaki, H. Matsumoto, S. Watanabe and S. Hanada. *Materials Trans* **45**, 2776 (2004)
- [2] J.J. Gutiérrez-Moreno, Y. Guo, K. Georgarakis, A.R. Yavari, G.A. Evangelakis, Ch.E. Lekka, *Journal of Alloys and Compounds*, DOI: 10.1016/j.jallcom.2014.05.024
- [3] M. Calina, A. Helth, J. J. Gutierrez Moreno, M. Bönisch, V. Brackmann, L. Giebelera, T. Gemming, Ch. E. Lekka, A. Gebert, R. Schnettler, J. Eckert (under review in *Journal of the Mechanical Behavior of Biomedical Materials*)

Effects of curvature on the equilibrium properties of nanostructures

T. Leontiou*

Frederick University

P.C. Kelires

Cyprus University of Technology

There exist various strain relaxation mechanisms, that effect the properties of epitaxially grown nanostructures, such as Ge nanoislands on a Si substrate. The epitaxial strain is typically relaxed through a mechanism involving some sort of plastic deformation (such as dislocations) and the equilibrium composition profile at device temperatures is the result of the interplay between such strain relaxation mechanisms and inter-diffusion. Recently [1] there have been experimental studies illustrating the possibility of yet another mechanism through the bending of the substrate (e.g. Ge nanoislands grown on SOI), resulting in defect free structures. Atomistic simulations can be used in order to probe the effect of such a mechanism on the equilibrium properties at various temperatures and thus provide a comparison between flat and curved geometries, the former of which has been already extensively studied [2]. We simulate the effect of a curved substrate, similar to what is experimentally observed using continuous space Monte Carlo simulations and we notice a considerable alteration of the curved vs the flat composition profiles (Fig. 1).

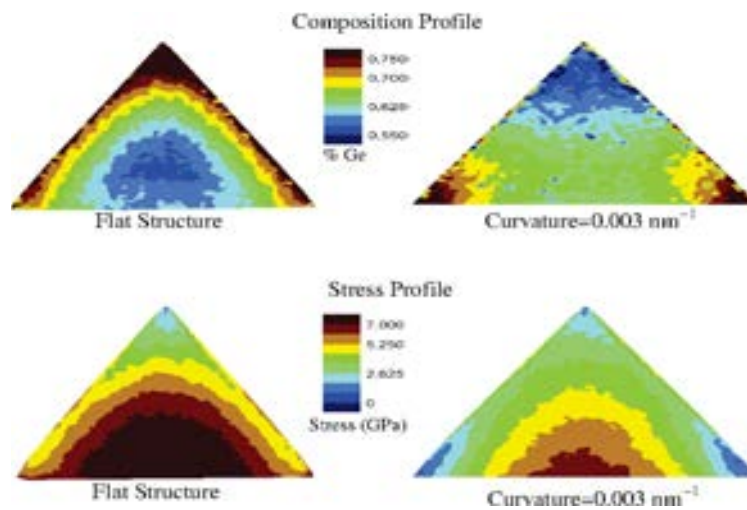


Figure 1: Top: The equilibrium composition profile after intermixing at 900K for a flat and a curved pyramid composed of 65% Ge. Bottom: The stress profile prior to intermixing.

References

- [1] F. Cavallo and M.G. Lagally, *Nanoscale Research Letters* Volume 7 (2012) ; F. Liu et al, *Nature* **416**, 498 (2002)
- [2] C. Georgiou, T. Leontiou and P.C. Kelires, submitted in *Applied Physics Letters* ; G. Hadjisavvas and P. C. Kelires, *Phys. Rev.* **72**, 075334 (2005)

* eng.lt@frederick.ac.cy

Modeling of plasmonic nanostructures for enhanced graphene-based photodetectors

E. Lidorikis*, A. Dagkli, N. Myoung, S. Evangelou
*Department of Materials Science & Engineering, University of Ioannina, 45110
 Ioannina, Greece*

T.J. Echtermeyer, M. Wu, A. Lombardo, A. Colli, S. Milana, A.C. Ferrari
*Department of Engineering, University of Cambridge, Cambridge CB3 0FA,
 United Kingdom*

Graphene, due to its unique optical properties, offers great opportunities for light harvesting and photodetection in a wide spectrum from visible to THz [1,2]. In most of these applications graphene is the active layer for both light absorption and for electron-hole separation and transport, the latter being facilitated by both photovoltaic and photothermoelectric effects [3]. Given however the relatively low absorption efficiency of graphene (2.3% when suspended and even lower when on a substrate) structural variations such as decoration of graphene with quantum dots [4] or plasmonic nanoparticles [5] have been found necessary to enhance performance. Here, we theoretically explore how different combinations of localized and propagating plasmons, plasmonic gratings (Fig. 1), lattice resonances and Fabry-Perot resonances, with different plasmonic materials such as noble metals, highly doped semiconductors and transparent conductive oxides can be utilized to optimize the absorption performance and/or tunability from the visible to the mid-IR. Specifically, we look at how the plasmonic near-fields, multiple scattering, and interference individually contribute to the enhanced absorption, and how their cumulative effect can be spectrally tuned and maximized.

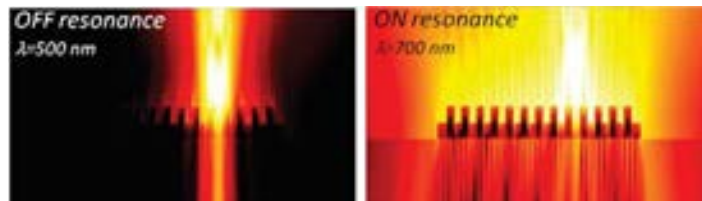


Figure 1: Field distribution of light scattering from a metallic grating

This work was funded by the EU Graphene Flagship (contract no.604391)

References

- [1] F. Bonaccorso et al., *Nature Photonics* **4**, 611 (2010).
- [2] T. Mueller et al., *Nature Photonics* **4**, 297 (2010).
- [3] T.J. Echtermeyer et al., *Nano Letters* (2014), DOI: 10.1021/nl5004762
- [4] G. Konstantatos et al., *Nature Nanotechnology* **7**, 363 (2012).
- [5] T.J. Echtermeyer et al., *Nature Communications* **2**, 458 (2011).

* elidorik@cc.uoi.gr

Magnetocaloric materials for room temperature refrigeration: the case of rare earth doped La-Ba manganites

G. Tonozlis and G. Litsardakis*

Laboratory of Materials for Electrotechnics,
Dept. of Electrical and Computer Engineering, AUTH, Greece

Magnetic refrigeration is an emerging technology, environmentally friendly and energetically more efficient than the widespread gas compression one. It exploits the magnetocaloric effect, which is a manifestation of the exchange between magnetic and lattice entropy when a material is subject to changing magnetic field in adiabatic conditions, resulting in a decrease or increase of temperature [1]. Commercial refrigeration systems are expected in the next years, but the development of a suitable magnetocaloric material is still a materials engineering challenge. Although the intermetallic iron alloys $\text{La}(\text{Fe}_{1-x}\text{Si}_x)_{13}$ are the choice of current prototypes, other compounds, such as $(\text{Mn,Fe})_2(\text{P,Si})$ and manganites of the type $\text{RE}_{1-x}\text{AE}_x\text{MnO}_3$, are proposed as room temperature refrigerants [2]. Especially the manganites present advantages over intermetallic alloys, such as low production cost, chemical stability, minimum eddy current loss and low thermal and magnetic hysteresis, as the magnetocaloric effect is associated to a second order magnetic transition [3].

We have been studying structural and magnetic properties of substituted La-Ba manganites and their potential as magnetocaloric materials [4,5]. In this presentation we report on Nd or Gd doped $(\text{La}_{1-x}\text{RE}_x)_{0.7}\text{Ba}_{0.3}\text{MnO}_3$ ($x=0.05, 0.10, 0.15$) and summarize our findings in rare earth (Y, Dy, Nd, Gd) doped La-Ba manganites. Samples are prepared by standard ceramic process and they all present a sharp ferromagnetic-paramagnetic transition of second order type. Due to change in A site average cation size, the transition temperature and the crystal structure type vary with composition. Calculation from isothermal magnetization curves and analysis of magnetic entropy change vs temperature or field curves provide insight of the effect of substitution on the materials properties. With Nd substitution we obtain at 305 K the performance of $\text{La}_{0.7}\text{Ba}_{0.3}\text{MnO}_4$ (330 K).

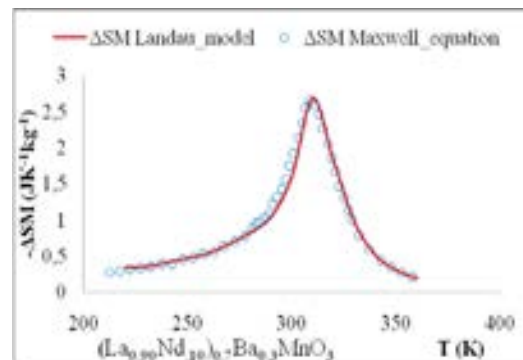
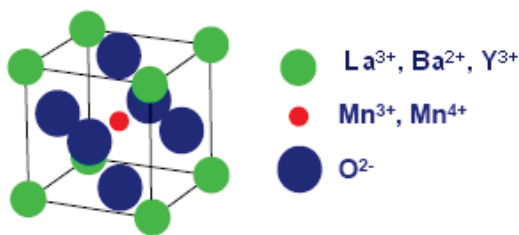


Fig. 1: The perovskite structure Fig. 2: Magnetic entropy change for 2T field change

References

- [1] K. A. Gschneidner, V. K. Pecharsky, and A. O. Tsokol, Rep. Prog. Phys. **68**, 1479 (2005).
- [2] K. G. Sandeman, Scr. Mater. **67**, 566 (2012)
- [3] M.H. Phan, S.C. Yu, J. Magn. Magn. Mater. **308**, 325 (2006).
- [4] G.Tonozlis and G.Litsradakis, pss(c) **11** 1133 (2014).
- [5] G.Tonozlis and G.Litsradakis, Intermag Conference, Dresden 2014

* Lits@eng.auth.gr

Porosity-moderated ultrafast electron transport in Au nanowire networks

E. Magoulakis^{1,2}, A. Kostopoulou^{1,3}, G.N. Arvanitakis^{1,2}, A.G. Kanaras⁴, A.N. Andriotis¹, A. Lappas¹, P.A. Loukakos^{1,*}

¹Foundation for Research and Technology – Hellas, Institute of Electronic Structure and Laser, N. Plastira 100, P.O. Box 1385, 71110 Heraklion, Greece

²Physics Department, Un. of Crete, P.O. Box 2207, 71409 Heraklion, Greece

³Chemistry Department, Un. of Crete, Voutes, 71003 Heraklion, Greece

⁴Physics & Astronomy, Un. of Southampton, Southampton SO17 1BJ, Hants, UK

We demonstrate for the first time the ultrafast properties of a newly formed porous Au nanostructure (Fig 1-up-left). The properties of the porous nanostructure are compared with those of a solid gold film using time-resolved optical spectroscopy. The experiments suggest that under the same excitation conditions the relaxation dynamics are slower in the former (Fig. 1-up-right). Our observations are evaluated by simulations based on a phenomenological rate equation model (Fig.1 down-left). The impeded dynamics has been attributed to the porous nature of the structure in the networks, which results in reduced efficiency during the dissipation of the laser-deposited energy. Importantly, the porosity of the complex three-dimensional nanostructure is introduced as a geometrical control parameter of its ultrafast electron transport. [1]. The results are of great importance to modern applications in photovoltaics, nanocircuits and nanocatalysts where the active elements are based on extended size three-dimensional porous nanostructures.

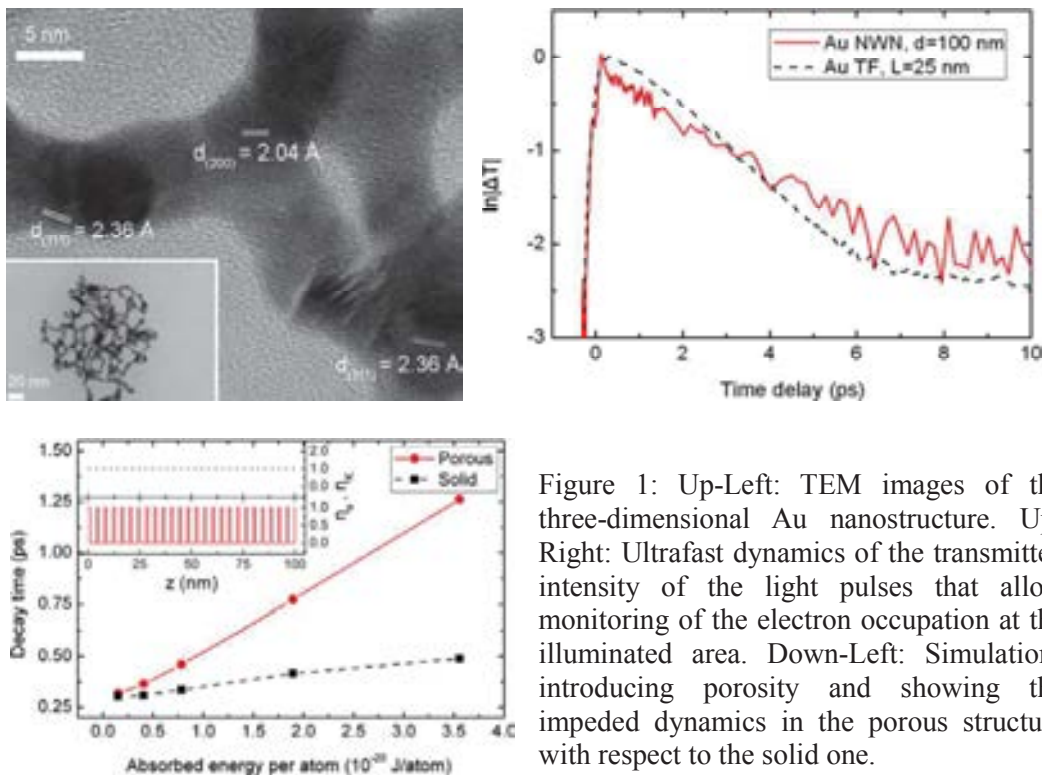


Figure 1: Up-Left: TEM images of the three-dimensional Au nanostructure. Up-Right: Ultrafast dynamics of the transmitted intensity of the light pulses that allow monitoring of the electron occupation at the illuminated area. Down-Left: Simulations introducing porosity and showing the impeded dynamics in the porous structure with respect to the solid one.

References

[1] E. Magoulakis, A. Kostopoulou, G.N. Arvanitakis, A.G. Kanaras, A.N. Andriotis, A. Lappas, P.A. Loukakos, Appl. Phys. A **111**, 711 (2013).

* loukakos@iesl.forth.gr

Electronic-Properties Engineering of TMDs: Strained Monolayers and Nanoribbons

A. E. Maniadaki, D. Davelou,
G. N. Kioseoglou, I. N. Remediakis, G. Kopidakis*
*Department of Materials Science and Technology,
University of Crete, Heraklion, Crete, Greece*

We present theoretical results for the structural, electronic and optical properties of nanoribbons (quasi-1D) and single-layer (2D) transition metal dichalcogenides MX_2 (M = Mo, W; X = S, Se, Te) under various types of strain. Our results are obtained through Density Functional Theory (DFT) calculations.

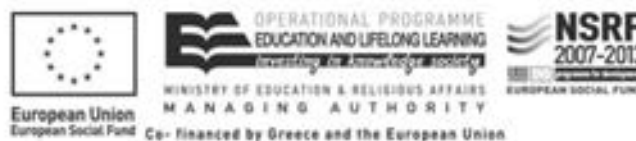
We find that the direct gap of single-layer MX_2 changes to an indirect gap for biaxial strain and uniaxial strain in the x- and y- direction, whereas for shear strain the structure remains a direct gap material. For both, tensile and compressive strain the gap decreases, with the reduction rate being smaller for tensile strain.

We also investigate the behaviour of the optical properties that are obtained using linear response theory. The results show qualitatively similar behaviour between the MX_2 materials and strain types. We show that the static dielectric constant decreases when the structure is under tensile strain and increases under compressive strain. Our DFT results are interpreted with simple models and are shown to be consistent with available experimental data.

For the quasi-1D structure, as far as the static dielectric constant is concerned, the behaviour under strain remains similar to the 2D structure. Additionally the dielectric constant increases with increasing ribbon width, reaching values which approach the dielectric constant found for the single-layer [1]. We interpret our results with a simple model by separately considering the contributions of the metallic edges and the semiconducting interior of the ribbons.

References

- [1] Davelou et al, Solid State Commun., 192 (2014) 42.



*kopidaki@materials.uoc.gr

Photodegradable Acetal block copolymer for drug delivery

T. Manouras^{1*}, G. Pasparakis², P. Argitis³ and M. Vamvakaki^{1,4}

¹*Institute of Electronic Structure and Laser, FORTH, 71110 Heraklion, Greece*

²*University College London, School of Pharmacy, WC1N 1AX London, UK*

³*Institute of Nanoscience and Nanotechnology, NCSR ‘Demokritos’, 15310 Aghia Paraskevi, Greece*

⁴*Department of Materials Science and Technology, University of Crete, 71003 Heraklion, Greece*

The development of polymers or other type of materials that degrade upon application of a light-stimulus would be highly desirable in a number of applications in nanomedicine and biofabrication such as exogenous activated drug delivery, and handling/manipulation of precious biological samples at the microscale (i.e. cell sorting, on-chip patterning, light directed cell migration, etc.).

In the present study, we demonstrate for the first time, the application of photochemical internalization in combinatorial photo-chemotherapy against cancer cells using a new class of dual degradable nanoparticles loaded with a potent chemotherapeutic anticancer compound (CPT) and a phototoxic drug (hematoporphyrin, HP). We recently reported on a new class of polymers based on the ketal family [1] that exhibits remarkably low ablation thresholds owing to their very low photolysis threshold. Furthermore, polyacetals have got a well-established hydrolysis profile under mildly acidic conditions (pH 5.5) found in the late endosome. In an effort to introduce red shifted photolability on the backbone of the polymer in the visible 2-nitroresorcinol monomers were used. Our system can be activated using visible and potentially infrared wavelengths at very low doses and exhibits simultaneous photo- and chemo- degradation, ideal for concerted light and pH controlled intracellular trafficking of drug cocktails, allowing for aggressive photoinduced cancer cell death.

In conclusion, we have developed new materials that exhibit mild and tunable photolytic cleavage under clinically relevant conditions. We demonstrated the use of dual photo- and chemo degradable NPs in photochemical internalization-mediated delivery of cytotoxic agents and proved the concept of enhanced cytotoxicity against cancer cell lines in vitro [2].



Figure 1: Our proposed generalized strategy

References

[1] G. Pasparakis, T. Manouras, A. Selimis, M. Vamvakaki and P. Argitis, *Angewandte Chemie International Edition* 50, 4142–4145 (2011).

[2] G. Pasparakis, T. Manouras, A. Selimis, M. Vamvakaki and P. Argitis, *Nature Comm.*, 5, 3623 (2014).

* tman@iesl.forth.gr

Fabry-Perot vapour microsensor onto fiber endface fabricated by multiphoton polymerization technique

V. Melissinaki^{*1,2}, M. Farsari¹, S. Pissadakis¹

¹*Institute of Electronic Structure and Laser (IESL), Foundation for Research and Technology - Hellas (FORTH).*

²*Department of Physics, University of Crete, Heraklion, Crete, Greece.*

We report on a Fabry-Perot optical resonator fabricated on the endface of a SMF28 fiber, by employing the direct laser writing technique [1]. We explore this fiber sensing probe for measuring the vapour of common organic solvents [2]. The material used for the fabrication of the microstructure is a zirconium-silicon, photosensitive organic-inorganic hybrid material [3]. The sensing head consists of a “prism” like structure suspended on four pillars, attached onto the silica fiber endface (Fig. 1a). This architecture allows the formation of a small air cavity, between the fiber endface and the microstructure, which acts as a Fabry-Perot resonator, providing interrogation capabilities of the intermediate optical medium. To avoid a multiple Fabry-Perot resonance between the two surfaces of the fabricated microstructure, which can complicate the interrogation spectrum, an inclination of about 20° was given across the outer surface of the microstructure. Liquid or gaseous media can penetrate in the empty space of this microcavity, detecting refractive index or absorption changes occurring in reflection mode. The 20µm air cavity demonstrated here results a periodic modulation of the reflected optical spectrum by notches of ~20dB in amplitude strength and a free spectral range of ~88nm.

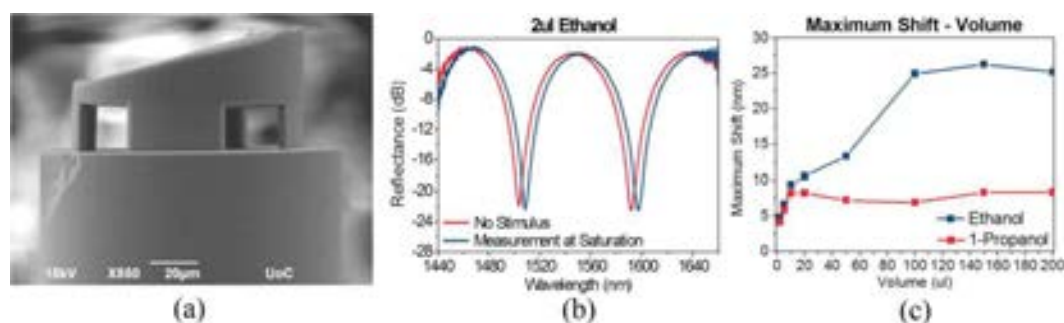


Figure 1: (a) SEM image of the microstructure on the endface of the fiber, (b) Reflection spectrums of 2µl Ethanol, (c) Shifts of the Fabry-Perot for two different alcohols for a variety of volumes.

We have tested the operation of this sensing probe for vapours of two different alcohols, those of 1-propanol and ethanol, at several different gaseous concentrations spanning from 11mbar to 65mbar. The behavior of the sensing probe presented herein has been also explained using standard physisorption mechanisms. Further work is carried out for fully characterizing and optimizing this novel sensing probe; there have been already demonstrated chemo-sensing and magnetosensing functionalities using this micro-optical configuration.

References

1. M. Malinauskas et al., *Phys. Rep.* **533**, 1 (2013).
2. M. Konstantaki et al., *Opt. Exp.* **20**, 8472 (2012).
3. I. Sakellari et al, *ACS Nano* **6**, 2302 (2012).

* melvas@iesl.forth.gr

Raman Characterisation of layered MoS₂ produced by a non-Catalytic CVD method

A. Michail¹, K. Papagelis^{1,2}, C. Galiotis^{1,2} and J. Parthenios^{*1}

¹Foundation for Research and Technology Hellas, Institute of Chemical Engineering Sciences P.O. Box 1414 GR-26504 Patras (Greece)

²Department of Materials Science University of Patras, GR-26504 Patras (Greece)

Molybdenum disulphide (MoS₂) is a layered semiconductor which exhibits an indirect (1.2eV) to direct (1.8eV) bandgap transition with decreasing number of layers. This makes MoS₂ a promising candidate to override graphene in some applications due to the absence of a bandgap of the former material. A non-catalytic CVD synthesis method to fabricate MoS₂ crystals on Si/SiO₂ substrate is presented. MoS₂ is produced by sulphurisation of MoO₃ in a quartz tube furnace under N₂ flow. The main aim is to refine the growth parameters (temperature, pressure, gas flow rate) in order to produce two-dimensional MoS₂ crystals with qualities comparable to their exfoliated counterparts. Preliminary results show that triangular crystallites of about 10 to 30 microns in lateral dimensions can be produced. The synthesized crystals are comprised of areas with different number of layers (monolayer to bulk) as it is evident from the Raman and Photoluminescence (PL) maps (fig.1c, d). The frequency difference value, $\Delta\omega$, of the A_{1g} and E_{2g} Raman modes of MoS₂ (fig. 1b) is indicative of the number of layers [1]. Additionally, the PL intensity increases dramatically by decreasing the layer number (fig. 1d), signifying the indirect to direct bandgap transition. Finally, CVD grown MoS₂ is compared with the one produced by micromechanical exfoliation.

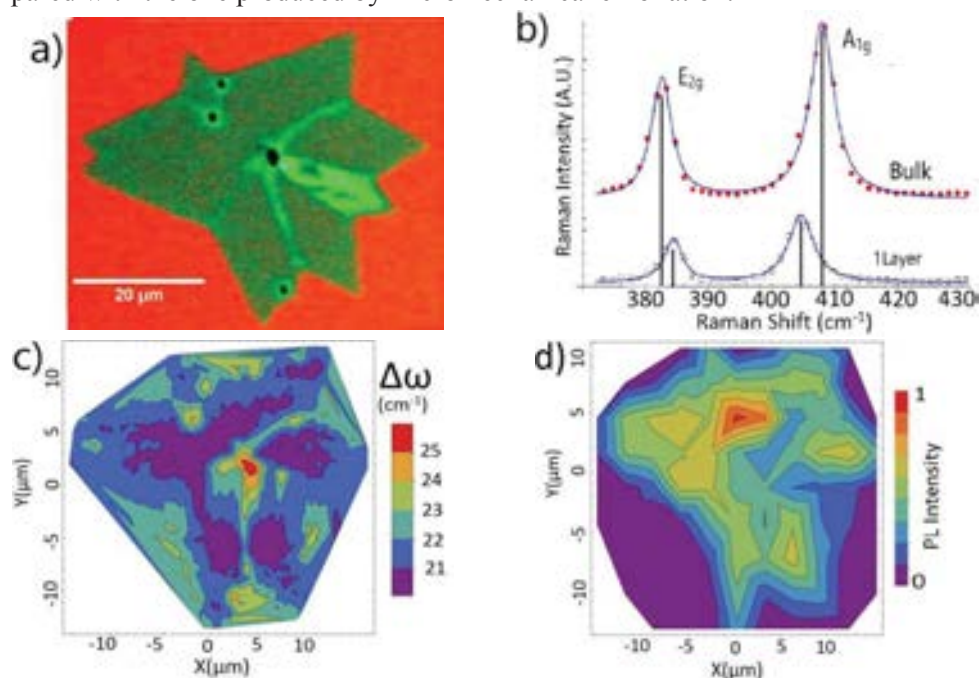


Figure 1: a) Optical image of MoS₂ crystallite, b) Raman spectra of bulk and monolayer MoS₂ where the difference $\Delta\omega$ is evident, c) $\Delta\omega$ and d) photoluminescence map of the crystallite shown in (a).

References

[1] Q. H. Wang, K. Kalantar-Zadeh, A. Kis, J. N. Coleman and M. S. Strano, *Nature Nanotechnology* **7**, 699-712 (2012)

* jparthen@iceht.forth.gr

Enhanced absorption in GaAs nanowire arrays grown on silicon substrates

K. Moratis^{1*}, R. Jayaprakash^{1,2}, S. Germanis¹, K. Tsagaraki², Z. Hatzopoulos^{2,3}, N. T. Pelekanos^{1,2}

¹Department of Materials Science and Technology, University of Crete, P.O. Box 2208, 71003 Heraklion, Greece.

²Microelectronics Research Group, IESL-FORTH P.O. Box 1385, 71110 Heraklion, Greece.

³Department of Physics, University of Crete, P.O. Box 2208, 71003 Heraklion, Greece

We report here on equivalent transmittance measurements in GaAs nanowires (NWs) grown on n+ Si(111) substrates, an example of which is shown in the SEM image of Figure 1. The GaAs NWs are grown by molecular beam epitaxy via the Ga-assisted Vapor-Liquid-Solid mechanism. The structural properties of the samples are controlled by varying various growth parameters such as the As-Ga stoichiometry, the substrate anneal time and temperature and Ga pre-deposition time. In order to control the NW diameter we follow a two-stage growth via Ga droplet removal.

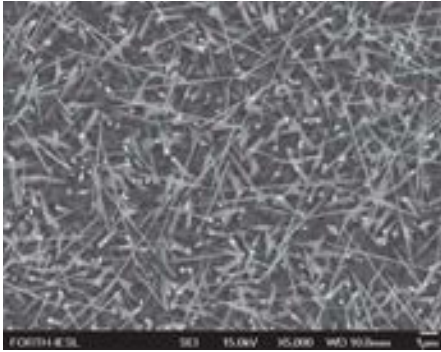


Figure 1: Top view SEM image of a NW Sample.

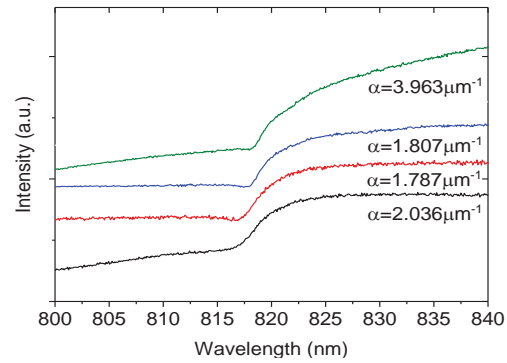


Figure 2: Transmittance spectra at T=20K.

Utilizing a common reflectivity setup, we deduce the transmittance spectra of several NW samples, as the ones shown in Figure 2, from which we estimate the effective absorption coefficient α , based on a modified expression of Beer-Lambert law, taking into account the non-uniform orientation of the NWs on the substrate surface, and neglecting any anisotropy effects,

$$\ln \frac{I}{I_0} = -2f_p l a - 2f_t \frac{d}{\cos(\theta)} a$$

where I_0 is the power of the incident light, I the power of the reflected light, f_p the filling factor of the vertical NWs, f_t the filling factor of the tilted NWs, l and d the average height and diameter of the NWs, respectively, and θ the average angle of the tilted NWs with respect to the substrate plane. The α -values in Figure 2 correspond to the low temperature absorption coefficient at the exciton gap for each sample, and clearly indicate pronounced absorption enhancement effects, at least compared to the bulk GaAs where $\alpha=1.1\mu\text{m}^{-1}$.

Acknowledgments: This work was supported by the European Social Fund and National resources through the ARISTEIA II Program “NILES”.

*moratisk@materials.uoc.gr

Photo-mechanical actuation of elastomer/carbon nanotubes nanocomposites

K. Czaniková, I. Krupa, M. Omastová^{i*}

*Polymer Institute, Slovak Academy of Sciences, Dubravská cesta 9,
845 41 Bratislava, Slovakia*

Enormous efforts of researcher are focused on the exploitation of carbon nanotubes (CNT) and their extraordinary properties in many applications as nanocomposites, sensors and actuators, field emission displays, nanoelectronics, etc. Tactile actuators based on polymer/CNTs composites are promising materials for the development of new types of visual-aid tablet for visually impaired people. However, when CNT are used as the nanofiller in polymeric matrices, problems appear with dispersion and agglomeration of CNT and compatibility with the polymeric matrix during the processing. One way to solve these problems is the surface modification of CNT which can be covalent or noncovalent. For preparing nanocomposites the non-covalent modification of MWCNT surface was carried out using compatibilizer consisting of pyrenyl and cholesteryl group [1, 2]. Nanocomposites based on ethylene-vinylacetate copolymer (EVA) and various amount of modified MWCNT were prepared by solution casting and tested as sensors and actuators. The photo-actuation measurements of the stretched nanocomposites containing modified CNT were performed using LED as light source. The photo-actuation measurements were performed on the stretched strips containing either the virgin EVA polymeric matrix or the EVA nanocomposite with MWCNT. The response of the materials to the light was studied by dynamical mechanical analysis (DMA) and scanning electron microscopy (SEM). DMA results showed that pure non-stretched EVA matrix exhibited expansion when exposed to the light. When composites in the form of strips are uniaxial pre-stretched more than 20 % of their original length, composites showed contraction when illuminated by LED. EVA nanocomposite containing 0.1 wt.% modified MWCNT showed the best results, exhibiting stresses between 33 to 165 kPa as a function of the light intensity and irradiation time. Very good repeatability of photo-actuation process up to 100 cycles was observed [3]. High optical-to-mechanical energy conversion factor of 55 MPa W⁻¹ for EVA nanocomposite containing 0.1 wt.% MWCNT during illumination by red light-emitted diode was found. Another important advantage of the present EVA/CNT nanocomposites is that all of their components are commercially available and their mixing process is easy to standardize, which enables its mass production and reduces costs.

Acknowledgements. This work was financially supported by the Slovak Research and Development Agency under contract No. APVV-0593-11, and by project VEGA 2/0149/14.

References

- [1]. K. Czaniková, M. Ilčíková, I. Krupa, M. Mičušík, P. Kasák, E. Pavlova, J. Mosnáček, D. Chorvát Jr., M. Omastová, *Smart. Mater. Struct.* Vol. 22, .No. 104001, 2013.
- [2]. K. Czaniková, I. Krupa, M. Ilčíková, M. Omastová, et al., *J. Nanophotonics*, Vol. 6, No. 063522, 2012.
- [3]. K. Czaniková, N. Torras, I. Krupa, M. Omastová, et al., *Sens. Act. B: Chem.* Vol. 186, page 701 – 710, 2013.

Study on the properties of VO₂ as thermochromic coating for smart windows

M. Panagopoulou*, D. Tsoukalas, and Y. Raptis

School of Appl. Math. & Phys. Sciences, NTUA, GR157- 80, Athens, Greece

D. Louloudakis, D. Vernardou, E. Spanakis, N. Katsarakis and E. Koudoumas
Electrical Engineering Department, School of Applied Technology, Technological Educational Institute of Crete, 710 04 Heraklion, Crete, Greece

E. Gagaoudakis, G. Michail, V. Kampylafka, E. Aperathitis and G. Kiriakidis
Institute of Electronic Structure & Laser (IESL), Foundation for Research and Technology (FORTH) Hellas, P.O. Box 1385, Heraklion 70013, Crete, Greece

G. Iliadis

UNIGLASS Ltd, 31st Vouliagmenis Av., 16675, Athens, Greece

In the present work, we present the latest **results of the National project EXOTHERMO on the properties of thermochromic VO₂ as coating for smart windows and energy efficient buildings**. It is well known that vanadium dioxide (VO₂) undergoes, at a critical temperature (T_c) of about 68°C, a semiconductor to metal (STM) transition, which is accompanied by a decrease in resistance and infrared transmittance, making the dioxide a promising material for smart window coatings in buildings.

VO₂ thin films were prepared by both the RF sputtering and the Atmospheric Pressure Chemical Vapor Deposition (APCVD) techniques, and the dependence of their thermochromic properties on substrate type, buffer layer, thickness and growth parameters employed were investigated. The substrates used were crystalline Si, uncoated glasses (fused silica and float glass) and pre-coated glasses with SiO₂, ZnON and SnO₂. The films were characterized using SEM, XRD, T-dependant micro-Raman, and spectral transmittance (200 to 2500 nm) as a function of temperature (25 to 90 °C).

Room temperature grown RF sputtered VO₂ films, initially amorphous with no thermochromic properties, they became polycrystalline monoclinic VO₂, after annealing in forming gas (95% N₂-5% H₂) at 500°C for 5min,. Films produced at temperatures less than 300 °C were polycrystalline V₂O₅ and annealing in forming gas at temperatures between 350-500°C was needed in order to get VO₂. The minimum substrate temperature required in order to get thermochromic films was 300°C to 400°C. These films exhibited transition temperature varying from 68 to 45°C. To reduce the transition temperature, two types of dopants (W or Mg) were introduced using simultaneous co-sputtering from two metallic targets (vanadium and the dopant). Lower T_c values have been obtained by adjusting the concentration percentage of the dopants. The lowest T_c , from the W-doped thermochromic films with 0.6 to 1.5 at% W, was measured at 20-25°C through T-dependant micro-Raman. Respectively, the Mg-doped films with 7 to 8.7 at% Mg display the lower T_c at 37.2°C, measured by transmittance hysteresis loop at 2000 nm.

The APCVD grown films (using vanadyl (V) triisopropoxide as single-precursor) were investigated for their properties in various growth conditions such as N₂ flow rate through the vanadium bubbler, deposition period and growth temperature. As found out, only coatings grown on SnO₂-precoated glass substrates presented thermochromic behaviour, this being optimized for a growth temperature of 450 °C, a deposition time of 30 min and a N₂ flow rate of 4 Lmin⁻¹. The respective transition temperature was found to be 66 °C, which was reduced down to 44 °C after doping with W.

This work was performed in the framework of the **EXOTHERMO** research project (**SYNERGASIA-Praksi I**, 09ΣYN-32-1185), that was funded by the G.S.R.T., Ministry of Education, Greece and the European Regional Development Fund (Sectoral Operational Programme: Competitiveness and Entrepreneurship, NSRF 2007-2013)/European Commission.

*Corresponding author: M. Panagopoulou, marpanag@mail.ntua.gr

Ultrafast laser-induced thermo-mechanical changes of Ti thin films on Si substrates

E. Tzianaki^{1,2}, Y. Orphanos¹, M. Bakarezos¹, G.D. Tsibidis³, P.A. Loukakos³, C. Kosmidis², M. Tatarakis¹, and N.A. Papadogiannis^{1,*}

¹Centre for Plasma Physics & Lasers, School of Applied Sciences, Technological Educational Institute of Crete, Rethymnon 741 00, Greece

²Physics Department, University of Ioannina, 451 10 Ioannina, Greece

³Foundation for Research and Technology-Hellas, Institute of Electronic Structure and Laser (FORTH-IESL), P.O. Box 1527, 711 10 Heraklion, Greece

Titanium (Ti) is a material for which theoretically calculated values of electron-phonon coupling constant are extremely high [1]. This makes Ti a favourable transducer for the conversion of absorbed ultrafast laser energy into high frequency mechanical waves. In this article, we present initial experimental results from thin Ti films on Silicon (Si) substrates, which support the previous theoretical calculations, and show interesting features both at the very early times of the interaction and, at later times, in which mechanical waves are created and propagate into the Ti film and the Si substrate. Preliminary theoretical modelling supports the extremely fast transfer of the electron energy to the lattice (of the order of 0.5ps) and addresses issues such as the role of the non-thermal electrons on the very early times of the interaction, as well as other dynamic features at later times such as rapid phase changes.

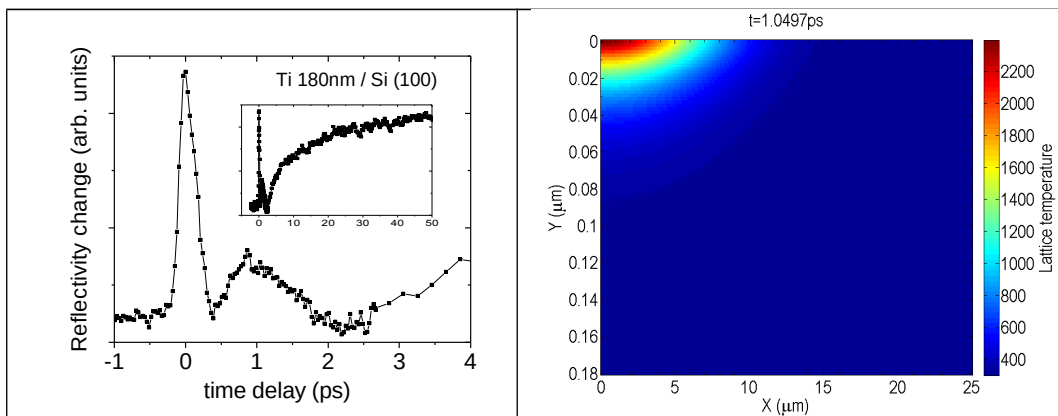


Figure 1: Left: Experimentally measured femtosecond transient reflectivity of a 180 nm Ti-film on Si (100) substrate at melting conditions. Right: Theoretical predictions for the temperature distribution inside the Ti film, at time 1.05 ps after the excitation. A melted depth of about 10 nm is illustrated.

References

[1] Z. Lin, L.V. Zhigilei, and V. Celli, Phys. Rev. B **77**, 075133 (2008).

ACKNOWLEDGEMENTS

This research has been co-financed by the European Union (European Social Fund – ESF) and Greek national funds through the Operational Program "Education and Lifelong Learning" of the National Strategic Reference Framework (NSRF) - Research Funding Program: ARCHIMEDES III. Investing in knowledge society through the European Social Fund (partially funded through Action 19: Innovative optoacoustic device for 3d spatiotemporal micro-characterization of composite materials based on ultrafast laser pulses). Authors would like to thank Dr George Konstantinidis and Prof. Panayiotis Patsalas for preparing and providing the samples.

* npapadogiannis@staff.teicrete.gr

High In-content InGaN films grown by Plasma-Assisted Molecular Beam Epitaxy for Photovoltaic Applications

E. Papadomanolaki¹, C. Bazioti², S. Kazazis¹, Th. Kehagias², A. Georgakilas^{1,3}, G. P. Dimitrakopoulos² and E. Iliopoulos^{1,3}

¹ *Physics Department, University of Crete, Heraklion, Greece*

² *Physics Department, Aristotle University of Thessaloniki, Thessaloniki, Greece*

³ *Micro/Nano-Electronics Research Group, IESL-FORTH, Heraklion, Greece*

InGaN alloys are a family of semiconductors with a direct bandgap that can span almost the entire solar range, a property that makes them particularly appealing for photovoltaic applications. For device development, however, several challenges have to be overcome: increased structural defects due to the large lattice mismatch between the alloy endpoints as well as phase separation phenomena caused by the immiscibility of the alloy components, especially at high temperatures. The RF-MBE growth of $\text{In}_x\text{Ga}_{1-x}\text{N}$ films on GaN(0001) substrates with a wide range of compositions and significant thickness ($>300\text{nm}$) under different growth conditions is considered in the present work. High resolution x-ray diffraction (HR-XRD), high resolution transmission electron microscopy (HR-TEM), scanning electron microscopy (SEM), atomic force microscopy (AFM), photoluminescence (PL) and Hall effect measurements were used to characterize the films.

The growth of high-In-content, single-phase InGaN films is reported. Analysis shows that In incorporation seems to depend on the preferable incorporation of Ga over In, InGaN decomposition, In desorption for higher growth temperatures especially and the interplay of such kinetic mechanisms.

Both HR-XRD and TEM studies show that phase separation in the films depends greatly on the growth conditions and, in particular, on the substrate temperature during growth: phase separation is more likely to occur at higher growth temperatures, while for lower temperatures it is significantly suppressed. The full width at half maximum (FWHM) of XRD (0002) rocking curves also shows a deterioration of the crystal quality as the temperature increases. Information from TEM suggests phase separation could be related to strain relaxation effects: at low temperatures, films exhibit V-defects, while for higher-temperature samples, stacking faults are observed and samples appear to form a sequestration layer at the base of the InGaN film. AFM shows low-temperature samples having ‘pits’ on the surface that are also consistent with V-defects, while high-temperature samples have much smoother surfaces. Furthermore, optoelectronic properties of the InGaN layers seem to be greatly affected by the substrate temperature: as the temperature rises there appears a redshift in the PL emission and a decrease of the carriers Hall mobility.

Acknowledgement: This research has been co-financed by the European Union (European Social Fund– ESF) and the Greek national funds through the Operational Program “Education and Lifelong Learning” of the National Strategic Reference Framework (NSRF) – Research Funding Program: THALES.

Single and few layer graphene flakes under uniaxial deformation

Konstantinos Papagelis^{1,2,*}

¹*Foundation of Research and Technology Hellas, Institute of Chemical Engineering Sciences, P.O. Box 1414, GR-26504 Patras (Greece)*

²*Department of Materials Science, University of Patras, GR-26504 Patras (Greece)*

Graphene is an amazing material exhibiting among the others superior mechanical properties such as extreme stiffness of about 1 TPa and breaking strength of 42 Nm^{-1} (or 130 GPa considering the thickness of graphene as 0.335 nm) [1,2]. Recently there has been a growing interest in bilayer, trilayer and few layer graphene materials because of their interesting properties. In these systems the electronic, optical and vibrational properties are distinct from those of single-layer graphene and strongly depended on the crystallographic stacking of the individual graphene layers] [3].

Raman spectroscopy has been proven a very successful technique to investigate the effect of mechanical deformation on graphene materials under uniaxial tension and compression [4, 5] or hydrostatic pressure [6]. Therefore, monitoring optical phonons it seems the clearest and simplest way to quantify the macroscopic stress/strain imparted to graphene sheets.

In this work, recent results on the uniaxial Raman response of single-, bi-, tri- and few-layer graphene samples will be discussed. Emphasis should be given on the perspectives in the design of graphene based nanocomposites and flexible electronics.

Acknowledgements: This research has been co-financed by the European Union (European Social Fund - ESF) and Greek national funds through the Operational Program “Education and Lifelong Learning” of the National Strategic Reference Framework (NSRF) - Research Funding Program: ARISTEIA II. Investing in knowledge society through the European Social Fund.



References

- [1] C. Lee, X. D. Wei, J. W. Kysar, J. Hone, *Science* 321, 385 (2008).
- [2] G. Kalosakas, N. N. Lathiotakis, C. Galiotis and K. Papagelis, *Journal of Applied Physics* 113, 134307 (2013).
- [3] K. Kim, S. Coh, L. Z. Tan, W. Regan, J. M. Yuk, E. Chatterjee, M. F. Crommie, M. L. Cohen, S. G. Louie, and A. Zettl, *Physical Review Letters* 108 246103 (2012).
- [4] O. Frank G. Tsoukleri, J. Parthenios, K. Papagelis, I. Riaz, R. Jalil, K. S. Novoselov and C. Galiotis, *ACS-Nano* 4, 3131 (2010).
- [5] O. Frank, M. Bouša, I. Riaz, R. Jalil, K. S. Novoselov, G. Tsoukleri, J. Parthenios, L. Kavan, K. Papagelis and C. Galiotis, *Nano Letters* 12, 687 (2012).
- [6] K. Filintoglou, N. Papadopoulos, J. Arvanitidis, D. Christofilos, O. Frank, M. Kalbac, J. Parthenios, G. Kalosakas, C. Galiotis and K. Papagelis, *Physical Review B* 88, 045418-1-6 (2013).

* kpapag@upatras.gr

Electrospun, pH-responsive microfibrinous membranes as adsorbents for bacteria removal from contaminated aqueous solutions

Petri Ch. Papaphilippou¹, Ioannis Virydes², Theodora Krasia-Christoforou¹

¹ *Department of Mechanical and Manufacturing Engineering, University of Cyprus, Nicosia, Cyprus*

² *Department of Environmental Science and Technology, Cyprus University of Technology, Limassol, Cyprus*

Water is one of the most essential elements in human life. Through many decades, humanity is facing a major problem of water contamination with subsequent high risks in human health and quality of life. During the last years there is an increased interest on the protection and purification of urban wastewater contaminated by pathogens [1]. Several techniques currently used to treat wastewater rely on direct chemical processes, (i.e. Chlorination and Advanced Oxidation Processes (AOPs)), which however, lead to the generation of harmful byproducts. Membrane filtration technologies are often employed for the decontamination and purification of water supplies including Microfiltration (MF), Ultrafiltration (UF), Nanofiltration (NF) and Reverse Osmosis (RO). Such technologies have been proved to be energy-efficient and in addition they do not require the use of chemicals [2].

Herein, novel materials in the form of microfibrinous membranes have been generated by means of the electrospinning technique and further evaluated as adsorbents for selected bacteria microorganisms. Electrospinning is a low-cost method that is used for the production of fibrous materials with fiber diameters ranging between a few nanometers up to a few micrometers [3]. Consequently, such materials are characterized by high surface-to-volume ratios rendering them appropriate in various applications including water remediation through filtration [4]. Random copolymers consisting of the hydrophobic methyl methacrylate (MMA) and the hydrophilic/pH-responsive 2-diethylamino ethyl methacrylate (DEAEMA) (pKa ~ 7.3) synthesized by conventional free radical polymerization have been electrospun under specific electrospinning conditions to yield cylindrical, beaded-free microfibrinous polymer membranes. The morphology and the thermal stability of the membranes were determined by scanning electron microscopy (SEM) and thermal gravimetric analysis (TGA), respectively. The aforementioned materials were assessed against the gram-negative bacteria of *Pseudomonas aeruginosa* and *Advenella species* in order to determine their performance as wastewater filtration systems. The bacteria removal by the microfibrinous membranes was studied by measuring the optical density (OD) of the microorganisms by UV-Vis spectrophotometry.

Acknowledgements

This work has been funded by the University of Cyprus and the University of Cyprus Grant "New Researchers".

References

- [1] Joao P.S. Cabral, "Water Microbiology. Bacterial Pathogens and Water", *Int. J. Environ. Res. Public Health*, 2010, 7, 3657-3703. [2] B. Van der Bruggen, C. Vandecasteele, "Distillation vs. membrane filtration: overview of process evolutions in seawater desalination", *Desalination*, 2002, 143(3), 207-218. [3] Z.-M. Huang, Y.-Z. Zhang, M. Kotakic, S. Ramakrishna, "A review on polymer nanofibers by electrospinning and their applications in nanocomposites", *Compos. Sci. Technol.*, 2003, 63, 2223-2253. [4] R. Gopal, S. Kaur, Z.W. Ma, C. Chan, S. Ramakrishna, T. Matsuura, "Electrospun nanofibrous filtration membrane", *J. Membr. Sci.*, 2006, 281(1-2), 581-586.

Intense femtosecond photoexcitation of bulk and monolayer MoS₂

I. Paradisanos^{1,2,*}, E. Kymakis³, C. Fotakis^{1,2}, G. Kioseoglou⁴, E. Stratakis^{1,4}

¹ *Institute of Electronic Structure and Laser (IESL), Foundation for Research and Technology-Hellas (FORTH), Heraklion, 71003, Greece*

² *Physics Department, University of Crete, Heraklion, 71003, Greece*

³ *Center of Materials Technology and Photonics & Electrical Engineering Department, Technological Educational Institute (TEI) of Crete, Heraklion, 71003, Greece*

⁴ *Department of Materials Science and Technology, University of Crete, Heraklion, 71003, Greece*

Transition metal dichalcogenides (TMDs) are layered compounds like graphite that can be reduced from three-dimensions to two-dimensional (2D) form up to the monolayer limit due to their strong in-plane bonding and weak interlayer van der Waals coupling. In contrast with their indirect gap character in the bulk, single layer TMDs are direct gap semiconductors with great promise for optoelectronic and photonic devices. Towards the development of such devices, the investigation of 2D materials response under intense photoexcitation by ultrashort pulses, as well as of their ultrafast optical properties, is undoubtedly important.

In this work, the effect of intense femtosecond laser excitation on the structure of bulk and monolayer MoS₂ (optical gaps of 1.30 and 1.90 eV respectively), under conditions ranging from lattice heating to material damage is systematically investigated. The evolution of the Raman active A_{1g} (out of plane) and E_{2g}¹ (in plane) vibrational modes was recorded as a function of irradiation intensity and total exposure time. Experiments reveal large differences in the ultrafast laser excitation response of monolayer compared to the bulk, as far as the lattice distortion as well as the lattice morphology at the onset of optical damage. The single-pulse optical damage threshold was determined for the monolayer and bulk under 800 nm and 1030 nm pulsed laser irradiation and the role of two-photon versus one photon absorption effects is discussed.

* iparad@iesl.forth.gr

Chimeric block copolymer/protein nanostructures via electrostatic self-assembly

S. Pispas*

Theoretical and Physical Chemistry Institute, National Hellenic Research Foundation, 48 Vassileos Constantinou Ave., 11635 Athens, Greece

Polyelectrolyte block copolymers constitute an intriguing class of macromolecules, as they combine the structural characteristics of amphiphilic block copolymers, polyelectrolytes and surfactants. [1] Equally interesting is the case of the electrostatic interaction between polyelectrolytes and proteins owing to a vast variety of possible technological applications concerning protein encapsulation, immobilization, purification and separation, as well as in the development of functional nanobiomaterials, while its study provides valuable insight into the interactions between charged biomacromolecules that take place in several biological systems. [2] Electrostatic interaction between polyelectrolyte block copolymers and proteins enables the formation of protein containing nanoparticles of varying structure and properties, suitable for nanobiotechnological and medical applications, e.g., protein/peptide drug delivery, biomacromolecules separation, surface modification, etc.

In this presentation novel nanostructures formed by electrostatic self-assembly between functional block copolymers and proteins will be discussed on the basis of elucidating effects of block copolymer architecture and responsiveness to external stimuli, component concentration, solution pH, temperature and ionic strength on the architecture and functionality of the formed hybrid/chimeric nanoassemblies in solution. Examples of chimeric nanostructures formed on solid surfaces will be also presented.

The work has been financed by the NANOMACRO 1129 project which is implemented in the framework of the Operational Program “Education and Life-long Learning” of the National Strategic Reference Program-NSRF (Action “ARISTEIA I”) and it is co-funded by the European Union (European Social Fund-ESF).

References

- [1] S. Förster, V. Abetz, and A. H. E. Müller, *Adv. Polym. Sci.* **166**, 173 (2004).
[2] a) M. A. Cohen Stuart, B. Hofs, I. K. Voets, and A. de Keizer, *Curr. Opin. Colloid Interface Sci.*, **10**, 30 (2005), b) C. L. Cooper, P. L. Dubin, A. B. Kayitmazer, and S. Turksen, *Curr. Opin. Colloid Interface Sci.* **10**, 52 (2005), c) A. Harada and K. Kataoka, *Prog. Polym. Sci.* **31**, 949 (2006).

* pispas@eie.gr

Study of Polymer/Graphene Interfacial Systems through Molecular Dynamics Simulations

Anastassia N. Rissanou^{*1,2}, Vagelis Harmandaris^{1,2}

¹ *Department of Mathematics and Applied Mathematics, University of Crete, GR-71409, Heraklion, Crete, Greece*

² *Institute of Applied and Computational Mathematics, Foundation for Research and Technology Hellas, GR-700 13 Heraklion, Greece*

Graphene nanocomposites have remarkable physical properties with important applications in many different areas. In the current work we present results, which are part of a general computational approach, based on a hierarchical simulation methodology [1], for the study of realistic polymer/graphene systems. Our primary goal is to study the effect of the graphene layers on the structural and dynamical properties of polymer systems. The work which has been accomplished up to now concerns the study of three hybrid polymer/graphene interfacial systems (polystyrene/graphene, poly(methyl methacrylate)/graphene and polyethylene/graphene) through detailed atomistic molecular dynamics (MD) simulations. [2,3,4] Various properties are being studied related to:

(a) Density profile: The time-averaged molecular density profiles, $\rho(z)$, as a function of the distance from the graphene surfaces (z -direction) of the model films are calculated.

(b) Structural characteristics: Molecular orientation tendencies induced by the confinement are being studied by calculating the second rank order parameter and the polymer chain's conformation tensor.

(c) Mobility aspects: We study the dynamics of polymer chains, both in the level of the monomer and the chain center-of-mass, by monitoring the evolution of the mean square displacements, as well as through time auto-correlation functions of a vector along the molecule.

All above properties are examined, as a function of the distance from the substrate (Figure 1) for a series of film widths, ranging from [2.85-14] nm. Finally, the properties of the macromolecular chains are being compared to the properties of the corresponding bulk systems at the same temperature.

The second stage of our work involves the extension of the proposed methodology to mesoscopic description using proper coarse-grained (CG) models. This approach allows us to extend simulations in much longer systems and for much longer times.

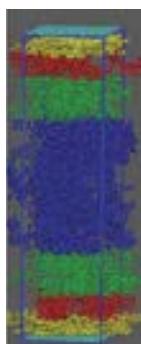


Figure 1: A snapshot of PS/graphene model system. Different colors correspond to different adsorption layers with respect to the surface.

References

- [1] Harmandaris, V. et al. *Macromolecules* **39**, 6708-6719 (2006); **40**, 7026-7035 (2007).
- [2] Rissanou, A. N. and Harmandaris, V. J. *Nanopart. Res.* **15**, 1589_1-14 (2013).
- [3] Rissanou, A. N. and Harmandaris, V. *Macromol. Symposia* **331-332**, 43-49 (2013).
- [4] Rissanou, A. N. and Harmandaris, V. *Soft Matter* **10**, 2876–2888 (2014).

* rissanou@tem.uoc.gr

Nanowires as a generic technology for basic science and future applications

Lars Samuelson*

*Lund University, Solid State Physics and Nanometer Structure Consortium,
Box 118, S-221 00 Lund, Sweden*

Very often, progress in science and technology comes as consequences of new achievements in materials science and technology. I will here describe one such technology step related to the realization of guided self-assembly for the growth of semiconductor nanowires. Beside the obvious importance this has had for materials science, this has also enabled progress in many other areas of science and technology, such as in low-dimensional physics, in life-science, in nanoelectronics as well as in energy and optoelectronics applications. I will in this talk review the development of the field of semiconductor nanowires and indicate the opportunities it offers for future applications especially related to energy and optoelectronic applications.

*lars.samuelson@ftf.lth.se

Effect of various parameters on morphological structure of PCL nanofibers

P.I Siafaka*¹, M.Mone¹, E.Pavlidou² and D.Bikiaris¹

¹Laboratory of Polymer Chemistry and Technology, Department of Chemistry, Aristotle University of Thessaloniki, 54124, Thessaloniki, Macedonia, Greece ,

²Laboratory of Solid State Physics, Department of Physics, Aristotle University of Thessaloniki, 541 24, Thessaloniki, Greece

Nanofibers have been the subject of recent intensive research due to their unique properties, such as large surface-area-to-volume ratio, flexibility in surface functionality, superior mechanical properties (stiffness ,tensile strength), and the fact that they can be produced from a wide range of organic and inorganic polymers . Electrospinning process with needle is the most desirable method for producing nanofibers, because it is a low-cost and effective method . Polymer nanofibers are the optimal candidates for providing novel applications in many research areas, such as medical areas, textiles, filtration etc .The characteristics of the electrospun jet and the morphology of the resultant fibres are highly dependent on the properties of the polymer solution ,applied voltage, distance of collector etc. PCL is biodegradable polyester and is used for many applications such as a drug delivery device, suture or adhesion barrier. [1-4]

Aim of this study, was the investigation of different parameters in order to produce PCL nanofibers, using solvents such as dichloromethane (DCM), chloroform and acetone. It was found that increment of the concentration, produced higher diameter nanofibers. Also, it was derived that a relation between applied voltage and distance of the collector, affect the formulation of fibers or beads.

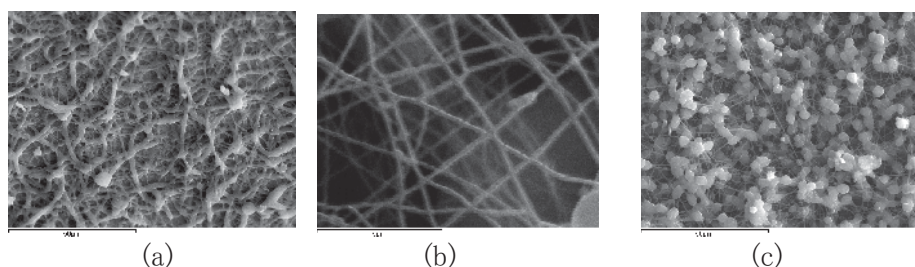


Figure 1: Electrospun nanofibers of (a) 30% PCL-solvent DCM, Flow rate=0.01ml/min, Distance(d)=4.5cm (b) 15 %PCL- solvent DCM, Flow rate=0.01ml/min, d=4.5cm, V=12KV and (c) beads-V= 17KV

References

- [1]D. Li, Y. Xia, Advanced Materials V. 16, 14, 1151-1170, (2004)
- [2]D.H. Reneker, A.L. Yarin, E. Zussman, H. Xu V. 41, 43-195, 345-346, (2007)
- [3]S. Shendokar,A. Kelkar ,R. Mohan,R. Bolick ,IMECE -12188, 2009
- [4]B. Cramariuc, R. Cramariuc, R. Scarlet, L. Rozemarie Manea, I. G. Lupu, O. Cramariuc, , Journal of Electrostatics, 1-10, (2013)

* psiafaka@chem.auth.gr Tel:+30-2310-997812

Structural and magnetotransport properties in granular $\text{Co}(c=0.8)\text{Bi}(1-c)$ thin films

Th. Speliotis*, A. Melitsiotis and D. Niarchos

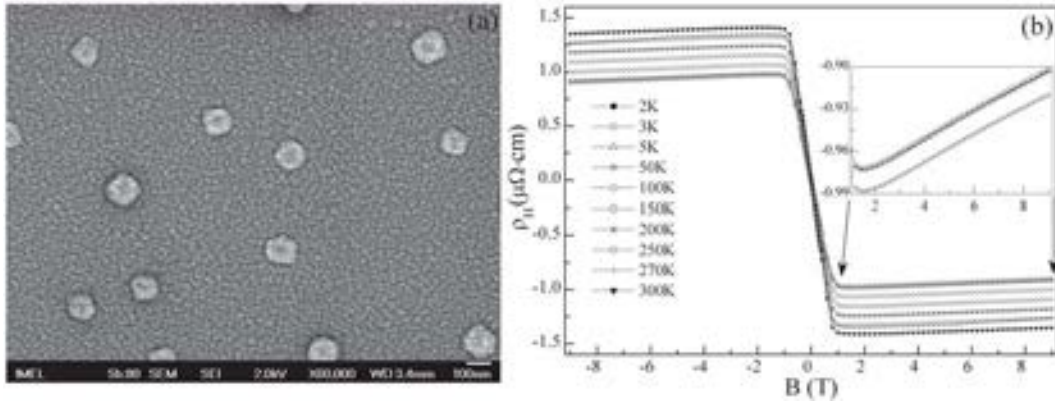
Institute of Advanced Materials, Physicochemical Processes, Nanotechnology and Microsystems, NCSR "Demokritos", 15310 Athens, Greece

P. Athanasopoulos and C. Christides

Dept. of Computer Engineering & Informatics, University of Patras, 26504, Greece

In this work we present Semimetal/Magnetic granular thin film nanostructures with structure of $\text{Co}(c=0.8)\text{Bi}(1-c)$ which were grown by magnetron sputtering.

X-ray diffraction (XRD) measurements reveal that the structure is polycrystalline. The predominant texture with $(00l)$ indices ($l=3, 6$), that observed in pure Bi films, decrease towards to zero intensity as Co thickness increases, indicating a progressive change in texture of Bi layers depending from the thickness of Co. Field Emission Scanning Electron Microscopy (FESEM) (figure a) show a bimodal distribution of grain sizes with average values of 95 nm for the embedded structures, and 10 nm for Co-rich nano-grains in the background.



AHE loops (figure b) exhibit a significant increase of the anomalous Hall (AH) coefficient R_S by 50%, from 2K up to 300K. It shows that the conduction mechanism in these films is not due to tunneling effect through grain boundaries, or variable-range-hopping (VRH) mechanism. A first explanation is that Hall resistance measures the amount of electrons trapped by magnetic gradients in boundaries between magnetic Co nano-grains and Bi surface states. It can be considered that Hall resistance measures channeling by snake and cycloid orbits in the regions of high magnetic gradient, as reported in ref. [1].

References

[1] A. Nogaret, D. N. Lawton, D. K. Maude, J. C. Portal, and M. Henini, *Phys. Rev. B*, **67**, 165317 (2003).

Acknowledgements

This research has been co-financed by the European Union (European Social Fund – ESF) and Greek national funds through the Operational Program "Education and Lifelong Learning" of the National Strategic Reference Framework (NSRF) - Research Funding Program: Greece – Hungary bilateral cooperation (HUN82). Investing in knowledge society through the European Social Fund

* tspeliotis@ims.demokritos.gr

Micro-FTIR: From Plasmon Frequency to Dopant Concentration Mapping

E.C. Stefanaki^{(1)*}, G.S. Polymeris^(1,3), M. Ioannou⁽²⁾ E. Pavlidou⁽¹⁾,
E. Hatzikraniotis⁽¹⁾, Th. Kyratsi⁽²⁾, K.M. Paraskevopoulos⁽¹⁾

⁽¹⁾Physics Department, Aristotle University of Thessaloniki, GR-54124, Thessaloniki, Greece

⁽²⁾Department of Mechanical & Manufacturing Engineering University of Cyprus, 1678 Nicosia, Cyprus

⁽³⁾Institute of Nuclear Sciences, Ankara University, Tandogan Campus, 06100 Ankara, Turkey

Traditionally, FTIR is used in order to characterize the phonon features for a material, or in the case of doped semiconductors towards the identification of the plasmon frequency that is correlated with the free carrier concentration. The aim of this work is to present an innovative process towards the mapping of the dopant concentration in a semiconductor using μ -FTIR technique.

Materials used in this study were $Mg_2Si_{1-x}Bi_x$ ($0 \leq x \leq 0.035$) hot pressed pellets. Room temperature IR measurements were performed with near normal light incidence in the range of $500-4000\text{cm}^{-1}$ using the microscope i-series Perkin Elmer, with $100\mu\text{m}$ iris, which enables FTIR mapping of the sample. Each obtained experimental reflectivity spectrum was fitted by applying the conventional Drude model.

The chemical composition of the sample was determined by EDS and SEM analyses using a Jeol 840A scanning microscope with an energy-dispersive spectrometer attached (model ISIS 300; Oxford). Room temperature Hall effect measurements were carried out using Van der Pauw configuration, with the magnetic field up to 1.2 T.

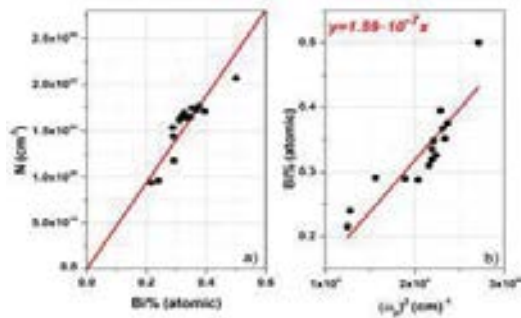


Figure 1

(a) Theoretical (line) and experimental (points) increase of the free carrier concentration (N) vs. Bi-content (b) Plasma minimum (ω_p)² as derived from the fitting of reflectivity spectra. Theoretical curve assumes that each Bi atom contributes to one free electron per unit cell in Mg_2Si .

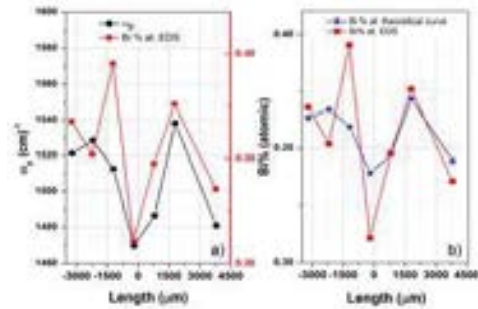


Figure 2

(a) Variation of the plasma frequency (black circles, yielded from μ -FTIR) as well as of the Bi content (red squares, by EDS in right y-axis) across the length of a sample with $x=0.35\%$ Bi. b) Bi% content variation defined through two approaches; SEM/EDS and through μ -FTIR.

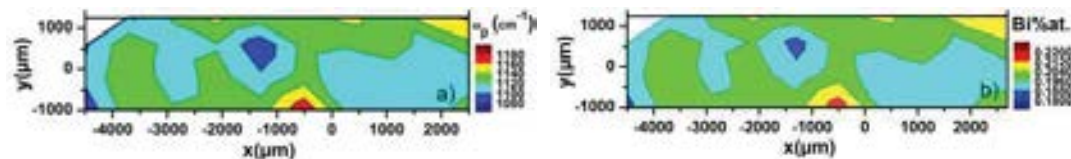


Figure 3

Contour plots of a bar-shaped sample with average Bi content 0.2% at. Left plot presents the mapping of the plasmon frequency. Right plot depicts the dopant concentration mapping.

* elste@physics.auth.gr

High Nuclearity, High Spin Clusters and Single Molecule Magnets from the Use of Diols in Mn Chemistry

A. J. Tasiopoulos* , E. E. Moushi, M. Charalambous, C. Papatriantafyllopoulou

Department of Chemistry, University of Cyprus, 1678 Nicosia, Cyprus

C. Lampropoulos, T. C. Stamatatos, G. Christou

Department of Chemistry, University of Florida, Gainesville, Florida 32611-7200, USA

Single Molecule Magnets (SMMs) represent a molecular approach to nanomagnetism [1] and have been proposed for several technological applications including high-density information storage, molecular spintronics and qubits for quantum computation. One of the most successful synthetic approaches towards new high spin molecules and SMMs involves the use of chelates containing alcohol groups, since alkoxides are good bridging groups and thus favour the formation of polynuclear products. [2] Recently, we have been investigating the use of 1,3-propanediol (H_2pd) and other diols in Mn carboxylate chemistry. [3] We will report, the synthesis, crystal structures and magnetic properties of a series of new compounds that were prepared from the use of various diols in Mn - carboxylate chemistry, including the families of Mn_{17} octahedra, $Mn_{40}M_4$ ($M = Na^+$ or Mn^{2+}) loops of loops and $Mn_{36}Ni_4$ 'loop-of-loops-and-supertetrahedra' aggregates.

References

- [1] G. Christou, D. Gatteschi, D. N. Hendrickson and R. Sessoli, *MRS Bull.* **25**, 66 (2000).
- [2] a) E. K. Brechin, *Chem. Commun.*, 5141 (2005). b) A. J. Tasiopoulos and S. P. Perlepes, *Dalton Trans.*, 5537 (2008).
- [3] a) E. E. Moushi, C. Lampropoulos, W. Wernsdorfer, V. Nastopoulos, G. Christou and A. J. Tasiopoulos, *J. Am. Chem. Soc.* **132**, 16146 (2010). b) M. Manoli, R. Inglis, M. J. Manos, V. Nastopoulos, W. Wernsdorfer, E. K. Brechin and A. J. Tasiopoulos, *Angew. Chem. Int. Ed.* **50**, 4441 (2011). c) M. Charalambous, E. E. Moushi, C. Papatriantafyllopoulou, W. Wernsdorfer, V. Nastopoulos, G. Christou and A. J. Tasiopoulos, *Chem. Commun.* **48**, 5410 (2012). d) M. Manoli, R. Inglis, M. J. Manos, G. S. Papaefstathiou, E. K. Brechin, A. J. Tasiopoulos, *Chem. Commun.* **49**, 1061 (2013).

Acknowledgements: This work was supported by University of Cyprus and Cyprus Research Promotion Foundation (ANABAΘMIΣH/ΠAΓIO/0308/12).

* atasio@ucy.ac.cy

On the possibility of photocatalytic water splitting on rutile TiO₂(110): a theoretical study

G.A. Tritsaris*, D. Vinichenko, G. Kolesov, E. Kaxiras
*School of Engineering and Applied Sciences, Harvard University,
Cambridge, MA, United States*

Solar-based hydrogen production by photocatalytic water splitting offers a route towards the delivery of clean fuel. Semiconductor metal oxides have been typically employed to mediate the photon-induced catalytic process but a comprehensive description of the elementary reaction pathways and charge-carrier dynamics is largely lacking even for the widely used TiO₂ [1]. We performed Ehrenfest molecular dynamics within the framework of time-dependent density functional theory to assess the possibility of water oxidation by photogenerated hole on rutile TiO₂. We find that molecular water adsorbed on a clean TiO₂(110) surface readily dissociates under extreme ultraviolet irradiation, and that dissociation on defect-containing surfaces could be thermally assisted under weaker excitation.

References

- [1] A. Fujishima and K. Honda, *Nature* **238**, 37 (1972).

* gtritsaris@seas.harvard.edu

Capacitive and Threaded Chain Plasmons in metallic nanoparticle strings

C. Tserkezis*, J. Aizpurua

Donostia International Physics Center and Centro de Física de Materiales CSIC-UPV/EHU, Donostia-San Sebastián, Spain

J.S. Barnard

Department of Materials Science and Metallurgy, University of Cambridge, Cambridge, U.K.

S. Kasera, O.A. Scherman

Melville Laboratory for Polymer Synthesis, Department of Chemistry, University of Cambridge, Cambridge, U.K.

L.O. Herrmann, V.K. Valev, J.J. Baumberg

Nanophotonics Centre, Cavendish Laboratory, University of Cambridge, Cambridge, U.K.

Nanophotonics is one of the most rapidly growing fields in Condensed Matter Physics nowadays. Recent advances in nanofabrication techniques have led to a large diversity of plasmonic nanostructures, which offer unique control of light-matter interactions. Here, we demonstrate an efficient way to exploit light for threading plasmonic nanoparticle strings, that is, creating chains of gold nanospheres conductively connected via gold threads with well-controlled dimensions. Gold nanosphere clusters are first self-assembled with use of appropriate rigid organic molecular linkers, namely cucurbiturils, which fix the interparticle gaps at precisely 0.9 nm. In such self-assemblies the excitation of collective plasmonic modes (called Capacitive Chain Plasmons, CCP) along linear and quasi-linear nanoparticle chains within the clusters leads to long-wavelength extinction resonances, accompanied by huge near-field enhancement at the interparticle gaps. This near-field enhancement is then exploited for threading, which is achieved by illuminating with ultrafast lasers whose wavelength coincides with that of the CCP mode, thus enabling non-thermal melting of gold at the gaps. This formation of plasmonic threads allows charge transfer within the entire nanoparticle strings, leading to the appearance of new, hybrid chain/rod modes in the infrared, Threaded Chain Plasmons (TCP). Nanoparticle size, chain length, and laser power offer unique control of the thread widths, which can be identified with a precision significantly exceeding that of electron microscopy by comparing experimental and simulated extinction spectra.

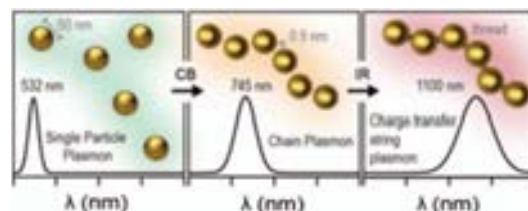


Figure 1: Schematic representation of the nanoparticle chain and string assembly, and the corresponding excitation of chain plasmons (CCP modes) and charge transfer plasmons (TCP modes), respectively

*christos_tserkezis001@ehu.es

Novel Ultra High Temperature Composites for Extreme Space Applications

G. Vekinis, G. Xanthopoulou and A. Marinou

Institute of Nanoscience and Nanotechnology, NCSR “Demokritos”, 15310, Agia Paraskevi Attikis

Space exploration requires materials with extreme properties and capabilities. Materials used in exploratory spacecraft have to display high strength and toughness at minimum mass and with very high reliability. The craft have to operate flawlessly after extended periods in vacuum, exposed to both extreme cold (close to absolute zero) and extreme heat (e.g. when close to the sun), all the while bombarded by high energy charged particles.

Among all capabilities that spacecraft sub-systems need to demonstrate, two stand out by their thermal superlatives. Firstly, an exploratory spacecraft, on its return to earth, needs to be able to withstand the extreme heat fluxes generated by friction during high speed entry into the atmosphere. Such heat fluxes can reach as much as 15MW/m^2 (at a speed of about 12km/sec) and induce a high temperature plasma in the shock wave in front of the craft. By way of comparison, the earth receives only about $300\text{-}700\text{W/m}^2$ from the sun at best. All “earth-return capsules” need to be protected by a “heat shield” (Figure 1) otherwise they would explode and/or evaporate in seconds!

Significantly, the heat fluxes though the wall of a rocket combustion chamber (Figure 2) can also reach levels approaching 10MW/m^2 and temperatures well in excess of 3000°C . Usually all rocket engines use dynamic cooling, but what if cooling is only by radiation to space?

Extreme conditions require extreme materials systems and creative solutions. What materials can we use for a heat shield? What materials can we use for a combustion chamber if we are restricted to cooling by radiation only? This brief review will introduce these two challenges and discuss the possible solutions used worldwide. In particular, some of the results obtained from the ESA (European Space Agency) project “HybridTPS” and the EC/FP7 projects “RastasSpear” (2010-2013) and “Pulcher” (2013-2015) will be presented and discussed.



Figure 1. The Heat-shield demonstrator tested and built for FP7/RastasSpear



Figure 2. A satellite rocket combustion chamber (glowing) undergoing static tests

Switching properties of a waveguide directional coupler based on quantum nanostructures with decay interference

Antonios Fountoulakis* and Emmanuel Paspalakis

Materials Science Department, University of Patras, Patras 265 04, Greece

Optical nonlinearity plays a crucial role in the switching characteristics of the two-waveguide directional coupler and leads to several interesting phenomena, such as soliton switching [1]. In a particular study, Wabnitz and co-workers [2,3] analyzed the switching properties of a nonlinear two-waveguide directional coupler where the constituent waveguides are made of a linear host material doped with two-level type resonant impurities. For the propagation of ultrashort pulses they showed that this device can work as a self-induced transparency soliton switch, with digital transmission characteristics.

Controlled propagation of electromagnetic pulses and the creation of slow light have been studied in several quantum nanostructures that exhibit decay interference [4-7]. Here, we propose a two-waveguide directional coupler where the constituent waveguides are made of a linear host material doped with a quantum system that exhibits decay interference. For the analysis of the propagation dynamics of electromagnetic pulses in the proposed device we use a modified coupled-mode theory analogous to that of reference [3]. Solving analytically, under proper approximations, and numerically the generalized coupled Maxwell-Bloch equations we show that the dynamics of the pulse propagation depends critically on the parameters of the quantum system and on the duration of the electromagnetic pulse. Loss-free propagation and slow light switching between the two waveguides are found to occur in the studied system.

References

- [1] M. Romagnoli, S. Trillo, and S. Wabnitz, *Opt. Quantum Electron* **24**, S1237 (1992).
- [2] A. Guzman, M. Romagnoli, and S. Wabnitz, *Appl. Phys. Lett.* **56**, 614 (1990).
- [3] A. Guzman, F. S. Locati, M. Romagnoli, and S. Wabnitz, *Phys. Rev. A* **46**, 1594 (1992).
- [4] E. Paspalakis, N. J. Kylstra, and P. L. Knight, *Phys. Rev. Lett.* **82**, 2079 (1999).
- [5] J. H. Wu, J. Y. Gao, J. H. Xu, L. Silvestri, M. Artoni, G. C. La Rocca, and F. Bassani, *Phys. Rev. A* **73**, 053818 (2006).
- [6] A. Fountoulakis, A. F. Terzis, and E. Paspalakis, *Phys. Rev. A* **73**, 033811 (2006).
- [7] W.-X. Yang, J.-M. Hou and R.-K. Lee, *Phys. Rev. A* **77**, 033838 (2008).

* antonisf@sch.gr

The temperature dependence of the transient photoconductivity of ZnO films

T. Georgakopoulos*, K. Pomoni

Department of Physics, University of Patras, 26500 Patras Greece

D. Karageorgopoulos, A Apostolopoulou, E. Stathatos

Department of Electrical Engineering, Technological-Educational Institute of Western Greece, 26334 Patras, Greece

ZnO is attractive for optoelectronic devices operating in the ultraviolet due to their excellent optical properties. It has a wide and direct band gap (3.37eV) and high exciton binding energy (60 meV). Persistent photoconductivity and slow photoconductive decay transients have been observed for ZnO, indicating the strong influence of trap levels. 0.183 g of Zinc chloride were dissolved in 6 ml of isopropanol (*i*-prOH) for the preparation of ZnO films. Then, poly(propylene glycol) bis(2-aminopropyl) ether oligomer was added under vigorous steering in a molar ratio [BAPPG]:[ZnCl₂]=1/5. Films on FTO glasses were formed with dip-coating from the above solution and were finally calcined up to 500°C for 45 minutes total time. The SEM image and XRD spectra are given in Figs. 1 and 2 respectively. The transient photoconductivity (σ_p) of the ZnO sample, in vacuum, is given in Figs. 3 and 4 in the temperature region 50-300 K. The sample follows the known sublinear behavior with no saturation evidence, suggesting the existence of traps within the bandgap. The increase in temperature causes the rise of σ_p as it is expected. The observed significant asymmetry between the two subsequent rises, with σ_p reaching much higher values at the end of the second illumination period, is due to the fact that some traps remained filled even at the end of the first decay period [1].

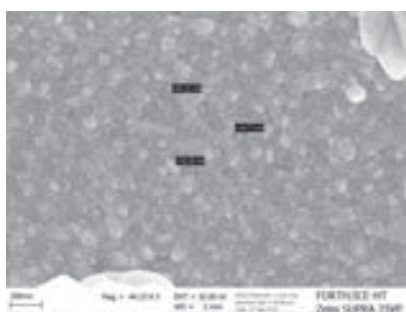


Fig. 1. Sem of ZnO film

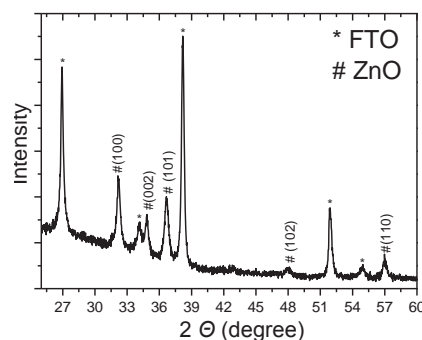


Fig. 2. XRD pattern of the ZnO film

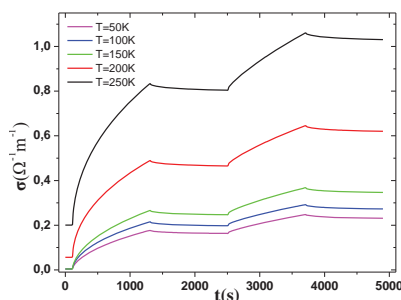


Fig. 3. The photoconductivity responses at 50, 100, 150, 200, 250 K, in vacuum

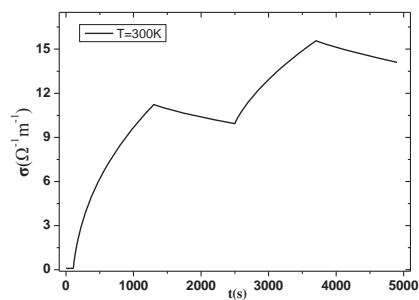


Fig. 2 The photoconductivity response at 300 K, in vacuum

References

- [1] K. Pomoni, T. Georgakopoulos, M.V. Sofianou, C. Trapalis, Journal of Alloys and Compounds 558 (2013) 1–5

* tgeorgakop@upatras.gr

Near room temperature emission from single (211)B InAs QD and clear antibunching behaviour up to 60K

S. Germanis^{1,2*}, L. Monniello³, R. Hostein³, A. Stavrinidis², G. Konstantinidis², Z. Hatzopoulos^{2,4}, V. Voliotis³, N.T. Pelekanos^{1,2}

¹*Department of Materials Science and Technology, University of Crete, Heraklion, Greece*

²*Microelectronics Research Group, IESL-FORTH, Heraklion, Greece*

³*UPMC Univ Paris 06, UMR 7588, Institut des NanoSciences de Paris, France*

⁴*Department of Physics, University of Crete, Heraklion, Greece*

We propose here a new system based on epitaxial self-assembled InAs/GaAs quantum dots (QDs), grown on a high-index (211)B GaAs substrate. This system incorporates all the well-known benefits of standard (100) InAs/GaAs QDs and in addition possesses a fascinating characteristic: the presence of a huge vertical piezoelectric (PZ) field inside the QDs, bringing in a number of significant advantages. First, the PZ field preserves the high symmetry of the confining potential, leading to negligible fine structure splitting values in this system [1], which is essential for entanglement applications. Second, it generates large exciton-biexciton splittings which allow for single photon applications at high temperatures. Towards this end, we report here temperature-dependent photoluminescence (PL) measurements on (211)B InAs single QDs, embedded inside GaAs/AlAs short-period superlattices, enhancing carrier confinement and allowing high temperature emission, as well as preliminary findings from photon anti-bunching experiments up to 60K from a PZ QD.

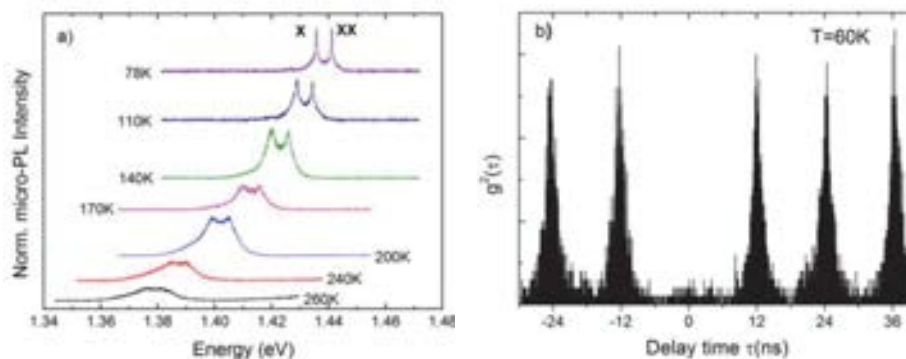


Figure 1.a): Temperature dependent μ -PL spectra from a single PZ InAs QD, embedded in GaAs/AlAs short-period superlattice, showing emission up to 260K. b): Second order correlation function $g^2(\tau)$ measured on exciton line at 60K.

As can be seen from Fig.1.a, the exciton-biexciton (X-XX) doublet with energy difference about 5.38meV from a single QD remains visible up to 260K, in spite of line broadening due to phonon and spectral diffusion effects. Arrhenius plots of PL intensities show activation energies ≥ 180 meV which correspond well to the difference between energy positions of wetting layer and QD emission. To our knowledge, this is the first time that the X and XX emission from a single InAs QD is resolved at such high temperatures. In Fig.1.b, a clear photon anti-bunching behavior from a single piezoelectric QD at 60K is depicted and we strongly feel that this preliminary result is a first step towards achieving practical single photon emitters at room temperature.

Acknowledgements: This work was supported by the European Social Fund and National resources through the THALES program "NANOPHOS".

Reference

[1] S. Germanis et al., Phys. Rev. B., 86, 035323 (2012)

* Corresponding author: germanis@materials.uoc.gr

Microcavity-enhanced emission from single (211)B InAs QDs for the generation of entangled photon pairs

S. Germanis^{1,2*}, A. Stavrinidis², G. Konstantinidis², Z. Hatzopoulos^{2,3}, N.T. Pelekanos^{1,2}

¹*Department of Materials Science and Technology, University of Crete, Heraklion, Greece*

²*Microelectronics Research Group, IESL-FORTH, Heraklion, Greece*

³*Department of Physics, University of Crete, Heraklion, Greece*

Semiconductor quantum dots (QDs) are the ultimate sources for single and entangled photon pairs “on demand”, with many applications in quantum communication and quantum computing. Towards the realisation of an efficient single QD emitter, we propose an optically pumped scheme with a piezoelectric (PZ) (211)B InAs QD, embedded in an appropriately designed GaAs/AlAs microcavity in order to improve its photonic yield. A main advantage of PZ QDs is the presence of a large PZ field, which preserves the high symmetry of the confining potential, compensates the lateral anisotropies and leads to negligible fine structure splitting (FSS) values for the majority of the as-grown QDs, a necessary condition for entanglement applications.

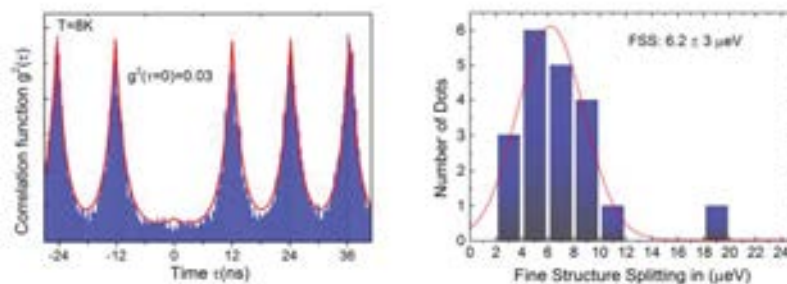


Figure 1: (*left*) Second order correlation function $g^2(\tau)$ exhibiting clear anti-bunching at zero delay time. Negligible FSS values for the majority of the as-grown PZ QDs.

The InAs QDs are grown at the center of a λ -thick GaAs microcavity, sandwiched between a top and bottom distributed Bragg reflectors, consisting of 3 and 14 $\lambda/4$ GaAs/AlAs mirror pairs respectively. The growth conditions are such that the self-assembled QDs have a density of about 10^9 cm^{-2} . Circular micro-pillars of different diameters are fabricated with e-beam lithography for μ -PL experiments. Fig.1 (left) shows clear anti-bunching behaviour in the statistics of photons emitted from a single QD exciton inside a micro-pillar. On the right hand side, are shown the inherently small exciton FSS values measured in this QD system. Such low FSS values, along with the clear single-photon emission characteristics of Fig.1, as well as the factor of 5 improvement in the photonic yield of these QDs due to microcavity effect, make the PZ InAs QDs good candidates for the implementation of highly efficient single and entangled photon sources.

Acknowledgements: This work was supported by the European Social Fund and National resources through the PROENYL research project, Action KRIPIS, project MIS-448305 funded by the General Secretariat for Research and Technology, Ministry of Education, Greece and the European Regional Development Fund (Sectoral Operational Programme: Competitiveness and Entrepreneurship, NSRF 2007-2013)/ European Commission.

* germanis@materials.uoc.gr

Study of resonant energy transfer between GaN/AlGaN quantum wells and polyfluorene

R. Jayaprakash*, F. Kalaitzakis, N. T. Pelekanos
Materials Science and Technology Department, University of Crete, and Microelectronics Research Group, IESL-FORTH, Heraklion, Greece

J. Bleuse, B. Gayral, E. Monroy
CEA-CNRS Group of Nanophysics and Semiconductors, CEA/INAC/SP2M, Grenoble, France

We seek evidence for Förster Resonance Energy Transfer (FRET) between a 200 nm-thick nitride film, containing 33 pairs of shallow GaN/AlGaN quantum wells (QW's), grown on a n+ GaN/sapphire template, and a 13 nm-thick polyfluorene layer, spun directly on top. Two types of samples, with and without polymer, are used for characterization in time-resolved and time-integrated photoluminescence (PL) experiments, at temperatures as low as 5K up to 300K. Our results show a systematic reduction, in the samples with polymer, of both the GaN QW PL intensities and decay times, which can be pursued up to room temperature. The effect could possibly be attributed to a FRET energy transfer process from the “donor” GaN QW to the “acceptor” polymer, provided that the drop of GaN QW PL intensity is met by an equal increase in the blue polymer emission. In our case, this condition is satisfied to less than 20%, clearly suggesting that the presence of the polymer layer on the surface mainly activates a, different than FRET, non-radiative carrier recombination mechanism, which induces the large reduction in QW PL intensities and lifetimes. Ongoing experiments aim at observing such resonant energy transfer effects in GaN samples where the polyfluorene molecules are chemically bound to the GaN surface.

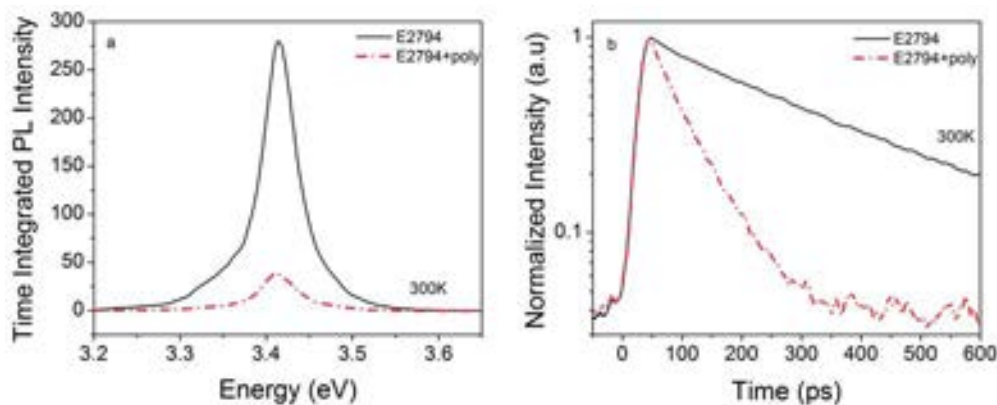


Figure 1: a) Time integrated PL and b) Time resolved PL of GaN/AlGaN QWs, with and without polymer

This work is supported by the European Social Fund and National resources through the THALES program “NANOPHOS” and the ARISTEIA II program “NILES”.

* rahul.jp@materials.uoc.gr

Effect of Rapid Thermal Annealing on Polycrystalline InGaN Deposited on Fused Silica Substrates

S. A. Kazazis¹, E. Papadomanolaki¹, M. Androulidaki², K. Tsagaraki²,
A. Kostopoulos², E. Aperathitis² and E. Iliopoulos^{1,2}

¹ Physics Department, University of Crete, Heraklion, Greece

² Micro/Nano-Electronics Research Group, IESL_FORTH, Heraklion, Greece

InGaN alloys are very promising candidates for efficient photovoltaic applications, since their engineered bandgap can cover the entire Air-Mass 1.5 solar spectrum. Deposition of amorphous-polycrystalline alloy films is potentially very interesting for low cost, large area solar cells deployment.

In this work we report on rapid thermal annealing (RTA) studies of polycrystalline InGaN films deposited on amorphous fused silica substrates. The films were grown at low substrates temperatures (200 °C) by exposure of the substrates to indium and gallium beams under radiofrequency nitrogen plasma. Films with compositions in the range of 20% to 50% indium content were obtained. In order to study the annealing effects, the films were subsequently subjected to consecutive RTA treatments, under N₂ ambient for 10 mins. Annealing temperatures spanned the range from 400 to 900 °C. X-ray diffraction (XRD), atomic force microscopy (AFM), photoluminescence (PL), Hall effect measurements and energy dispersive x-ray spectroscopy (EDXS) were utilized to characterize films properties. The optical properties of the films were systematically studied, employing variable angle spectroscopic ellipsometry (VASE).

As deposited films were polycrystalline and showed a preferential (0002) orientation. Annealing promoted crystallization, resulting in an increase in the grain size of the original crystallites, which was more evident in the high indium mole fraction films. Also, in this case, a phase separation was observed above 850 °C. Upon annealing, films' resistivity reduced by at least two orders of magnitude and PL intensity was enhanced. In the high indium content films, a monotonic bandgap increase at temperatures greater than 500 °C was found utilizing VASE. This bandgap increment can be attributed to the Urbach tails reduction due to the disorder lowering and to the Burstein-Moss shift due to the higher electron concentration, upon increasing temperature.

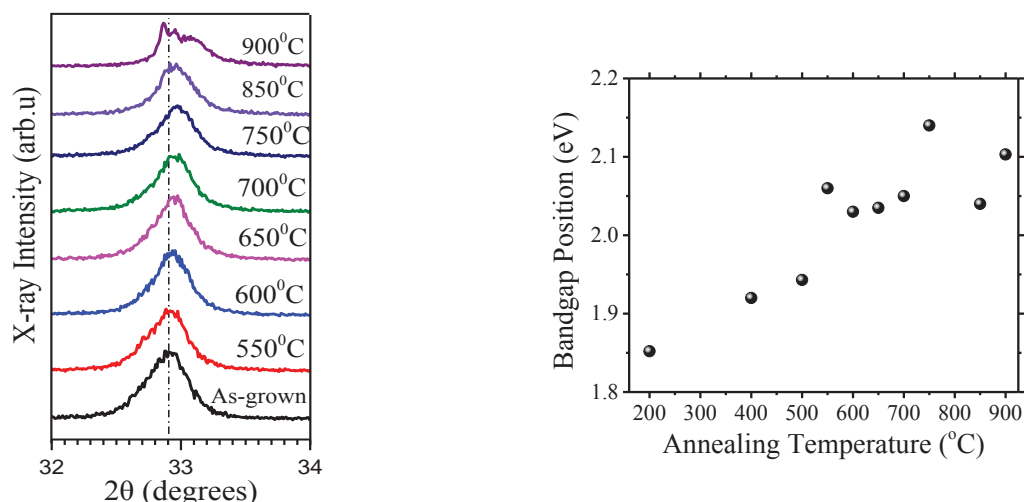


Fig.1. XRD of polycrystalline InGaN film on FS with 50% In composition, after RTA at different temperatures and the corresponding evolution of bandgap position as measured by VASE.

Acknowledgement: This research has been co-financed by the European Union (European Social Fund– ESF) and the Greek national funds through the Operational Program “Education and Lifelong Learning” of the National Strategic Reference Framework (NSRF) – Research Funding Program: THALES.

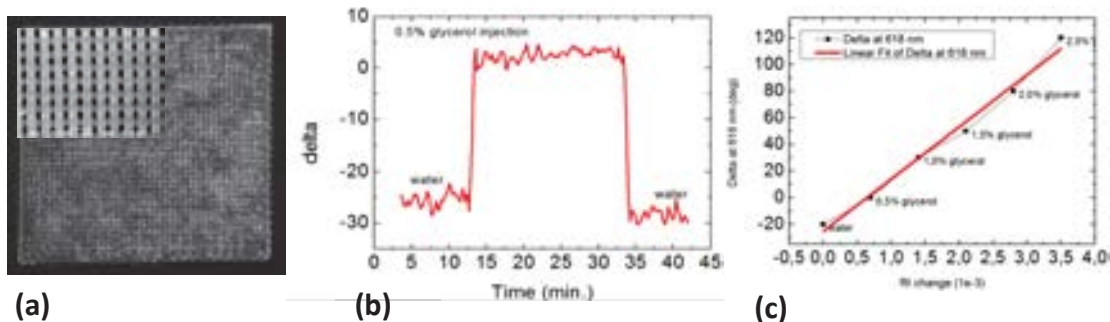
3D Photonic Crystal structures for Sensing Applications

Maria Manousidaki^{1,*}, Andrey Aristov², Maria Farsari¹, Andrei Kabashin²

¹IESL – FORTH, N.Plastira 100, 70013, Heraklion Crete, Greece

²Laboratoire Lasers, Plasmas et Procédés Photoniques (LP3 UMR 7341 CNRS), Aix-Marseille University, Campus de Luminy, Case 917, 13288 Marseille, France

We present our research which focuses on the fabrication of 3D metallic Photonic Crystal (PhC) structures using Direct Laser Writing, for sensing applications. When a fs infrared laser is tightly focused into the volume of a photosensitive resin (which is transparent in the infrared), the laser pulses can cause multi-photon polymerization (MPP) and produce structures with sub-100nm resolution. We have made dielectric 3D nanostructures using a metal-binding organic-inorganic hybrid material. The PhC structure had the woodpile geometry with 700nm interlayer periodicity [1]. These structures were selectively covered with silver (Ag) using electroless plating [2,3]. The resulting metallic photonic nanostructure was applied as a phase-sensitive plasmonic biosensor, exhibiting sensitivity of 5×10^4 deg. of phase shift per refractive index unit (RIU). The optical properties were examined with the use of a Woollam M-2000 ellipsometer, which is based on measurements of phase-polarization properties of light reflected from the PhC structure, and sensing results were noticed.



Figures: (a) SEM image of the 3D PhC structure with 700nm interlayer periodicity; (b) Delta reflection data for the woodpile structure: response of phase Δ under the addition of 0.5% glycerine in water solution; (c) Delta as a function of the refractive index of the medium, as conditioned by different concentrations of glycerine: the resonant position linearly shifts under a relatively wide range of refractive index variations, measured sensitivity of 5×10^4 deg. of phase shift per refractive index unit (RIU).

References:

[1] Gabija Bickauskaite, **Maria Manousidaki**, Konstantina Terzaki, Elmina Kambouraki, Ioanna Sakellari, Nikos Vasilantonakis, David Gray, Costas M. Soukoulis, Costas Fotakis, Maria Vamvakaki, Maria Kafesaki, Maria Farsari, Alexander Pikulin, and Nikita Bityurin, *Advances in OptoElectronics*, Volume, (2012), Article ID 9279312012 doi:10.1155/2012/927931.

[2] Nikos Vasilantonakis, Konstantina Terzaki, Ioanna Sakellari, Vytautas Purlys, David Gray, Costas M. Soukoulis, Maria Vamvakaki, Maria Kafesaki, and Maria Farsari, *Adv.Mater.*, 24, 1101(2012)

[3] Konstantina Terzaki, Nikos Vasilantonakis, Arune Gaidukeviciute, Carsten Reinhardt, Costas Fotakis, 1,3 Maria Vamvakaki, and Maria Farsari, *Optical material express*, August (2011) / Vol. 1, No. 4

*marymanou@iesl.forth.gr

Spontaneous emission modification in photonic structures

Ch. P. Mavidis^{1,2,*}, M. Kafesaki^{1,2}, E. N. Economou^{1,3}, C. M. Soukoulis^{1,4}

¹*Institute of Electronic Structure and Laser, FORTH, 71110 Heraklion, Crete, Greece*

²*Department of Materials Science and Technology, University of Crete, 71003 Heraklion, Crete, Greece*

³*Department of Physics, University of Crete, 71003 Heraklion, Crete, Greece*

⁴*Ames Laboratory and Department of Physics and Astronomy, Iowa State University, Ames, Iowa 50011, USA*

Photonic structures, such as photonic crystals and metamaterials, have the potential to tailor the spontaneous emission rate [1-2] of emitters embedded into them or placed in their vicinity, due to modified density of electromagnetic modes that they offer. This can have great impact on the performance photonic devices such as antennas, light sources and quantum information processing platforms.

In this work we examine the modified emission rate in different photonic crystal and metamaterial structures. For each system, rates are calculated numerically as a function of frequency for different emitter orientations, locations and system sizes, by employing the Finite Difference Time Domain Method (FDTD) and the Boundary Element Method (BEM).

Depending on the specific geometry and the material composition of the structures, large inhibition or enhancement (compared to free space) of the emission rate is observed in most of the systems analyzed,

References

[1] E. Yablonovich, Phys. Rev. Lett, **58**, 2059 (1987)

[2] S. John, Phys. Rev. Lett. **58**, 2486, (1987)

* mavidis@iesl.forth.gr

Study of sputtered NiO and NiAl₂O₄ spinel thin films deposited in oxygen deficient plasma

G. Michail* ⁽¹⁾, V. Kambylafka ⁽¹⁾ E.Aperathitis ⁽¹⁾, K. Tsagaraki ⁽¹⁾

(1) IESL, FORTH Hellas, P.O. Box 1385, Heraklion 70013, Crete, Greece

G. Kiriakidis ⁽²⁾ and Gagaoudakis ⁽²⁾

(2) Physics Dep., Univ.of Crete, P.O. Box 2208, 71003 Heraklion, Crete, Greece.

N. Pelekanos ⁽³⁾

(3) Materials science & Technology Department, University of Crete, P.O. Box 2208, 71003 Heraklion, Crete, Greece.

Nickel oxide (NiO) is an attractive material for use as an antiferromagnetic layer, p-type transparent conductive film, as an active electrode in electrochromic devices and as a functional sensing layer for gas sensor devices. NiO exhibits p-type semiconducting nature with wide band gap energy in the range of 3.5–4.0eV. Stoichiometric NiO is an insulator but Ni vacancies, interstitial oxygen atoms and Ni ions with different valences can modify its electrical and optical properties. Li, Al and Cu have been reported recently as possible dopants in NiO which might enhance its properties.

In this work, NiO and Ni–Al–O thin films were prepared by R.F. sputtering from metallic Ni and Ni–Al targets, in Ar+O₂ atmosphere. The RF power was 300W while the total pressure was 5mTorr. The structural, surface morphology and optical properties of thin films were studied by XRD, AFM, SEM, EDX and UV–NIR transmittance respectively. All measurements were performed on as-prepared films as well as after annealing in vacuum from 200°C to 600 °C.

NiO thin films were indicated as polycrystalline having the (200) preferred orientation, grain size about 4nm and the RMS roughness was 1.64nm. The highest visible transmittance (20–35%) was observed for as-deposited film in 2.8% O₂ in plasma with optical band gap at 3.64eV. The surface morphology was compact and homogeneous. After annealing at 500 °C the transmittance increased to 75% for the films with 2.8%O₂ in plasma.

Films deposited from Ni–Al composite target showed a completely different structure than that of NiO, with diffraction peak of XRD corresponding to the (311) peak of NiAl₂O₄ spinel phase. EDX confirmed the existence of Al in the structure (4,5 at.%). The RMS roughness was 2.87nm with compact and smooth surface morphology. Only the films deposited in plasma containing 2.8% O₂ showed high visible transmittance at 45–60%, with optical band gap at 3.76eV. As-deposited NiAl₂O₄ spinel films in 2.8% oxygen plasma were 20–25% more transparent than the respective NiO film. In addition, the transmittance of NiAl₂O₄ increased even more after annealing at 600 °C recording an average value of 75–80% in visible spectrum.

This work was partially supported by the European Social Fund and National Resources Fund through the THALES program “NANOPHOS” and the FP7/2007–2013 project “Oxide Materials Towards a Matured Post–silicon Electronics Era –ORAMA” (contract no. NMP3–LA–2010–246334).

Optical properties of core-shell GaAs-AlGaAs nanowires on silicon

K. Moratis^{1*}, K. Tsagaraki², Z. Hatzopoulos^{2,3}, J. Bleuse⁴, F. Donatini⁵, N. T. Pelekanos^{1,2}

¹Department of Materials Science and Technology, University of Crete, P.O. Box 2208, 71003 Heraklion, Greece.

²Microelectronics Research Group, IESL-FORTH P.O. Box 1385, 71110 Heraklion, Greece.

³Department of Physics, University of Crete, P.O. Box 2208, 71003 Heraklion, Greece

⁴CEA-CNRS Group of Nanophysics and Semiconductors, CEA/INAC/SP2M, Grenoble, France

⁵CNRS, Inst. NEEL, F-38042 Grenoble, France

During the last years, core-shell nanowires based on III-As compounds are extensively studied due to their enhanced optoelectronic properties. GaAs nanowires (NWs) are prominent candidates for novel devices due to their one-dimensional geometry, the ability to form radial or axial heterostructures, whilst they are characterized by unique waveguiding effects and increased absorption compared to their bulk counterparts. Nevertheless their efficiency is directly affected by the poor quality native oxide present at the NW surface and the increased number of traps. In order to avoid the aforementioned factors which deteriorate the NW optoelectronic properties, an AlGaAs shell is grown around them, acting as an efficient passivation layer, increasing drastically the PL yield and carrier lifetimes. In addition, the AlGaAs shell induces significant piezoelectric fields, improving the electron hole separation, and thus reducing recombination losses, which is a key factor for high efficiency solar cell devices. In this work we investigate the optical properties of core-shell GaAs-AlGaAs nanowires grown on n⁺ Si(111) substrates. The samples are grown by molecular beam epitaxy via the Ga-assisted Vapor-Liquid-Solid (VLS) mechanism. In order to achieve the core-shell architecture, we follow a two-stage growth, where initially the GaAs core is grown, subsequently the Ga droplet is removed and finally an Al_{0.3}Ga_{0.7}As shell is deposited around the NW following the nominal conditions for a 2D growth. The diameter of the GaAs core is approximately 75nm, while the overall NW diameter ranges from 150nm-280nm, depending on the 2D growth time. Here, we report on a combination of experimental methods applied to these NWs such as photoluminescence (PL) (Fig. 2), time-resolved PL, μ PL, cathodoluminescence (CL) (Fig. 1), which allowed us to demonstrate the high optical quality of these nanostructures.



Figure 1: CL measurements in a single NW depicting the emission from different regions.

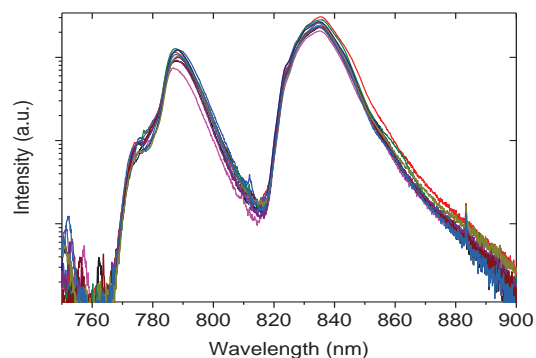


Figure 2: PL spectra at T=15K

Acknowledgments: This work was supported by the European Social Fund and National resources through the THALES program “NANOPHOS”.

*moratisk@materials.uoc.gr

Optical power limiting of laser radiations by carbon nanostructures

I. Papagiannouli*, P. Aloukos, S. Couris

Department of Physics, University of Patras, 26504 Patras, Greece & Institute of Chemical Engineering Sciences (ICE-HT), Foundation for Research and Technology, Hellas, 26504 Patras, Greece

In recent years considerable efforts have been put in understanding the nonlinear optical response of various materials in order to realize photonic devices of practical use. [1-3] In that view, achieving a deeper insight into the physical mechanisms from which nonlinearities of materials arise is an essential step in order to optimize the required performance. On the other hand, with the increasing use of lasers in daily life there is an increased concern of protecting both the human eyes and/or optical sensors/detectors against laser induced damage. To address this issue continuous efforts are being made, focusing on the synthesis and characterization of new optical limiting materials, with increased sensitivity and capacity to cover broadband optical radiations, ranging from UV to IR wavelengths. Among the various investigated materials suitable for optical limiting applications, nanocrystalline diamonds and carbon dots are considered as important candidates. The former having been developed very recently, can be easily synthesized in a variety of shapes and dimensions while their surface functionalization allows the attachment of different organic, inorganic, polymeric and biological species, imparting them with high water solubility, ionic character and a lot of other attractive properties. [4-7] The latter nanostructures, have also attracted considerable attention as promising materials for many applications including optoelectronics, all-optical switching and optical limiting. [7-9] However, their NLO response has not been investigated in details. Herein, in this study, the optical limiting properties of some crystalline NDs and amorphous CDs have been investigated and the results are discussed and compared with other past studies.

References

- [1] A. B. Bourlinos *et al.*, Carbon **61**, 640 (2013).
- [2] E. Koudoumas *et al.*, Chem. Phys. Lett. **357**, 336 (2002)
- [3] V. Vanyukov *et al.*, Appl. Opt. **52**, 4123 (2013).
- [4] S. N. Baker *et al.*, Angew. Chem. Int. Ed. **49**, 6726 (2010).
- [5] A. B. Bourlinos *et al.*, Chem. Mater. **20**, 4539 (2008).
- [6] A. B. Bourlinos *et al.*, Small **4**, 455 (2008).
- [7] J. C. G. Esteves da Silva, **30**, 1327 (2011).
- [8] V. Yu Dolmatov Russ. Chem. Soc. **76**, 339 (2007).
- [9] M. Kozak *et al.*, Physica E **44**, 1300 (2012). -

* epapag@iceht.forth.gr

The authors acknowledge financial support by the European Union (European Social Fund-ESF) and Greek national funds through the Operational Program "Education and Lifelong Learning" of the National Strategic Reference Framework (NSRF)-Research Funding Programs: THALIS (ISEPUMA): Investing in knowledge society through the European Social Fund. D. Potamianos and E. Kakkava are acknowledged for their assistance.

Laser printing and laser reduction of graphene oxide

S. Papazoglou¹, Y.S.Raptis¹, I. Zergioti^{1*}

¹*National Technical University of Athens, Physics Department, Iroon Polytehneiou 9, 15780 Zografou, Athens, Greece*

V. Tsouti², S. Chatzandroulis²

²*Institute of Microelectronics, NCSR Demokritos, Athens, Greece*

In this work, we present our recent results on the laser printing, using the Laser Induced Forward Technique, and the irradiation-mediated reduction of graphene oxide, exploiting the restoration of the sp^2 hybridized graphitic network, for the fabrication of resistive chemical sensors. Printing and reduction experiments were carried out using a pulsed ns Nd:YAG laser along with a high-power mask projection micromachining setup. A dedicated CCD camera was coupled with the optical setup, to monitor the deposition and reduction processes.

In general, three approaches (chemical, thermal and irradiation) have been used for the removal of the functional oxygenous groups from the hydrophilic graphene oxide basal plane, in order to obtain its reduced form [1], [2]. The restoration of the electrical conductivity can therefore be exploited in resistive chemical sensors. In this framework, we investigated the laser-assisted reduction of graphene oxide, using a pulsed laser (266 nm), so as to investigate the effect of pulse number and laser fluence on the reduction yield. Moreover, the laser printing conditions were also investigated, in terms of the fluence threshold for succesful deposition and the distance between the donor and receiver substrates, aiming to achieve the transfer of well-defined graphene oxide droplets, with homogeneous and reproducible flake dispersion.

The morphology of the deposited graphene oxide droplets has been characterized by optical microscopy, while the laser reduced graphene oxide structural and electrical properties, have been studied by means of optical microscopy, Raman spectroscopy and electrical measurements.

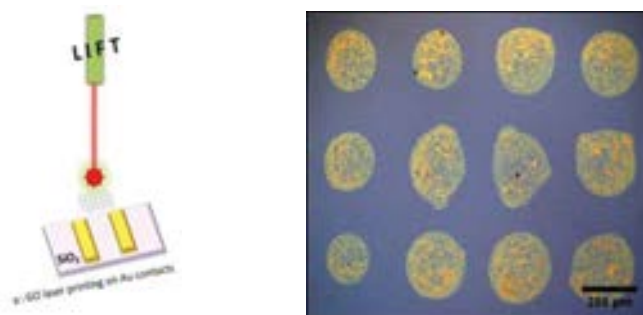


Figure 1: Schematic representation of GO printing on Au contacts (left) and laser printed GO droplets on SiO₂ (right)

References

- [1] S. Pei et al., The reduction of graphene oxide, *Carbon* **50**, pp. 3210-3228, 2012.
- [2] Emmanuel Kymakis et al., Flexible Organic Photovoltaic Cells with In Situ Nonthermal Photoreduction of Spin-Coated Graphene Oxide Electrodes, *Advanced Functional Materials*, 2013.

* zergioti@central.ntua.gr

Beam shaping and manipulation in photonic crystal structures

Anna C. Tasolamprou^{1*}, Maria Kafesaki^{1,2}

¹*Institute of Electronic Structure and Laser,
FORTH, 71110, Heraklion, Crete, Greece*

²*Department of Materials Science and Technology,
University of Crete, 71003, Heraklion, Crete, Greece*

Lei Zhang³, Thomas Koschny³, Costas M. Soukoulis^{1,3}

³*Ames Laboratory and Department of Physics and Astronomy,
Iowa State University, Ames, Iowa 50011, USA*

Photonic crystals (PCs) are well known materials mostly due to their band gap properties. Additionally it has been shown, both theoretically and experimentally, that PCs support the propagation of surface waves, provided that they are properly terminated. This termination consists of a corrugated outer periodic layer which may differ in shape and/or lattice constant from the bulk material. Introducing a line defect acting as a waveguide in a bulk photonic crystal structure and properly designing the corrugated layer enables the excitation of the surface states within the band gap. The surface layer alone leads to reduced transmission efficiency along the waveguide axis; nevertheless an additional grating like layer may facilitate the coupling of the surface waves to outgoing propagating waves [1]. The surface energy radiation results in enhanced transmission and directionality of the beam. The key feature of this configuration is the grating layer which under specific conditions, leads to constructive interference of the diffracted waves and beaming. This work investigates and demonstrates how the proper design of the grating layer allows for selective interference and provides control over the beam shape and emission angle. Apart from the PCs, it has been discovered that even a single dielectric layer can support surface states, whereas a surface and grating bilayer may couple the surface states to outgoing propagating waves. Here we also demonstrate both experimentally and theoretically, that such a bilayer dielectric structure allows for the collimation and enhanced transmission of a Gaussian incident beam, while a system of multiple cascading bilayers can sustain the beam for large propagation distances.

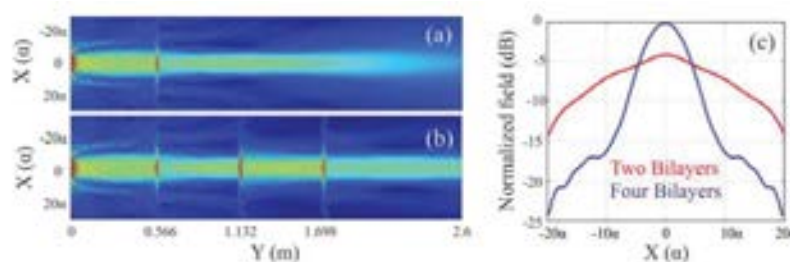


Figure 1: Field strength of (a) two bilayer and (b) four bilayer structure. (c) x cross section field distribution for two and four bilayers at a propagation distance of 100λ .

References [1]

R. Moussa, B. Wang, G. Tuttle, T. Koschny, and C. M. Soukoulis, "Effect of beaming and enhanced transmission in photonic crystals", *Phys. Rev. B* **76**, 235417 (2007).

* atasolam@iesl.forth.gr

Three-dimensional photonic crystals and metamaterials made by direct laser writing

Aggelos Xomalis^{1,2*}, G. Kenanakis¹, A. Selimis¹, M. Kafesaki^{1,2}, M. Farsari¹

¹*Institute of Electronic Structure and Laser, Foundation for Research and Technology Hellas, 71110 Heraklion, Crete, Greece*

²*Department of Materials Science and Technology, University of Crete, 71003 Heraklion, Crete, Greece*

In this work we design and fabricate three-dimensional (3D) metallic photonic crystals and metamaterials operating in the THz region (see Fig. 1) and targeting asymmetric wave transmission and circular polarization filtering. The design and theoretical analysis of the structures is done using commercial software based on the finite element method. The fabrication is done by Direct femtosecond Laser Writing (DLW) of an organic-inorganic polymer with metal-binding moieties and selective silver coating using electroless plating. [1]. The DLW by multi-photon polymerization which is used here is a nonlinear optical technique which allows the fabrication of 3D structures with a resolution beyond the diffraction limit. The resolution of our structures is of the order of 100nm.

Theoretical analysis and preliminary electromagnetic characterization of some of our fabricated structures shows significantly large asymmetric transmission (diode-like response), which can have great impact in polarization isolation applications.

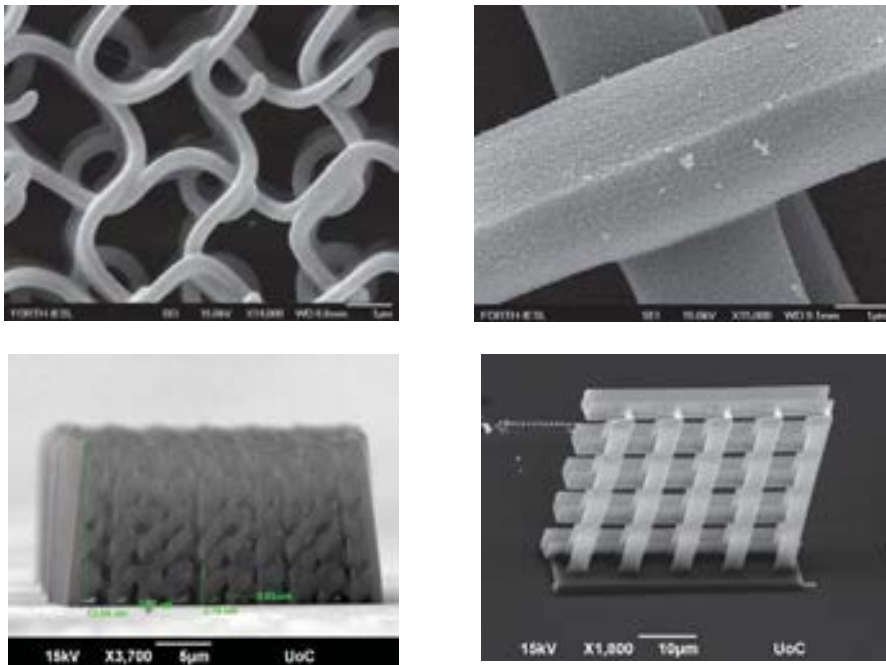


Figure 1: SEM pictures of the structures with the silver parts at the surface of the polymer material.

References

[1] Three-dimensional metallic photonic crystals with optical bandgaps, N. Vasilantonakis et al., *Advanced Materials* 24 (8), 1101-1105

* aggelos@iesl.forth.gr

Application of the equation of motion method for the determination of the EXAFS Debye-Waller factors

M. Katsikini*, F. Pinakidou, E. C. Paloura, J. Arvanitidis, S. Ves
 Aristotle University of Thessaloniki, School of Physics, 54124 Thessaloniki

A. Georgakilas

Department of Physics, University of Crete & IESL, FORTH, 71110 Heraklion

One of the puzzling parameters in the analysis of EXAFS spectra is the Debye-Waller factor (DWF) that accounts for the static and thermal disorder. In hexagonal semiconductors, e.g. GaN, the epitaxial growth of thin films as well as growth along non-polar orientations, result in strain-induced distortions of the nearest neighbor distances. The reliability and accuracy of the assessment of such distortions is increased drastically if the DWFs can be estimated independently by an appropriate method. Here we use the equation of motion (EM) subroutine of the FEFF8 package to calculate the DWFs and then to simulate the Ga-K-edge EXAFS spectra of GaN epilayers. The parameters used were the a and c lattice constants, as determined by XRD. The best values for the stretching force constants for the Ga-N, N-N and Ga-Ga interactions were found equal to 115, 38 and 23 N/m, respectively. These values reproduce very satisfactorily the Raman vibrational density of states (VDOS) as shown in Fig. 1. We point out that the Raman spectrum of the ion-implanted GaN is analogous to the VDOS due to relaxation of the selection rules. The contribution to the VDOS of the particular photoelectron scattering paths, depicted in the inset, is shown in the bottom panel of Fig.1. In Fig. 2 the experimental EXAFS spectra of an a -plane sample recorded at near-normal and near-grazing incidence are plotted along with the simulations in the k - and R -space.

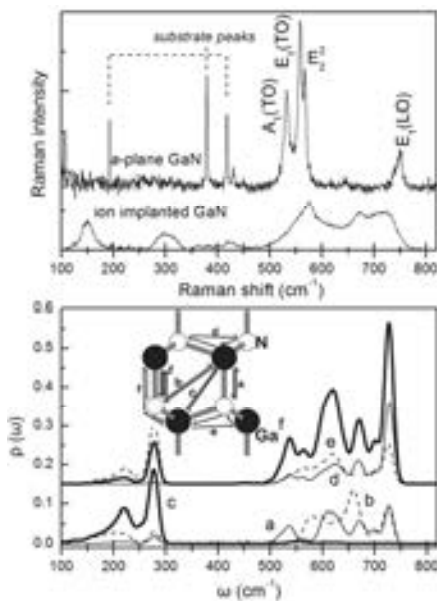


Figure 1: (top) Raman spectra of a crystalline- (a -plane) and a highly defective - (ion-implanted) GaN sample (bottom) Vibrational density of states of single (a,b,c), double (e,d) and triple (f) scattering paths indicated in the inset.

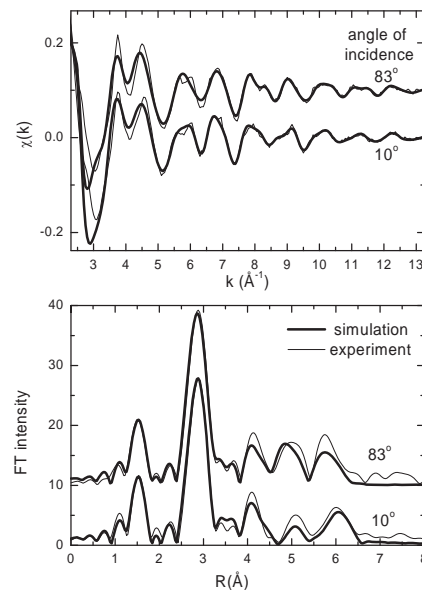


Figure 2: (top) $\chi(k)$ and (bottom) Fourier Transform amplitude of Ga-K-edge EXAFS spectra of an a -plane GaN sample for near-normal (83°) and near-grazing (10°) incidence. The c -axis was lying on the polarization plane of the synchrotron beam.

Acknowledgement: This research has been co-financed by the European Union (European Social Fund - ESF) and Greek national funds through the Operational Program "Education and Lifelong Learning" of the National Strategic Reference Framework (NSRF) - Research Funding Program: ARCHIMEDES III. Investing in knowledge society through the European Social Fund.

* katsiki@auth.gr

Study of plastic deformation and fracture of polar and nonpolar GaN single crystals: A multiscale approach

P. Kavouras*, G.P. Dimitrakopoulos, Th. Kehagias, Ph. Komninou
 Department of Physics, Aristotle University of Thessaloniki, 54 124 Thessaloniki,
 Greece

I. Ratschinski, H.S. Leipner
 Interdisziplinäres Zentrum für Materialwissenschaften, Martin-Luther-Universität
 Halle-Wittenberg, 06099 Halle, Germany

G. Leibiger, F. Habel
 Freiburger Compound Materials GmbH, 09599 Freiberg, Germany

Quasi-static nano-indentation and static micro-indentation techniques were utilized to induce localized deformation on polar *c*-plane (0001) and nonpolar *m*-plane ($\bar{1}010$) surfaces of GaN single crystals. Both samples were studied for two orientations of Berkovich and Vickers indenter tips, in order to study the effect of crystal anisotropy on the plastic and elastic behaviour. It was found that fracture behaviour is more sensitive to the orientation of the indenter tip, compared to plastic behaviour. The indentation-induced plastic deformation was studied by cathodoluminescence imaging (Figure 1, left). Polar GaN was harder than *m*-plane GaN at the nano-scale, while marginally harder at the micro-scale. Pop-in discontinuities were narrower at *c*-plane than *m*-plane GaN (Figure 1, right), following an analogous behaviour compared to polar and nonpolar GaN thin films [1]. Dislocation arrangements were more isotropic at the *c*-plane than the nonpolar *m*-plane orientation, since dislocations propagate along the basal plane alone, at both cases. Polar GaN was more susceptible to crack initiation compared to *m*-plane, when indented with a Vickers indenter. Nano-indentation did not produce cracking at both samples and indenter orientations. Micro-indentation fostered radial and lateral crack formation at both indenter orientations at polar GaN. Lateral cracks did not reach the surface, i.e. they did not produce surface flaking as in the case of heavily damaged GaN thin films [2].

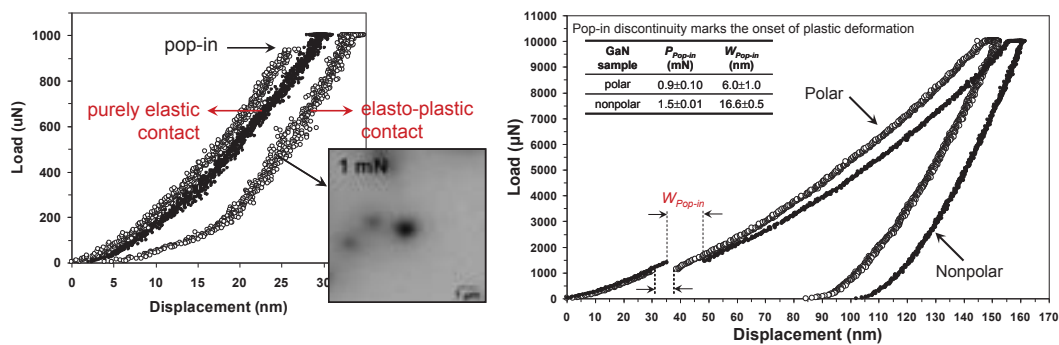


Figure 1: (Left) Load-displacement curves for polar GaN sample at 0° tip orientation for maximum load of 10^{-3} N. Solid circles correspond to purely elastic contact. Open circles correspond to elastoplastic contact. The inset contains the indentation print left by the elasto-plastic indentation as recorded by CL imaging. (Right) Load-displacement curves for polar and nonpolar GaN samples at 0° tip orientation for maximum load of 10^{-2} N.

References

- [1] Kavouras *et al.*, Phys. Stat. Sol. A **210**, 213 (2013).
 [2] Kavouras *et al.*, Thin Solid Films **515**, 3011 (2007).

* pkavo@physics.auth.gr

Strain accommodation in InGaN epilayers and interlayers with high alloy content towards efficient photovoltaics

Th. Kehagias, C. Bazioti, G. P. Dimitrakopoulos

Physics Department, Aristotle University of Thessaloniki, 54124 Thessaloniki, Greece

Th. Walther

Department of Electronic & Electrical Engineering, University of Sheffield, Sheffield S1 3JD, UK

E. Papadomanolaki, E. Iliopoulos

Microelectronics Research Group, Physics Department, University of Crete, P.O. Box 2208, 71003 Heraklion-Crete, Greece, and, IESL, FORTH, P.O. Box 1385, 71110 Heraklion-Crete

High alloy content InGaN thin films are promising for high efficiency photovoltaics. To this end, it is required to elucidate the mechanisms of strain relaxation through defect introduction in conjunction to the indium content and phase separation phenomena. A systematic study was performed using samples deposited by plasma-assisted molecular beam epitaxy (PAMBE) which is a technique that can take advantage of metastability due to the lower growth temperatures. The change of growth temperature was employed in order to vary the indium content and observe the pertinent chemical and structural phenomena by transmission electron microscopy (TEM) techniques. We considered (0001) interlayers and epilayers of thicknesses starting from 1 nm and up to ~500 nm, and a 10-60% alloy content. The films were characterized using TEM, quantitative high resolution TEM (qHRTEM), scanning TEM (STEM) and energy dispersive x-ray spectroscopy (EDXS). In thin films, we observed that with decreasing growth temperature, distinct mechanisms of strain relaxation become dominant with a concurrent increase of the indium content. At high growth temperature, strain relaxation is accommodated by the opening up of V-defects connected to screw or mixed-type threading dislocations that continue from the GaN template. This mechanism is superseded by the so-called sequestration mechanism that comprised the self-formation of a strained buffer-like InGaN layer between the GaN template and the main film. Such a region is gradually suppressed with further lowering the growth temperature. In addition to epilayers, InGaN interlayers of increasing thickness were deposited in order to assess early stage phenomena such as material interdiffusion, interfacial roughening and introduction of extended defects (Fig. 1). Indium incorporation efficiency was found to increase with interlayer thickness up to a critical thickness of ~5 nm and a ~40% content, whereby the onset of gradual plastic relaxation was determined. On the other hand, the elastic thinner layers exhibited strain fluctuations attributed to alloy inhomogeneities.

Acknowledgement Research co-financed by the EU (ESF) and Greek national funds - Research Funding Program: THALES, project NITPHOTO.

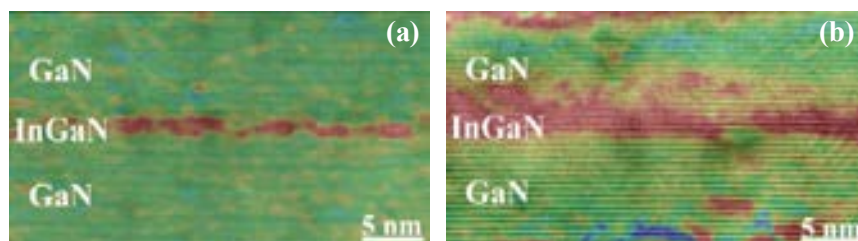


Figure 1: HRTEM images of InGaN interlayers with superimposed strain maps depicting the relative variation of the d -spacing of (0002) planes. (a) A nominally 1 nm thick layer with strain fluctuations. (b) A partially relaxed layer of nominally 5 nm thickness with strain grading at the InGaN/GaN interface.

Reordering of Cr atoms during proton irradiation in a Fe-5 at.% Cr alloy

Z. Kotsina,* G. Apostolopoulos, K. Mergia, S. Messoloras
I.N.Ra.S.T.E.S., National Centre for Scientific Research "Demokritos"

A. Lagoyannis, S. Harissopoulos
I.N.P.P., National Centre for Scientific Research "Demokritos"

The Fe-Cr alloy system is the base of ferritic/martensitic steels with a Cr concentration up to 15 at.%. Because of their low activation, resistance to radiation damage accumulation and good mechanical properties, Fe-Cr alloys are considered as prime candidates for the internal structure of future Fusion Power Plants. However, the behaviour and the evolution of their microstructure under irradiation is not yet fully understood. One of the greatest obstacles in understanding both thermodynamic and kinetic properties of Fe-Cr under irradiation is the uncertainty relating to the low temperature equilibrium state ($T < 700$ K). Currently the low temperature part of the Fe-Cr phase diagram is derived only from high-temperature experiments.

In an effort to elucidate the existence of solute ordering effects during irradiation, which may affect phase stability and microstructure evolution, proton irradiations were performed at the NCSR "Demokritos" 10MV TANDEM accelerator at a temperature of 400 K. It was shown that atomic migration is still possible even at such a low temperature, enabled by the energy imparted to the lattice atoms during collisions with the irradiating particles. The radiation-enhanced diffusion constant associated with this effect has been estimated by performing experiments at different proton fluxes. Irradiation induced modifications were detected by means of in-situ measurements of the electrical resistivity, which is sensitive to solute ordering in alloys. It was found that significant re-ordering of Cr atoms takes place during irradiation of Fe-5 at.% Cr alloys, leading to enhanced short-range order.

*kotsina@ipta.demokritos.gr

Non-linear Dynamics in Small World and Scale Free Networks

K.A. Skoufaris^{*a}, G.P. Tsironis^{bc}

^aUniversity of Crete, Materials Science and Technology Department.

^bUniversity of Crete Physics Department and FORTH, P. O. Box 2208, Heraklion 70113, Greece.

^cCrete Center for Quantum Complexity and Nanotechnology.

Wave propagation, self-trapping and transport properties in non-linear complex networks [1] are investigated. The structure complexity is introduced by the use of Small World [2] and Scale Free networks [3]; these two types of networks can be found quite often and in very different scientific areas. In that framework, I will present a non-linear dynamical study which incorporates the competition of bond and on site energy disorder, long range interaction and non-linearity for wave propagation. The Discrete Non-linear Schrödinger (DNLS) equation is used for this studies as it is a prototypical equation with a large number of applications in condensed matter physics, optics, etc. [4]

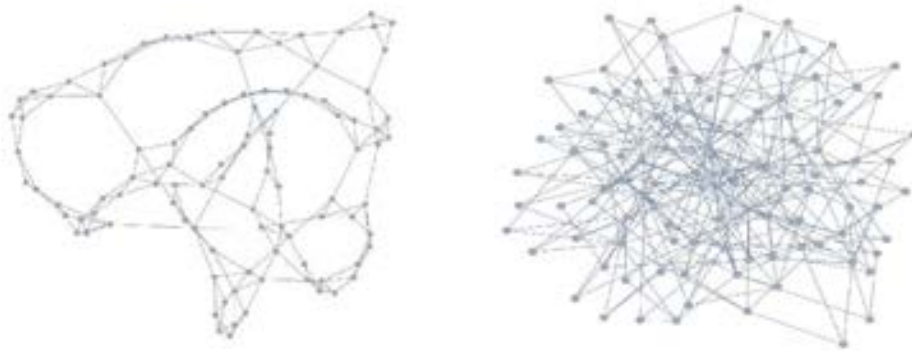


Figure 1: On the left is a Small World network with 100 nodes and 200 bonds. On the right is a Scale Free network with 100 nodes and 285 bonds.

References

- [1] F. Perakis, G.P. Tsironis, Phys. Lett. A 375 (2011) 676.
- [2] D.J. Watts, S.H. Strogatz, Nature (London) 393 (1998) 440.
- [3] Barabasi, A.-L., and R. Albert, 1999, Science 286, 509.
- [4] T. Holstein, Ann. Phys. 8 (1959) 325, S.M. Jensen, IEEE J. Quant. Electron. QE-18 (1982)

*kysk@materials.uoc.gr

Magnetoelectricity in two-dimensional manganites

E. Aza*^{1,2}, I. Bakaimi¹, A.M. Abakumov³, B. Klemke⁴, K. Kiefer⁴ and A. Lappas¹

¹*Institute of Electronic Structure and Laser, Foundation for Research and Technology - Hellas, Vassilika Vouton, 71110 Heraklion, Greece*

²*Material Science and Engineering Department, University of Ioannina GR 451 10 Ioannina, Greece*

³*EMAT, University of Antwerp, Groenenborgerlaan 171, B-2020 Antwerp, Belgium*

⁴*Helmholtz Center Berlin for Materials and Energy, D-14109 Berlin, Germany*

NaMnO₂ belongs to the family of ABO₂ type complex oxides. In this two-dimensional rock-salt type of structure, layers of monovalent Na and trivalent Mn that alternate one another, provide a paradigm where polymorphism and geometrical frustration (Fig. 1) have remarkable impact on the physical properties of the materials [1].

Two polymorphs of NaMnO₂ have been identified by transmission electron microscopy (TEM). In the present study we demonstrate that due to the inherent polymorphism, the magnetic ground state (Fig. 1) of the quasi-1D spin system in the α -polymorph evolves through complex modulated structures to a quasi-2D magnet for the β -polymorph [2].

Furthermore, we examined possible coupled phenomena in these compounds through a series of magneto-dielectric measurements. The results at both low and high frequencies demonstrate the unique potential of such manganite lattices to generate spatial regions with symmetry-breaking pinning sites that favour coupled degrees of freedom. The above lead us to believe that when structural complexity arises from spin-frustration, magnetoelectricity may be stabilised in otherwise collinear magnetic systems.

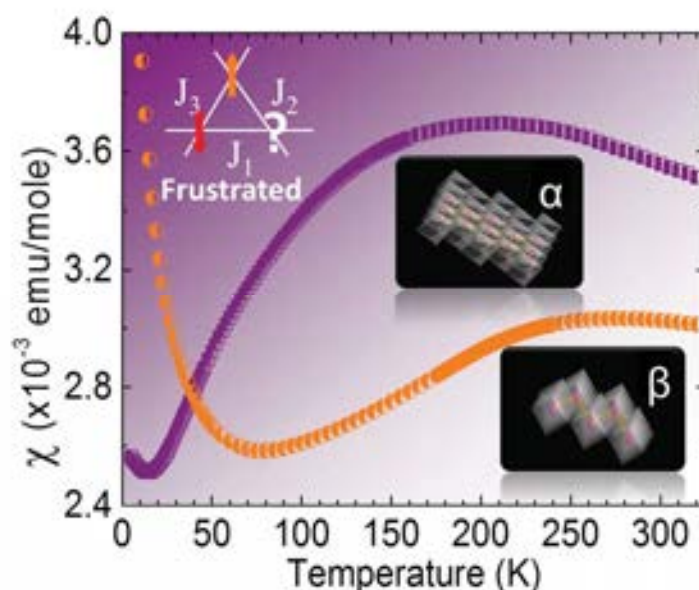


Figure 1: dc magnetic susceptibility of the two-polymorphs.

References

- [1] A. Zorko, O. Adamopoulos, M. Komelj, D. Arcon, and A. Lappas, Nat. Commun. **5**, 3222 (2014).
 [2] A.M. Abakumov, A.A. Tsirlin, I. Bakaimi, G. Van Tendeloo, and A. Lappas, Chem. Mater. **26**, 3306 (2014).

* elaza@iesl.forth.gr

Structural, magnetic and electrical properties of $\text{La}_{1-x}\text{Bi}_x\text{MnO}_{3+\delta}$ ($\delta=0.09$) perovskite compounds

N. Biniskos, M. Calamiotou, E. Syskakis*

Section of Solid State Physics, Department of Physics, University of Athens, Panepistimiopolis, Gr-15784 Zografos, Athens.

*email: esysk@phys.uoa.gr

LaMnO_3 is an antiferromagnetic insulator with orthorhombic symmetry, while BiMnO_3 is a ferromagnetic insulator with monoclinic symmetry. These remarkably different properties are unambiguously established despite the fact that the A-site in both compounds is occupied only by trivalent cations with similar ionic radii. The polarizability of the $6s^2$ lone pair of Bi [1,2] seems to be responsible not only for the above mentioned differences, but also for the multiferroic properties of BiMnO_3 . In the present work phase and magnetic transitions of $\text{La}_{1-x}\text{Bi}_x\text{MnO}_{3+\delta}$ ($0.00 < x < 0.30$) with high O_2 excess ($\delta=0.09$) have been investigated by electrical resistance ($R(T)$), ac susceptibility (χ_{ac}) and low field magnetoresistance (LFMR) in the region $80 < T < 300\text{K}$. The phase composition and structural properties were also investigated by X-ray diffraction (XRD) at $T=300\text{K}$. The compounds were synthesized by solid state reaction at $T=1030^\circ\text{C}$ in air, using high purity La_2O_3 , MnO_2 and Bi_2O_3 .

According to X-ray powder diffractometry the samples are single phase perovskites crystallizing with rhombohedral symmetry (R3c) (see Fig.1a). The electrical conductivity, $\sigma(T)$, can be described by the small polaron model and is strongly correlated with the observed long range FM order at $T < 150\text{K}$ in the frame of the double exchange (DE) mechanism. Bi doping in the specimen causes an increase of the unit cell volume. With the assumption that δ is independent of Bi content this can only be understood if the $6s^2$ lone pair of Bi is active. The observed decrease of the Curie temperature, T_C , and the accompanied weakening of the LFMR (see Fig.1b) might be explained as a consequence of structural deformation caused by the $6s^2$ lone pair too.

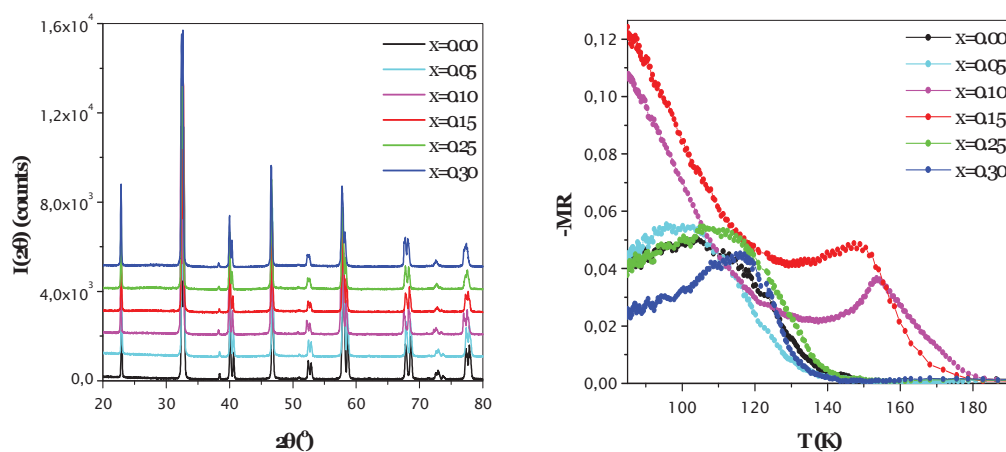


Fig 1: (a) X-Ray Diffractograms, (b): MR(T) measurements of Bi-doped specimen treated in O_2 at $T=1030^\circ\text{C}$ for 100h.

[1]: Nicola A. Hill, J. Phys. Chem. B, 104, 6694-6709 (2000)

[2]: T. Kimura et al, Nature 426, 55 (2003)

Magnetic order of transition-metal δ -doped cubic ZnO

Iosif Galanakis

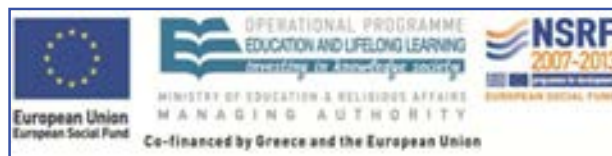
Department of Materials Science, School of Natural Sciences, University of Patras

The implication of the spin-degree freedom in conventional semiconducting electronic devices offers a new degree of freedom leading to the rapid expansion of the field of spintronics.¹ A plausible route to achieve the implementation of the electrons spin in devices is the doping of semiconductors using transition metal atoms.² The interplay between these impurity atoms and the holes/electrons doping of semiconductors can lead to novel magnetic phenomena.

ZnO is a well-known wide-band semiconductor crystallizing in the wurtzite structure which has been widely studied.³ When grown as a thin film the lattice structure adopted is the cubic zinc-blende structure, while a pressure of about 6 GPa induces the cubic rock-salt structure.³ ZnO has started to attract considerable attention in spintronic/magnetoelectronic research since it was discovered that the occurrence of Zn/O antisites or defects can lead to the appearance of magnetism.⁴

The properties of transition-metal (V, Cr, Mn, Fe, Co, Ni) δ -doped ZnO are reported based on ab-initio electronic structure calculations where the on-site electronic correlations are included using the Hubbard parameters. Calculated electronic and magnetic properties are considerably altered with respect to usual first-principles band-structure calculations. Most of the studied systems are found to be either half-metals or ferromagnetic/antiferromagnetic semiconductors and thus can be employed in a variety of spintronic applications as spin-filter materials.⁵

This research has been co-financed by the European Union (European Social Fund - ESF) and Greek national funds through the Operational Program "Education and Lifelong Learning" of the National Strategic Reference Framework (NSRF) - Research Funding Program: THALES. Investing in knowledge society through the European Social Fund.



*email: galanakis@upatras.gr

References

- ¹ I. Zutic, J. Fabian, and S. Das Sarma, *Rev. Mod. Phys.* **76**, 323 (2004).
- ² K. Sato et al., *Rev. Mod. Phys.* **82**, 1633 (2010).
- ³ S. Singh et al., *J. Phys. D: Appl. Phys.* **40**, 6312 (2007).
- ⁴ F. Oba, M. Choi, A. Togo, and I. Tanaka, *Sci. Technol. Adv. Mater.* **12**, 034302 (2011).
- ⁵ I. Galanakis, *Phys. St. Sol. (RRL)* **8**, 274 (2014).

Study of CMR effect and magnetic order in perovskite (La, Pr, Nd)MnO_{3+δ} (δ ≈ 0.09, 0.12) compounds.

K. Georgalas*, E. Syskakis

Section of Solid State Physics, School of Physics, University of Athens, Panepistimiopolis, Gr-15784 Zografos, Athens.

**email: kogeorg@phys.uoa.gr*

In the present work, magnetoresistance and magnetic properties of bulk polycrystalline specimen of La_{1-x}Pr_xMnO_{3+δ} (x=0.00-1.00) and La_{1-y}Nd_yMnO_{3+δ} (y=0.00-0.50) perovskite type compounds were investigated by LFMR(T) (H≈2kG) and χ_{ac} (T) (80<T<300 K) measurements. The compounds were synthesized by solid state reaction using high purity La₂O₃, Pr₆O₁₁, Nd₂O₃, MnO₂ in air. Series of pressed samples with different x, y were exposed to oxidative conditions (P_{O₂}=0.21, 1 bar T=900°C/100h) after sintering at high temperature, in order to achieve a high and homogeneous O₂ distribution in the specimen.

The χ_{ac} (T) measurements show that both the Pr-, as well as the Nd-doped specimen exhibit FM transitions at T<150 K. In the long range FM state established at low doping (x,y≤0.20) the Curie temperatures, T_C, and the spontaneous susceptibility decrease monotonously with the dopant concentration. The values of T_C are systematically lower for the Nd-doped samples. These variations indicate progressive weakening of the long range FM state resulting by increasing distortion introduced by the smaller radii of the ions (r_{Nd³⁺}=1.27Å < r_{Pr³⁺}=1.30Å substituted at A-site for La. For intermediate dopant concentrations (0.20<x<0.80 and 0.20<y<0.50) the spontaneous χ_{ac} (T) shows an unusual thermal dependence. Two consecutive FM type transitions are clearly recognized, indicating the competition between FM double-exchange and AFM super-exchange interactions [1]. χ_{ac} (T) measurements on similarly treated powders show qualitatively same magnetic ordering behavior, thus ruling out phenomena of oxygen inhomogeneity in specimen. Finally, at still higher Pr-, and Nd- doping only the transition from PM to Canted-AFM state is observed.

The LFMR(T) measurements for specimen in the low doping regime (x,y≤0.20) show broad peaks close to the corresponding FM transitions. These peaks shift to lower T with increasing x, y as expected for the DE originating intrinsic phenomenon of CMR. The LFMR(T) for specimen with x>0.20 displays two successive broad peaks, supporting the existence of two FM phases, in good agreement with the χ_{ac} (T) measurements.

References

- [1] V. Dyakonov, et al, Phys. Rev. B **77**, 214428, (2008)

Structural and magnetic properties of strongly carbon doped Fe-Co thin films.

G. Giannopoulos¹, L. Reichel^{2,3}, A. Markou⁴, S. Kauffmann-Weiss^{2,3,5},
I. Panagiotopoulos⁴, A. Edström⁶, W. Wallisch⁷, J. Rusz⁶, S. Fähler^{2,5}, J. Fidler⁷,
D. Niarchos¹

¹ IAMPPNM, NCSR Demokritos, Athens 15310, Greece

² IFW Dresden, PO Box 270116, 01171 Dresden, Germany

³ TU Dresden, Institute for Materials Science, 01062 Dresden, Germany

⁴ Department of Materials Science and Engineering, University of Ioannina,
Ioannina 45110, Greece

⁵ Chemnitz University of Technology, Institute of Physics, 09107 Chemnitz, Germany

⁶ Uppsala University, Department of Physics and Astronomy, 75120 Uppsala, Sweden

⁷ Vienna University of Technology, Institute Solid State Physics, Vienna, 1040 Austria

Fe-Co is proposed as a possible candidate alloy for permanent magnet applications due to its high magnetic moment. Apart from high magnetic moment, a considerably high magnetocrystalline anisotropy is required for permanent magnets. In this work we present sputtered thin Fe-Co films doped with Carbon, in order to stabilize metastable tetragonal phases, by straining the unit cell and thus inducing magnetocrystalline anisotropy in the system [1]. Tetragonal distortion can be induced by epitaxial growth of the magnetic Fe-Co layer on appropriate substrate or buffer materials layer with different lattice parameters [2], thus changing the c/a . Adding a third element, Carbon, could stabilize the strain and increase the magnetocrystalline anisotropy of the system.

In our study, we alloyed high amounts of carbon to Fe-Co based on promising theoretical and experimental studies which investigated films with less C. ATC 2200-V high vacuum magnetron sputtering system supplied from AJA Inc was used to prepare the samples, with a base pressure of 4×10^{-9} Torr. The depositions were performed on single crystalline MgO (001) substrates. The layer structure consists of a 3nm Cr underlayer, a 30nm Au-Cu buffer and the Fe-Co magnetic layer with variable C content. In ultrathin layers, up to 2nm thickness, C addition can induce a strain in the Fe-Co films. Then, the observed magnetic anisotropy is more determined by the interface to the buffer where the film supposedly grows coherently. In thicker films above 3nm thickness, the high C content leads to the formation of separated Fe-Co grains. Although this avoids a coherent strain from the Au-Cu buffer layer, the overall strain is still above 1%. We argue that C may stabilize this low tetragonal strain up to higher thicknesses when the strain initializing buffer layer is applied.

Acknowledgements

Work is supported by the EU Programme REFREPERMAG

References

- [1] T. Burkert, L. Nordström, O. Eriksson, O. Heinonen PRL **93**, 027203 (2004)
- [2] B. R. Cuenya, M. Doi, S. Löbus, R. Courths, W. Keune Surf. Science 493, 338 (2001)

L₁₀ FePt/FeCo thin films towards rare earth free permanent magnets applications

G.Giannopoulos¹, L.Reichel^{2,3}, A.Markou⁴, M.Werwinski⁵, A.Edström⁵, J.Rusz⁵, I.Panagiotopoulos⁴, S. Faehler², D. Niarchos¹

¹*INN, NCSR Demokritos, Athens 15310, Greece*

²*IFW Dresden, PO Box 270116, 01171 Dresden, Germany*

³*TU Dresden, Institute for Materials Science, 01062 Dresden, Germany*

⁴*Department of Materials Science and Engineering, University of Ioannina, Ioannina 45110, Greece*

⁵*Uppsala University, Department of Physics and Astronomy, 75120 Uppsala, Sweden*

Permanent magnets are used in a wide variety of applications, from personal computers to cars and magnetic sensors. Rare-earth elements are extensively used in permanent magnets in order to achieve high anisotropies. Fe-Co is proposed as a possible alternative to rare-earth permanent magnet based alloys, due to its very high magnetic moment. The magnetocrystalline anisotropy can be induced via straining the FeCo unit cell as shown in theory [1] and confirmed by experimental studies on ultrathin films. For this reason several underlayers have been employed to cause tetragonal distortion to the cubic FeCo cell [2]. In this work we present our results on epitaxial growth of Fe₄₅Co₅₅ ultrathin films on L10 phase FePt thin underlayers, producing an exchange spring system [3-5] leading to high coercivities and very high energy products. We used magnetron sputtering to deposit FePt layers at 500°C to favor the fct phase formation and to deposit Fe-Co at 300°C. The thickness was varied between 5 and 7 monolayers for the FePt and up to 9 monolayers for the FeCo. In all samples full FePt fct phase transformation was observed according to structural analysis, along with epitaxial growth of Fe-Co on FePt. Coercive field was reduced from 1.3 T down to almost 0.2 T through exchange coupling of FePt and FeCo magnetic layers with increasing thickness. The anisotropy is out of plane while the energy product is estimated in the excess of 200kJ/m³.

Acknowledgements: This work was supported by the EU-REFREEPERMAG project

References

- [1] T. Burkert, L. Nordström, O. Eriksson, O. Heinonen PRL 93, 027203 (2004)
- [2] S. Kauffmann-Weiss, S. Hamann, L. Reichel, A. Siegel, V. Alexandrakis, R. Heller, L. Schultz, A. Ludwig, and S. Faehler APL Materials 2, 046107 (2014)
- [3] D. Kim, J. Hong Surface Science 606 (2012) 1960–1964
- [4] D. Kim, Ar. Hashmi and J. Hong Journal of the Korean Physical Society, Vol. 62, No. 6, March 2013, pp. 918~923
- [5] B. Wang, H. Oomiya, A. Arakawa, T. Hasegawa, and S. Ishio, J. Of Appl. Phys. 115, 133908 (2014)

A multifunctional approach focused on hyperthermia response of commercial ferrofluids

A. Makridis,^{*} M. Tziomaki, E. Myrovali, D. Sakellari, K. Simeonidis, M. Angelakeris

Department of Physics, Aristotle University, 54124 Thessaloniki, Greece

K. Topouridou, M.P. Yavropoulou, J.G. Yovos

Division of Molecular Endocrinology, AHEPA University Hospital, Aristotle University of Thessaloniki, Thessaloniki, Greece.

Magnetic ferrofluids have received special attention due to their various biomedical applications including cancer diagnosis and treatment. The aim of this study was to investigate the ability of commercial ferrofluids to work as multifunctional heat mediators. Samples under study are the MRI agents FeraSpin-XX series from nanoPET-Pharma (www.nanopet-pharma.com) where XX denotes XS, R, Re and XL with variable hydrodynamic diameters of iron-oxide magnetic nanoparticles. Magnetic nanoparticles being subjected to an AC magnetic field may show remarkable heating effects related to losses during the magnetization reversal process of the particles. Taking advantage of this behaviour of the nanoparticles it is possible to locally raise the temperature inside a tumor between 41°C and 45°C (a desirable hyperthermia limit) to promote cell death, a treatment known as magnetic particle hyperthermia (MPH). Calorimetric measurements were taken using two different AC magnetic field frequencies (210 and 765 kHz) corresponding to similar magnetic field amplitudes (15-25 kA/m) and varying solution concentration (0.5-2 mg_{Fe}/mL). The magnetic heating characteristics of the ferrofluids were investigated and determined by estimating the quantifiable index of heating efficiency, the Specific Loss Power (SLP), which is measured in watts per gram of magnetic material (Fig. 1). Iron oxide nanoparticles with optimum performance were used to an *in vitro* hyperthermia study that performed on human osteosarcoma cell line Saos-2 cells. Finally, our work revealed a size-dependent cytotoxicity profile, tunable SLP together with fast thermal response, features that are crucial for adequate thermal efficiency combined with minimum treatment duration. The heating efficiency along with their non-cytotoxic behaviour of these commercial magnetic ferrofluids reveal their multifunctional role in modern theranostics. The wide range of accessible features of magnetic nanoparticles underscores their potential as the most promising platform material available for theranostics.

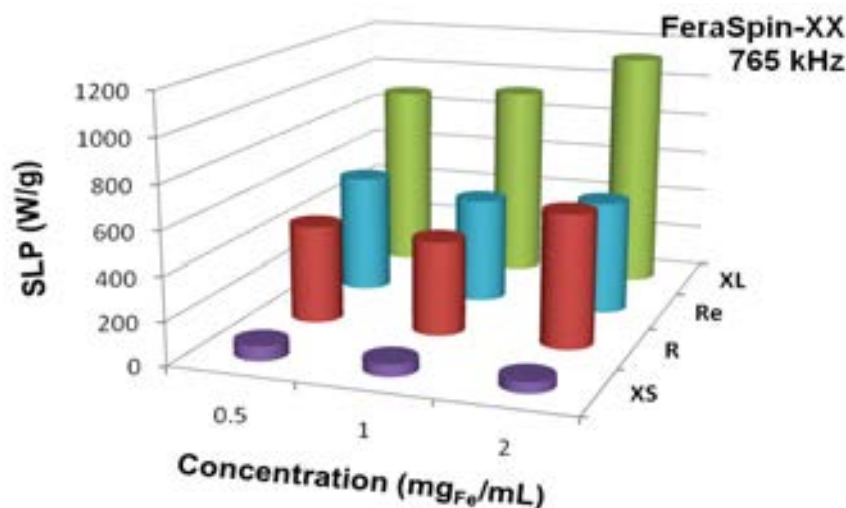


Figure 1: SLP at various concentrations of FeraSpin-XX (XS, R, Re and XL) under AC magnetic field frequency 765 kHz at 25 kA/m.

^{*} anmakrid@physics.auth.gr

Magnetic nanoparticle arrays: Effect on magnetic hyperthermia

E.Myrovali*, V.Ntomprougidis, D.Sakellari, K.Simeonidis, M. Angelakeris
 Physics Department, Aristotle University of Thessaloniki, 54124 Thessaloniki,
 Greece

Magnetic particle hyperthermia is a synergistic cancer treatment technique that takes advantage of heat released by magnetic nanoparticles (MNPs) when are exposed in an alternating magnetic field and may lead cancer cells either to a severe shock or even to apoptotic death. The thermal response of MNPs solution depends on a large number of parameters, such as the intrinsic properties of nanoparticle (e.g. size, magnetization), the medium parameters (e.g. viscosity, stability) of the solution and the field features (amplitude, frequency). In this work, we investigate how MNPs arrays (comprised of magnetite nanoparticles arranged in lines) may affect thermal response in comparison to the individual randomly dispersed MNPs (control samples). For this reason MNPs arrays where prepared, using as solvent a mix of agarose gel (agar) and water in magnetite nanoparticle solutions prepared by aqueous coprecipitation (shown in Fig.1a), by varying agar solution concentration (0.05-10 mg/mL) under two configurations of static magnetic field (100-400 G) parallel ($\theta=0^\circ$) and perpendicular ($\theta=90^\circ$) with respect to hyperthermia field direction (Figs. 1b-1d). Scanning Electron Microscopy (SEM) results reveal the successful formation of MNPs arrays (Fig. 1e). Moreover, hyperthermia measurements in two experimental setups (frequencies: 210, 765kHz, amplitudes: 250-300 Oe), revealed the enhanced thermal response of samples subjected parallel in magnetic field with respect to perpendicular and control samples (Fig. 2) for both concentrations as quantified by Specific Loss Power (SLP), a heating efficiency index. The effect of solution viscosity tuned by the agar concentration to the formation of the chains, and subsequently to SLP values is discussed together with the dipolar interactions governing array formations and their stability.

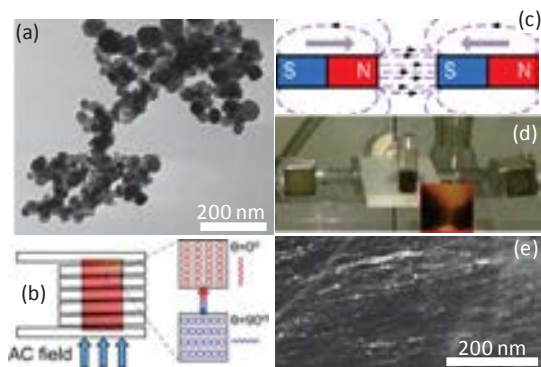


Figure 1: (a) TEM imaging of magnetite nanoparticles, (b) experimental setup of magnetic hyperthermia setup at two configurations: $\theta=0^\circ$ (parallel) and $\theta=90^\circ$ (perpendicular). (c) schematic magnetic field representation, (d) MNPs array formation under static magnetic field, (e) SEM imaging of MNPs arrays.

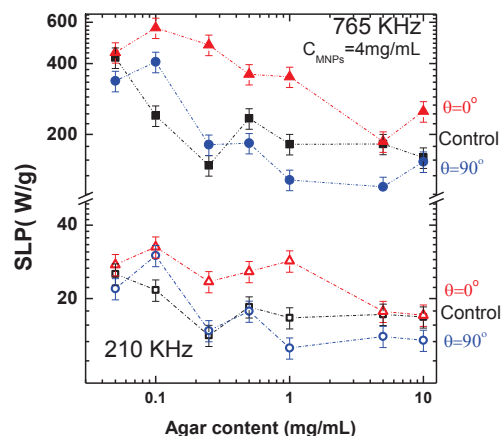


Figure 2: SLP values for varying agar content, under two different field frequencies (210 and 765kHz) and amplitude (300Oe).

* emiroval@physics.auth.gr

Orbital and magnetic order in $\text{LaMn}_{1-x}\text{Cr}_x\text{O}_{3+\delta}$ ($x=0.0-0.25$) compounds

A. Samartzis, and E. Syskakis

Department of Solid State Physics, School of Physics, University of Athens, Panepistimiopolis, Gr-15784 Zografos, Athens.
 email: esysk@phys.uoa.gr

The effect of Cr substitution for Mn on the orbital order-disorder (Jahn-Teller) transition, prototypically exhibited by stoichiometric LaMnO_3 at 750 K, remained unexplored to present times. Recent work (1, 2) on $\text{LaMn}_{1-x}\text{Cr}_x\text{O}_{3+\delta}$ compounds mainly focused on their magnetic/structural properties addressing questions like the nature of the magnetic Mn^{3+} - Cr^{3+} (double exchange (DE) or super exchange(SE)) which is responsible for the FM behaviour observed upon increasing x in hole-free specimen. In the present work Cr doping at Mn site was employed to investigate its influence on the J-T distortion. Cr^{3+} , with an ionic radius (0.615 Å) comparable to that of high-spin Mn^{3+} (0.64Å) should not cause extensive lattice distortion. However, Cr^{3+} , being isoelectronic to Mn^{4+} should introduce non-distorted Cr^{3+}O_6 octahedra, randomly distributed at spatially fixed Mn^{3+} sites.

The $\text{LaMn}_{1-x}\text{Cr}_x\text{O}_{3+\delta}$ samples ($0.00 \leq x \leq 0.25$) were investigated by electrical resistivity, $\rho(T)$, differential thermal analysis, DTA, (300-1100K) and χ_{ac} measurements (80-300 K). The powders of the compounds have been prepared using high purity La_2O_3 , $\text{Cr}(\text{NO}_3)_3 \cdot 9\text{H}_2\text{O}$ and MnO_2 by solid state reaction and were exposed finally to $T=1300^\circ\text{C}$ in air. Pressed samples of different Cr content were simultaneously subjected to heat treatments–densification at $T=900-1300^\circ\text{C}$, under controlled atmospheres ($P_{\text{O}_2}=210 \cdot 10^{-6}$ mbar), to obtain specimen with successively lower O_2 -excess up to $\delta \approx 0$.

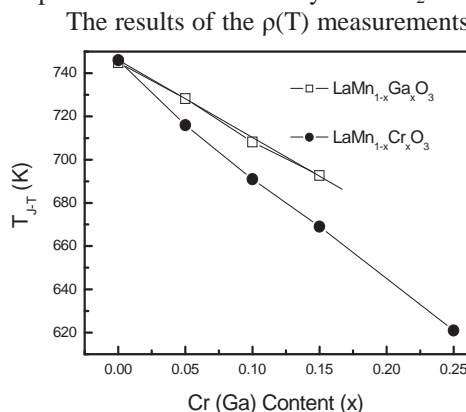


Fig.1: Displacement of the Jahn Teller transition by $\text{B}=\text{Cr}^{3+}$, Ga^{3+} in $\text{LaMn}_{1-x}\text{B}_x\text{O}_3$ compounds.

shown in Fig.1, Cr^{3+} clearly causes a significantly stronger displacement of T_{J-T} than the isoelectronic nonmagnetic Ga^{3+} despite their size similarity ($r_{\text{Ga}^{3+}}=0.62$ Å).

The results of the χ_{ac} measurements for O_2 -rich specimen ($\delta \approx 0.09$) show DE-dominated FM transitions, with non-monotonic variation of the Curie temperatures with Cr doping, in accordance with literature data(4). For specimen with low Mn^{4+} content, $\delta < 0.04$, transitions to the CA-AFM have been observed at $T_{\text{CA}} < 140\text{K}$. The spontaneous susceptibility exhibits a steep increase suggesting a considerable enhancement of the FM interactions in specimen with $x \geq 0.15$. On the other hand, T_{CA} shows a minimum at $x=0.10-0.15$. As the position of the minimum apparently depends on the Mn^{4+} content it rather indicates a competition of magnetic DE and SE interactions. The enhancement of FM interactions resulting in a strengthening of the CA-AFM state seems therefore to be favored in Mn^{4+} -free specimen.

References:

- (1) Y. Sun et al. PRB **63**, 174438, (2001); J. Deisenhofer et al., PRB **66**, 054414, (2002)
- (2) L.W. Zhang et al. J. Magn. Magn. Mat. **219**, 236. (2000); L. Morales et al. J. Solid state Chem. **180**, 1824 (2008)
- (3) A. Ramos et al. PRB **87**, 220404(R), (2013)
- (4) L. Morales et al. PRB **72**, 132413, (2005)

Ultrashort pulse laser assisted generation of layered nanomaterials in liquid

K.Alexaki^{1,2}, C.Fotakis^{1,2}, E.Stratakis^{1,2},

1. Institute of Electronic Structure and Laser, Foundation for Research & Technology Hellas, (IESL-FORTH), P.O. Box 1527, Heraklion 711 10, Greece.

2. University of Crete, Heraklion 714 09, Greece.

This paper will present our recent work on the application of ultrafast lasers for the generation of layered nanomaterials. In particular, the photo-exfoliation of MoS₂ and WS₂ targets upon femtosecond laser processing in liquid media is presented. This procedure took place in low fluences and gave rise to the formation of few layer MoS₂ and WS₂ nanoflakes which was confirmed by Transmission Electron Microscopy and Raman Spectroscopy. Furthermore, the formation of fullerene-like spherical nanoparticles (NP) of MoS₂ and WS₂, using femtosecond laser ablation in water or ethanol is demonstrated. This procedure took place in high fluences, while remarkable dependence of the NP's morphology and structure on the repetition rate was observed. The NP colloids were characterized by Scanning Electron Microscopy, X-ray Diffraction, Transmission Electron Microscopy and Raman Spectroscopy. Raman Spectroscopy revealed large localized strain effects in the electronic band structure of atomically thin MoS₂ and WS₂. The mechanism of photo-exfoliation was investigated and discussed.

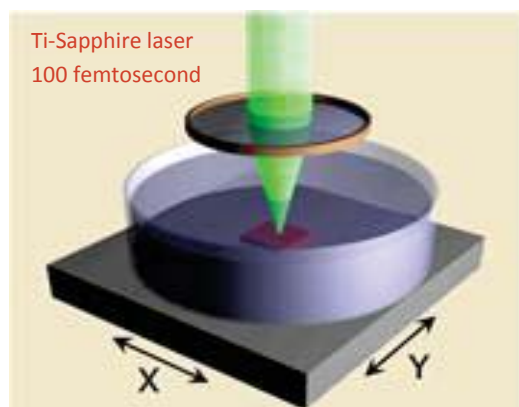


Figure 1: Experimental Setup of ablation in liquid by ultrashort laser pulses

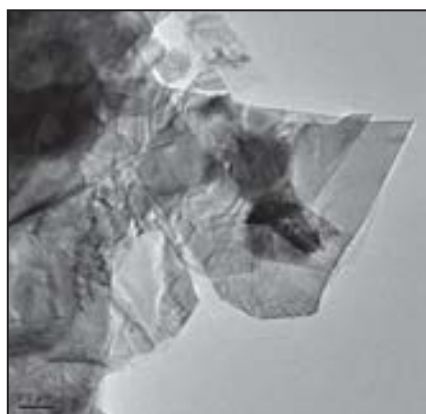


Figure 2: TEM view of MoS₂ flakes in water

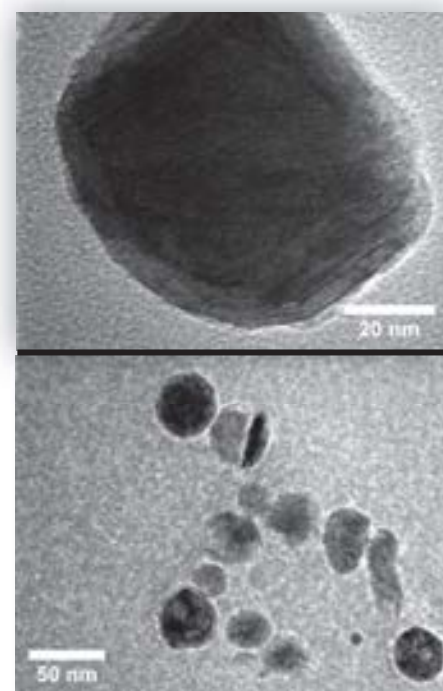


Figure 3: TEM view of WS₂ NPs in ethanol

* konale11@hotmail.com

Mechanical Properties of Graphene and Boron Nitride sheets and ribbons

S. Alexandri^{1*}, G. Kalosakas^{2,3}, N. N. Lathiotakis⁴, C. Galiotis^{2,3} and K. Papagelis^{2,3}

¹*Interdepartmental Programme in Polymer Science and Technology, University of Patras, Patras (Greece)*

²*Foundation of Research and Technology Hellas, Institute of Chemical Engineering Sciences, P.O. Box 1414, GR-26504 Patras (Greece)*

³*Department of Materials Science, University of Patras, 26504 Patras (Greece)*

⁴*Theoretical and Physical Chemistry Institute, National Hellenic Research Foundation, Vass. Constantinou 48, Athens GR-11635, Greece*

The study of atomically thin 2D crystals is expected to remain one of the hottest fields in nanomaterials for many years [1]. Among the 2D materials, graphene is an ideal one to model its mechanical properties. In particular, the elastic modulus of single layer graphene and its elastic response have been a subject of intensive theoretical research [2]. Hexagonal boron nitride (BN) is a structural analogue of graphene exhibiting large band gap (5.5eV) and partially ionic sp^2 hybridized bonds which are responsible from its notably different properties compared to graphene.

In this work, we have calculated and compared the mechanical properties of graphene and boron nitride sheets and ribbons. We have used empirical force fields derived from first principles' calculations to describe the bond stretching and angle bending interactions between the atoms in graphene and BN. By using molecular dynamics simulations, Young modulus, fracture stress, fracture strain and Poisson ratio for zigzag and armchair directions of graphene and boron nitride nanoribbons are determined.

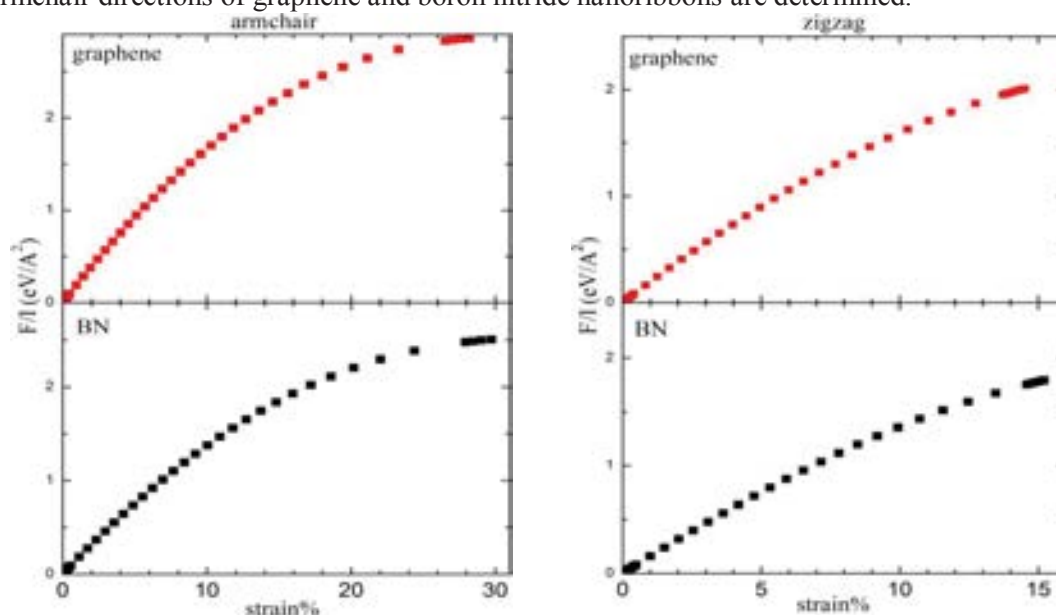


Figure 1: Stress-strain relation of bulk graphene and BN under uniaxial tensile loading along the armchair and zigzag directions.

References

[1] A. K. Geim and I. V. Grigorieva, *Nature* **499**, 419 (2013).

[2] G. Kalosakas, N. N. Lathiotakis, C. Galiotis and K. Papagelis, *Journal of Applied Physics* **113**, 134307 (2013).

* sotiria.th.al@gmail.com

Acknowledgements: This work has been supported by the Thales project GRAPHENCOMP, co-financed by the European Union (ESF) and Greek national funds (ΕΣΠΑ).

The influence of Au film thickness and annealing conditions on SERS enhancement

S. Andrikaki^{1,2*}, K. Govatsi^{1,3}, K.S. Andrikopoulos¹,
S.N. Yannopoulos¹, G.A. Voyatzis¹

¹FORTH/ICE-HT, P.O. Box 1414, GR-265 04, Rio-Patras, Greece

²Department of Materials Science, Univ. of Patras, GR-26500, Rio-Patras, Greece

³Department of Chemistry, Univ. of Patras, GR-26500, Rio-Patras, Greece

Surface enhanced Raman scattering (SERS) offers the possibility to perform quantitative measurements and/or identification of molecular species at extremely low concentrations. The technique is based on the enhancement of the weak Raman scattering signal when the probed species are in the vicinity of nanostructured metallic substrates. Colloidal SERS substrates are advantageous with respect to their easy preparation and low cost with concurrent high enhancement [1]. In comparison, solid substrates enable flexibility in sampling [2]. In the current work, Au films of various thicknesses (< 5 nm) were deposited by sputtering onto Si wafers <100>. The solid state thermal dewetting of Au films at 400 °C resulted in the formation of Au nanoparticles with morphologies such as those shown in Fig. 1. The initial film thickness controls the resulting particle size distribution [3]. The optical properties of the substrates were studied by UV-Vis spectroscopy and their enhancement on the Raman signal was evaluated by observing the Raman features of an active agent MTX that was properly spin coated on the substrates. Correlation of SERS signal with the optical properties as well as the mean particle size of Au was attempted and optimum conditions for maximum SERS signal were investigated.

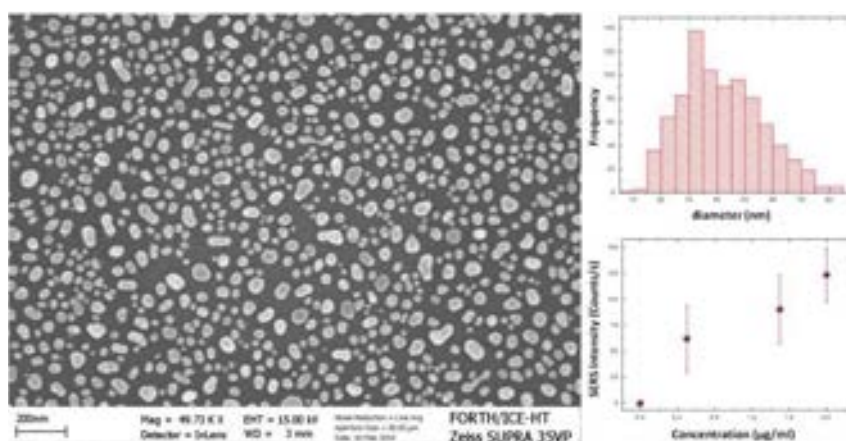


Figure 1: SEM image of a sample with 30 nm average Au nanoparticle size. The particle size distribution and the correlation of SERS intensity with the concentration of MTX.

Acknowledgement: The present work was funded from the European Union's Seventh Framework Programme (FP7/2007-2013) under the grant agreement N° NMP4-LA-2012-280759 and the acronym 'NanoBarrier'.

References

- [1] J. Anastasopoulos, A. Soto Beobide, G. Voyatzis, *J Raman Spectrosc.* **44**, 401 (2013).
- [2] E. Kammer, et al., *Phys Chem Chem Phys* **16**, 9056 (2014).
- [3] K. Govatsi, A. Chrissanthopoulos, V. Dracopoulos, S. Yannopoulos, *Nanotechnology* **25**, 215601 (2014).

* andrikaki@iceht.forth.gr

Shaping core-shell iron oxide nanocrystals

G. Antonaropoulos^{*1,2}, K. Brintakis^{1,3}, A. Kostopoulou¹ and A. Lappas¹

¹*Institute of Electronic Structure & Laser, Foundation for Research & Technology – Hellas, Vassilika Vouton, 71110 Heraklion, Greece*

²*Department of Chemistry, University of Crete, Voutes, 71003 Heraklion, Greece*

³*Department of Physics, Aristotle University of Thessaloniki, 54124 Thessaloniki, Greece*

Over the past years, the potential applications of iron oxide nanoparticles in various fields have been widely acknowledged. Wüstite-type (FeO) nanoparticles have attracted particular attention due to their interesting defect-related magnetic properties. The formation of FeO_x, which is highly unstable at room temperature, is only achievable in the nanoscale form [1]. By controlling the oxidation process of the metastable FeO, we are able to create a core/shell type morphology of FeO/Fe₃O₄ nanostructures [2]. The interface between the antiferromagnetic FeO core and the ferrimagnetic Fe₃O₄ shell leads to a technologically exploitable effect known as “exchange bias”[3] (Figure 1). This makes such nanostructured materials excellent candidates for magnetic storage media.

The elevated temperature, wet-chemical techniques employed for the synthesis of our nanocrystals (Figure 2), give us the ability to tune the size and the shape of the particles. Developing the growth conditions so that particles with less-regular morphological characteristics are attained (namely, from spherical to cubic - Figure 2c), is of particular interest due to the achievable higher magnetic anisotropy of the nanomaterials. We discuss the potential of such monodisperse nanocrystals to self-assemble on appropriate substrates with the purpose to provide low-dimensional, multifunctional magnetoelectric systems.

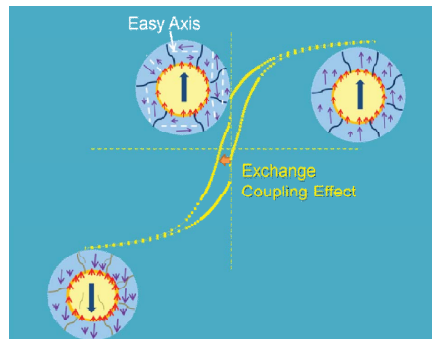


Figure 1: Schematic of the exchange-coupling effect [4].

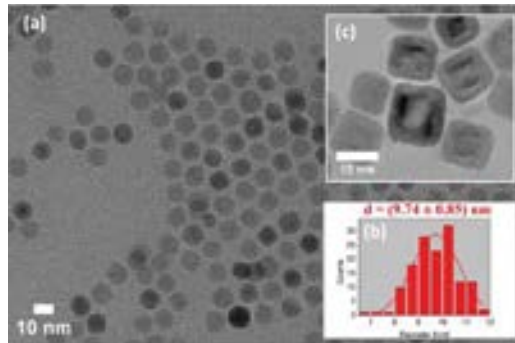


Figure 2: (a) Spherical core/shell nanocrystals exhibiting a tendency to self-assemble, (b) their size distribution and (c) high-resolution image of cubic core/shell nanocrystals

References

- [1] F. X. Redl, C.T. Black., G. C. Papaefthymiou, R. L. Sandstrom, M. Yin, H. Zeng, C. B. Murray and S. P. O'Brien, *J. Am. Chem. Soc.* **126**, 14583 (2004).
- [2] Y. L. Hou, Z.C.Xu and S.H.Sun, *Angew. Chem., Int. Ed.* **46**, 6329 (2007).
- [3] J. Nogues and I.K. Schuller, *J. Magn. Magn. Mater.* **192**, 203 (1998).
- [4] A. Kostopoulou, F. Thetiot, I. Tsiaoussis, M. Androulidaki, P.D. Cozzoli and A. Lappas, *Chem. Mater.* **24**, 2722 (2012).

* ganton@iesl.forth.gr

High pressure Raman and PL study of $\text{In}_x\text{Ga}_{1-x}\text{N}$

V. Gkrana, K. Filintoglou, J. Arvanitidis*, D. Christofilos, M. Katsikini,
C. Bazioti, G. P. Dimitrakopoulos, S. Ves, G. A. Kourouklis
Physics and Chemical Engineering Departments, A.U.Th., Greece

A. Georgakilas, E. Iliopoulos
Department of Physics, University of Crete and IESL, FORTH, Greece

The direct bandgap of the $\text{In}_x\text{Ga}_{1-x}\text{N}$ alloys ranging from UV to NIR renders these materials suitable for short wavelength laser diodes and photovoltaic devices. Raman and photoluminescence (PL) spectroscopies are non-destructive tools for the characterization of their structural quality and stress distribution. In this work, the pressure response of a polar $\text{In}_x\text{Ga}_{1-x}\text{N}$ ($x \sim 0.37$) film grown by MBE on a GaN/sapphire template was studied by combined Raman and PL mappings, allowing for the precise location of sample sites exhibiting different residual stress (Figure 1). In the Raman spectrum of the as-grown sample three Raman peaks appear at ~ 544 , ~ 682 and $\sim 706 \text{ cm}^{-1}$, attributed to the in-plane E_2 mode, an alloy disorder-activated shoulder (S-peak), and the $A_1(\text{LO})$ mode along the c -axis, respectively. The PL peak is located at $\sim 1.97 \text{ eV}$, very close to the absorption edge energy, indicating that PL is unaffected by the presence of any defect states, composition fluctuations or In clustering. Breakage of the sample causes the significant softening of the Raman peaks and the redshift of the PL peak, indicative of position dependent relaxation of the epilayer due to random crack formation. Powdering of the sample further decreases the PL peak energy and the Raman frequencies with the latter approaching the strain-corrected values. [1]

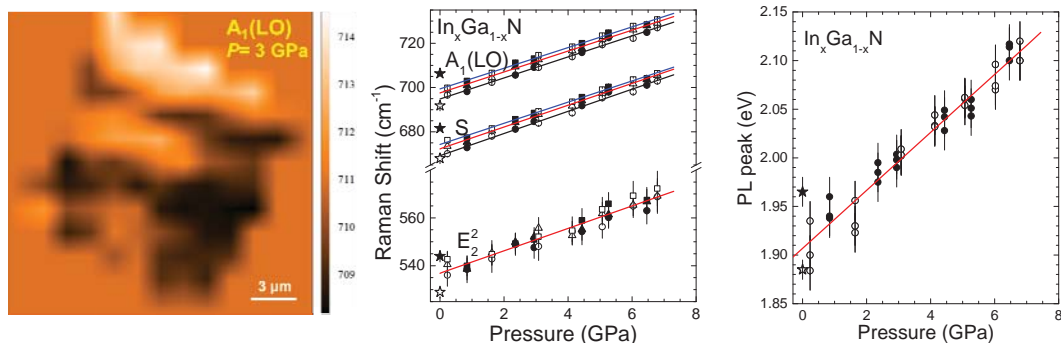


Figure 1: Raman mapping of the $A_1(\text{LO})$ frequency at $P=3 \text{ GPa}$ and pressure dependence of the Raman frequencies and the PL peak.

The analysis of our high pressure data demonstrates that in our experiments the residual stress state and the presence of the substrate do not affect the pressure response of the Raman and PL peaks. Pressure application causes blueshift of the Raman ($\sim 4.7 \text{ cm}^{-1}/\text{GPa}$ for all modes and for different sample sites) and the PL peak ($\sim 30 \text{ meV}/\text{GPa}$). The pressure slopes for the Raman peaks are suggestive of the intermediate, between GaN and InN, stiffness of the alloy. The pressure slope of the PL peak obtained here is very similar to that of the bandgap energy (E_g) for $x \sim 0.4$ from absorption measurements and that theoretically predicted assuming uniform arrangement of the In atoms. [2,3]

Acknowledgement: This research has been co-financed by the European Union (European Social Fund - ESF) and Greek national funds through the Operational Program "Education and Lifelong Learning" of the National Strategic Reference Framework (NSRF) - Research Funding Program: ARCHIMEDES III. Investing in knowledge society through the European Social Fund.

References

- [1] R. Oliva, J. Ibanez, R. Cusco et al., *J. Appl. Phys.* **111**, 063502 (2012).
- [2] M. Millot, Z. M. Geballe, K. M. Yu et al., *Appl. Phys. Lett.* **100**, 162103 (2012).
- [3] I. Gorczyca, A. Kaminska, G. Staszczak et al., *Phys. Rev. B* **81**, 235206 (2010).

AlN/GaN HEMTs with thin GaN/AlN buffer layers on sapphire (0001) substrates

A. Bairamis^{1,2,*}, Ch. Zervos^{1,2}, A. Adikimenakis¹, A. Kostopoulos¹,
 M. Kayampaki¹, K. Tsagaraki¹, G. Konstantidis¹ and A. Georgakilas^{1,2}
¹*Microelectronics Research Group (MRG), Institute of Electronic Structure and Laser (IESL), Foundation for Research and Technology-Hellas (FORTH) P.O. Box 1385, 71110, Heraklion-Crete, Greece*
²*Physics Department, University of Crete, Heraklion-Crete, Greece,*
 * e-mail: bairamis@physics.uoc.gr

High Electron Mobility Transistors (HEMTs) should combine high electron mobility channels and high resistivity buffer layers on insulating substrates. The efficient confinement of the carriers in the channel can be enhanced by the presence of a barrier underneath the channel. The thinnest possible epitaxial structure may be important for specific applications, but also satisfies the condition for reduced manufacturing cost.

With the above motivation, in this work we have studied the performance capabilities of AlN/HEMT structures with narrow GaN buffer layer (300nm) on a thin AlN back barrier (200 nm) grown directly on insulating sapphire substrates. The double barrier AlN/GaN/AlN HEMT structure can enhance the channel confinement, decrease electron spill-over effects and suppress the buffer leakage, as needed for high frequency performance and high breakdown fields.

Spontaneous and strain induced polarization, which are two determinant factors in nitride semiconductors research, lead to a high positive polarization in the AlN, resulting in a 2DEG induced at the AlN/GaN interface. Since our structures contain GaN layers, grown on AlN buffer layer, it also follows a negative polarization charge which can cause an accumulation of holes. The AlN/GaN heterojunction offers the highest polarization discontinuity for GaN channel transistors and HEMT devices can be realized with ultra-shallow channels and very high current density. Enhancement-mode AlN/GaN HEMTs have also received great attention recently, especially for high power switching applications. A particular subject of interest was to assess the possibility of realizing normally-off HEMT devices, only by scaling of the AlN top barrier thickness without any other surface or gate treatment (gate recess, plasma treatment).

Material and device characterization, as well as two-dimensional electron gas density calculations, produced very consistent results for the scaling of material and device properties with the AlN top barrier thickness. It is shown that the transistor threshold voltage could be scaled linearly from +0.2 V to -2.7 V by varying the AlN barrier thickness from 1.5 nm to 4.5 nm, respectively. The maximum drain current was 1.1 A/mm for intermediate AlN barrier thicknesses. The results demonstrate the strong performance capabilities of thin AlN/GaN/AlN heterostructures and their potential use for normally-off devices.

Fig. 2 shows the variation of the 300K 2DEG mobility, as well as the theoretical and experimental results of N_S for different AlN barrier thicknesses. For AlN thickness between 1.5 nm and 3nm, the electron mobility increases rapidly from 46 to 900 cm^2/Vs . A small reduction was observed for higher AlN barrier thicknesses, reaching the value of 703 cm^2/Vs for 4.5 nm AlN. The theoretical and experimental N_S values of 2DEG densities are in a very good agreement, with the highest value being $2.2 \times 10^{13} \text{ cm}^{-2}$ for the HEMT structure with 4.5 nm AlN barrier thickness.

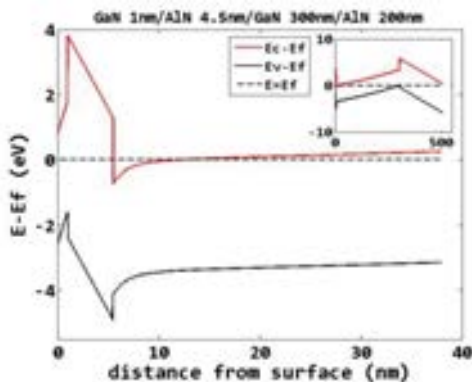


Fig. 1. Simulated band diagram of the GaN/AlN double heterostructure for AlN thickness at 4.5nm. The insert diagram presents the band profile for the whole structure.

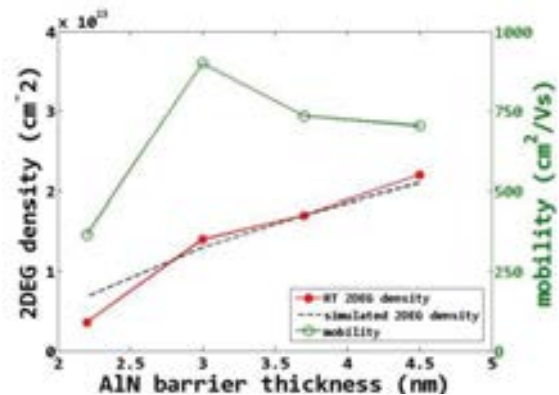


Fig. 2. Theoretical and experimental 2DEG sheet density (N_S) and electron mobility, as functions of AlN barrier thickness.

Low temperature porous Ta_2O_5 films. Towards hybrid molecular/high-k oxides for non-volatile memory applications.

A. Balliou*, G.Papadimitropoulos, N.Glezos, D.Davazoglou
*Institute of Microelectronics, NCSR Demokritos,
 Agia Paraskevi Attikis, 153 10 Athens, Greece*

In this work we study the potential of utilization of porous Ta_2O_5 oxide films grown under ambient temperature conditions either as gate dielectrics in hybrid molecular/semiconductor memory elements or as charge trapping medium reliant on interface dipole engineering. The partially ionic nature of the incorporated charged molecules induces the presence of interface dipoles, changing the band lineup across the interfaces of the MOS stack [1]. This phenomenon can be exploited to modulate the flat band voltage shift and improve the properties of the high-k dielectric at the same time [2].

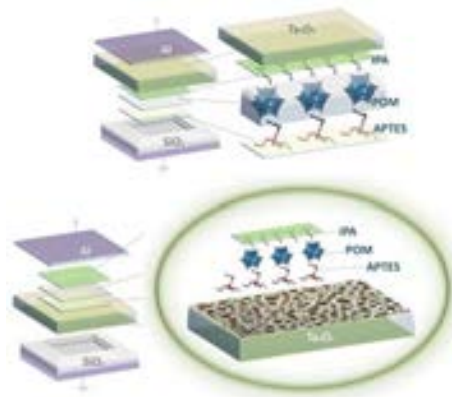


Figure 1: Schematics of the fabricated MIS capacitor memory stacks incorporating low temperature Ta_2O_5 and self-assembled POM oligolayer on SiO_2 . On top the tantalum oxide layer is grown on the active molecular oligolayer playing the role of gate oxide. At the bottom the porous surface of the oxide serves as a large effective templating surface for the self-assembly of the active molecules. The latter results in a high density molecular layer with well-defined structural and interfacial properties.

References

- [1] Yasuyuki Hikita, Mitsuru Nishikawa, Takeaki Yajima and Harold Y. Hwang, *Phys. Rev. B*, **79**, 073101, (2009).
- [2] A. A. Pavel and N. Islam, *IEEE Trans. Nanotechnol.* **9**, 345, (2010).

*aballiou@imel.demokritos.gr

ALD deposited thin HfO₂ films: electrical and structural characterization.

M.A. Botzakaki* S.N. Georga, C.A. Krontiras,
University of Patras, Department of Physics, 26504 Rion-Patras Greece

G. Skoulatakis, S. Kennou and S. Ladas
University of Patras, Department of Chemical Engineering, 26504 Rion-Patras Greece

P. Svarnas
University of Patras, Department of Electrical and Computer Engineering, High Voltage Laboratory, 26504 Rion-Patras Greece

C.Tsamis, E. Makarona

NCSR "Demokritos", Inst. of Advanced Materials, Physicochemical processes, Nanotechnology & Microsystems, GR 15310 Aghia Paraskevi, Athens, Greece

The further dimensional shrinking of MOS devices is necessary in order to follow the continuous requirement of faster devices for technological applications. Towards this goal, new substrates, such as s-Si, Ge and III-V semiconductors, with higher carrier mobility than Si are studied [1,2]. On the other hand, in order to replace SiO₂, "new" high-k materials such as ZrO₂, Al₂O₃, HfO₂ are also studied [3,4].

ALD is one of the most promising deposition technique in microelectronics because it gives the opportunity to deposit ultra thin films at relatively low temperatures with absolute control of the thickness. HfO₂ is a promising gate dielectric material mainly due to the high dielectric value (20–25). In this study we deposit HfO₂ dielectric films, in pre-cleaned p-Ge substrates via ALD technique in three different deposition temperatures. X-ray Photoelectron Spectroscopy (XPS) analysis revealed that stoichiometrical HfO₂ was deposited in all three deposition temperatures.

AFM analysis reveals that HfO₂ films are uniform, cohesive with very low roughness. In order to electrically characterize these structures, Pt/HfO₂/p-Ge structures were constructed through photolithography and lift off methods. The electrical response as well as the Density of Interfacial traps (D_{it}) of the structures were tested/evaluated through C-V, C-f and G-V measurements. A passivation layer of plasma grown GeO₂ (2nm) was developed in between the gate dielectric and the Ge substrate. The structures were also characterized by C-V, C-f and G-V measurements.

References

- [1] K.C. Saraswat et al. *Microelectron. Eng.*, **80**, 15 (2005).
- [2] M.A. Botzakaki et al., *Microelectron. Eng.* **112**, 208 (2013).
- [3] J.M. Rafi et al. *J. Electrochem. Soc.* **158** (5) G108 (2011).
- [4] Z. Tan et al. *ECS Solid State Lett.* **2** (8) P61–P62 (2013).



in knowledge society through the European Social Fund.

This research has been co-financed by the European Union (European Social Fund – ESF) and Greek national funds through the Operational Program "Education and Lifelong Learning" of the National Strategic Reference Framework (NSRF) - Research Funding Program: Heracleitus II. Investing

* mpotzakaki@physics.upatras.gr

Raman study of $^{12}\text{C}/^{13}\text{C}$ Double Layer Graphene

D. Kokkinos, K. Filintoglou, D. Christofilos*, J. Arvanitidis, S. Ves,
G. A. Kourouklis

Physics and Chemical Engineering Departments, A.U.Th., Greece

O. Frank, M. Kalbac

J. Heyrovsky Institute of Physical Chemistry, Czech Republic

Graphene is one of the most promising materials for revolutionizing contemporary technology. Growth of large area single layer graphene (SLG) has been facilitated by the use of copper substrates. [1] Double layer graphene (DLG) differs from SLG as a gap opens in the electronic structure, crucial for nanoelectronic applications. In this context, the properties of the constituent layers of DLG and interlayer interaction are of particular interest. Raman spectroscopy is the tool of choice for the identification and study of graphene through the most prominent G and 2D Raman bands. [2] Here, we present our Raman study of DLG/Cu grown by chemical vapour deposition in a chamber operating at 1273 K, resulting in DLG regions with the lower layer consisting of ^{13}C and the upper of ^{12}C isotope atoms. [3] The isotopically marked carbon layers enable their optical spectroscopic discrimination. Four characteristic sample areas are identifiable by mapping and careful analysis of the frequencies and line shapes of the Raman bands: SLG and DLG solely consisting of ^{13}C as well as DLG $^{12}\text{C}/^{13}\text{C}$ layers with turbostratic (t) or AB (bernal, b) stacking (Fig. 1).

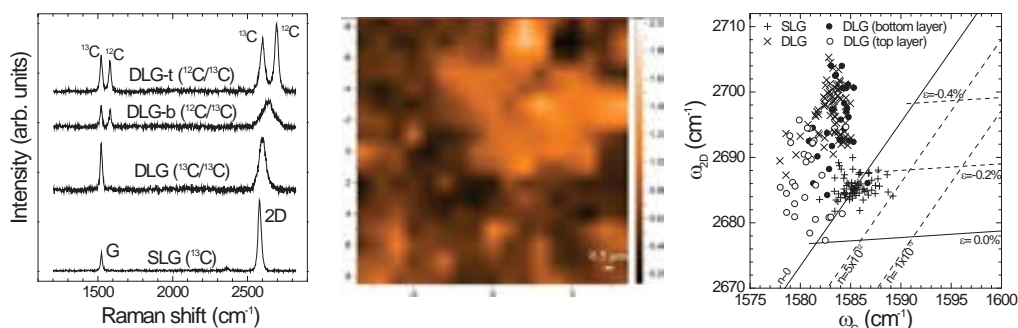


Figure 1: Indicative Raman spectra, $I_G(^{12}\text{C})/I_G$ map and mass normalized $\omega_{2D}-\omega_G$ plot.

The $\omega_{2D}-\omega_G$ plot has been proved very useful in deducing the local strain and doping state of SLG. [4] Although such a diagram is not appropriate for quantitative data interpretation for DLG, it can provide a qualitative picture of the interactions involved. Our Raman data can be introduced in the plot by appropriate mass normalization of the ^{13}C peak frequencies. The SLG appears compressively strained with small-to-zero doping. As for the DLG data, they lie outside the strain/doping grid, which should be interpreted as a consequence of the interlayer interaction. They group in two distributions with their relative position indicating a higher strain of the bottom layer that can be understood as a consequence of the substrate-graphene interaction. Further, isotopic marking permits to separately follow the pressure evolution of the two layers. Their G band pressure slopes are similar to each other and to that of the SLG ($\sim 10 \text{ cm}^{-1}/\text{GPa}$), suggesting that it is the substrate that determines the pressure response in both systems.

References

- [1] X. Li, W. Cai, J. An et al., *Science* **324**, 1312 (2009).
- [2] A. C. Ferrari and D. M. Basko, *Nature Nanotech.* **8**, 235 (2013).
- [3] P. T. Araujo, O. Frank, D. L. Mafra et al., *Sci. Rep.* **3**, 2061 (2013)
- [4] J. E. Lee, G. Ahn, J. Shim et al., *Nature Commun.* **3**, 1024 (2012).

* christof@eng.auth.gr

MoS₂ Nanostructures: Semiconductors with metallic edges

Daphne Davelou*, Georgios Kopidakis, George Kioseoglou and Ioannis N. Remediakis

Department of Materials Science and Technology, University of Crete, Greece

**d.davelou@materials.uoc.gr*

We present theoretical simulations based on Density-Functional Theory (DFT) for MoS₂ nanoribbons. We calculate electronic band structure and use linear-response theory to simulate the optical absorption of the material via dielectric function calculations. In addition, we calculate optoelectronic properties such as static relative permittivity, refractive index and reflectivity. Calculations are performed with the Grid-based Projected Augmented Wave (GPAW) package.

By studying nanoribbons with different widths, a single layer MoS₂ and bulk MoS₂, we observe that the electronic and optical properties of the material depend strongly on the dimensionality. The static relative permittivity drops from 7.1 in 3D to 3.7 in 2D, consistent with experimental data, and down to 2.4 for the quasi-1D nanoribbon. This dramatic change in optoelectronic properties is attributed to the presence of metallic edges in the 1D MoS₂, an otherwise semiconducting material (see Fig. 1). By studying nanoribbons with different widths, we are able to provide quantitative characteristics of these quasi-metallic states such as their spatial extent and permittivity [1].

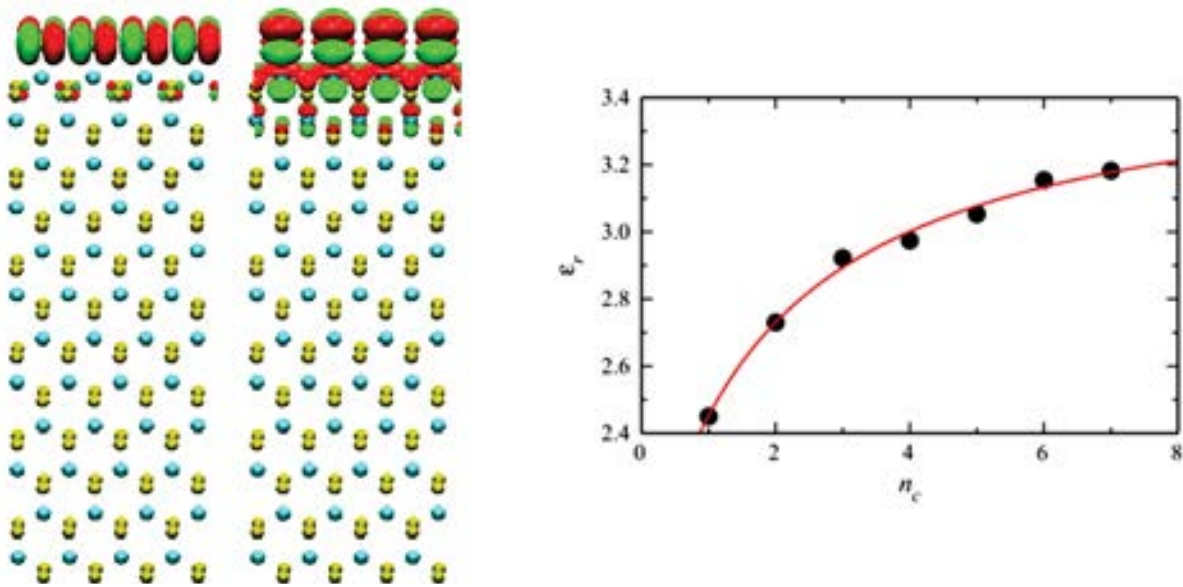


Figure 1:**left:** Isosurfaces of the electronic wavefunctions at the HOMO (left) and the LUMO state (right) for a nanoribbon with a width of $n_c=6$ cells. Mo and S atoms are represented by blue and yellow spheres, respectively. Different colors correspond to different sign of the wavefunction.**right:**Static relative permittivity as a function of nanoribbon width.

Acknowledgment: This work is supported by the research committee of the University of Crete.

Reference

[1] D. Davelou, G. Kopidakis, G. Kioseoglou and I. N. Remediakis, Solid State Commun. **192** 42 (2014)

Surface doping of exfoliated and CVD graphene on Si/SiO₂ substrate

Nikos Delikoukos^{1*}, Labrini Sygellou¹, John Parthenios¹, Dimitrios Tasis¹, Costas Galiotis^{1,2} and Konstantinos Papagelis^{1,2}

¹Foundation of Research and Technology Hellas, Institute of Chemical Engineering Sciences, P.O. Box 1414, GR-26504 Patras (Greece)

²Department of Materials Science, University of Patras, GR-26504 Patras (Greece)

Graphene is a very special material, since it has the advantage of being both conducting and transparent. It has received much interest due the combination of extremely high mobility of carriers up to $2.5 \times 10^5 \text{ cm}^2 \text{V}^{-1} \text{s}^{-1}$ and Young's modulus values up to 1 TPa. There are mainly two approaches to produce large area ($<50 \times 50 \mu\text{m}^2$) graphene membranes, namely the mechanical exfoliation method where graphene can be detached from an already existing graphite crystal ("HOPG" or "graphenium flakes") and the chemical vapor deposition (CVD) method where the graphene membrane can be grown directly on the top of a metallic substrate. In contrast to traditional semiconductors, the two-dimensional structure of graphene confines the doping process to surface adsorption or edge decoration. Dyes, polymers as well as fused aromatic systems have been used to realize *n*-type and *p*-type doping in the liquid phase [1, 2].

In this work, we present the gradual *p*-type doping of large area exfoliated flakes (Monolayer(1LG), Bilayer(2LG), Trilayer(3LG)) and CVD graphene transferred onto Si/SiO₂ wafers. In this approach, HNO₃ molecules are thermally deposited to form self-assembled charge transfer complexes. The charge transfer mechanism is experimentally interrogated by Raman spectroscopy. Raman spectroscopy, owing to its sensitivity on the structural and electronic characteristics of graphene, has been proven to be a valuable non-destructive tool to detect, among the others, the doping state of graphene by probing the changes of the so-called G and 2D Raman active bands [3].

Figure 1(Left panel) shows the optical microscope image of large bilayer graphene onto Si/SiO₂ substrate, which has an area of about $100 \times 50 \mu\text{m}^2$ indicated by the closed red line. In figure 1(Right panel) the frequency position and the full width at half maximum (FWHM) of the G band for untreated and doped CVD graphene is presented. As can be clearly inferred from the figure the G band characteristics are position dependent and show a clear trend as a function of the doping level.

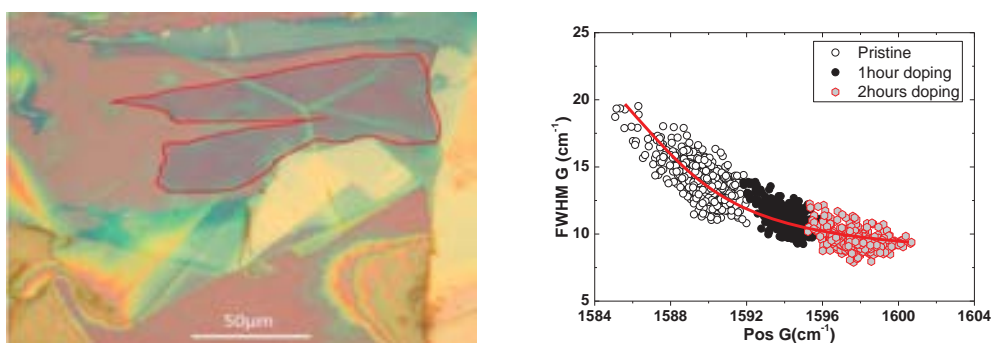


Figure 1: (Left panel) Optical micrograph of large area bilayer graphene (~85 μm) laying on the top of Si/SiO₂ substrate. (Right panel) Pos(G) as a function of FWHM(G) for CVD graphene before and after two doping steps ($\lambda_{\text{exc}} = 514 \text{ nm}$).

References

- [1] Lee, W., Suk, J., Hao, Y., Park, J., Yang, J., Ha, H., Murali, S., Chou, H., Akinwande, D., Kim, K., and Ruoff, R., ACSNano**6**, 1284 (2012).
- [2] Lv, R., Terrones, M., Materials Letters **78**, 209 (2012).
- [3] Ferrari, A. C. and Basko D. M., Nature Nanotech.**8**, 235 (2013).

* nickdelik@hotmail.com

Acknowledgements : This research has been financed by a GSRT project (ERC-10), entitled "Deformation, Yield and Failure of Graphene and Graphene-based Nanocomposites" which is greatly acknowledged.

Theoretical Study of CO₂ adsorption in functionalized MOFs

M. G. Frysalis, E. M. Klontzas, G. E. Froudakis
Department of Chemistry, University of Crete
P.O.Box 2208, Voutes 71003 Heraklion, Crete, Greece

As carbon dioxide is the primary greenhouse gas contributing to global warming, its storage and conversion has attract great attention in the scientific community. Many materials have been investigated for CO₂ adsorption¹. Among all these types of materials Metal Organic Frameworks (MOFs)² have been attracting the major scientific interest. MOFs are organic-inorganic hybrid materials made of metal ions or clusters interconnected through an organic linker.

In present work we study the interactions between carbon dioxide and a range of functionalized aromatic molecules by using quantum chemistry methods (MP2). This study focus on design of linker molecules which could be the organic part of new metal organic framework, with the aim of improving the CO₂ adsorption capacity of the material³.

Møller–Plesset perturbation theory within ri approximation using the def2-TZVPP basis sets was used to compute the interaction energy between CO₂ and the various molecular functional groups. From a total of forty-four different functional groups the ten substituents with the best binding energies are:

OLi>OSO₃H>CNH₂NOH>SO₃H>CHNOH>OOH>SOOH>COOH>CONH₂>CH₂OH
The results indicate that the incorporation of the OLi (8.6 kcal/mol) and OSO₃H (4.7kcal/mol) substituents in the MOF structure increases the interaction energy of the molecule with CO₂ at the most.



This research has been co-financed by the European Union (European Social Fund–ESF) and Greek national funds through the Operational Program "Education and Lifelong Learning" of the National Strategic Reference Framework (NSRF) - Research Funding Program: Heracleitus II. Investing in knowledge society through the European Social Fund

¹ J.C.M. Pires, F.G. Martins, M.C.M. Alvim-Ferraz, M. Simões Chemical Engineering research and design **89** 1446–1460 (2011)

² Deanna M. D Alessandro, Berend Smit, and Jeffrey R. Long, Angew. Chem. Int. Ed. **49**, 6058 – 6082 (2010)

³ Maria G. Frysalis, Emmanuel Klontzas and George. E. Froudakis ChemPhysChem **15**, 905-911 (2014)

Structural characterization of Al-induced crystallized amorphous Si thin films for photovoltaic applications

C. Gkanatsiou*, N. Vouroutzis, N. Frangis
*Department of Physics, Aristotle University of Thessaloniki, GR-54124
Thessaloniki, Greece*

V. Gianneta, A. G. Nassiopoulou
*NCSR Demokritos/INN, Terma Patriarchou Grigoriou, Aghia Paraskevi, 15310
Athens, Greece*

We present the structural characterization of p-doped polycrystalline Si films, formed by Al-induced crystallization and doping of amorphous Si thin films. The initial test structure consists of a bilayer of Al and α -Si, deposited on SiO_2/Si . The Al layer was deposited by electron gun evaporation, while the α -Si layer by sputtering. After extended annealing at 450°C for several hours, α -Si crystallization and layer reversal takes place. The crystallized Si layer is highly doped with Al. The obtained structure is adequate for use in high efficiency solar cell devices¹. Two different samples were used, namely sample D2001 and sample F2001. In both of them the nominal thickness of the SiO_2 layer was 100nm, while that of the Al and the α -Si layers was 200nm. Annealing was performed in N_2 ambient at 450°C for 7.5 h in sample F2001 and for 10h in sample D2001. The structural characterization of these films was performed by using conventional and high resolution transmission electron microscopy (TEM). In both cases, full layer reversal took place, so as the Al layer was fully situated on top of the polycrystalline Si layer, of thickness in the range of 200-250 nm. The polycrystalline layer was of high crystalline quality, with grains having size between: a) 150nm and $2.2 \mu\text{m}$ for D2001 and b) 100 nm and 800 nm for sample F2001. The difference in crystal size is attributed to the different annealing time. Twins and other defects are observed in the Si grains and they are analysed. [1]



Figure 1: Combination of Bright Field TEM images showing the structure of the sample D2001



Figure 2: Bright Field TEM image showing the structure of the sample F2001

References

[1] S. Gardelis, A. G. Nassiopoulou, P. Manoussiadis, N. Vouroutzis, and N. Frangis, *Appl. Phys. Lett.* **103**, 241114, 2013

* c.gkanatsiou@hotmail.com

Atomic models for interfaces in multilayer structures grown on SiC

A. Gkanatsiou*, Ch. B. Lioutas, N. Frangis
*Department of Physics, Aristotle University of Thessaloniki,
GR-54124 Thessaloniki, Greece*

Multilayer (5 layers) and multicomponent structures (based on GaN and related materials) were grown on 4H and 6H-SiC (with a misorientation of ± 0.5 -2 degrees off from the (0001) plane) substrates using the MOVPE method. The layers were grown epitaxially, as it was confirmed from the corresponding electron diffraction patterns. Several types of interfaces were observed between the layers that either ran parallel to the interface or formed V-shaped defects (e.g. the SiC/AlN, GaN/AlN, GaN/AlGaN interfaces etc.)

In this study, atomic models of the interfaces are presented based on experimental High Resolution TEM (HRTEM) micrographs and corresponding computer simulation images.

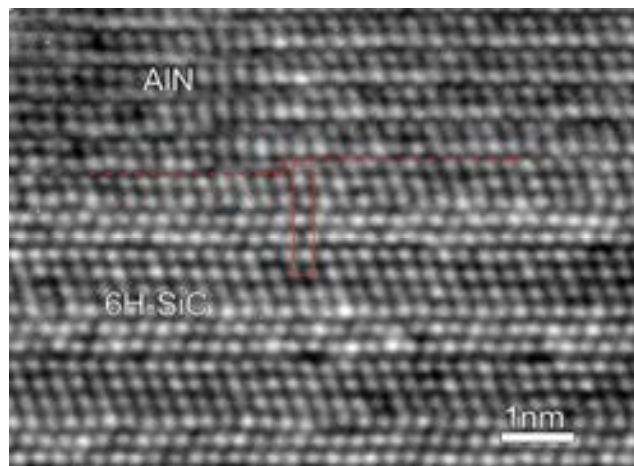


Figure 1: HRTEM image showing an atomic scale step in the 6H-SiC/AlN interface

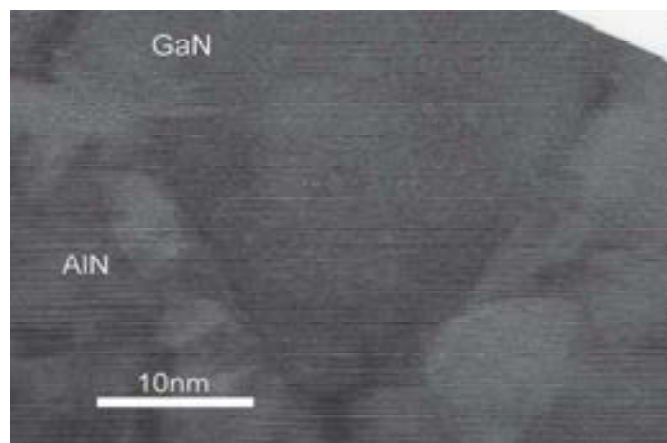


Figure 2: HRTEM image showing a V-shaped defect in the AlN/GaN interface

Supported by IKY FELLOWSHIPS OF EXCELLENCE FOR POSTGRADUATE STUDIES IN GREECE-SIEMENS PROGRAM, the JU ENIAC Project LAST POWER Grant agreement no. 120218 and the Greek G.S.R.T., contract SAE 013/8 - 2009SE 01380012.

* alexgkan@auth.gr

Gas Sorption Properties of a Functionalized NbO-type Metal Organic Frameworks

Charis Gryparis*, Ioannis Spanopoulos and Pantelis N. Trikalitis

Department of Chemistry, University of Crete, Voutes 71003 Heraklion, Greece

Metal organic frameworks (MOFs) or porous coordination polymers is an important class of open-framework solids synthesized by the coordination of suitable organic linkers to metal ions or clusters. The hybrid nature of MOFs could give rise to a plethora of advanced nanoporous materials with unique properties.[1] MOFs are considered very important for gas storage and separation applications, including CO₂ selective capture, however framework stability as well as gas uptake and selectivity needs to be improved.[2]

The NbO-type MOFs, made of 4-connected di-isophthalate ligands and 4-connected dicopper paddlewheel units, show excellent framework stability, high porosity, and improved gas adsorption capacity, especially for CO₂ and H₂. [3] We have shown recently that MOFs with functionalized organic ligands can further enhance the gas sorption properties of the resulting material.[4] In this way, by taking advantage the unique NbO platform and using suitable functionalized organic ligands we have successfully synthesized and characterized a series of MOFs with interesting gas sorption properties, including CO₂, CH₄ and H₂. These solids are air stable as shown in Figure 1. Important details will be presented and discussed.

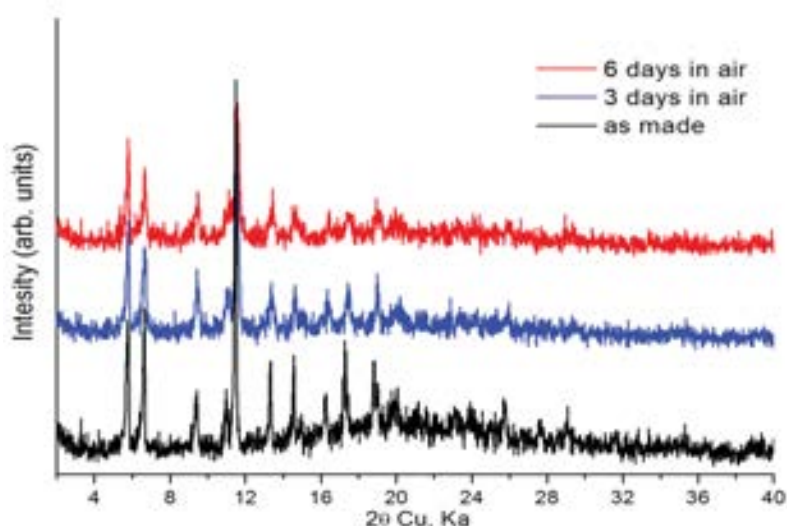


Figure 1. Powder X-Ray diffraction patterns of a copper-based functionalized MOF exposed to air for several days.

References

- [1] G. Ferey, *Chem. Soc. Rev.* **37**, 191 (2008).
 [2] Sumida K., Rogow D. L., Mason J. A., McDonald T. M., Bloch E. D., Herm Z. R., Bae T., Long J. R., *Chem. Rev.* **112**, 724 (2012).
 [3] Lin X., Telepeni I., Blake A. J., Dailly A. Brown C. M., Simmons J. M., Zoppi M., Walker G. S., Thomas K. M., Mays T. J., Hubberstey P., Champness N. R, Schroder M., *J. Am. Chem. Soc.* **131**, 2159 (2009).
 [4] Spanopoulos I., Xydias P., Malliakas D. C., Trikalitis N. P., *Inorg. Chem.*, **52**, 855 (2013).

* gryparis@chemistry.uoc.gr

Perpendicular Magnetic Anisotropy on W-based Spin-Orbit Torque CoFeB | MgO MRAM Stacks

A. Kaidatzis* and D. Niarchos

NCSR "Demokritos", Inst. of Nanoscience and Nanotechnology, Athens, Greece

O. Boulle and G. Gaudin

SPINTEC, CEA/CNRS/UJF/GINP, INAC, Grenoble, France

C. A. Avci, K. Garello, and P. Gambardella

Department of Materials, ETH Zurich, Switzerland

Spin-Orbit Torque Magnetic RAM (SOT-MRAM) is a novel memory concept recently proposed [1], promising a fast access, energy-efficient, scalable, high density non-volatile memory technology. A typical SOT-MRAM stack is composed of a Magnetic Tunnel Junction (MTJ), two ferromagnetic layers separated by an insulating oxide, grown on top of a metal with high spin-orbit coupling, which acts as the read/write current line. The structures principally studied are Ta | CoFeB | MgO | CoFeB stacks, due to the high spin-orbit coupling of Ta, the readily obtainable perpendicular magnetic anisotropy (PMA) of CoFeB and the more effective spin-dependent tunnelling through the monocrystalline MgO barrier [2]. Recently, there has been a focus on W for use as current line metal, due to its reported giant spin-orbit coupling [3]. In this context, we study W | Ta | Co₂₀Fe₆₀B₂₀ | MgO and WTa-alloy | Co₂₀Fe₆₀B₂₀ | MgO half-MTJ sputter deposited stacks. Series of samples with CoFeB thickness between 0.6 nm and 1.8 nm have been deposited and thereafter annealed in high vacuum for 1 hour, at temperatures between 200°C and 350°C. X-ray diffraction (XRD) and anomalous Hall effect (AHE) magnetometry have been performed to characterize the samples. AHE magnetometry reveals a clear PMA for the samples deposited on top of W/Ta underlayers, with CoFeB thickness between 0.9 and 1.2 nm. We will present a systematic study of these half-MTJs providing further insight on the CoFeB | MgO system.

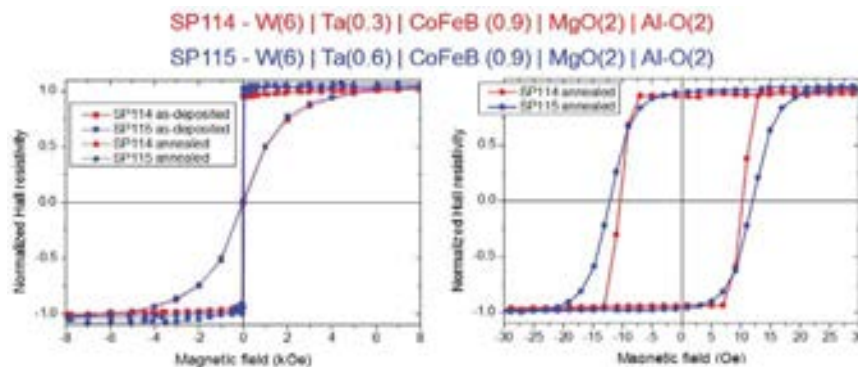


Figure: Anomalous Hall effect magnetometry of W | Ta | Co₂₀Fe₆₀B₂₀ | MgO stacks before and after annealing at 350°C. The magnetic field is applied perpendicular to the sample.

Acknowledgements

Funding from the E.C. through a FP7-ICT project (Grant No. 318144) is acknowledged (www.spot-research.eu/).

References

- [1] I. M. Miron et al., *Nature* **476**, 189 (2011).
- [2] S. Ikeda et al., *Nature Materials* **9**, 721 (2010).
- [3] C.-F. Pai et al., *Appl. Phys. Lett.* **101**, 122404 (2012).

* kaidatzis@ims.demokritos.gr

Sol-gel grown compound ZnO thin films for photovoltaic applications

P. Koralli, M. Kandyla, G. Mousdis, M. Kompitsas*

Theoretical and Physical Chemistry Institute, National Hellenic Research Foundation, 48 Vasileos Constantinou Avenue, 11635 Athens, Greece

M. Girtan

Photonics Laboratory, Angers University, 2, Bd. Lavoisier, 49045 Angers, France

Zinc oxide (ZnO) and composite ZnO thin films were deposited on microscope glass by applying the sol–gel spin coating technique, with the purpose to be used as transparent front contacts in thin-film solar cells. Aluminium or indium was incorporated in the ZnO matrix, in order to improve the electrical resistivity of the films. The incorporation of gold or silver nanoparticles aimed at increasing the efficiency of the solar cell.

The resistivity of the films was measured by the four-point van der Pauw method. The film structure was studied by X-ray diffraction (XRD). It was observed that all undoped and doped films, regardless of the impurity element, have a hexagonal wurtzite structure, showing a high degree of orientation along the c axis (002 peak), indicating the preferred grain growth along this plane. In addition, topographical and morphological studies of the doped and undoped ZnO films were performed by Atomic Force Microscopy (AFM).

The optical properties of the pure and composite ZnO thin films were investigated. It was shown that the incorporation of aluminium or indium improves the average film transmission. Further, the presence of gold or silver nanoparticles was verified with the aid of their plasmonic resonance on the optical transmittance spectra around 600 and 430 nm, respectively. The band gap for all ZnO thin films was estimated from the optical spectra and the film thickness was obtained by profilometry. In general, all films were of high quality with an average optical transmission over 80%, which decreases sharply at approximately 380 nm due to the band gap absorption of ZnO. The effect of the concentration of the impurity elements on the film properties was investigated.

* mcomp@eie.gr

Electrical percolation in incandescent lamps' tungsten wires

I. Karagiannis¹, I.Samaras²

¹ Physics and Technology of Materials, Physics Department of Aristotle Univ. of Thessaloniki, Greece

² Solid State Physics Section, Physics Department of Aristotle Univ. of Thessaloniki, Greece

Tungsten wires in incandescent lamps are one of the oldest bulk nanometals in nanotechnology. Using severe plastic deformation (SPD) techniques before the 1960's, an application driven thermo-mechanical technology of tungsten wires morphology solved many problems of the devices (incandescent lamps). The optimum solution found with highly elongated clusters of W-grains and nano-vacancies. The nano-vacancies in the order of 100nm are filling with potassium impurities upon heating forming a percolation system of a W-metal and a dielectric K-nanobubbles. Low weight percentage w% ($\ll 0.01\%$), potassium based, nanosize solid impurities transform into nanobubbles upon weak heating. This potassium solid-(63.5°C)-liquid-(759°C)-gas phase transition results into a huge volumetric v% increase due to solid-gas volume expansion. The fine control of insulating nanobubbles' volume percentage due to the DC electrical heating and the AC electrical measurement of the complex impedance $Z (= Z_r + jZ_i)$ allows the investigation of percolation problems, with the controlled variable being the nano-size of the insulating phase. Upon initial heating, the real component Z_r of the complex impedance Z represents both the Joule effect and an abrupt-additional increase due to a virtual decrease in metallic tungsten wires' diameter. Also, the imaginary component Z_i of Z represents the abrupt increase in nanobubbles' size of insulating phase, resulting in a volume percentage v% increase. The heating evolution versus electrical power P, of the calculated lumped parameters (R_1/R_2C) in an equivalent circuit (Fig.1). Using normalized (%) electrical parameters H_p , H_v and H_i (H_p for power P, H_v for voltage V, and H_i for current i), almost all devices present universal electrical behavior. A percolation regime is found from 0 to 1% of power P having a percolation threshold at 1% ($\text{Log}H_p=0$, in Fig.2), just before visual light appears at 2 to 3%. New “particles”, the photons, affect strongly the percolation problem and this new (2nd) percolation regime will be addressed in a future presentation.

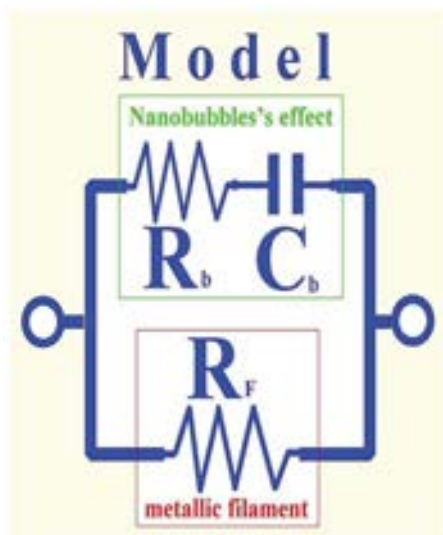


Fig.1: Equivalent circuit (a simple 3-elements model)

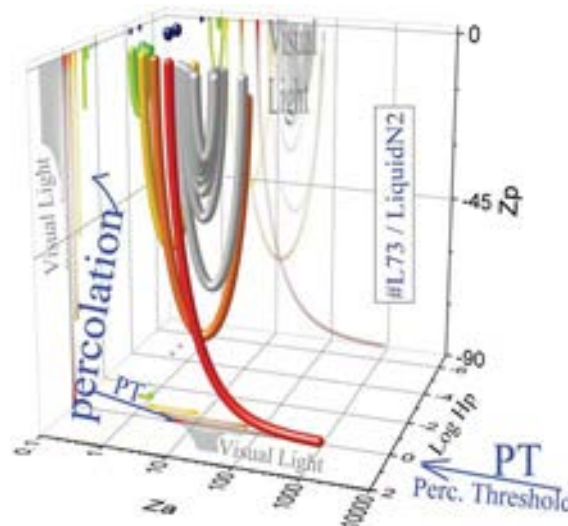


Fig.2: Complex impedance Z of a W-wire. The Z-phase (Z_p) shows the percolation regime (0% up to 1% of power P).

Energetics and electronic properties of GaN nanowires with embedded $\text{In}_x\text{Ga}_{1-x}\text{N}$ nanodisks

T. Pavloudis, J. Kioseoglou, Th. Kehagias, Ph. Komninou, Th. Karakostas*
*Department of Physics, Aristotle University of Thessaloniki, GR-54124
Thessaloniki, Greece*

C. D. Latham, M. I. Heggie
*Department of Chemistry, Faculty of Engineering and Physical Sciences,
University of Surrey, Guildford, GU2 7XH, UK*

P.R. Briddon
*Physics Centre, School of Natural Science, University of Newcastle upon Tyne,
Newcastle, NE1 7RU, UK*

M.J. Rayson
Institutionen för matematik, Luleå Tekniska Universitet, SE-97187 Luleå, Sweden

M. Eickhoff
*Institute of Experimental Physics I, Justus-Liebig-University Giessen, D-35392
Giessen, Germany*

In the present work we investigate the influence of strain on the energetics and the electronic properties of nanowires (NWs) consisted of a GaN base part followed by a superlattice part of successive $\text{In}_x\text{Ga}_{1-x}\text{N}$ nanodisks (NDs) (x ranging from 3% to 25%) separated by GaN spacers. $\text{In}_x\text{Ga}_{1-x}\text{N}/\text{GaN}$ supercells were modelled and simulations were implemented with the LAMMPS code for Molecular Dynamics, using a bond-order interatomic potential under the III-species environment approach [1], and with AIMPRO for Density Functional Theory calculations.

It has been found by both simulation approaches that among three possible types of strain (biaxial, hydrostatic and uniaxial), the biaxially strained NW superlattice is the one with the lowest excess energy for all indium concentrations. However the energy difference between biaxially and hydrostatically strained states for In concentration below 10% in the NDs is small. It is deduced that up to $\sim 10\%$ of In, the hydrostatic strain state is competitive with the biaxial and above this value the preferable strain model is the biaxial one. Hence, hydrostatic and biaxial strain components should be both considered in the embedded NDs and they are of different physical origin. The biaxial strain originates from growth on lattice mismatched layers, while the hydrostatic strain component originates from the lateral surfaces. Concerning the optoelectronic properties, the strained $\text{In}_x\text{Ga}_{1-x}\text{N}$ NDs do not induce states in the bandgap of the NWs. However, a bowing parameter of 4.5 should be taken into account in the quadratic Vegard's equation for the bandgaps in the different concentrations for such $\text{In}_x\text{Ga}_{1-x}\text{N}$ ND in GaN NW structure.

References

[1] Kioseoglou et al, pss (b) **245** (2008) pp 1118-1124

Acknowledgments: Work supported from EU under the FP7 STREP Project "DOTSENSE" (Grant Agreement 224212). The computations were supported by the LinkSCEEM-2 project, funded by the European Commission under the 7th Framework Program through Capacities Research Infrastructure, INFRA-2010-1.2.3 Virtual Research Communities, Combination of Collaborative Project and Coordination and Support Actions (CP-CSA) under grant agreement no RI-261600.

* karakost@auth.gr

Exchange-bias effect in core-shell nanoparticles with non-spherical shape and rough interfaces

V.A. Dimitriadis, D. Kechrakos*

School of Pedagogical and Technological Education (ASPETE), GR-14121

O. Chubykalo-Fesenko

Instituto de Ciencia de Materiales de Madrid, CSIC, ES-28049

We study the isothermal magnetic hysteresis of nanoparticles with FM core - AF shell morphology for various sizes and different shapes, in order to elucidate the sensitivity of the exchange bias effect on the shape of the particles and the structural imperfections at the core-shell interface. We use classical Heisenberg Hamiltonian with different local anisotropy terms for the core, the shell and the surface. The field-cooled process and the isothermal hysteresis loop are simulated implementing the Metropolis Monte Carlo algorithm. The coercive (H_C) and exchange bias (H_{eb}) fields for spherical and cubical nanoparticles with similar nominal sizes are compared. At low temperatures ($T \ll K_{1FM}$), we show that (i) cubical particles exhibit higher coercivity and lower exchange bias field than spherical ones, owing to the lower number of uncompensated spins (N_{unc}), and (ii) with increasing interface roughness, the differences between spherical and cubical particles are gradually smeared out.

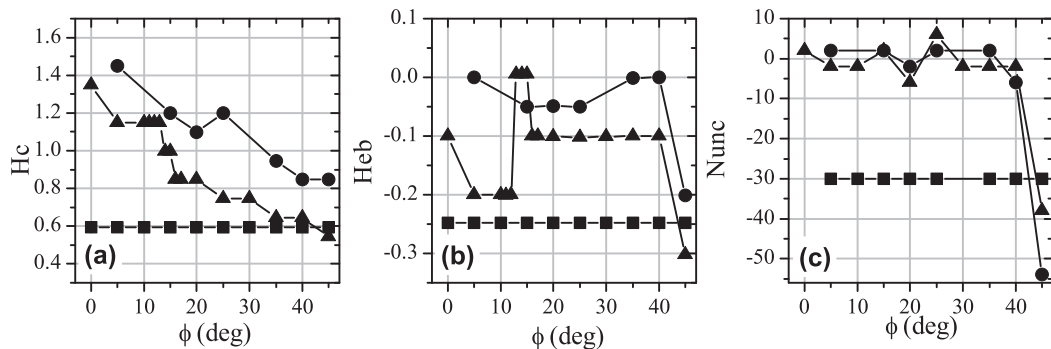


Figure 1: Dependence of (a) the coercive field, and (b) the exchange-bias field on the crystallographic orientation of the underlying SC lattice for two cubical particles (circles: $R_{ext} = 11a, R_c = 8a$, triangles: $R_{ext} = 8a, R_c = 5a$) and a spherical particle (squares: $R_{ext} = 11a, R_c = 8a$). The z-axis is taken along [001], the x and y-axes are rotated by the polar angle ϕ with respect to the [100] axis. The number of uncompensated spins (N_{unc}) depends on the polar angle ϕ as shown in (c).

Acknowledgement. Research co-financed by the European Social Fund and Greek national funds through the Research Funding Program "ARCHIMEDES-III".

*dkehrakos@aspete.gr

Adsorption and Electrochemical Behaviour of Cyt-c on Carbon Nanotubes/TiO₂ Nanocomposite Films Fabricated at Various Annealing Temperatures

P.A. Kolozoff, S. Katsiaounis, G. Avgouropoulos, E. Topoglidis*
Department of Materials Science, University of Patras, Rio 26504, Greece

The achievement of electron mediator free communication between the cofactors of redox proteins and a solid electrode surface could provide a simple and efficient way for studying fundamental protein function and structure and for developing novel amperometric biosensors. However, direct electrical contact of redox proteins on bare solid electrodes is usually prohibited due to deeply buried redox centers by the protein matrix and/or the denaturation of bioentities on the electrode surface.

In recent years, nanostructured metal oxide materials such as mesoporous TiO₂ films have overcome such problems and offer an ideal surface for protein immobilization from aqueous solutions with high binding stability and undetectable protein denaturation [1]. It has been demonstrated that these films offer excellent biocompatibility, high surface area, electrical conductivity, optical transparency, a simple and low cost fabrication method and therefore could be used for the development of electrochemical biosensors [2]. However, the fact that these films are semiconductors and exhibit limited conductivity at low negative potentials limits the quality of the electrochemical signals obtained.

In this work, carbon nanotubes (CNTs) were incorporated into mesoporous TiO₂ films resulting in TiO₂/CNT nanocomposites with improved electrical conductivity. Characterization of novel nanocomposite films was carried out with XRD, SEM and Raman, while conductivity and electrochemical properties were examined via cyclic voltammetry and spectroelectrochemistry. The immobilization and electrochemical behavior of a redox protein, such as Cytochrome-c, supported on these TiO₂/CNT films was studied in detail and particularly the effect of CNTs on the interfacial electron-transfer process between the electrode and the adsorbed biomolecules [3].

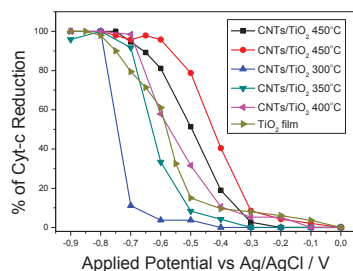


Figure 1: Percentage of Cyt-c reduced on DWCNTs/ TiO₂ films prepared at various annealing temperatures as a function of the applied potential determined from the relative spectroelectrochemical data

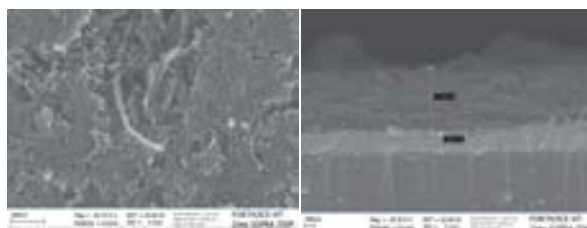


Figure 2: SEM images of a DWCNTs/TiO₂ film (top view and cross section).

References

- [1] E. Topoglidis, T. Lutz, J. R. Durrant and E. Palomares, *Bioelectrochemistry* **517**, 142 (2008).
- [2] C. Tiflidou and E. Topoglidis, *Colloids and Surfaces B: Biointerfaces*, in preparation (2014).
- [3] P. A. Kolozoff, S. Katsiaounis, G. Avgouropoulos and E. Topoglidis, *Electrochemistry Communications*, in preparation (2014).

* etop@upatras.gr

GaAs/AlGaAs core-shell nanowires for energy applications: A structural study

Th. Kehagias, N. Florini, G. P. Dimitrakopoulos, J. Kioseoglou, Ph. Komninou*
Physics Department, Aristotle University of Thessaloniki, 54124 Thessaloniki, Greece

K. Moratis, Z. Hatzopoulos, N. T. Pelekanos
Materials Science & Technology and Physics Departments, University of Crete and IESL/FORTH, GR-71003 Heraklion, Greece

III-V compound semiconductors based solar cells present much higher efficiencies, due to their increased light absorption and charge mobility. Incorporating the photovoltaic properties of III-V semiconductors into nanowire (NW) structures, efficiencies similar to today's best solar cells are expected, with much less material. Furthermore, by decoupling light absorption from carrier collection pathways in core-shell NWs, excellent optical quality and long carrier lifetimes can be achieved.

GaAs/AlGaAs core-shell NWs were grown on Si(111) by plasma assisted molecular beam epitaxy (PAMBE) via the vapor-liquid-solid mechanism. Their nanostructure was explored by high-resolution and scanning transmission electron microscopy (HRTEM-STEM). NWs are zinc-blende (ZB) single crystals that emerge directly from the Si surface despite the presence of the thin amorphous native oxide. Then, growth proceeds by a continuous succession of (111) mirror twins. The core-shell structure was revealed by both diffraction contrast TEM and annular dark-field (ADF) STEM imaging, showing that the AlGaAs shell occupies at least one half of the projected diameter of the NWs, ranging from 80 nm to 200 nm. The Al content of the shell was estimated at ~35-38% by energy dispersive X-ray (EDX) analysis (Figure 1). Moreover, molecular dynamics (MD) simulations of plan-view NW slices were applied to calculate the variation of the energy, the stress tensors, the displacement field and the strain components of the core-shell configuration.

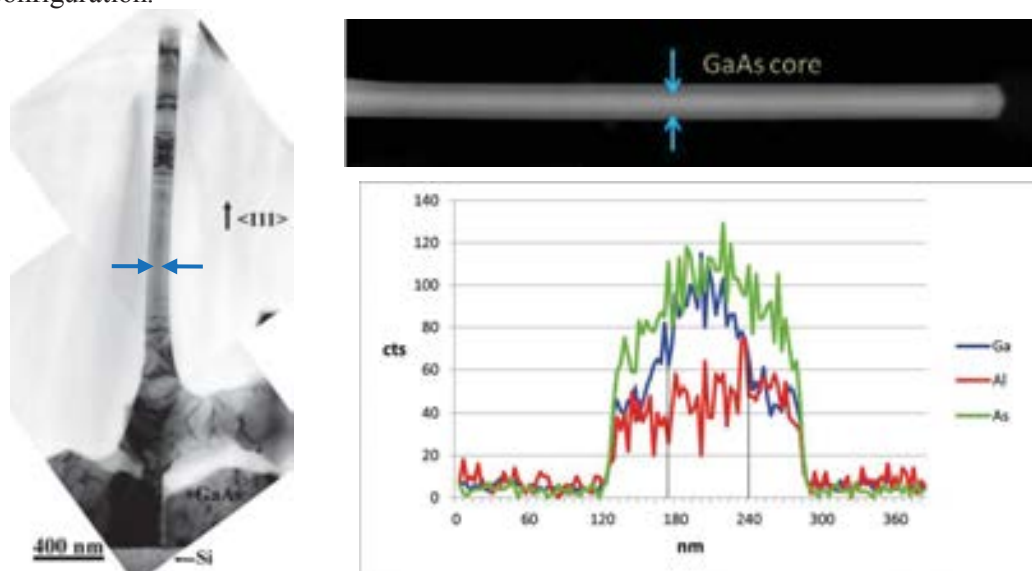


Figure 1. TEM image (left) of a GaAs/AlGaAs NW and the corresponding ADF image (top right). Arrows indicate the GaAs core. The EDX scan of the NW reveals the boundary between the core and the AlGaAs shell.

Acknowledgement

Research co-financed by the European Union (European Social Fund–ESF) and Greek national funds - Research Funding Program: ARISTEIA II, project NILES.

* komnhnoy@ auth. gr

OH-IRMOF-16 as potential drug carrier for Gemcitabine delivery. A DFT study.

Marianna Kotzabasaki, Emmanuel Klontzas, George E. Froudakis

Department of Chemistry, University of Crete, Vasilika Vouton, Iraklion 71003, Crete, Greece

The unique physical and chemical characteristics of Metal Organic Frameworks (MOFs) make them promising candidates for drug storage and drug delivery. MOFs are organic – inorganic hybrid materials made of metal ions or clusters interconnected through an organic linker. In order to develop new and much-improved drug delivery regimes in IRMOF-16 we functionalized each organic linker with a hydroxyl group. Then, the interaction of gemcitabine with the strategically modified organic linker of IRMOF-16 (non-toxic, high-loading MOF) has been investigated by employing DFT methods (PBE/TZVP). Our results indicate that the introduction of a hydroxyl group in the organic linker of IRMOF-16 was critical for gaining key acid-base and hydrogen-bond interaction sites. The maximum interaction energy with gemcitabine was found to be 24 kcal/mol for the modified IRMOF-16. Semi-empirical calculations (PM7) were also performed in order to study the interactions of gemcitabine with larger fragments of the modified IRMOF-16 unit cell.

Interfacial phenomena in GaN core-AlN/GaN shell nanowires

T. Koukoula^{*}, Th. Kehagias, Th. Pavloudis, J. Kioseoglou, Ph. Komninou
Physics Department, Aristotle University of Thessaloniki, GR-54124 Thessaloniki, Greece

S. Eftychis, J. Kruse, A. Georgakilas
Microelectronics Research Group, Physics Department, University of Crete, P.O. Box 2208, GR-71003 Heraklion, and IESL/FORTH, P.O. Box 1385, GR-71110 Heraklion, Crete, Greece

III-Nitrides core-shell nanowires (NWs) comprise non-polar $\{10\bar{1}0\}$ interfaces between the core and the shell, free from extended defects, allowing for a controlled band-gap and strain engineering in the development of novel optoelectronic devices. Transmission electron microscopy (TEM) methods were implemented to investigate the interfacial phenomena of GaN core- AlN/GaN shell NWs. The NWs were grown by plasma-assisted molecular beam epitaxy (PAMBE) on Si(111) with a thin AlN nucleation layer, consisting of a GaN base part, two intermediate, 10-15 nm thick, AlN spacers and a GaN cap layer. High-resolution TEM (HRTEM) observations revealed the core-shell structure with 2-3 monolayers (MLs) thick AlN shell around the GaN core and a second GaN shell overlaying the AlN one with a thickness of 7-10 MLs (Fig. 1). Quantitative measurements on the HRTEM images, along the growth axis, showed that this particular configuration imposes the *c*-lattice constant of the AlN shell to be adapted to the *c*-lattice constant of the GaN core. Therefore, a full elastic accommodation of the AlN on GaN is determined, considering the absence of misfit dislocations from the GaN/AlN interface. Regarding the AlN spacers, geometrical phase analysis (GPA) showed a gradual relaxation towards their central region, both along the axial and lateral directions, yet again without the presence of misfit dislocations. Finally, the core-shell NWs were investigated by Molecular Dynamics (MD) and Density Functional Theory (DFT) simulations of the experimental HRTEM images and the variation of the energy, stress tensors, strain components, displacement field and band-gap was calculated. The results shed light on the energetic, structural and electronic properties of the system.

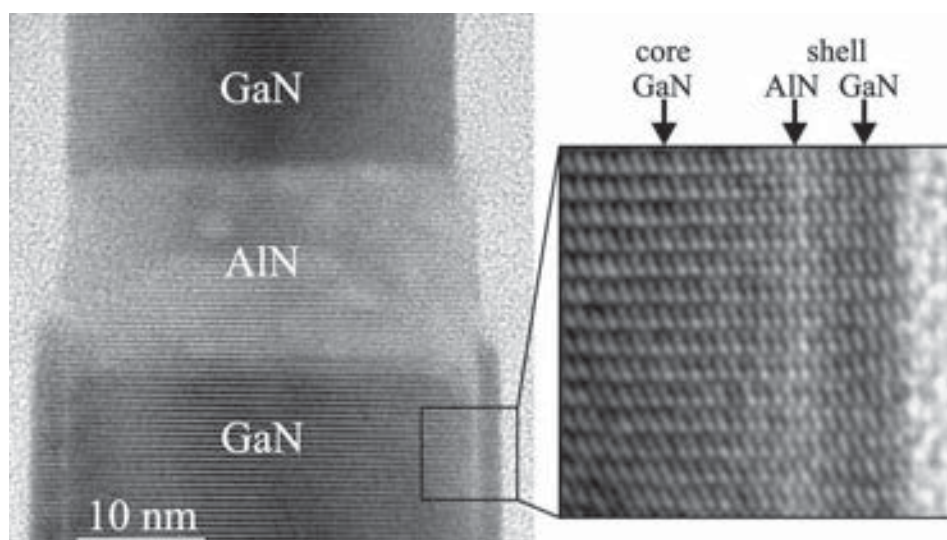


Figure 1: HRTEM image, along the $[11\bar{2}0]_{\text{GaN}}$ projection direction, illustrating the GaN core-AlN/GaN shell configuration.

Acknowledgments Research co-financed by the European Union (ESF) and Greek national funds - Research Funding Program: THALES, project “NanoWire”.

^{*} tkouk@physics.auth.gr

Nanoscale properties of GaN nanowires grown on Si substrates with an AlN interfacial layer

T. Koukoula^{*}, Th. Kehagias, J. Kioseoglou, Ph. Komninou

Physics Department, Aristotle University of Thessaloniki, GR-54124 Thessaloniki, Greece

S. Eftychis, J. Kruse, A. Georgakilas

Microelectronics Research Group, Physics Department, University of Crete, P.O. Box 2208, GR-71003 Heraklion, and IESL/FORTH, P.O. Box 1385, GR-71110 Heraklion, Crete, Greece

It is well established that self-assembled GaN nanowires (NWs) on Si(111) substrates grow on a thin amorphous Si_xN_y layer, that forms either due to intentional nitridation of the Si surface, or the intense N-rich conditions used for NWs growth by plasma-assisted molecular beam epitaxy (PAMBE). This layer is closely related to NWs misorientation from the growth direction, resulting in a high degree of NWs coalescence and consequently, affects their overall structural, electronic and optical properties. Transmission electron microscopy (TEM) techniques were employed to determine the optimum substrate surface treatment of GaN NWs growth on bare Si with or without nitridation of the surface, and on top of an AlN interfacial layer (IL) of varying thickness. High-Resolution TEM (HRTEM) observations have shown that formation of the amorphous Si_xN_y layer takes place inevitably when the Si was nitridated, intentionally or not, prior to NWs growth. However, the axial inclination of NWs was improved when the surface was intentionally nitridated, owing to the formation of a thicker Si_xN_y at the GaN/Si interface and the atomically flat Si surface. The amorphous Si_xN_y layer was not prevented even when a 0.2 nm AlN IL was foremost deposited (Fig. 1(a)). In contrast, when the thickness of the AlN IL exceeded 0.4 nm, either as-grown or annealed under active nitrogen, the Si_xN_y layer was suppressed, leading to GaN NWs with superior axial alignment and crystal quality (Fig. 1(b)). Moreover, GaN nanoislands (NIs) appeared along with GaN NWs in all cases, which evolved into a compact faceted GaN layer including sparse GaN NWs with increasing thickness of the AlN IL.

It appears that in the initial stages of IL growth, AlN forms strained 3D islands that act as nuclei for the spontaneous growth of GaN NWs. Subsequently, during annealing, the AlN IL transforms into a partially-relaxed compact 2D layer that favors the formation of GaN faceted domains along with the NWs, while in the case of a fully relaxed 20 nm thick AlN IL, a compact GaN layer is formed.

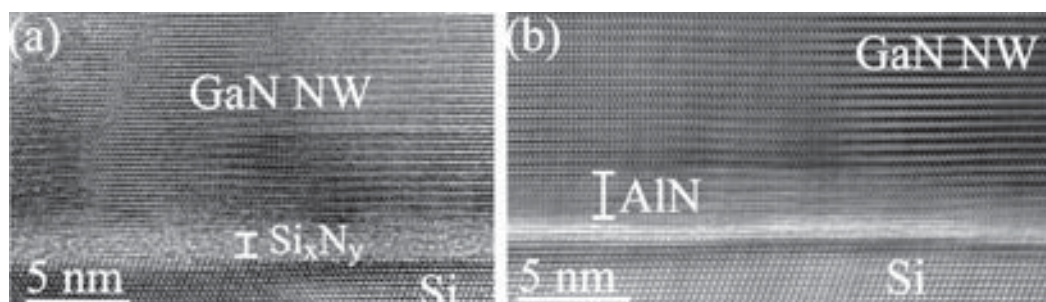


Figure 1: HRTEM images of the GaN/Si interfacial area, when (a) a 0.2 nm AlN IL was deposited prior to NWs growth, and (b) a 2 nm as-grown AlN IL was used.

Acknowledgments Research co-financed by the European Union (ESF) and Greek national funds - Research Funding Program: THALES, project “NanoWire”.

* tkouk@physics.auth.gr

Size dependence of ultrafast electron dynamics and nonlinear optical response of γ -Fe₂O₃ nanoparticles

N. Liaros¹, S. Couris

*Department of Physics, University of Patras, 26504 Patras, Greece
Institute of Chemical Engineering Sciences (ICE-HT), Foundation for Research
and Technology, Hellas, 26504 Patras, Greece*

During the last two decades, transition metal oxides (TMO) provided a novel platform for the study of several emerging complex phenomena, such as colossal magneto resistance, superconductivity, ferroelectricity etc. [1] Among them, γ -Fe₂O₃ Magnetic Iron Oxide Nanoparticles (MIONS) comprise an important class of nano-sized particles showing unique physical properties (i.e. magnetic and electronic), strongly dependent on the particle size, shape and surface morphology. [2] In this work, we report on the ultrafast time-resolved absorption spectroscopy and the third order nonlinear optical properties of novel MIONS coated with poly-acrylic acid-co-maleic acid (pAcMa) and having various sizes ranging from 3 to 14 nm. The nonlinear optical response as well as the ultrafast relaxation dynamics in the different energy and time domains are analysed and associated with the size of the nanoparticles. In particular, as evidenced by Z-scan measurements, [3] the nonlinear optical response decreases with the size of the nanoparticle. Furthermore, the time resolved spectroscopy measurements indicate that the relaxation dynamics shows a clear dependence on the particle size, with the dynamics being accelerated as the size decreases. The combined results of the nonlinear optical and time resolved experiments will be compared and discussed.

References

- [1] N. J. Cherepy *et al.*, J. Phys. Chem. B, 102, 770-776 (1998).
- [2] Y. P. He *et al.*, Phys. Rev. B, 71, 125411 (2005).
- [3] M. Sheik-Bahae *et al.*, IEEE J. of Quant. Electr., 26, 760-769 (1990).

¹ nliaros@iceht.forth.gr

The authors acknowledge support by the European Union (European Social Fund-ESF) and Greek national funds through the Operational Program "Education and Lifelong Learning" of the National Strategic Reference Framework (NSRF)-Research Funding Programs: THALIS (ISEPUMA): Investing in knowledge society through the European Social Fund. D. Potamianos and E. Kakkava are acknowledged for their assistance.

Structural properties of inclined GaN nanowires

A. Lotsari*, G. P. Dimitrakopoulos, Th. Kehagias, Ph. Komninou
Physics Department, Aristotle University of Thessaloniki, 541 24 Thessaloniki, Greece

A. Adikimenakis, A. Georgakilas
Microelectronics Research Group (MRG), IESL, FORTH, P.O. Box 1385, 71110 Heraklion Crete, Greece; and Physics Department, University of Crete, Heraklion Crete, Greece

We present a structural characterization of self-assembled inclined GaN nanowires (NWs) on *r*-plane sapphire grown by plasma-assisted molecular beam epitaxy (PAMBE), under nitrogen rich conditions and excessive substrate nitridation. The size and the density of the NWs are depended in the nitridation conditions. Photoluminescence measurements of these NWs showed excellent crystal quality and strong emission even at room temperature.

The GaN NWs were grown along the *c*-axis subtending a 61° angle to the *r*-plane sapphire substrate as shown in the TEM image of Figure 1. A rough and discontinuous nonpolar *a*-plane GaN thin film was formed between the NWs.

High-resolution transmission electron microscopy (HRTEM) techniques were employed for the elucidation of the grown origin of the NWs. The sapphire nitridation pre-treatment appears to enhance roughness that promotes the nucleation of both nonpolar and semipolar nanocrystals [1,2]. This is further confirmed by the Moiré fringes close to the interface that suggest interfacial areas of different materials overlap. By combining the TEM observations in cross-section and plan-view geometries, the crystallographic model of the NWs was constructed. Convergent-beam electron diffraction (CBED) was employed to identify the polarity of the NWs.

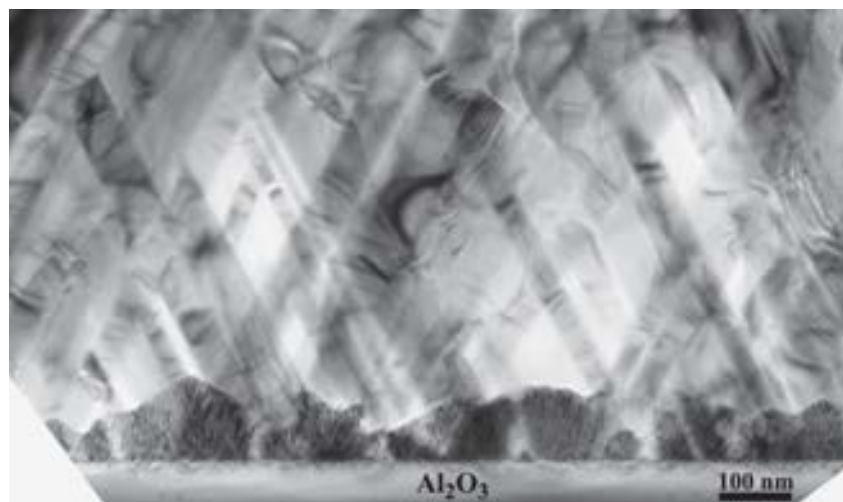


Figure 1: TEM image of the inclined GaN NWs along $[0001]_{\text{a-GaN}} \parallel [1\bar{1}01]_{\text{Al}_2\text{O}_3}$ zone axis. Between the NWs, a rough thin film of nonpolar *a*-plane GaN is formed.

References

- [1] J. Smalc-Koziorowska *et al.*, Applied Physics Letters **93**, 021910 (2008).
- [2] J. Smalc-Koziorowska *et al.*, Journal of Applied Physics **107**, 073525 (2010).

Acknowledgments: Research co-financed by the European Union (ESF) and Greek national funds - Research Funding Program: THALES, project NANOWIRE.

* alotsari@physics.auth.gr

Ultrafast laser-induced processes and processing on semiconductor surfaces at the micro/nano-scale by temporally shaped fs laser pulses

P. A. Loukakos*, E. Stratakis, G. D. Tsiibidis and C. Fotakis

Foundation for Research and Technology – Hellas, Institute of Electronic Structure and Laser, P.O. Box 1385, Heraklion GR-71110, Greece

The application of temporally shaped femtosecond laser pulses in the micro/nano-structuring of semiconductor surfaces is studied experimentally and theoretically. As an initial step towards full pulse shaping, sequences of double pulses with variable temporal spacing in the ps time domain with equal intensity have been used. Craters decorated with nm-sized ripples are formed following the laser-surface interaction depending on the irradiation conditions. The area, depth and strikingly the ripple periodicity show a dependence on the temporal delay between the individual components of the double pulses for the examined semiconductor surfaces, namely Si (Fig. 1) and ZnO.

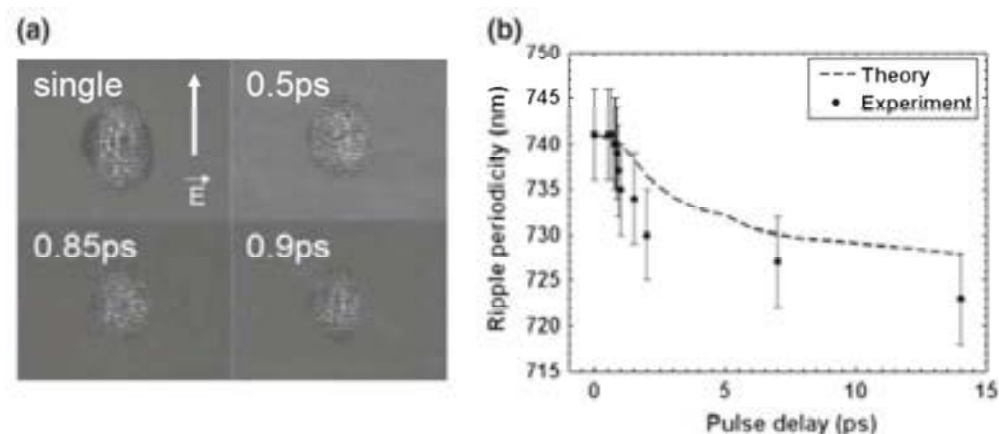


Figure 1: (a) Ripples generated on Si surfaces resulting from Laser-Plasmon interference, shown for different inter-pulse delay times. (b) The ripple periodicity exhibits a dependence (decrease) on the (increasing) temporal distance between the two components of the double femtosecond laser pulse sequences.

Our analysis and explanation for the dependence of the micro and nano-morphological features on the pulse delay is based on our recently developed theoretical model that combines the laser-triggered ultrafast excitation and relaxation mechanisms on a semiconductor surface such as carrier excitation, ultrafast carrier-lattice energy exchanges and energy transport along with the slower phenomena of melting, the corresponding hydrodynamics and re-solidification that follow until the final surface morphology is established. The details of our model and our recent experimental investigations on laser-irradiated Si and ZnO surfaces will be discussed [1-4].

References

- [1] G. D. Tsiibidis, M. Barberoglou, P. A. Loukakos, E. Stratakis, and C. Fotakis, *Phys. Rev. B* **86**, 115316 (2012).
- [2] M. Barberoglou, D. Gray, E. Magoulakis, C. Fotakis, P. A. Loukakos, and E. Stratakis, *Opt. Express* **21**, 18501 (2013).
- [3] M. Barberoglou, G. D. Tsiibidis, D. Gray, E. Magoulakis, C. Fotakis, E. Stratakis, and P. A. Loukakos, *Appl. Phys. A* **113**, 273 (2013).
- [4] G. D. Tsiibidis, E. Stratakis, P. A. Loukakos, and C. Fotakis, *Appl. Phys. A* **114**, 57 (2014).

*loukakos@iesl.forth.gr

Aqueous corrosion of Ni-Al Composite Coatings by Combustion-Assisted Flame Spraying

A. Marinou^{1,2}, G. Xanthopoulou¹, G. Vekinis¹, A. Lekatou²

¹Institute of Nanoscience and Nanotechnology, NCSR “Demokritos”, 15310, Athens, Greece

²Univ. of Ioannina, Dept. of Materials Science and Engineering, Ioannina 45110, Greece

A new, cost-efficient and on-site-applicable thermal spraying process for depositing NiAl metallic overlay coatings or bond-coats for high temperature applications has been developed by synthesizing the desired intermetallic phases from base-metals *in-flight* during oxy-acetylene flame spraying. By adjusting the spraying conditions, excellent Ni-Al-based coatings have been achieved on various substrates, including mild steel, stainless steel and aluminium alloys. The new method is called “Combustion-Assisted Flame Spraying”, (“CAFSY”) and its viability has been demonstrated at a pre-industrial level for coating various metallic parts. The Ni-Al-based coatings produced by CAFSY exhibit very high integrity with good adhesion, very low porosity, high surface hardness and high erosion resistance at a substantially lower cost than equivalent coatings using ready alloy powders, since they are made using only simple oxy-acetylene flame spraying. Thermal treatment of the coatings after spraying (fig. 1b) results in increased concentration of hard intermetallic phases (e.g. NiAl) in comparison with coatings without thermal treatment (fig.1a), at least equivalent to coatings produced by plasma spraying.

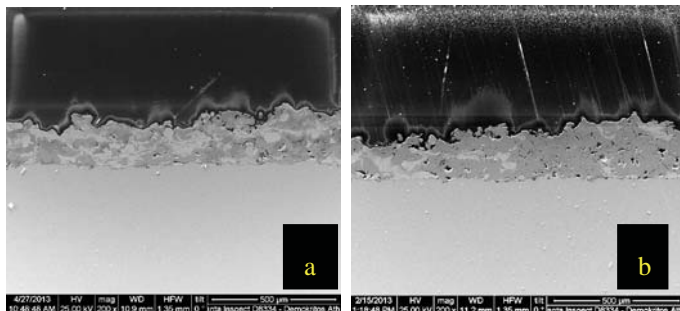


Figure 1. SEM of the coating a) without and b) with thermal treatment of the coating after thermal spraying. The enrichment of the NiAl phase (grey) is evident

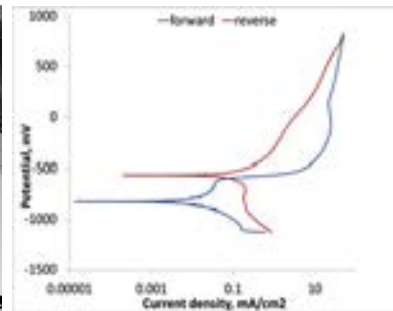


Figure 2. Electrochemical behavior of a NiAl coating in 3.5% NaCl

The coatings have been characterized by measurement of their adhesion strength, air-born erosion, etc, as well as aqueous corrosion. The corrosion performance of the coatings in 3.5% NaCl, at 25 °C was measured by potentiodynamic polarization, chronoamperometry followed by SEM/EDS analysis. Extended immersion of the materials in 3.5% NaCl induces a multiple stage passivation/pseudopassivation, as indicated by the large passive current density. The current density corresponding to the reverse anodic polarization scan was lower than the current densities during the forward anodic polarization scan, as shown in Figure 2. This indicates that these coatings exhibit a high resistance to localized corrosion in 3.5% NaCl.

The work is continuing with adaptation of the CAFSY method for industrial use and for coating other types of intermetallics.

Comparative SERS and UV-Visible measurements for low concentration detection of biocidal groups

G. Mathioudakis^{1,2*}, A. Soto Beobide¹, G. A. Voyiatzis¹

¹FORTH/ICE-HT, P.O. Box 1414, GR-265 04, Rio-Patras, Greece

²Department of Chemistry, University of Patras, GR-265 00, Patras, Greece

Raman spectroscopy is widely applied for analytical studies since it combines high selectivity and ability to analyse materials with no prior sample preparation. Surface Enhanced Raman spectroscopy (SERS) might be a more valuable detection method because it is a very sensitive technique manifested as an enhancement by many orders of magnitude of the intensity of Raman radiation by molecules in the immediate vicinity to nano-rough metal surfaces and nano-structured metal systems such as nanocolloid clusters of noble metals. A novel surface enhanced Raman scattering excitation/collection configuration with a new oscillating cell combined with right angle scattering collection geometry has been recently introduced [1]. The present work constitutes an attempt to introduce SERS in the monitoring of release processes of biocidal analytes and to compare the detection limits obtained by this method with a most traditional and common technique used in quantitative analysis controlled release as UV-Vis absorption. These analytes are novel polymeric materials with enhanced and controllable antifouling properties, which are promising for potential applications in the field of “clean” surfaces, either for sanitary purposes or as antifouling paints.

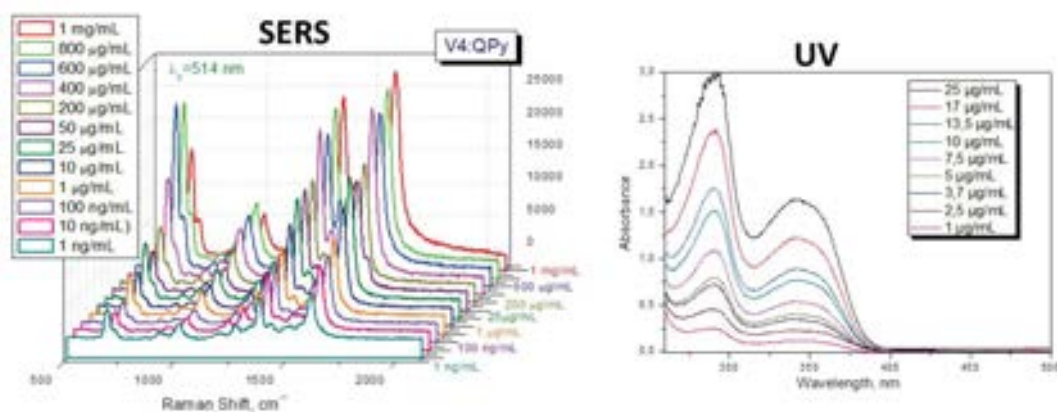


Figure 1: Comparison of the low concentration (detection limits) for the same biocidal analyte using UV-Vis spectroscopy (1 µg/mL) and SERS (1 ng/mL)

Acknowledgement: This research has been co-financed by the European Union (European Social Fund – ESF) and Greek national funds through the Operational Program "Education and Lifelong Learning" of the National Strategic Reference Framework (NSRF) - Research Funding Program: THALES. Investing in knowledge society through the European Social Fund. “Development of Novel Functional Copolymers and Surfaces with Permanent and/or Controlled released biocidal species” (MIS: 379523).

References

[1] A.C. Manikas, A. Soto Beobide, G.A. Voyiatzis, *Analyst* 134 (2009) 587.

* mathiou@iceht.forth.gr

Modelling of 3D Nanographene

C. Mathioudakis*, P.C. Kelires

*Research Unit for Nanostructured Materials Systems,
Department of Mechanical and Materials Science Engineering,
Cyprus University of Technology,
P.O. Box 50329, 3603 Lemesos, Cyprus*

In the low-density regime of carbon materials, nanoporous formation along with nanostructuring and coexistence of various hybridizations give rise to three-dimensional (3D) structures with outstanding properties. Carbon nanofoams (CNFs) belong to this class of materials. They are open, random and light structures resembling a foam. We have recently studied [1]. CNFs made up of schwarzites, nanostructures with negative Gaussian curvature. Here, we investigate another form of this exciting material - the 3D Nanographene (3D-NG) - which is made of graphene nanoflakes. This 3D randomly interconnected structure offers an alternative route for promising applications. Our studies are based on Monte Carlo simulations for the network formation, followed by tight-binding molecular dynamics simulations for full relaxation and calculation of the mechanical and optoelectronic properties. We find that 3D-NG is rigid, despite its porous nature, so it can be utilized in applications (catalysis, tribology, energy storage) as thin films. It, also, exhibits high conductivity, approaching that of single-layer graphene, and high optical absorptivity. Similar properties are exhibited by the CNT foams. This makes this 3D manifestation invaluable for applications in electronics and optics.

References

- [1] C. Mathioudakis and P. C. Kelires, *Phys. Rev. B* **87**, 195408 (2013).

* c.mathioudakis@cut.ac.cy

The influence of epitaxial strain on the structure of iron oxide thin films on Pt(111) and Ru(0001)

N. Michalak¹, Z. Miłosz¹, M. Lewandowski^{1,2*}, R. Ranecki¹, S. Jurga², T. Luciński¹

¹ *Institute of Molecular Physics, Polish Academy of Sciences, M. Smoluchowskiego 17, 60-179 Poznań, Poland*

² *NanoBioMedical Centre, Adam Mickiewicz University, Umultowska 85, 61-614 Poznań, Poland*

* *lewandowski@amu.edu.pl*

FeO(111) grows epitaxially on Pt(111), forming a Moiré superstructure [1]. In case of FeO(111) on Ru(0001), due to significant lattice mismatch and the corresponding epitaxial strain, not only a Moiré superstructure is formed, but also dislocations/domain boundaries appear [2]. FeO(111) is an interface layer used for the growth of thicker iron oxide films, such as Fe₃O₄(111) or α -Fe₂O₃(0001). For Pt(111), the Moiré superstructure does not significantly influence the morphology of Fe₃O₄(111) [1]. In case of Ru(0001), the morphology of Fe₃O₄(111) is complex which is believed to be driven by strain-induced defects in the FeO(111) film.

This work was financially supported by the Polish Ministry of Science and Higher Education (grant No. IP2011 030071 – Ru(0001) part) and the National Science Centre of Poland (grant No. 2012/05/D/ST3/02855 – Pt(111) part).

References

- [1] W. Weiss and W. Ranke, *Progress in Surface Science* **70** (2002), 1.
- [2] K. Ketteler and W. Ranke, *The Journal of Physical Chemistry B* **107** (2003), 4320.

Oxidation study of hafnium nanoparticles through grazing incidence x-ray diffraction

I. Michelakaki*, D. Tsoukalas

*Department of Applied Physics, National Technical University of Athens,
15780 Zografou, GREECE*

Application of nanoparticles is of importance in various fields ranging from electronics to medicine. In our study we are interested to investigate metal oxide nanoparticles as building blocks of resistive memory switches a major candidate of future Non-Volatile Memories. HfO₂ thin films are among the strongest candidates for such memories [1] and investigation of nanoparticles made from this material could be of particular interest towards miniaturization of such devices. Furthermore the switching properties of such memories are affected by the crystallinity of the oxide films. In this context, towards application into resistive memory devices, we conduct a material study which involves fabrication and structure characterization of thin films composed from HfO₂ nanoparticles.

In the present work we examine the synthesis and characterization of HfO₂ nanoparticles obtained after oxidation of Hf nanoparticles that were fabricated by an inert gas condensation method. A vapor of Hf atoms metal is produced by dc sputtering of a hafnium target in a high pressure Ar atmosphere. The high pressure leads to aggregation of the atoms into particles. The particles are forced due to a pressure difference to enter a deposition chamber, where they soft land on the substrate. This method allows the fabrication of Hf nanoparticles with mean diameter about 5 nm.

The oxidation of the Hf nanoparticles into HfO₂ was performed either during the deposition by a beam of O₂ before they land on the substrate, or after the deposition with heating under O₂ flow to temperatures from 150°C to 600°C. The oxidized nanoparticles films were characterized by grazing incidence x-ray diffraction (GIXRD). This method is introduced as a direct, non-destructive, surface-sensitive technique for analysis of thin films. The method can be applied to polycrystalline thin films in order to determine the composition and structure of ultra-thin surface layers.

From the XRD spectra the determination of the conditions for the Hf nanoparticles oxidation was possible. The spectra reveals that oxidation of the Hf nanoparticles into HfO₂ is performed during the deposition of the nanoparticles under O₂ flow without application of temperature. Furthermore oxidation of the nanoparticles after their deposition in oxidizing atmosphere was also possible when the samples were heated to temperatures above 300°C. Also information about the changes in the polycrystalline structure of the HfO₂ nanoparticles film as a function of temperature was obtained. For low oxidation temperature the structure of the nanoparticles film consists of both monoclinic and tetragonal crystal lattices, while for higher oxidation temperatures only the tetragonal structure is observed. Furthermore the increase of the oxidation temperature leads to narrower peaks, which is indicative of the enhancement of the film crystallinity.

The authors would like to acknowledge financial support from research program “Aristeia II” (Grant No. 4543). This research has been co-financed by the European Union (European Social Fund ESF) and Greek national funds through the Operational Program “Education and Life long Learning” of the National Strategic Reference Frame work(NSRF).

References

[1] S. Long et al. ‘Quantum-size effects in hafnium-oxide resistive switching’, Appl. Phys. Lett. 102, 183505 (2013)

*michelakaki.irini@gmail.com

Gas sensing properties and structural characterization of hot-wire porous metal oxides thin films

G. Papadimitropoulos^{a,*}, I. Kostis^b, N. Stathopoulos^b, D. Davazoglou^a

^a NCSR Demokritos, Institute of Nanoscience and Nanotechnology, Greece

^b Department of Electronics, Technological and Educational Institute of Piraeus

The suitability of a material to be used in the fabrication of chemical sensors depends on its ability to return its resistance to its initial state upon removal of the cause that induced the change of its properties. Many materials have been used up to now for the formation of chemical sensors. Among them are a lot of metal oxides like WO₃, Ta₂O₅ and MoO₃ [1, 7]. The above oxides are of great interest and have been investigated extensively owing to their promising physical and chemical properties [2-3]. Many techniques are being used for the fabrication of metal oxides thin films, including thermal evaporation [4], chemical vapor deposition [5] and sputtering [6].

The aim of our research is to examine hot-wire metal oxides (hwMO) thin films as sensory materials in chemical sensors [7] and to investigate their structural properties. These films are deposited very easily compared to other methods by a heated metallic filament under vacuum. This deposition method can be applied for all metallic oxides having higher vapor pressure than the corresponding metal. The deposited oxides are porous [8] and exhibit reversible resistance changes stimulated by their environment; render them suitable for gas sensing applications.

The resistance variations of these configurations caused by changes in their environment were monitored. Reversible changes of resistance, of the order of several KOhms and MOhms, were observed in these metal oxides films caused by the presence or upon removal of gases (H₂ and CO). The magnitude of these changes, related to the sensitivity, was found to depend on hydrogen and carbon monoxide concentration and temperature of measurement (150 °C - 450 °C). The time needed (response time) for the resistance to drop or to rise after gas exposure was found comparable to that needed to recover to its initial value after gas removal. Response times of the order of a few seconds were measured on hwMO films, much shorter than those measured on metal oxides samples deposited by other methods, like chemical vapor deposition [5].

Acknowledgment: Dr. G. Papadimitropoulos acknowledges financial support by IKY FELLOWSHIPS OF EXCELLENCE FOR POSTGRADUATE STUDIES IN GREECE-SIEMENS.

- [1] C.Wang, L. Yin, L. Zhang, D. Xiang, R. Gao, *Sensors*, 10, 2088 (2010).
- [2] C. Sanrato, M. Odziemkowski, M. Ulmann, J. Augustynski, *Am. Chem. Soc.*, 123, 10639 (2001).
- [3] G. C. Granqvist, *Sol. Energy Mater. Sol. Cells*, 60, 201 (2000).
- [4] M W Qu, W Wlodarski, *Sens. Actuators, B* 64 (2000).
- [5] D. Davazoglou, A. Moutsakis, V. Valamontes, V. Psycharis, D. Tsamakis, *J. Electrochem. Soc.*, 144, 595 (1997).
- [6] M. Bendahan, R. Boulmani, L. J. Seguin, K. Aguir, *Sens. Actuators B*, 100, 320 (2004).
- [7] G. Papadimitropoulos, I. Kostis, R. Triantafyllopoulou, V. Tsouti, M. Vasilopoulou, D. Davazoglou, *Miroelectronic Eng.*, 90, 51 (2012).
- [8] G. Papadimitropoulos, N. Vourdas, K. Giannakopoulos, M. Vasilopoulou, D. Davazoglou, *Journal of Applied Physics*, 109, 103527 (2011).

*e-mail: gpapad@imel.demokritos.gr

Fe+ Irradiation Effects on Iron Films

K. Papamichail^{1*}, K. Mergia¹, Yves Serruys², Th. Speliotis¹, G. Apostolopoulos¹
and F. Ott³

¹*National Center for Scientific Research "Demokritos", 15310 Athens, Greece*

²*CEA-Saclay – DEN/DMN/SRMP – Laboratoire JANNuS, France*

³*Lab. Léon Brillouin CEA/CNRS Saclay, 91191 Gif sur Yvette Cedex, France*

For fusion energy applications FeCr based steels are candidate structural materials. Understanding the neutron irradiation effects on Fe and FeCr steels is of paramount importance for the development of radiation resistance materials and the implementation of future fusion reactor.

The initial interaction of neutrons with lattice atoms can lead to the production of high energy recoils, known as Primary Knock-on Atoms (PKA). The energy of the incident fusion neutrons is 14 MeV. However, as the neutrons penetrate within the material they lose energy and thus the PKAs of Fe have a range of energies with a mean energy of 490 keV. Consequently, the main part of the damage arising from neutron or other ions irradiation is due to energetic Fe atoms which create the radiation damage cascades. This phenomenon can be studied by employing Fe ion irradiation of Fe or FeCr alloys. Since the penetration of 490keV energetic Fe ions is 400 nm, thin films need to be investigated. By the selection of the film thickness, radiation damage and implantation can be introduced in the film.

The aim of the current work is to investigate the effects of the two different mechanisms taking place as far as structural and magnetic properties are concerned. Simulations on the interaction of 490 keV Fe+ with Fe films were carried out. The simulations showed that in Fe film thickness of around 50 nm the Fe implantation is negligible whereas the radiation damage considerable, while for 300 nm thickness the implantation is accompanied by radiation damage effects in the film. With this reasoning films of 50 and 300 nm thickness were fabricated. The irradiations were carried out with 490 keV for different irradiation doses.

The structural and magnetic changes prior and after the irradiation were assessed by X-ray diffraction, X-ray reflectivity, magnetometry and polarized neutron reflectivity measurements. No amorphicity is observed even for the highest irradiation dose of 1.3×10^{17} ions/cm². The lattice constant and the grain size present exponential growth as the irradiation dose increases and follow a universal curve.

The irradiation has a drastic effect on the magnetic properties of iron films revealing the different contribution of the two mechanisms. For the case of radiation damage effects, the magnetic moment per atom increases with irradiation dose, changing from 2.1 μ_B /at in the non irradiated film to 2.45 μ_B /at in the film with the maximum irradiation dose of 3.8×10^{16} ions/cm² [1]. This increase is attributed to the creation of vacancy clusters as it is known that the neighbouring and next neighbours Fe atoms of the cluster have increased magnetic moments. When radiation damage and implantation effects occur, the magnetic moment varies with depth. For the depth up to which radiation damage is predominant the magnetic moment increases with dose, whereas deeper in the Fe film where the implantation phenomena become significant the magnetic moment decreases with the increase of the irradiation dose.

Acknowledgments: This work was funded by the EU under the contract of Association between EURATOM and the Hellenic Republic Association and was carried out within the framework of the European Fusion Development Agreement.

References

[1] K. Mergia *et al.*, "Polarized neutron reflectivity reveals enhanced moment on Fe⁺ irradiated iron films", LLB, CEA, 2013 Annual Report.

PEO crystallization and dynamics close to SiO₂ surfaces

H. Papananou,^{1,2,*} K. Chrissopoulou,¹ and S. H. Anastasiadis^{1,2}

¹*Institute of Electronic Structure and Laser, Foundation for Research and Technology-Hellas, Heraklion, Crete, Greece*

²*Dept. of Chemistry, University of Crete, Heraklion Crete, Greece*

K. S. Andrikopoulos,³ G. A. Voyiatzis,³ A. Avgeropoulos,⁴ M. Labardi,⁵ D. Prevosto⁵

³*Institute of Chemical Engineering Sciences, Foundation for Research and Technology-Hellas, Patras, Greece*

⁴*Dept. of Materials Science Engineering, Univ. of Ioannina, Ioannina, Greece*

⁵*CNR-IPCF, Department of Physics, University of Pisa, Pisa, Italy*

Addition of nanosized inorganic materials in a polymeric matrix results to nanohybrids with optimized properties with respect to the initial components. On the other hand, the behaviour of polymers when they are restricted in space or when they are close to surfaces can be very different from that in the bulk. In this work, we investigate the morphology, crystallization and dynamics of a hydrophilic, semi-crystalline polymer, poly(ethylene oxide), PEO, when mixed with silica, SiO₂, nanoparticles in a broad range of compositions. The good dispersion of the nanoparticles was verified by Transmission Electron Microscopy (TEM), whereas the morphology and crystallization behaviour of the hybrids were investigated with, X-ray diffraction (XRD), Fourier Transform Infrared Spectroscopy (FTIR) and Differential Scanning Calorimetry (DSC). All techniques show a gradual decrease of polymer crystallinity with increasing the amount of nanoparticles; nevertheless, polymer crystallization is observed for all silica loadings. Moreover, DSC measurements showed the existence of two melting and crystallization transitions in hybrids with polymer content lower than 50wt%, indicating that the polymer crystallizes differently than the bulk near the silica surface.

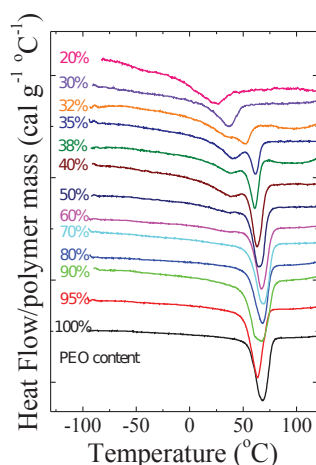


Figure 1: DSC thermograms of PEO/silica nanohybrids with varying polymer content

The effect of the proximity to the silica surface on polymer dynamics was investigated with Broadband Dielectric Spectroscopy, (BDS) as well. The dynamic behaviour of hybrids with different composition is compared with the respective of the bulk polymer and with the one of nanohybrids comprised of a different additive i.e. layered silicates. In the latter case, the effect of the size and geometry of the additive is examined.

This work was performed in the framework of PROENYL research project, Action KRIPIS, project MIS-448305 (2013SE01380034), funded by the General Secretariat for Research and Technology, Ministry of Education, Greece and the European Regional Development Fund (Sectoral Operational Programme: Competitiveness and Entrepreneurship, NSRF 2007-2013)/ European Commission and the COST Action MP0902-COINAPO (STSM-MP0902-14971).

hellpap@iesl.forth.gr

Chemical functionalization of carbon nanomaterials for magnetic drug delivery applications

S. Papazoglou¹, S. Samothrakitis¹, I. Theodorakos¹, I. Zergioti^{1*}
¹National Technical University of Athens, Physics Department, Iroon Polytehneiou 9, 15780 Zografou, Athens, Greece

A. Ntziouni², K. Kordatos²
²National Technical University of Athens, Department of Chemical Engineering, Iroon Polytehneiou 9, 15780 Zografou, Athens, Greece

A. Klinakis³
³Biomedical Research Foundation Academy of Athens, 4 Soranou Ephessiou St., 115 27, Athens, Greece

Carbon nanomaterials have attracted major interest, due to their unique mechanical and electrical properties, for drug delivery applications. In particular, CNTs offer the ability to chemically functionalize their surface, by covalent or non covalent bonding approaches between CNTs and other materials of interest. In this context, iron nanoparticles originated from magnetite (Fe_3O_4), were attached on the multi-walled carbon nanotube's (MWCNTs) outer core, aiming to form a magnetically controlled nano-platform. [1] The nanoparticles dispersion and binding yield were also studied, so as to achieve an homogeneous distribution of iron nanoparticles across the nanotube surface and minimize their aggregation in larger agglomerates, which could lead to the formation of thrombus, thus blocking the blood flow. In a later stage, the nano-platform will be also equipped with antibodies for the identification of surface proteins expressed in tumour sites, fluorescent molecules for visualization and chemotherapeutic drugs.

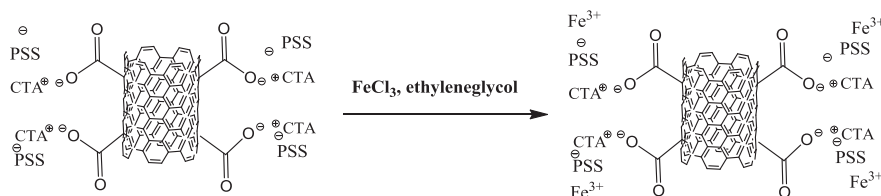


Figure 1: Last step of the CNTs functionalization approach with iron nanoparticles.

References

[1] M. Lewin, et al., *Nature Biotechnology*, **4**, pp. 410-414, (2010).

* zergioti@central.ntua.gr

Atomistic Molecular Dynamics simulation study of a hybrid Poly (ethylene oxide) / Silica nanoparticle system

V.S. Petrakis^{*1}, A.N. Rissanou³, V. Harmandaris^{2,3}

K. Chrisopoulou³, S. Anastasiadis^{1,3}

1. Department of Chemistry, University of Crete, Heraklion, Greece

2. Department of Mathematics and Applied Mathematics, University of Crete, Heraklion, Greece

3. IACM / FORTH & IESL / FORTH, Heraklion, Greece.

The goal of the present work is to study hybrid poly (ethylene oxide), PEO, silica nanoparticle systems. Poly (ethylene oxide), PEO, is a non-ionic, water - soluble, semi crystal polymer with many applications due to its flocculent, thickening, sustained-release, lubrication, dispersing and water-retention properties. Its hydrophilicity, biocompatibility, and versatility make it attractive as biomaterial as well. Additionally, PEO nanocomposites with non-crystalline nanoparticles are of important technological interest. [1-3]

In this work we perform detailed atomistic Molecular Dynamics simulations on a hybrid system of PEO with a Silica nanoparticle, in order to study and understand the structural and dynamical properties of the hybrid system. In more detail we directly calculate the density profile, chain conformations, segmental and terminal dynamics of PEO chains as a function of distance from the silica nanoparticle. [4-5] In a further step we will compare the simulation results to experimental data.

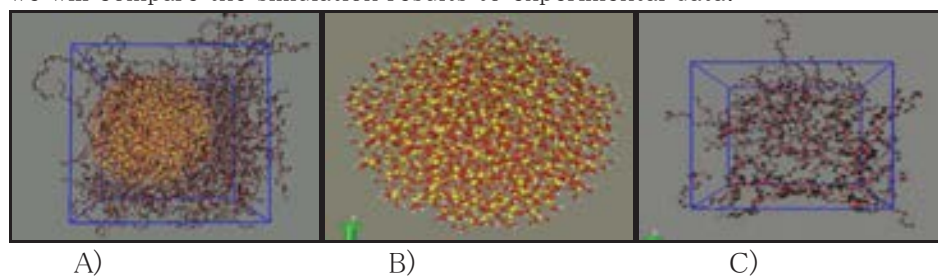


Figure 1:A) Snapshot from a hybrid PEO/Silica nanoparticle system B) snapshot from a Silica nanoparticle C) snapshot from a PEO bulk

References

- [1] B.Hong , F.Escobedo,A.Z.Panagiotopoulos, Journal of chemical engineering data **55**, 4273(2010)
- [2] B.Hong and A.Z.Panagiotopoulos, Journal of Physical chemistry B **116** , 2385(2012)
- [3] S.Anastasiadis, K.Chrisopoulou, K.S.Andrikopoulos, S.Fotiadou, S.Bollas, C.Karageorgaki, D.Christofflos,G.A.Voyiatzis , Macromolecules **44** , 9710(2011)
- [4] M.Doxastakis and Y.N.Pandey journal of chemical physics **136**, 94901(2012)
- [5] A.N.Rissanou and V.Harmandaris , Soft Matter **10** , 2876(2014)

Micro and Nanostructure of Mg₂Si after Ageing

G.S. Polymeris^{(1,2)*}, E.C. Stefanaki⁽¹⁾, C.B. Lioutas⁽¹⁾, K. Mars⁽³⁾, E. Godlewska⁽³⁾,
A. Burkov⁽⁴⁾, M. Fedorov⁽⁴⁾, E. Hatzikraniotis⁽¹⁾, K.M. Paraskevopoulos⁽¹⁾

¹ *Solid State Physics Section, Physics Department, Aristotle University of Thessaloniki, 54124 Thessaloniki, Greece*

² *Institute of Nuclear Sciences, Ankara University, 06100 Beşevler, Ankara, Turkey*

³ *AGH University of Science and Technology, Faculty of Materials Science and Ceramics, Al. A. Mickiewicza 30, 30-059 Krakow, Poland*

⁴ *IOFFE Physical and Technical Institute of the Russian Academy of Sciences, 194021 St Petersburg, Russia*

Due to the rich reserves of the raw materials, along with their low cost and nontoxic nature, Mg₂Si-based compounds are well known as promising thermoelectric materials with moderate temperature operation. Despite the voluminous literature dealing with structural characterization as well as in-homogeneity studies of those materials, there is a lack of reports related to ageing studies, useful for the extensive use. Therefore, the present work provides characterization studies for the binary Mg₂Si doped with 2% Bi.

Long (20mm) bar-shaped samples were subjected to artificial ageing, by keeping its edges at elevated temperature for a prolonged time. Structural characterization was performed by using Electron Microscopy in both Scanning (SEM) coupled with EDS and Transmission (TEM) configurations. Room temperature IR measurements were performed with near normal light incidence in the range of 500-4000cm⁻¹ using a Perkin Elmer i-series microscope, with 100µm iris. Scanning Seebeck and micro-FTIR measurements enable the mapping of dopant content in the samples after ageing.

The aim of this study is the investigation of the effect of thermal treatment on micro/nanostructure of magnesium silicide, as well as on dopant in-homogeneity. Elevated temperature at the edges of the sample cause crystallites that grow in size and thus, the concentration of larger crystallites (of the order of 1µm) was found higher at the edges, while nano-crystals (average size ~15nm) were more numerous at the center of the sample (Fig. 2, 3). The Seebeck coefficient (micro Seebeck scanning) was higher (in absolute values) at the edges of the sample (Fig. 1) in agreement with the lower local free carrier concentration in the same sample following from micro FTIR measurements.

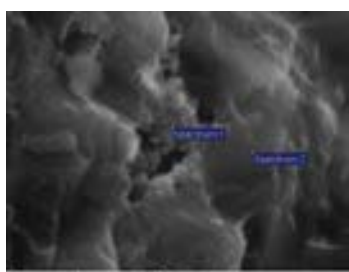


Figure 1 (SEM)

Smaller crystallites are numerous at the center part of the sample. EDS reveal that smaller crystallites have higher Bi content.



Figure 2 (TEM)

Small crystallites (average size ~15nm) are more frequently observed, and are more numerous in the center part than at the edges

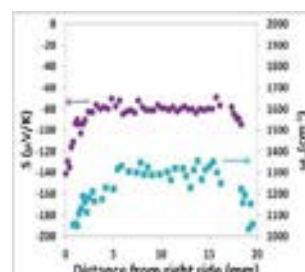


Figure 3 (Seebeck/FTIR)

Seebeck coefficient (S) and plasmon frequency (ω_p) variation along the long axis of the sample, after aging.

* polymers@auth.gr

Raman spectroscopy probes stress transfer efficiency in monolayer graphene/polymer systems

G. Anagnostopoulos¹, C. Androulidakis¹, G. Tsoukleri¹, J. Parthenios^{1,2},
I. Polyzos¹, K. Papagelis^{1,3}, C. Galiotis^{1,2,3*}

¹*Institute of Chemical Engineering and High Temperature Chemical Processes, Foundation for Research and Technology – Hellas (FORTH), P.O. BOX 1414, Patras 265 04, Greece*

²*Interdepartmental Programme in Polymer Science & Technology, University of Patras, Patras 26504, Greece*

³*Department of Materials Science, University of Patras, Patras 26504, Greece*

In this work, we investigate the stress/strain transfer mechanism in simply-supported and embedded graphene flakes on polymer substrates using the 4-point bending approach in tandem with Raman spectroscopy. At each strain level, a mapping (ω_{2D} & ω_G profiles) across specific lines on 1LG flakes is made. As seen (Fig.1), systematic shifts of the ω_{2D} are obtained as one move at steps of 100 nm from the edge of the flake towards the middle. These systematic shifts are evident at all strain levels but also in the as-received material. At 0.00% applied strain, there is almost a constant distribution of ω_{2D} Raman wavenumbers starting from ~ 2600 cm^{-1} for both edges. For the left side and up to 1.5 μm there is no significant shift of ω_{2D} line, while for the right side a similar trend is appeared up to 2.5 μm from the edges but at ~ 2605 cm^{-1} . Within the bulk of the flake, the ω_{2D} line varies up to 5 cm^{-1} . It is a shift, which cannot only be attributed to strains induced by the exfoliation procedure. According to Das et al. [1], the ω_{2D} phonon frequencies are sensitive to electrostatic interactions (in our case probably emanating from the substrate) causing its shifting to higher or lower values depending on doping. The above mentioned fluctuations at the edges, which are more intense at lower levels, are present in all applied strain levels, implying the presence of additional influences, such as doping that occurs via contact with the substrate.

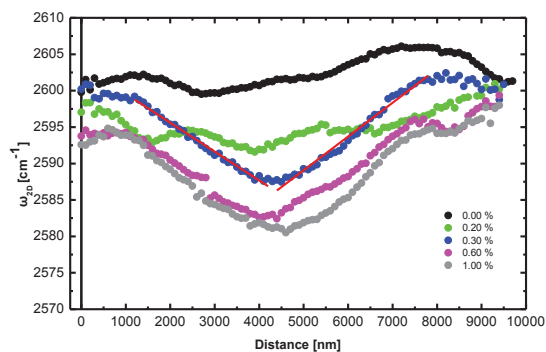


Fig.1: The ω_{2D} distributions for various levels of strain are shown along a sampling line in the simply-supported flake

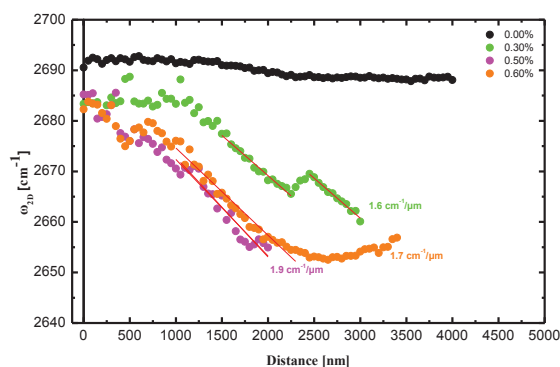


Fig.2: The ω_{2D} distributions for various levels of strain are shown along a sampling line in the embedded flake

In the embedded case (Fig.2), the ω_{2D} shifts clearly to lower wavenumbers as one move from the edge towards the middle of the flake, indicating axial stress transfer through shear at the interface [2]. As in the case of the simply supported specimen some fluctuations of the ω_{2D} values are observed close to edges (< 1.0 μm) particularly at low strain levels.

References

- [1] A. Das, S. Pisana, B. Chakraborty, S. Piscanec, S. K. Saha, U. V. Waghmare, K. S. Novoselov, H. R. Krishnamurthy, A. K. Geim, A. C. Ferrari and A. K. Sood, *Nature Nanotechnology* **3**, pp. 21-215 (2008)
[2] L. Gong, I. A. Kinloch, R. J. Young, I. Riaz, R. Jalil, K. S. Novoselov, *Adv. Mater.* **22**, pp. 2694–2697 (2010)

*Whom all correspondence should be sent to: c.galiotis@iceht.forth.gr

Wavelength dependence of suspended single layer graphene Raman spectra

Ioannis Polyzos^{1*}, John Parthenios¹, Konstantinos Papagelis^{1,2}, [Massimiliano Bianchi](#)³, Roman Sordan³ and Costas Galiotis^{1,4}

¹ *Institute of Chemical Engineering and High Temperature Chemical Processes, Foundation of Research and Technology-Hellas (FORTH/ICE-HT), Patras, Greece*

² *Materials Science Department, University of Patras, Patras, Greece*

³ *L-NESS, Department of Physics, Politecnico di Milano, Polo di Como, Via Anzani 42, 22100 Como, Italy*

⁴ *Department of Chemical Engineering, University of Patras, Patras, Greece*

Graphene is a perfect 2D covalent crystal and forms the basis of all graphitic structures. Due to its inherent properties and the great variety of possible applications graphene has attracted a lot of interest from both experimentalists and theoreticians. Although during the last years a lot of work has been made on supported graphene, there is a lack of experimental research on suspended one. In the present work suspended, mechanically exfoliated, single-layer graphene (SLG) was fabricated. Raman Spectroscopy, a non destructive optical technique, was employed to produce detailed Raman maps of the sample. Raman maps of the frequency distribution and the full width at half maxim of the graphene typical G and 2D peaks, with spatial resolution down to 0.1 μm , are presented. No D-line was observed revealing the good crystal quality. The effect of charge doping and strain on Raman spectra is investigated[1]. Furthermore, the observed spectral shifts and peak profile changes are discussed. The 2D line for suspended graphene found here to have a bimodal profile, as referenced in the literature [2,3]. Three different excitation wavelengths, 488nm, 514.5nm and 785 nm, were used to examine its spectral characteristics dependence on wavelength.

References

- [1] D. Metten, F. Federspiel, M. Romeo, S. Berciaud, *physica status solidi (b)* 250 (2013) 2681.
- [2] S.p. Berciaud, S. Ryu, L.E. Brus, T.F. Heinz, *Nano letters* 9 (2008) 346.
- [3] Z. Luo, C. Cong, J. Zhang, Q. Xiong, T. Yu, *Applied Physics Letters* 100 (2012) 243107.

* ipolyzos@iceht.forth.gr

Acknowledgements: The research project is implemented within the framework of the Action «Supporting Postdoctoral Researchers» of the Operational Program "Education and Lifelong Learning" (Action's Beneficiary: General Secretariat for Research and Technology), and is co-financed by the European Social Fund (ESF) and the Greek State.

Properties of hybrid polymer/gold nanocomposite materials through a classical molecular dynamics approach.

A.J. Power^{*a}, I.N. Remediakis^a, V. Harmandaris^{bc}

^a Department of Materials Science and Technology, Univ. of Crete, 71003 Heraklion, Crete, Greece.

^b Department of Mathematics & Applied Mathematics, Univ. of Crete, GR-71409 Heraklion, Crete, Greece.

^c IACM FORTH, GR-71110 Heraklion, Crete, Greece.

The properties of polyethylene chains around of a gold nanoparticle at a temperature of 450 K are investigated using a combination of density functional theory calculations and classical atomistic simulations. A classical Morse-type potential, used to describe the interaction between the polymer and the gold nanoparticle, was parameterized based on the results of density functional calculations [1]. Several gold nanoparticles with Wulff construction were studied, with diameter ranging from around 2.5-12 nm [2] and polyethylene chains consist of 22 monomers [3]. The structural, conformational, and dynamical properties of the chains were analyzed and compared to the behavior of the bulk polyethylene system. In more detail we report data concerning polymer density profiles, bond order parameter, segmental and terminal dynamics.

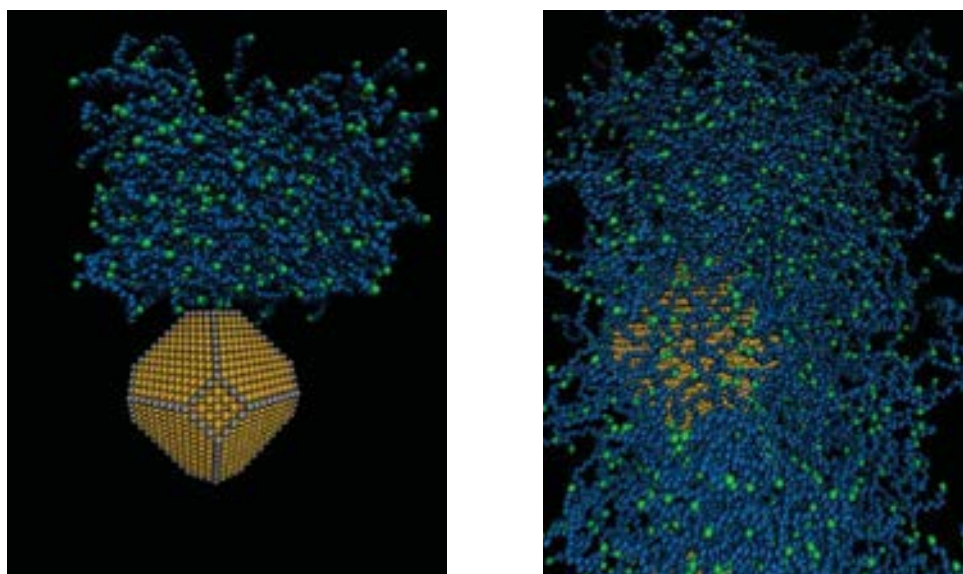


Figure 1: Snapshot from MD simulation of hybrid polyethylene/gold nanocomposite at 450K. Au nanoparticle (3101 atoms, diameter of 5.02 nm) and polyethylene (420 chains, 22-mers per chain) are shown. With yellow is the Au and with grey are the edges of Au nanoparticle. With blue are the CH₂ and with green the CH₃ monomers.

Acknowledgement:



The work of Albert Power was supported by a Scholarship from the **Alexander S. Onassis foundation**.

References:

- [1] K. Johnson, V. Harmandaris, *Soft Matter*, **8**, 6320–6332 (2012).
- [2] G. D. Barmparis, I. N. Remediakis, *Phys. Rev. B*, **86**, 085457 (2012).
- [3] A. Rissanou, V. Harmandaris, *Soft Matter*, **10**, 2876 (2014).

* ajpower@materials.uoc.gr

LPCVD Electrochromic WO₃ Layers on FTO Glass Substrates Using Different Substrate Temperatures

K. Psifis^{*1,2}, D. Louloudakis^{1,3}, G. Papadimitropoulos⁴, D. Davazoglou⁴, N. Katsarakis^{1,2}, C. Savvakis^{1,5}, E. Spanakis⁶, D. Vernardou^{1,2} and E. Koudoumas^{1,2}

¹Center of Materials Technology and Photonics,

Technological Educational Institute of Crete, Greece

²Electrical Engineering Department, School of Applied Technology,

Technological Educational Institute of Crete, Greece

³Department of Physics, University of Crete 711 00 Heraklion, Crete, Greece

⁴NCSR "Demokritos", Institute of Microelectronics, POB 60228, 153 10 Agia

Paraskevi, Attiki, Greece

⁵Mechanical Engineering Department, School of Applied Technology,

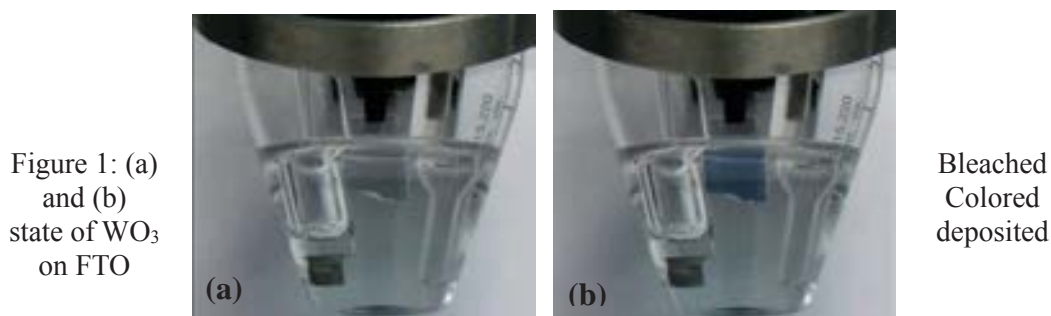
Technological Educational Institute of Crete, Greece

⁶Department of Materials Science & Technology, University of Crete 711 00

Heraklion, Crete, Greece

Electrochromism is a reversible change in a material's optical properties (transmittance, absorbance and reflectance) under an applied voltage. Tungsten trioxide (WO₃) is a material with remarkable electrochromic properties, suitable for application such as solar permeability control in buildings (i.e. smart windows), variable reflectance mirrors and light shutters [1].

Thin films of WO₃ were deposited on Fluorine-doped tin oxide (FTO) coated glass substrates, using low pressure chemical vapor deposition. The structure, morphology and the subsequent electrochromic properties were found to be strongly depended on the growth temperature. The structural and morphological characterization of the samples was performed using x-ray diffraction, Raman spectroscopy and scanning electron microscopy respectively, while, using cyclic voltammetry, their time response from bleached to colored state (Figure 1), as well as the charge involved in the electrochromic process were determined.



References

[1] C.G. Granqvist, Handbook of Inorganic Electrochromic Materials, Elsevier Science, Amsterdam, 1995.

Acknowledgements: This project is implemented through the Operational Program "Education and Lifelong Learning" action Archimedes III and is co-financed by the European Union (European Social Fund) and Greek national funds (National Strategic Reference Framework 2007 - 2013).

* psifiskostas@gmail.com

Interactions of polyaspartic-*b*-poly(ethylene glycol) copolymer with magnetite nanoparticles

I. Rousalis,¹ A. Bakandritsos,^{1*} G. Moudrichas,² S Pispas²

¹University of Patras, Department of Materials Science, Patras, 26504, Greece,

²Theoretical and Physical Chemistry Institute N.H.R.F., Athens, Greece

Surface engineering of magnetite nanoparticles (MNPs) is a key aspect of their effective application as therapeutic and diagnostic systems.[1] The coating should impart high colloidal stability, bio-repellent properties for stealth behavior and drug loading ability. The block copolymer of polyaspartic-*b*-poly(ethylene glycol) (pAsp-*b*-pEG), with the free carboxylates is considered appropriate for coordination on the surface Fe atoms of the MNPs, while it's PEG block secures the high steric stability and low protein bonding (stealthiness).

In this study a pAsp block of 8 monomers and PEG (Mw of 5kDa) was added during or after the synthesis of MNPs. Alkaline precipitation with a single FeII or FeII-FeIII precursors were studied and several synthetic conditions were varied, such as the type and amount of base, metal salt and polymer concentrations. The nanoparticles produced were purified by isolation with centrifugation, and addition of new amount of distilled H₂O, twice. The products were evaluated with colloidal stability assays in neat H₂O and high ionic strength aqueous solutions.

A few pAsp-*b*-pEG derivatized magnetic nanoparticles were identified to be stable for several months in neat H₂O, with hydrodynamic diameters in the range of 100–50 nm. The best performing product regarding stability and size was only obtained after the post-reaction addition of the polymer to the preformed MNPs. Nevertheless the systems were destabilized after two successive washing and redispersion steps. Therefore, an alternative pathway was explored by first synthesizing cationically charged magnetite colloids and following their interaction with the anionic carboxylates of pAsp-*b*-pEG was studied. It was found that this pathway produced assemblies stable not only after successive washings, but in high-ionic media as well. The latter is critical for evaluating the effective PEGylation of the systems.[2]

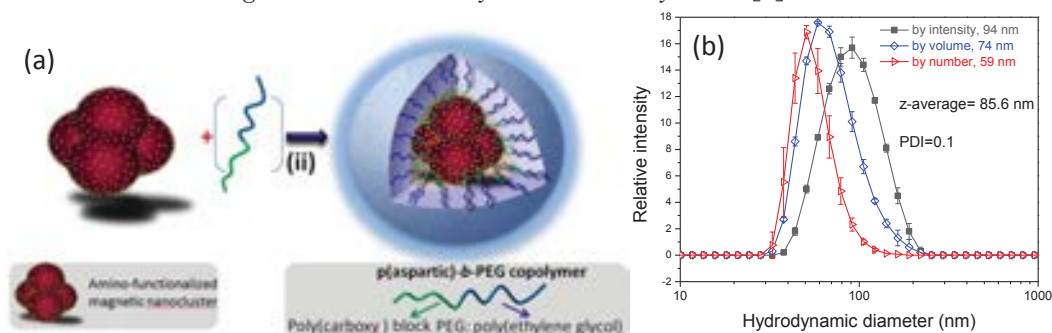


Figure1: (a) Schematic illustration of the probable interaction between cationic magnetic nanoparticles and the anionic block of poly(aspartic-*b*-ethylene glycol) copolymer, and (b) the respective dynamic light scattering results of the assemblies.

References

- [1] Ling, D.; Hyeon, T. Chemical Design of Biocompatible Iron Oxide Nanoparticles for Medical Applications. *Small* **9**, 1450 (2013).
- [2] Honda, S.; Yamamoto, T.; Tezuka, Y. *Nat. Commun.* **4**, 1574 (2013).

Graphene deposited on the top of a highly corrugated polymer substrate

L. Seremetis^{*1}, J. Parthenios¹, C. Galiotis^{1,2} and K. Papagelis^{1,2}

¹*Institute of Chemical Engineering Sciences - Foundation of Research and Technology Hellas, 26504 Patras, Greece*

²*Materials Science Department, University of Patras, 26504, Greece*

Graphene and other materials, structures, and devices are increasingly influenced by surface forces as their size moves into the nm-range. This occurs because (i) the materials are often separated by small distances from the underlying substrate and are sensitive to the operant range of surface forces, (ii) the structural stiffness decreases as its size decreases, and (iii) both the surface forces and structural stiffness scale nonlinearly with relevant dimensions. For example, van der Waals energy between two molecules varies with separation, d , as $1/d^6$ over the range of ~ 1 – 10 nm and then transitions to $1/d^7$ for separations $d > \sim 100$ nm due to retardation effects, and the bending stiffness of a beam varies with thickness, t , as t^3 [1].

Adhesion of graphene with neighboring materials and structures plays an important role in its behavior, both scientifically and technologically. Adhesive interactions are complicated due to the interplay between surface forces and topography.

In this work, the interaction of single graphene layers with the highly corrugated polydimethylsiloxane (PDMS) surface has been examined, by means of Raman spectroscopy and atomic force microscopy (AFM). Initially, AFM images show that the corrugation on PDMS is long-range with a wavelength of about $1.5\mu\text{m}$ and graphene is not fully conformed to the substrate. In fig.1a graphene shows rippling in between hills of the substrate. Using Raman spectroscopy and imaging, a correlation between topography and graphene conformation can be achieved. Particularly, by Raman mapping of high spatial resolution ($\sim 100\text{nm}$ step), it can be concluded that the redshift of either G or 2D Raman bands appear in locations corresponding to the corrugation hills (fig. 1b), where graphene is fully conformed. In locations where graphene partially conforms the redshift of the Raman bands is suppressed.

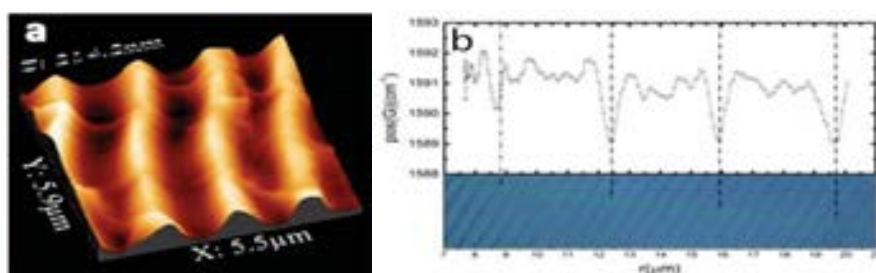


Figure 1: a) AFM image of graphene on corrugated PDMS, b) Raman spatial mapping along the designated line using 514.5nm excitation wavelength.

References

[1] J.S. Bunch, M.L. Dunn, Phys. Solids **152**, (2012) 1359–1364.

Acknowledgement

This research has been supported and financed by a GSRT project (ERC-10), entitled “Deformation, Yield and Failure of Graphene and Graphene-based Nanocomposites”.

* lseremetis@iceht.forth.gr

Ar⁺ bombardment as a tool for controllable defect creation on large scale CVD Single Layer Graphene

Lambrini Sygellou¹, Ioannis Polyzos^{1*}, John Parthenios¹, Konstantinos Papagelis^{1,2} and Costas Galiotis^{1,3}

¹ Institute of Chemical Engineering and High Temperature Chemical Processes, Foundation of Research and Technology-Hellas (FORTH/ICE-HT), Patras, Greece

² Materials Science Department, University of Patras, Patras, Greece

³ Department of Chemical Engineering, University of Patras, Patras, Greece

Ion beam (Ar⁺) bombardment with various energies was used to controllably induce defects into individual graphene specimens. The samples were 1cm² copper chips with single layer graphene on top, produced with the CVD method. Ar⁺ ion irradiation ($P_{Ar} = 3 \times 10^{-6}$ mbar) performed for 12 s in a preparation chamber with ion energies ranging from 36 up to 200eV at an incidence angle of 0° with respect to the normal direction of the sample's surface. After ion bombardment the samples were exposed to H₂ atmosphere. X-ray photoelectron spectroscopy (XPS), ultraviolet photoelectron spectroscopy (UPS) and Raman Spectroscopy (RS) were used to characterize the samples [1-3] before and after the irradiation / H₂ exposure process. Our analysis revealed that the density of defects increases as the irradiation dose increases with the exception of the 36eV ion energy, which stands below the threshold for stable defect creation.

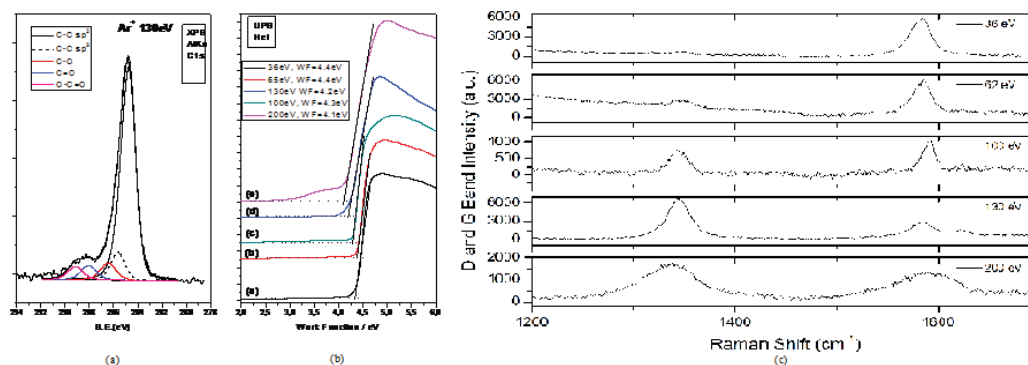


Figure 1 (a) Deconvoluted C1s XP peak for graphene/Cu after 130eV Ar⁺ bombardment, (b), (c) HeI UPS and RS ($\lambda_{exc}=514.5$ nm) for graphene/Cu after 36eV, 65eV, 100eV, 130eV and 200eV Ar⁺ bombardment.

References

- [1] D. Marton, H. Bu, K.J. Boyd, S.S. Todorov, A.H. Al-Bayati, J.W. Rabalais, Surface Science 326 (1995) L489.
- [2] M.M. Lucchese, F. Stavale, E.H.M. Ferreira, C. Vilani, M.V.O. Moutinho, R.B. Capaz, C.A. Achete, A. Jorio, Carbon 48 (2010) 1592.
- [3] L.G. Cançado, A. Jorio, E.H.M. Ferreira, F. Stavale, C.A. Achete, R.B. Capaz, M.V.O. Moutinho, A. Lombardo, T.S. Kulmala, A.C. Ferrari, Nano letters 11 (2011) 3190.

** ipolyzos@iceht.forth.gr

Acknowledgements: This research has been financed by a GSRT project (ERC-10), entitled “Deformation, Yield and Failure of Graphene and Graphene-based Nanocomposites”

Gas Sorption Properties of Microporous Magnesium Formate

Ioannis Spanopoulos* and Pantelis N. Trikalitis

Department of Chemistry, University of Crete, Voutes 71003 Heraklion, Greece

Metal-organic frameworks (MOFs) are crystalline nanoporous materials comprised of metal clusters connected three-dimensionally by multi-topic organic ligands. This hybrid architecture opens the possibility to design and synthesize a great variety of new porous materials.[1] However, many MOFs are sensitive to moisture, limiting in this way their potential utilization in industrial applications. To overcome this problem the use of small, hard metal ions (Mg^{2+} , Al^{3+}) in MOF could lead to air and water stable materials.[2]

We report here the synthesis and gas sorption properties of fully evacuated microporous magnesium formate, $[\text{Mg}_3(\text{O}_2\text{CH})_6]$, a porous 3-D network with 1-D channels. The material exhibits permanent porosity with $496 \text{ m}^2 \text{ g}^{-1}$ BET surface area. Gas sorption studies showed a 1.38 wt% H_2 uptake at 77 K/1 bar, a 2.18 mmol g^{-1} CO_2 at 298 K/1 bar and a high NH_3 uptake of 5.37 mmol g^{-1} at 298 K/1 bar. The framework holds its structural integrity upon various circles of NH_3 adsorption and desorption rendering the material a potential candidate in applications for the removal of harmful gases and contaminants.

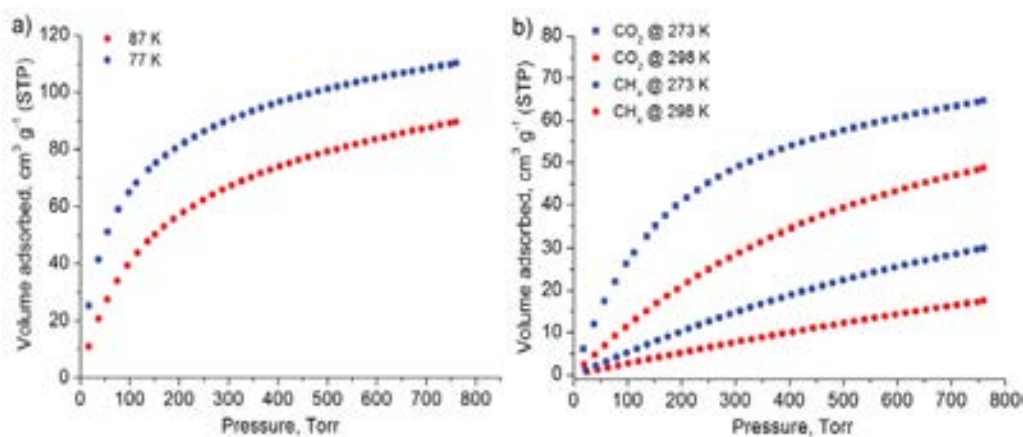


Figure 1. (a) Hydrogen adsorption isotherms at 77 K and (b) CO_2 and CH_4 adsorption isotherms at 273 K and 298 K.

References

- [1] Wang C., Liu D., Lin W., *J. Am. Chem. Soc.* **135**, 13222 (2013).
 [2] McDonald T. M., Lee W. R., Mason J. A., Wiers B. M., Hong C., Long J.R., *J. Am. Chem. Soc.* **134**, 7056 (2012).

* ioaspan@chemistry.uoc.gr

Sensing characteristics of NiO and NiO:Li thin films deposited by sol gel method onto glass substrate

I.Sta^{1,*}, M. Jlassi¹, M. Kandyla³, M.Hajji^{1,2}, P. Koralli³, M. Kompitsas³
and H. Ezzaouia¹

¹ *Laboratoire de Photovoltaïque, Centre de Recherche et des Technologies de l'Energie, Technopole de Borj-Cédria, BP 95, 2050 Hammam-Lif, Tunisie.*

² *Institut Supérieur d'Electronique et de Communication de Sfax, Université de Sfax, BP 868, 3018 Sfax, Tunisie.*

³ *National Hellenic Research Foundation, Theoretical and Physical Chemistry Institute, 48, Vasileos, Konstantinou Ave., 11635 Athens, Greece.*

* email of corresponding author: imenstalpv@yahoo.fr

Abstract

Undoped NiO and NiO doped lithium films fabricated by spin coating method were studied for hydrogen sensing applications. The sensor response was found to depend essentially on four parameters: chemical composition, structure, morphology and operating temperature. The crystallinity and morphology of the as-prepared films were analyzed using X-Ray Diffraction (XRD) and Atomic Force Microscopy (AFM). The sensing properties of NiO and NiO:Li toward H₂ were investigated at different operating temperatures and H₂ concentrations. Optimization of the preparation conditions show that NiO:Li 8% thin films exhibit the highest sensitivity.

Keywords: Nickel Oxide; lithium doping; semiconductor; sol gel method; hydrogen sensors.

Synthesis and characterization of NiO and NiO with Pd nanoparticles on the surface

I.Sta^{1*}, M. Jlassi¹, M. Kandyla³, M.Hajji^{1,2}, P. Koralli³, M. Kompitsas³

and H. Ezzaouia¹

¹ *Laboratoire de Photovoltaïque, Centre de Recherche et des Technologies de l'Energie, Technopole de Borj-Cédria, BP 95, 2050 Hammam-Lif, Tunisie.*

² *Institut Supérieur d'Electronique et de Communication de Sfax, Université de Sfax, BP 868, 3018 Sfax, Tunisie.*

³ *National Hellenic Research Foundation, Theoretical and Physical Chemistry Institute, 48, Vasileos, Konstantinou Ave., 11635 Athens, Greece.*

* email of corresponding author: imenstalpv@yahoo.fr

Abstract

Nickel oxide (NiO) was synthesized by sol gel method and subsequently their surface partially covered by Pd nanoparticles with the aid of PLD for different deposition times. The effect of the Pd nanoparticles on the properties of NiO matrix was investigated. The Structural, morphological, and compositional properties were studied by X-ray diffraction (XRD), atomic force microscopy (AFM), scanning electron microscopy (SEM), and energy dispersive X-ray (EDX) spectroscopy respectively. The optical properties of the films were characterized by UV-visible spectrophotometry. The transmittance of the films decreases as the Pd content is increased. The dependence of the refractive index (n), extinction coefficient (k), and absorption coefficient (α) of the films on the wavelength was investigated. The band gap estimated was to $E_g = 3.88, 3.94$ and 3.91 eV, for NiO, NiO:Pd (1min) and NiO:Pd (2min), respectively.

Keywords: Nickel Oxide; palladium ; sol gel method; PLD.

Novel 3D SiC and BN pillared nanostructures: design principles, electronic and H₂ storage properties.

T. Stergiannakos*, E. Klontzas, G.E. Froudakis
Department of Chemistry, University of Crete, P.O. Box 2208, 71003, Heraklion, Crete, Greece

E. Tylianakis
Department of Materials Science and Technology, University of Crete, P.O. Box 2208, 71003 Heraklion, Crete, Greece

T. Vegge
Department of Energy Conversion and Storage, Technical University of Denmark, Frederiksborgvej 399 Building 238, DK-4000 Roskilde, Denmark

Novel three dimensional Silicon Carbide (SiC) and Boron Nitride (BN) nano-structured materials have been designed, based on Pillared Graphene (PG) architecture [1]. These novel materials, similar to PG, combine graphene-like sheets and nanotubes to form periodic 3D SiC and BN structures. The general Euler's rule for polygons was used to create the junctions that connect the 2D sheets with the nanotubes, by choosing proper combinations of different polygons (three octagons, six heptagons ...). These novel materials present by design interesting features such as versatile geometric characteristics, tunable pore sizes and surface areas. Their structural and electronic properties were investigated by performing DFT calculations, while their Hydrogen adsorption properties were investigated by following a multi-scale theoretical strategy. Our results indicate that SiC-PG and BN-PG act as semiconductors and have better H₂ adsorption properties than carbon PG. This enhancement is attributed to the increased electrostatic nature of H₂ interactions with the consisting atoms of these materials [2][3]. Further enhancement of the H₂ storage characteristics was achieved by doping these materials with metal atoms.

References

- [1] G.K. Dimitrakakis, E. Tylianakis and G.E. Froudakis, *Nano Lett*, **8**, 10 (2008).
- [2] A. Maurantonakis and G.E. Froudakis, *Nano Lett*, **3**, (2003)
- [3] G. Mpourmpakis, and G.E. Froudakis, *Catalysis Today*, **120**, (2007)



This research has been co-financed by the European Union (European Social Fund–ESF) and Greek national funds through the Operational Program "Education and Lifelong Learning" of the National Strategic Reference Framework (NSRF) - Research Funding Program: Heracleitus II. Investing in knowledge society through the European Social Fund

* sterg_t@chemistry.uoc.gr

The synergistic effect of hybrid fillers on the thermomechanical properties of epoxy nanocomposites

A. Z. Stimoniaris*, C.G. Delides

Department of Environmental Engineering, T.E.I. of Western Macedonia, Greece

C. A. Stergiou

Laboratory of Inorganic Materials, Centre for Research and Technology-Hellas, Greece

M. A. Karakassides

Department of Materials Science and Engineering, University of Ioannina, Greece

Nanocomposites show different properties than the bulk polymer matrix because of the small size of the filler and the corresponding increased specific surface area. Additionally, certain polymer nanocomposites based on hybrid fillers have been shown to undergo more substantial improvements in mechanical, thermal, electrical and dielectric properties, than those containing a single filler type. The synergy of fillers, which may even differ in terms of chemical structure, shape and size, seems to play a dominant role on the properties of the composites [1-4]. For our investigation, specimens were prepared by dispersing two types of conductive fillers (CB and/or MWCNTs) and clay in an epoxy matrix, in different proportions. Particularly, we used diglycidyl ether of bisphenol A (DGEBA) resin with triethylenetetramine (TETA) hardener for the host material, while different amounts of CB, amine modified MWCNTs and organomodified nanoclay (Cloisite 30A) were used as fillers. The production procedure is fully presented elsewhere [5]. For the characterization of the nanocomposites, Scanning and Transmission Electron Microscopy (SEM and TEM), Dynamic Mechanical Analysis (DMA), Raman and IR spectroscopy techniques were carried out. It was found that the addition of low amounts of clay into carbon-loaded epoxy nanocomposites can modify several of its properties such as mechanical, electrical, glass transition and crystallization processes. A major parameter explaining these effects is the excluded volume created by the μm -scale clay clusters forming a segregated network of nanoparticles [1].

Acknowledgements

Thanks are expressed to the technician Domna Nalbantidou for her contribution to sample preparation and some of the measurements.

References

- [1]. G. D. Liang, S. P. Bao, S. C. Tjong, *Mater. Science Eng., B*, **142**, 55 (2007).
- [2]. L. Liu, J. C. Grunlan, *Adv. Funct. Mater.*, **17**, 2343 (2007).
- [3]. H. Palza, B. Reznik, M. Wilhelm, O. Arias, A. Vargas, *Macromol. Mater. Eng.*, **297**, 474 (2012).
- [4]. A.B. da Silva, J. Marini, G. Gelves, U. Sundararaj, R. Gregório Jr., R. E.S. Bretasa *Europ. Pol. J.* **49**(10), 3318 (2013).
- [5]. Th.V.Kosmidou, A.S. Vatalis, C.G. Delides, E. Logakis, P. Pissis, G.C. Papanicolaou, *e-xpress Polymer Letters*, **5**(2), 364 (2008).

* adamstimoniaris@gmail.com

Epoxy resin / fly ash composites: Effect of sonication time on thermo-mechanical behavior

A. Z. Stimoniaris^{*}, C.G. Delides

Department of Environmental Engineering, T.E.I. of Western Macedonia, Greece

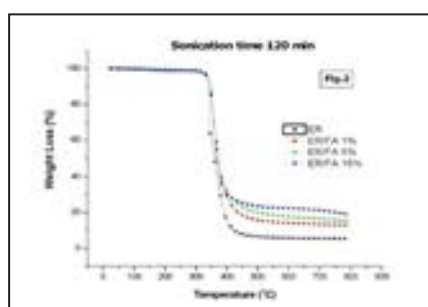
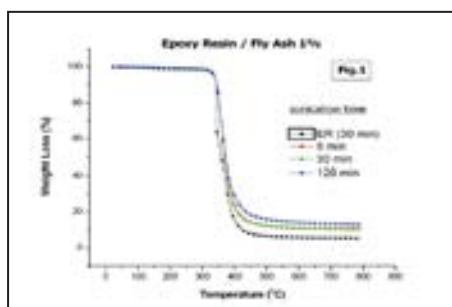
A. Kanapitsas

Department of Electronic Engineering, T.E.I. of Stereas Elladas, Lamia, Greece

H. Zois

Merchant Marine Academy of Epirus Vathi, Preveza, Greece

In this work the thermo-mechanical properties of epoxy resin (ER) composites filled with fly ash (FA) has been investigated [1-3]. Fly ash was produced at the power stations of Kozani region and it is rich in CaO, due to the origin of the burned lignite. When embedded into a polymer matrix, FA appears in the form of aggregates. In order to suppress the possible formation of fly ash agglomerates and/or bundles, high speed shearing for 15 minutes and sonication for 5, 30 or 120 minutes was applied. Fly ash weight content was equal to 1, 2 or 5 %. Several complementary experimental techniques (such as SEM, DMA, DSC and TGA) were employed to study the dispersion of fly ash particulates within the epoxy matrix, the dynamic mechanical behavior and the thermal properties of the composites. SEM examinations reveal that, after longer sonication time, the fly ash morphology changes from a discontinuous set of aggregated clusters to a more homogeneous dispersion of the fly ash particles. It was also found that the storage modulus (E') for the sample with 1% of FA after 120 min of sonication is 16,7% higher than that of the pure epoxy. However, it is slightly affected in the rubbery state. Glass transition temperature (T_g), as estimated by DMA and DSC measurements, is slightly decreasing by increasing the fly ash content and the sonication time. In addition, in the filled samples, T_g is lower than that of the neat resin. These variations could be explained on the basis of deaggregation and better dispersion of the fly ash particulates and to free volume increase due to sonication process. TGA experiments confirm that the incorporation of fly ash inclusions enhances the thermal properties of the epoxy matrix. All the composites studied show good thermal stability for temperatures up to 330 °C with a maximum decomposition temperature higher than 360 °C (Figures 1,2). A small increase to the calculated residual weight (char content) with increasing fly ash concentration is also observed.



Figures 1 and 2: Typical TGA plots for the epoxy resin / fly ash composites

References

- [1]. K.W.-Y. Wong and R.W. Truss, *Compos. Science and Technology*, **52**, 3, 361(1994).
- [2]. J. Gu, G. Wu and Q. Zhang, *Materials Sc. and Engineering: A*, **452**, 614 (2007).
- [3]. I. Ahmad and A. Mahanwam, *Journal of Minerals & Materials Characterization & Engineering*, **9**, 3,183 (2010).

* adamstimoniaris@gmail.com

Pulsed laser assisted decoration of 2D materials with plasmonic nanoparticles

M. Sygletou^{1,2*}, C. Petridis³, E. Kymakis³, C. Fotakis^{1,2}, E. Stratakis^{1,2}

1. Institute of Electronic Structure and Laser, Foundation for Research & Technology Hellas, (IESL-FORTH), P.O. Box 1527, Heraklion 711 10, Greece

2. University of Crete, Heraklion 714 09, Greece

3. Center of Materials Technology and Photonics & Electronic Engineering Department, Technological Educational Institute (TEI) of Crete, Heraklion, 71003, Greece

In recent years, two-dimensional materials (2D) attract the interest of various scientific disciplines because of their unique optical properties and the potential applications of these materials including optical, electrochemical devices and transistors. In our study, we report on an one-step method for effective decoration of graphene, molybdenum disulfide (MoS_2) and hexagonal Boron Nitride (h-BN) 2D layers with plasmonic metallic nanoparticles (NPs). Following single pulse UV laser irradiation of 2D sheets in AgNO_3 or HAuCl_4 solution, Ag and Au NPs are synthesized and grow on the layers' surface, respectively. The obtained plasmonic sheets are characterized by Scanning and Transmission Electron Microscopy as well as Raman and UV-vis spectroscopy. Our method is unique and important since no reducing agent is required in the reaction. The potential application of the synthesized plasmonic sheets in various components in solution processable transparent electronics is envisaged.

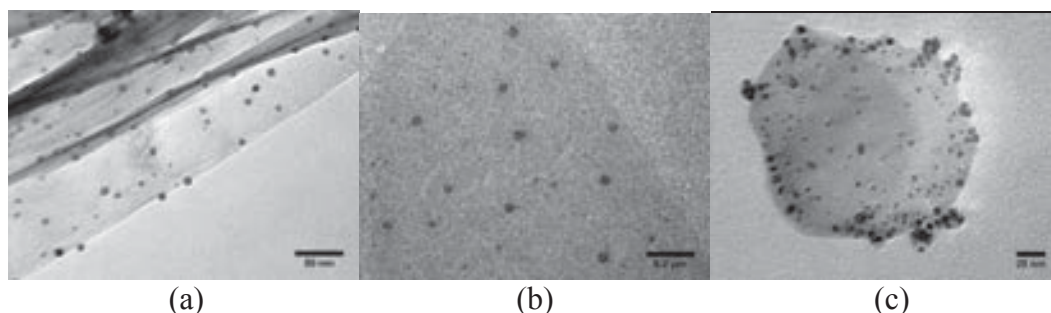


Figure 1 : a) GO_Ag NPs, b) GO_Au NPs and c) BN_Au NPs after single UV pulse laser irradiation

References

- [1]Xianjue Chen *et al.*, Chemical Communications 49, 1160-1162 (2013).
- [2]Hyosung Choi *et al.*, Nature Photonics 7, 732–738 (2013).
- [3]Yazhuo Shang *et al.*, Solid State Sciences 15, 17-23 (2013).

* masyg@iesl.forth.gr

Carbon-Based Nanoporous Networks as Media for the Separation of CH₄/CO₂ Mixtures: A Molecular Dynamics Approach

G. Tamiolakis, I. Skarmoutsos, G. E. Froudakis
Department of Chemistry, University of Crete
P.O.Box 2208, Voutes 71003 Heraklion, Crete, Greece

Gas adsorption and separation are very important processes for industrial and environmental applications. These processes can lead to an important reduce of the release of harmful gases in the environment. Porous solids acting as adsorbents or membrane fillers are playing key roles in capture, adsorptions, separations and purifications of various chemicals that we encounter in our daily activities, directly or indirectly¹. There are several families of porous materials that have been synthesized in the last few years^{2,3}. They exhibit advanced properties, compared to traditional porous materials such as zeolites or polymeric membranes. Carbon based (CB) materials are promising candidates of this kind.

In present work molecular dynamics simulation techniques have been employed to investigate the adsorption and separation of equimolar binary mixture CH₄/CO₂ at ambient temperature, using recently design 3D-carbon-based nanostructure: a 3D Porous Nanotube Network (PNN)⁴. The calculation performed have shown that CO₂ molecules are preferentially adsorbed over CH₄ ones, yielding a very satisfactory selectivity for carbon dioxide. Mean square displacements of CO₂ and CH₄ molecules have also been calculated predicting higher diffusivities for CH₄ molecules inside the PNN compared to CO₂ ones, but significantly lower than in bulk gas mixture⁵.

The results obtained signify that rational design of novel CB nanostructured porous networks might lead to the development of promising candidates for CH₄/CO₂ separation.

References

1. A. Samanta, A. Zhao, G.K.H. Shimizu, P. Sarkar, R. Gupta, *Industrial & Engineering Chemistry Research* **51** 1458-1463 (2012)
2. J. Li, R.J. Kuppler, H.C. Zhang, *Chemical Society Reviews* **38** 1477-1504 (2009)
3. X. Zhang, X. Shao, W. Wang, D. Cai, *Separation and Purification Technology* **74** 280-287 (2010)
4. E. Tylianakis, G.K. Dimitrakakis, S. Melchor, J.A. Dobado, G.E. Froudakis, *Chemical Communications* **47** 2303-2305 (2011)
5. I. Skarmoutsos, G. Tamiolakis, G.E. Froudakis, *Journal of Physical Chemistry C* **17** 19373-19381 (2013)

This research has been co-financed by the European Union (European Social Fund – ESF) and Greek national funds through the Operational Program "Education and Lifelong Learning" of the National Strategic Reference Framework (NSRF) - Research Funding Program: THALES



Adsorption and Electrochemical Behaviour of Cyt-c on Transparent Mesoporous TiO₂ Films

C. Tiflidou, E. Topoglidis*

Department of Materials Science, University of Patras, Rion 26504, Greece

The immobilization of biomolecules upon electrodes and other surfaces is important not only for studying their function and structure but also for the development of bioanalytical devices such as biosensors. We investigate in this study the use of mesoporous optically transparent TiO₂ films as substrates for protein immobilization.

TiO₂ films with developed mesoporous architecture are among the best candidates as host matrices for the incorporation of various optoelectroactive guest molecules. The films have a high surface area, are optically transparent, exhibit good electrical conductivity (wide bandgap ~ 3.2 eV) and can be prepared by low cost screen printing technologies for the development of dye sensitized solar cells, electrochromic displays, electrode devices and colorimetric chemical sensors.

Therefore in this study, their ability to provide a novel and versatile immobilization surface for biomolecules and the development of an amperometric biosensor for H₂O₂ will be examined. The resulting TiO₂ films were structurally characterized by a variety of techniques such as SEM (see figure 1), TEM, XRD and BET analysis. In addition a thorough study of the binding of Cytochrome-c upon them [1] and the parameters that influence its adsorption are presented. [2] Finally, with the use of a 3-electrode electrochemical cell, electrochemical techniques such as cyclic voltammetry and spectroelectrochemistry (see figure 2) were used in order to investigate the electrochemical behavior of the immobilized biomolecules and their potential use for the development of an electrochemical biosensor for H₂O₂.

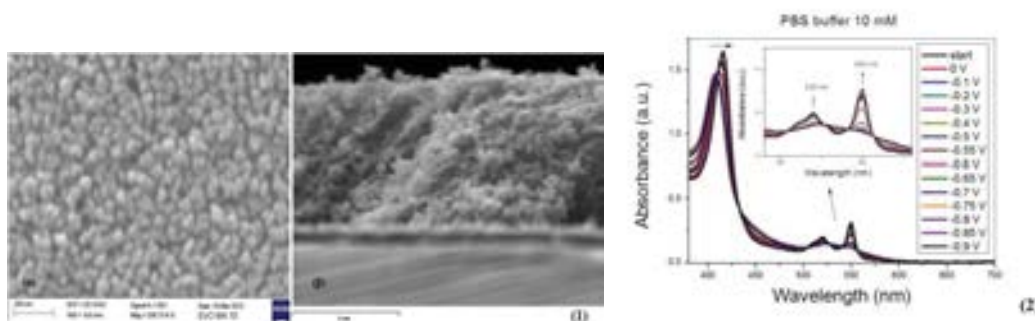


Figure 1: SEM images of TiO₂ thin film (top view and cross section).

Figure 2: Spectroelectrochemical study of Cyt-c/TiO₂ in PBS buffer 10 mM, pH 7.

References

- [1] C. Renault, V. Balland, E. Martinez-Ferrero, L. Nicole, C. Sanchez and B. Limoges, *Chem. Commun.*, 7494 (2009).
- [2] C. Tiflidou and E. Topoglidis, *Colloids and Surfaces B: Biointerfaces*, in preparation (2014),
- [3] E. Topoglidis, A. E. G. Cass, B. O'Regan, J. R. Durrant, *Journal of Electroanalytical Chemistry* **517**, 20 (2001).

* etop@upatras.gr

Gas Sorption Properties of New Mesoporous, Functionalized MOFs

Constantinos Tsangarakis*, Ioannis Spanopoulos and Pantelis N. Trikalitis

Department of Chemistry, University of Crete, Voutes 71003 Heraklion, Greece

Metal organic frameworks (MOFs) are a novel class of porous nanomaterials, containing both an organic and an inorganic part. Ultra high porosity and tunable functionalization of MOFs render them unique candidates for numerous applications.[1] Among them, gas-storage applications are considered very important especially for CO₂ and CH₄. [2] For these particular applications, MOFs with unsaturated metal sites and organic linkers functionalized with strong polarizing groups are considered very promising due to enhanced gas-framework interaction.[3] Mg-MOF-74, a material containing 1-D hexagonal channels and unsaturated metal sites, has shown a remarkable CO₂ uptake of 35.2 wt %, at 1 bar and 296 K.[4] Therefore, incorporation of polar functional groups into MOF-74 can further enhance its CO₂ uptake. We have successfully synthesized and characterized a series of expanded, mesoporous functionalized MOF-74 (Zn²⁺, Co²⁺, Mn²⁺, Mg²⁺) analogues. Detailed and extensive gas sorption properties will be presented and discussed.

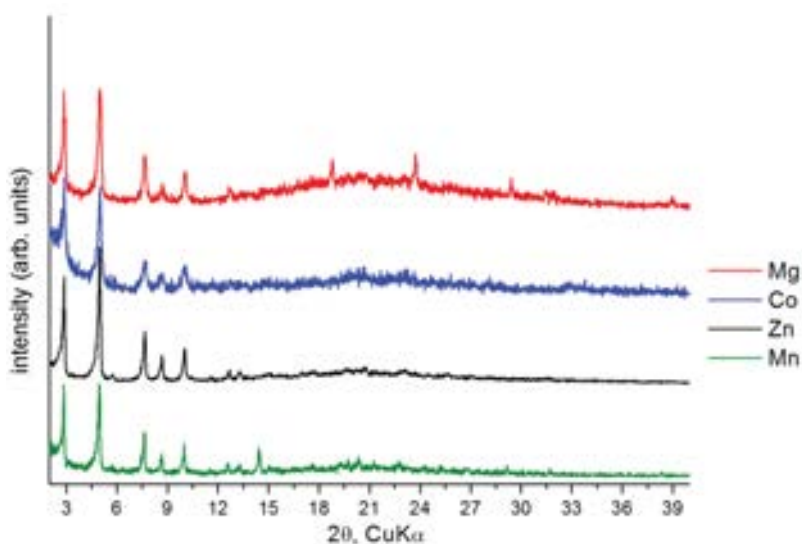


Figure 1. Powder X-Ray diffraction patterns of the as synthesized materials.

References

- [1] Kuppler R.J., Timmons D.J., Fang Q.-R., Li J.-R., Makal T.A., Young M.D, Yuan D., Zhao D., Zhuang W., Zhou H.-C., *Coord. Chem. Rev.* **253**, 3042 (2009).
- [2] Yang D.-A., Cho H.-Y., Kim J., Yang S.-T., Ahn W.-S., *Energy Environ. Sci.* **5**, 6465 (2012).
- [3] Xydias P., Spanopoulos I., Klontzas E., Froudakis E. G., Trikalitis N. P., *Inorg. Chem.* **53**, 679 (2014).
- [4] Caskey S. R., Wong-Foy A. G., Matzger A.J., *J. Am. Chem. Soc.* **130**, 10870 (2008).

* ktsagaros@chemistry.uoc.gr

Fundamentals of surface modification after irradiation of silicon with ultrashort laser pulses

G. D. Tsididis^{1*}, P. A. Loukakos¹, E. Stratakis^{1,2}, C. Fotakis^{1,3}

1) Institute of Electronic Structure and Laser (IESL), Foundation for Research and Technology (FORTH), N. Plastira 100, Vassilika Vouton, 70013, Heraklion, Crete, Greece

2) Department of Materials Science and Technology, University of Crete, 710 03 Heraklion, Crete, Greece.

3) Physics Department, University of Crete, Heraklion 71409, Crete, Greece

* tsibidis@iesl.forth.gr, phone: 00302810391912, fax: 0030-2810391569

Material processing with femtosecond (fs) pulsed lasers has received considerable attention over the past decades due to its multiple diverse applications ranging from micro-device fabrication to optoelectronics, microfluidics and biomedicine. Rapid energy delivery and reduction of the heat-affected areas are the most pronounced advantages and in view of the abundant applications a thorough knowledge of the fs laser interaction with the target material is required for enhanced controllability of the structuring process. The fundamentals of the physical mechanisms and simulation techniques are employed to conduct a thorough investigation of ultrashort pulsed laser induced surface modification due to conditions that result in a superheated melted liquid layer and material evaporation. The novel proposed theoretical model aims to address the laser-material interaction in conditions which lead to mass removal in combination with a hydrodynamics-based scenario of the crater creation and ripple formation following surface irradiation (Fig.1a) with single and multiple temporal separated pulses [1, 2]. The development of periodic structures (Fig.1b) with an orientation perpendicular to the electric of the laser beam is based on a synergy of electron excitation and capillary wave solidification and the interference of the incident wave with a surface plasmon wave [3]. The theoretical framework aims to offer a thorough elucidation of laser-matter interaction fundamentals and facilitate production of well-defined micro/nanostructures (Fig.1c) with preferable optical properties.

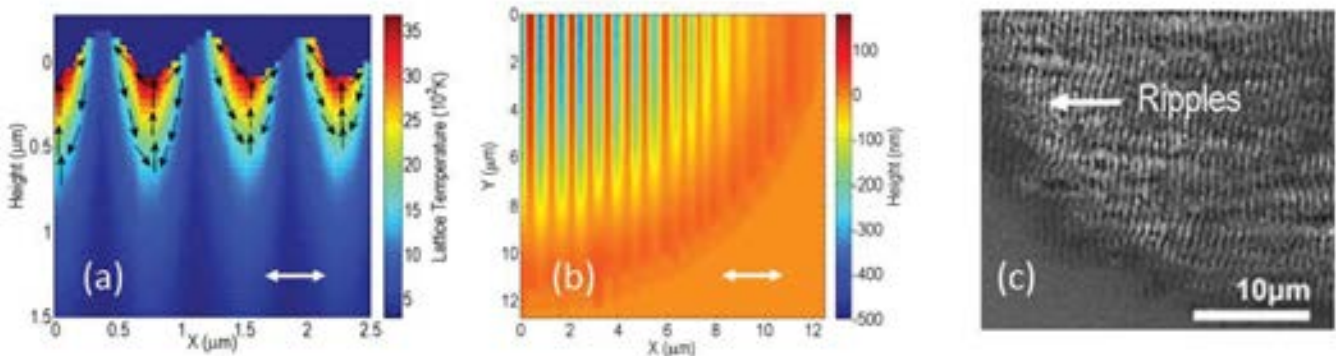


Figure 1. (a) Spatial distribution of lattice temperature at $t=1\text{ns}$ for ten pulses. (Arrows indicate flow movement), (b) Ripple pattern for ten pulses, (c) SEM image of surface modification (fluence= $0.6\text{J}/\text{cm}^2$, pulse duration= 430fs). (Double-ended arrow indicates the laser beam polarisation).

- [1] M. Barberoglou *et al.*, Applied Physics A: Materials Science and Processing **113**, 273 (2013).
- [2] G. D. Tsididis *et al.*, Applied Physics A **114**, 57 (2014).
- [3] G. D. Tsididis *et al.*, Physical Review B **86**, 115316 (2012).

Chemical functionalization of inorganic surfaces for organic LEDs applications

D. Gherca,^{1*} D. Tsikritzis,^{2*} S. Kennou,² M. Vamvakaki^{1,3}

¹*Institute of Electronic Structure and Laser, Foundation for Research and Technology Hellas, Heraklion, Crete, Greece*

²*Department of Chemical Engineering, University of Patras, GR 265 04 Patras*

³*Department of Materials Science and Technology, University of Crete, Heraklion, Crete, Greece*

Chemical modification of inorganic surfaces with silane molecules is commonly used for the development of functional surfaces for various applications [1]. In this study, the functionalization of inorganic surfaces (silicon, GaN) was achieved using a three-step chemical deposition method. First, the surfaces were cleaned by sonication in different solvents followed by the formation of a silicon dioxide layer by immersion in a freshly prepared piranha solution. Finally, an organosilane was deposited on the surfaces in the form of a self-assembled monolayer. The pristine surfaces, as well as those treated with piranha solution and those after APTES/APDMES deposition, were analysed by contact angle (CA) measurements, atomic force microscopy (AFM) and X-ray Photoelectron Spectroscopy. The static water CAs and AFM suggested the presence of the silane molecules on the inorganic surfaces. XPS analysis showed the presence of Si, O and C on all surfaces, whereas, N was only visible on the APTES treated surfaces, attributed to the primary amino groups of the silane molecule (Fig.1A). In the case of the surface modified with APDMES the N peak is hardly observed since it is in the detection limit of the technique. Fig.1B shows the deconvolution of the N1s spectra for the APTES modified sample in two N_A and N_B peaks, where N_A is attributed to the free amino groups and N_B is due to the protonated amino groups. The N_A/N_B ratio increases from 1.3 to 2.55 when the surface sensitivity of XPS is increased by turning the sample by 45° . From this it is concluded that the protonated amino groups are oriented close to the Si surface, whereas the free amino groups are positioned closer to the free surface [2].

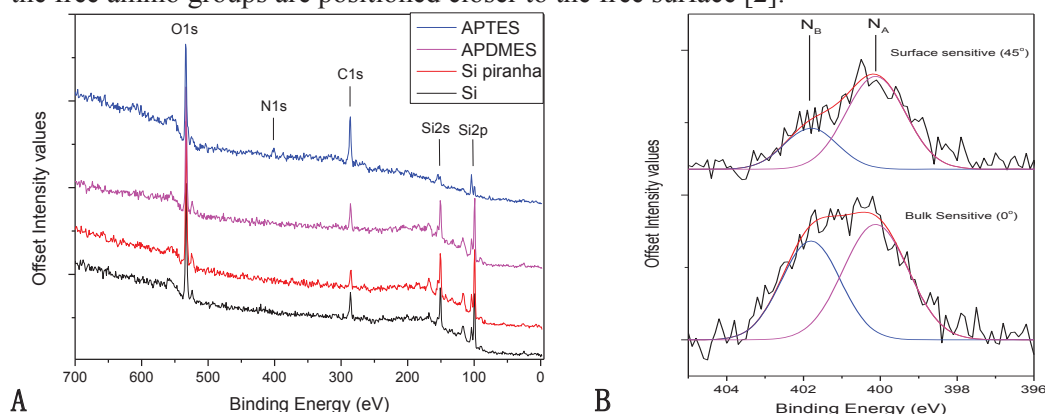


Figure 1: A) Wide scan survey spectra for all the surfaces. B) Deconvolution of the N1s spectra in the APTES modified Si surface.

Acknowledgements This research has been co-financed by the European Union (European Social Fund-ESF) and Greek national funds through the Operational Program "Education and Lifelong Learning" of the National Strategic Research Frame (NSRF)-Research Funding Program: ARISTEIA II, project NILES.

References

[1] J. Lopez-Gejo, A. Arranz, A. Navarro, C. Palacio, E. Munoz and G. Orellana, JACS 132, 1746 (2010)

[2] E. Vandenberg, L. Bertilsson, B. Liedberg, K. Uvdal, R. Erlandsson, H. Elwing and I. Lundström, Journal of Colloid and Interface Science 147, 103 (1991).

* daniel.gherca@iesl.forth.gr, tsikritzis@chemeng.upatras.gr

Ag loaded TiO₂ coupled onto reduced graphene oxide for enhanced visible-light photocatalytic activity

E. Vasilaki,^{1*} M. Kaliva,^{2,4} D. Vernardou,³ I. Georgaki,³ D. Konios,^{1,3}
E. Kymakis,³ M. Vamvakaki,^{2,4} N. Katsarakis^{3,4}

(1) Department of Chemistry, University of Crete, 71003, Heraklion, Crete, Greece. (2) Department of Materials Science and Technology, University of Crete, 71003, Heraklion, Crete, Greece. (3) Center of Materials Technology and Photonics, Technological Educational Institute of Crete, 71004, Heraklion, Crete, Greece. (4) Institute of Electronic Structure & Laser, FORTH, 71110, Heraklion, Crete, Greece.

TiO₂ is the semiconductor of choice for the degradation of numerous pollutants. However, its performance is limited due to its wide band gap and its high electron-hole recombination rate. Lately, the development of materials for visible-light driven photocatalysis has attracted particular attention and many approaches are being considered, such as the coupling of TiO₂ with noble metals [1] and carbonaceous materials [2]. In this work, silver nanoparticles were loaded onto TiO₂ by chemical reduction. Furthermore, TiO₂ and Ag-TiO₂ were deposited onto reduced graphene oxide (rGO). Characterization of the samples was conducted by UV-Vis and Raman spectroscopy, scanning and transmission electron microscopy, Fourier transform infrared (FTIR) spectroscopy and X-ray diffraction. The photocatalytic performance of the samples was evaluated by assessing the conversion of methylene blue under visible light irradiation. The rate of removal at first increases with Ag loading, but drops above a threshold loading value, while, the composite materials present enhanced photocatalytic activity compared to that of conventional TiO₂ (Fig. 1).

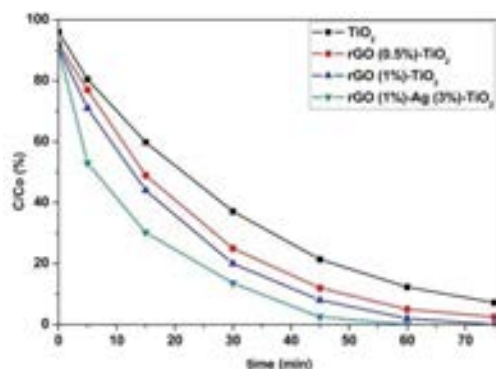


Figure 1: Photocatalytic performance of TiO₂ and Ag-TiO₂ coupled with rGO

References

- [1] Z. Zheng, B. Huang, X. Qin, X. Zhang, Y. Dai and, M. Whangbo, J. Mater. Chem. **21**, 9079 (2011).
[2] H. Zhang, X. Lv, Y. Li, Y. Wang, J. Li, ACS Nano **4**, 7303 (2010).

* met656@edu.chemistry.uoc.gr

Influencing the interactions on poly(ethylene oxide) / graphite oxide nanocomposites

N. Vasilakis,^{1,2,*} K. C. Vasilopoulos,¹ L. Syggelou,³ K. Chrissopoulou,¹ S. H. Anastasiadis^{1,2}

¹ *Institute of Electronic Structure and Laser, Foundation for Research and Technology–Hellas, Heraklion Crete, Greece*

² *Department of Chemistry, University of Crete, Heraklion Crete, Greece*

³ *Institute of Chemical Sciences, Foundation for Research and Technology–Hellas, Heraklion Crete, Greece*

Following the discovery of graphene and the demonstration of its properties by Konstantin Novoselov and Andrei Geim, [1] the scientific community is trying to utilize this promising material for industrial applications like hydrogen storage, solar cells and reinforcement of polymeric materials. In this work, we are investigating the effect of the interactions between a hydrophilic polymer, poly(ethylene oxide), PEO and graphite oxide, GO, on the dispersion of the additive and the final structure and properties of the nanocomposites. The attempt to influence the interactions is performed through varying the degree of oxidation and thus the hydrophilicity of GO. The Staudenmaier method is utilized to convert graphite to graphite oxide for varying oxidation times from 0.5 to 48 hours. The success of the oxidation is verified for most cases with X-ray diffraction, XRD, where a shift of the characteristic graphite diffraction peak towards lower angles is observed (Figure 1). Moreover, a quantitative measurement of the degree of oxidation is performed through X-ray photoelectron spectroscopy, XPS. The different GO's are utilized to synthesize PEO/GO nanocomposites. The structure of the nanohybrids is investigated with XRD, their thermal properties and stability with differential scanning calorimetry, DSC, and thermogravimetric analysis, TGA, respectively, whereas the effect of the GO on polymer conformation with infrared spectroscopy, ATR–FTIR.

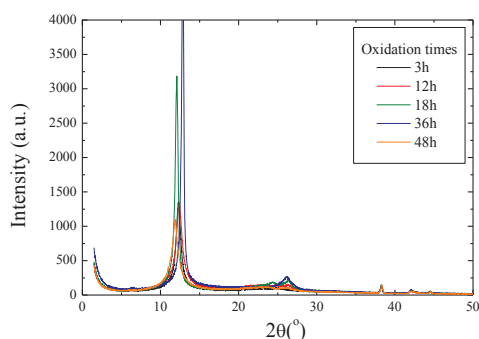


Figure 1: XRD measurements of GO with different oxidation times

References

[1] A. K. Geim and K. S. Novoselov, *Nature Materials* **6**, 183, (2007).

This research has been co-financed by the European Union (ESF) and Greek national funds through the Operational Program "Education and Lifelong Learning" of the NSRF – Research Funding Program: THALES – Investing in knowledge society through the European Social Fund (MIS 377278).

* vasinkos@iesl.forth.gr

Controlling the number and stacking of layers in CVD graphene on Nickel

J. Marquez Velasco¹, S.A. Giamini¹, N. Kelaidis¹, G. Kordas¹, Y.S. Raptis² and A. Dimoulas¹

¹ National Center for Scientific Research "Demokritos", 15310 Athens, Greece

² Department of Physics, National Technical University of Athens, Athens, Greece

Large area single layer graphene or few layer Bernal stacked (A-B) graphene is required for graphene device applications [1]. Chemical Vapour Deposition (CVD) provides a pathway to large area – high quality graphene growth, mainly on lower-cost Copper and Nickel substrates. Growth of graphene by CVD is a combination of surface growth and carbon diffusion from the substrate, making the control of the quality and number of layers challenging. Copper substrates are more suitable for predominantly single layer graphene growth while Ni substrates produce few or multi - layer graphene. Hydrogen is used in CVD graphene growth to regulate the catalytic dissociation of hydrocarbons but it can also be used as a graphene etchant [2]. We propose a method of controlling the number of graphene layers by a post growth annealing process in Hydrogen environment that reduces the number of layers without degradation of the graphene quality.

In this work, graphene is grown by CVD on Nickel substrates. Growth time and flow rate are intentionally increased in order to obtain multilayer graphene, where the top layers are preferably stacked in A-B order as verified by STM. Micro-RAMAN spectroscopy is performed in order to characterize graphene and the 2D peak is analysed to extract information about the number of layers and stacking order [3]. Knowing from the 2D peak analysis that graphene is in A-B stacking configuration an estimation of the number of layers is possible. On the other hand, in the case where turbostratic graphene is predominant, the number of layers cannot be revealed using this method [4]. A single step annealing process in Ar/H₂ at low temperature (450°C) is optimized as a graphene etching process. It is found that graphene etch can be achieved on metal catalysts at low temperature, without introducing defects into graphene.

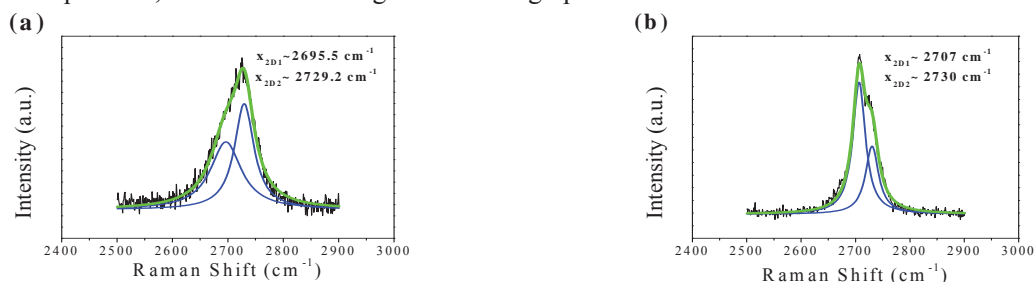


Figure 1: RAMAN 2D-peaks of graphene of (a) initial substrate of multi-layer (>7 layer) graphene (A-B stacked), grown on Nickel foil (b) after 10-mins post-growth etching graphene is reduced to 3-4 layer with an A-B stacking order.

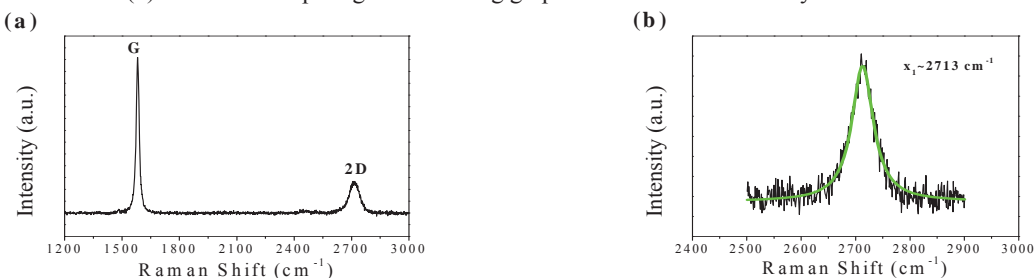


Figure 2: RAMAN spectrum after 12-mins of etching: (a) full spectrum showing the absence of D-peak (b) 2D-peak of after etching indicating a turbostratic graphene indicating the etching of the A-B stacked graphene overlayers.

References

- [1] Novoselov et al, Science **vol. 306**, 666-669
- [2] Zhang et al, ACS Nano. 2012 Jul 24;**6(7)**:6526
- [3] A. C. Ferrari et al, Nature Nanotechnology, **vol 8**, April 2013
- [4] Kwanpyo Kim et al., PRL **108**, 246103 (2012)

Structure – Activity Interrelationships of Combustion Synthesis Catalysts for the Oxidation of Diesel Soot

G. Xanthopoulou and G. Vekinis

Institute of Nanoscience and Nanotechnology, NCSR “Demokritos”, 15310, Greeceⁱ

Atmospheric aerosol particles are considered air pollutants because of their impact on the environment, climate and public health, including in-vitro mammalian cell chromosomal and DNA damage. Among such pollutants, diesel particulate matter (DPM) or diesel soot, primarily composed of carbon, has a significant adverse impact on both global warming and public health. DPM is typically trapped using diesel particulate filters (DPFs), which are periodically regenerated to oxidize the accumulated soot particulates. Because of the highly complex nature, ambiguity, and unpredictability of the multicomponent soot structure, as well as varying diesel engine operating conditions, optimized DPF operation and regeneration is a challenging task and parallel catalytic oxidation of the soot would offer definite advantages.

This work presents the results of an investigation on the structure-catalytic activity interrelationships for a range of combustion synthesis catalysts tested for oxidation of three different types of soot: diesel engine, activated carbon and heating burner. The catalytic activity of any catalyst depends on microstructure, but also on their redox behavior and lattice oxygen mobility. To study such dependencies, various catalytic materials were synthesised using Solution Combustion Synthesis (SCS) from aqueous solutions of manganese and cerium nitrates, copper potassium dichromate, chromium oxide (VI) and urea at a preheating temperature of 500 °C. The synthesised catalysts were characterized by SEM/EDAX, XRD, and nitrogen porosimetry. Their catalytic performance was studied in air flow at 1l/min at a heating rate of 10°C/min. In all cases a soot:catalyst mixture of 1:3, was placed in a ceramic reactor and the temperature for initiation and completion of oxidation was determined. It was found that crystallite size (fig.1) and lattice d spacing catalysts (fig.2) correlate with their activity. Other parameters found to correlate with the catalytic activity were the initial primary particle size, specific surface area, and crystallite stacking height in a self-consistent way.

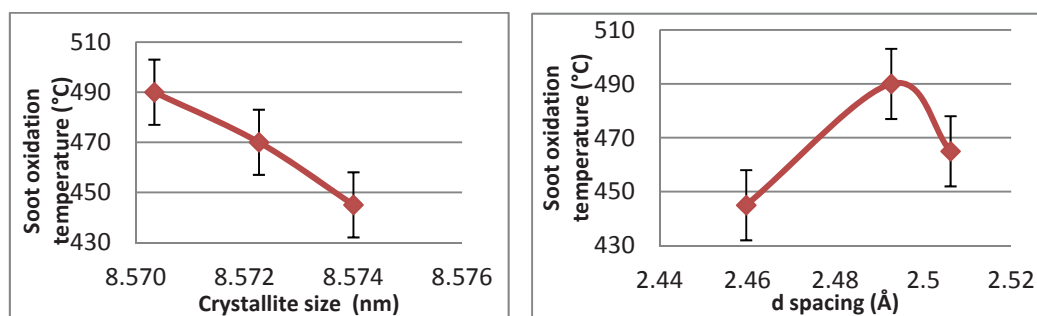


Fig.1 Influence of crystallite size of grains (D) at combustion temperatures of diesel soot, SCS Co-Ce-O catalyst. Influence of CuCrO₂ crystal structure parameters (d) of SCS Cu-K-Cr-O catalyst on the combustion temperatures of diesel soot

ⁱ gxantho@ims.demokritos.gr

Lattice strain control of the activity of cobalt catalysts produced by combustion synthesis

G. Xanthopoulou^a, K. Karanasios^{a,b}, G. Vekinis^a

^a*Institute of Nanoscience and Nanotechnology, NCSR "Demokritos", Agia Paraskevi 15310, Greeceⁱ*

^b*Department of Chemical Engineering, National Technical University, Iroon Polytechniou 9, Zografou 157 80, Athens, Greece*

Catalysts based on cobalt, aluminum and magnesium oxides, doped with Zn, Mg, Al, B and Ba were synthesized using combustion synthesis (either self-propagating high temperature synthesis, SHS or Solution Combustion Synthesis, SCS) and were investigated for dry reforming of methane. The doping atomic ratios of Co/metal ranged from 10:0.2 to 10:3.0. Solution combustion synthesis of Co(II) nitrates with one of Zn, Mg, Al, Ba metal nitrates and boric acid resulted in formation of high surface area nano-sized catalysts. The dry reforming reaction was carried out in a fixed bed reactor at 750 – 900°C and at atmospheric pressure with gas ratio in a stream of CO₂:CH₄:N₂ (1:1:1). The total flow rate of reactants was 860h⁻¹. Of all catalysts tested, Co/Me (10:0.5) and Co/Me (10:2) exhibited the highest activity at these specified conditions. X-ray diffraction (XRD) measurements revealed the presence of CoB₂O₄, CoAl₂O₄, Co₂AlO₄, CoO, ZnCo₂O₄, CoMg₃O₄, Co₃MgO₄, Ba₂CoO₄, Co₃(BO₃)₂ in the catalysts.

Lattice spacing analysis reveal that the dopant ions substitute for various metal ions in the oxides under the present synthesis conditions. A lattice expansion occurs in the case of the Co/Mg catalysts while a lattice contraction was found for the Co/Zn catalysts (fig.1). A correlation between cobalt spinel crystal lattice spacings and activity of catalysts (fig. 2) was observed. By considering lattice strains resulting from the above ionic substitutions it was possible to arrive at reactivity–lattice strains relationships that provides guidelines for tuning catalytic activity.

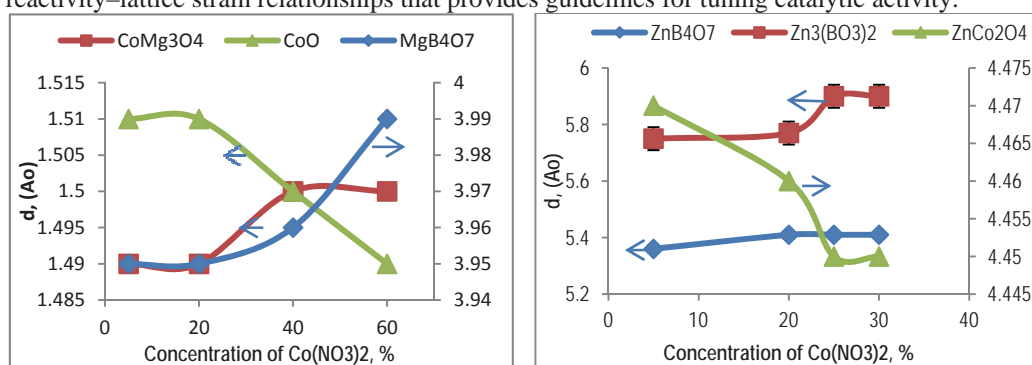


Fig.1. Influence of initial batch composition on the cobalt spinels crystal lattice spacings

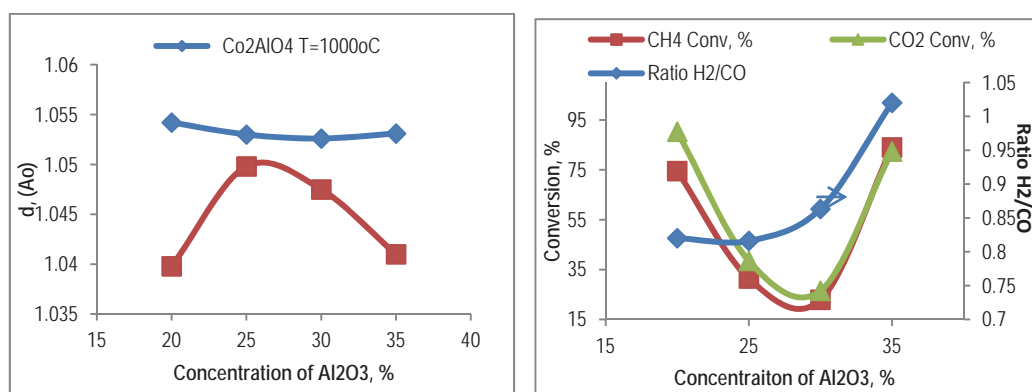


Fig.2 Influence of catalyst composition on the crystal lattice spacings and CH₄ and CO₂ conversion

ⁱgxantho@ims.demokritos.gr

Gas-sorption properties of functionalized Zr- and Hf-based MOFs

Pantelis Xydias^{*}, Ioannis Spanopoulos and Pantelis N. Trikalitis
Department of Chemistry, University of Crete, Herakleion 71003 Greece

Metal Organic Frameworks is a relatively new class of materials that are highly attractive for gas sorption applications due to the fact that they combine high porosities with functionalized surfaces. Herein we report the synthesis and study of Zr- and Hf-based MOFs made of ditopic and quadratopic carboxylated based ligands that have similar structures to the UiO-67, MOF-812 and PCN-521 materials. In the case of UiO-67 analogues (see Figure 1), different functional groups have been incorporated including -SO₂, NO₂ and -OH. The nature of the functional groups greatly affects the gas-sorption properties. These results will be presented and discussed in detail. [1-4]

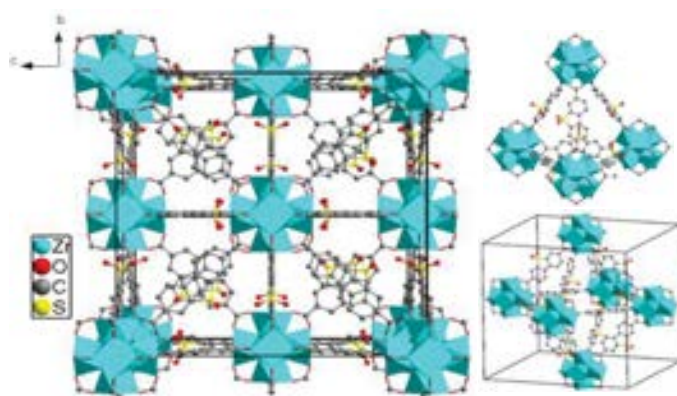


Figure 1. The ideal fcc structure for the sulphone functionalised UiO-67 along the a-axis. The structure contains tetrahedral and octahedral cages.

References

- 1 J. H. Cavka, S. Jakobsen, U. Olsbye, N. Guillou, C. Lamberti, S. Bordiga, K. P. Lillerud, *Journal of the American Chemical Society* **2008**, *130*, 13850-13851.
- 2 H. Furukawa, F. Gandara, Y. B. Zhang, J. C. Jiang, W. L. Queen, M. R. Hudson, O. M. Yaghi, *Journal of the American Chemical Society* **2014**, *136*, 4369-4381.
- 3 M. W. Zhang, Y. P. Chen, M. Bosch, T. Gentle, K. C. Wang, D. W. Feng, Z. Y. U. Wang, H. C. Zhou, *Angewandte Chemie-International Edition* **2014**, *53*, 815-818.
- 4 P. Xydias, I. Spanopoulos, E. Klontzas, G. E. Froudakis, P. N. Trikalitis, *Inorganic Chemistry* **2014**, *53*, 679-681.

^{*} xydias@chemistry.uoc.gr

Dynamics of cis-1,4 Polyisoprene and 1,4 Polybutadiene confined to Nanoporous Alumina

S. Alexandris^{1*}, G. Sakellariou², M. Steinhart³, G. Floudas¹

¹*Department of Physics, University of Ioannina*

²*Department of Chemistry, University of Athens*

³*Institut für Chemie neuer Materialien, Universität Osnabrück*

*salexan@cc.uoi.gr

We study the effect of confinement of two flexible polymers, one with attractive interactions with the pore walls (cis-1,4 Polyisoprene) and one with repulsive interactions (cis-1,4 Polybutadiene), as a function of molecular weight, pore diameter, temperature and frequency. Polyisoprene is a type-A polymer (Stockmayer) and as such it has a dipole moment parallel and perpendicular to the backbone. We employ molecular weights in the range from 300-20.000 g/mol and as confining medium we use self-ordered AAO templates with diameters in the range 400-25 nm. Our main interest is on the effect of confinement on the normal modes and segmental mode. Dielectric spectroscopy measurements over a broad range of frequencies and temperatures revealed a significant broadening of both modes on confinement and a slow-down of the normal mode dynamics in the lowest molecular weight. For the Polybutadiene case we study its behavior under the same confining media using molecular weights in the range from 500-55.00 g/mol. The feature that makes this case different of that of PI is that the segmental mode speeds-up as with decreasing pore diameters.

High Band Gap Indacenodithiophene and Indacenodithienothiophene Copolymers as Electron Donors in Organic Photovoltaics

Athanasios Katsouras, Christos L. Chochos and Apostolos Avgeropoulos
*Department of Materials Science and Engineering, University of Ioannina, Ioannina
45110, Greece*

Conjugated polymers represent one of the most important class of materials for the fabrication of many optoelectronic applications, such as light emitting diodes, field effect transistors, organic photovoltaics, sensors, etc. In the field of organic photovoltaics, the design of novel conjugated polymers with appropriate frontier orbital energy levels, optical band gap and suitable carrier transport properties are needed to improve the power conversion efficiency (PCE).^[1,2] Among various materials developed for bulk heterojunction devices, the multifused-ring conjugated polymers are particularly interesting due to their superior optical and electrical properties.^[3] The highly fused aromatic/heteroaromatic units enhance effective conjugation of the polymer backbone to facilitate electron delocalization and charge carrier mobilities.^[4] In this work, we present the design, synthesis and optoelectronic (absorption and electrochemical properties) characterization of a new family of Indacenodithiophene and Indacenodithienothiophene based copolymers. Finally, initial results on the performance of these copolymers in organic photovoltaic devices will be demonstrated.

Figure 1: Chemical structures of the indacenodithiophene and indacenodithienothiophene copolymers developed in this work

References

- [1] G. Li, R. Zhu, Y. Yang *Nature Photon.* **6**, 153 (2012).
- [2] C. L. Chochos, S. A. Choulis, *Prog. Polym. Sci.* **36**, 1326 (2011).
- [3] J. You, L. Dou, Z. Hong, G. Li, Y. Yang, *Prog. Polym. Sci.* **38**, 1909 (2013).
- [4] Y. Li, K. Yao, H.-L. Yip, F.-Z. Ding, Y.-X. Xu, X. Li, Y. Chen, A. K.-Y. Jen *Adv. Funct. Mater.* (2014), DOI: 10.1002/adfm.201303953

Synthesis and characterization of pH-sensitive hybrid janus nanoparticles

P. G. Falireas,* M. Vamvakaki

*Institute of Electronic Structure and Laser, Foundation for Research and
Technology – Hellas, 711 10 Heraklion, Crete, Greece*

*Department of Materials Science and Technology, University of Crete, 710 03
Heraklion, Crete, Greece*

Janus nanoparticles [1], named after the double-faced Roman god, are compartmentalized colloids with two sides of different chemistry or polarity. These particles have attracted significant attention in recent years due to their unique properties which derive from their anisotropic character. In this study, we present the synthesis and characterization of amphiphilic hybrid janus nanoparticles comprising an inorganic silica core and a shell consisting of compartmentalized poly(acrylic acid) (PAA) and poly (2-(dimethylamino)ethyl methacrylate) (PDMAEMA) polymer brushes.

In the first step, silica nanoparticles ($D = 100$ nm) were used to stabilize polystyrene colloidosomes [Figure 1]. The exposed surface of the silica nanoparticles was modified with an atom transfer radical polymerization (ATRP) initiator. After the functionalization, polystyrene was dissolved yielding janus nanoparticles bearing ATRP initiating sites. Next, surface-initiated ATRP of *tert*-butyl acrylate (*t*-BuA) was carried out from the one hemisphere of the initiator-functionalized silica nanoparticles followed by functionalization of the second hemisphere with the ATRP initiator. Finally, ATRP of DMAEMA was conducted to obtain amphiphilic hybrid janus nanoparticles. Acidic hydrolysis of the P(*t*-BuA) ester groups led to oppositely charged polyampholyte janus particles [2] decorated with PAA and PDMAEMA polymer chains.

The Janus character of the particles was confirmed by thermogravimetric analysis and scanning and transmission electron microscopies (SEM and TEM), whereas the molecular weights and molecular weight distributions of the P(*t*-BuA) and PDMAEMA polymer brushes were determined by gel permeation chromatography. The dual responsive behavior of the janus nanoparticles in water as a function of temperature and pH was investigated by dynamic light scattering and potentiometric titration.

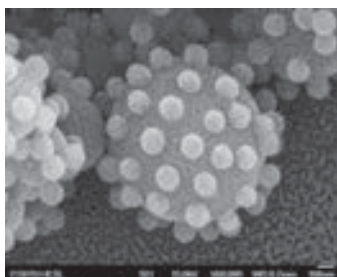


Figure 1: SEM image of the polystyrene-SiO₂ colloidosomes

References

- [1] de Gennes, P.G., *Soft Matter. Science* **256**, 495 (1992).
- [2] Berger, S., et al., *Macromolecules* **24**, 9669 (2008).

* pfalir@iesl.forth.gr

Porous Porphyrin-containing Polymer Nanoparticles for Gas Separation Applications

C. Flouraki,^{1, 2*} M. Kaliva,^{1, 2} G.S. Armatas² and M. Vamvakaki^{1, 2}

¹*Institute of Electronic Structure and Laser, Foundation for Research and Technology – Hellas, 711 10 Heraklion, Crete, Greece*

²*Department of Materials Science and Technology, University of Crete, 710 03 Heraklion, Crete, Greece*

Nanoporous organic polymer materials have gained significant attention lately for applications in gas storage and separation technologies. [1, 2] Among them aromatic polymers containing porphyrin or styrene moieties have been shown to exhibit significantly high surface area and good selectivity for CO₂. [3, 4] In this work, porous polymer nanoparticles were synthesized by free radical emulsion copolymerization of a mixture of styrene (S), tetra-vinyl functionalized 5,10,15,20-Tetrakis (4-hydroxyphenyl)-21H,23H-porphyrin (PO) and divinylbenzene (D) [Figure 1a]. The cross-link density of the polymer particles was varied by increasing progressively the PO content from 1.5 to 5 % with respect to D at a constant S/cross-linker (PO and D) mole ratio of 2:3. The morphology and size of the obtained nanoparticles were characterized by scanning electron microscopy, transmission electron microscopy and dynamic light scattering measurements. After synthesis, the particles were extensively purified by dialysis against water. The samples were then exchanged to ethanol or dimethylformamide and the solvent remaining in the pores was effectively removed by supercritical drying with CO₂ in order to obtain open-pore polymer structures (PO-S-D). The permanent porosity of the PO-S-D materials was confirmed by nitrogen and carbon dioxide adsorption experiments [Figure 1b]. Analysis of the adsorption data using the ideal adsorption solution theory reveals that the PO-S-D sample containing 5% PO has a CO₂/CH₄ separation factor of ~23 and ~12 at -10°C and 0°C, respectively, in the low pressure limit.

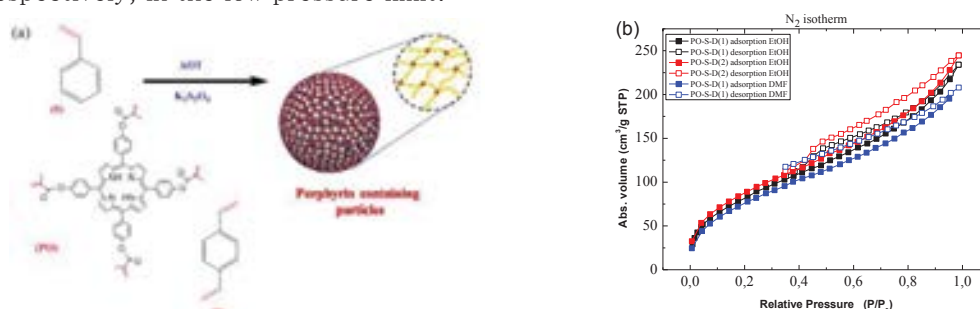


Figure 1: (a) Synthetic process followed for the preparation of the porous porphyrin-containing polymer particles; (b) Nitrogen adsorption and desorption isotherms at -197°C for the solvent-free PO-S-D (1) [1.5 % PO] and PO-S-D (2) [5 % PO] samples treated in ethanol and dimethylformamide.

References

- [1] S. Xu, Y. Luo, B. Tan, *Macromol. Rapid Commun.* **34**, 471–484 (2013).
- [2] M. S. Silverstein, *Polymer* **55**, 304–320 (2014).
- [3] A. Modak, M. Nandi, J. Mondal, A. Bhaumik, *Chem. Commun.* **48**, 248–250 (2012).
- [4] M. Kaliva, G. S. Armatas, M. Vamvakaki, *Langmuir* **28**, 2690–2695 (2012).

* xarafi@iesl.forth.gr

Immobilization of nanocatalysts-containing polymeric carriers onto solid surfaces

M. A. Frysalis,^{1,2*} C. Orfanou,² M. Kaliva,^{1,3} L. Papoutsakis,¹ M. Vamvakaki^{1,3} and S. H. Anastasiadis^{1,2}

1. *Institute of Electronic Structure and Laser, Foundation for Research and Technology-Hellas, Heraklion Crete, Greece*
2. *Department of Chemistry, University of Crete, Heraklion, Greece*
3. *Department of Materials Science & Technology, University of Crete, Heraklion Crete, Greece*

This study is concerned with the attachment of electrostatically stabilized polymeric microgel particles based on poly(acrylic acid), PAA, poly(methacrylic acid), PMAA, and poly(2-(diethylamino)ethyl methacrylate), PDEAEMA, onto inorganic surfaces. These microgels have been synthesized as hosts for the impregnation of metal nanoparticles (Ru, Pd, etc.), which will be utilized as nanocatalysts for various catalytic reactions of industrial interest carried out in microfluidic reactors. The attachment of the microgel particles onto glass substrates can be significantly improved by the utilization of functional groups, such as carboxylic acid moieties present on the surface of the microgels. Various routes were followed in order to deposit the particles onto the surfaces, such as the Pickering emulsion method, which is to trap the particles at the interface between two fluids [1]. Parallel to the above procedure, an amine coupling method was introduced, which leads to the covalent binding of the microgel particles onto the surface. The durability of the microgel particles attached onto the surfaces against hydration and shear forces was tested utilizing repeated immersion of the surfaces into water undergoing mechanically-generated hydrodynamic flow.

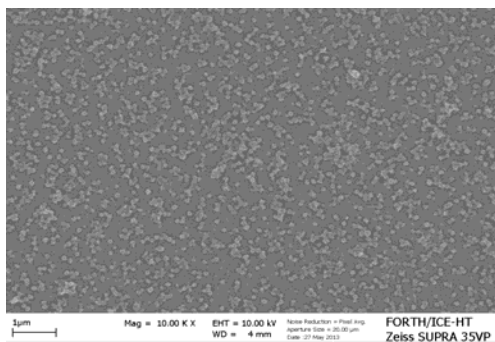


Figure 1: PMAA microgels carrying Pd nanocatalysts attached onto a glass surface with the amine coupling procedure.

Acknowledgements: Part of this research was sponsored by the European Union (POLYCAT; grant agreement CP-IP 246095-2).

References

- [1] M. Kaliva, M.A. Frysalis, C. Flouraki, L. Papoutsakis, M. Vamvakaki and S.H. Anastasiadis, *Macromol. Symp.* **331**, 17-25 (2013).

* melina@iesl.forth.gr

Polymeric surfaces with controlled wettability exhibiting unidirectional features

M. A. Frysalis,^{1,2,*} L. Papoutsakis,¹ G. Kenanakis,¹ E. Stratakis¹ and S. H. Anastasiadis^{1,2}

1. Institute of Electronic Structure and Laser, Foundation for Research and Technology-Hellas, Heraklion Crete, Greece

2. Department of Chemistry, University of Crete, Heraklion, Greece

The development of artificial smart surfaces has gained the interest of the scientific community the last decades. There have been great efforts by the researchers to understand and control the wettability of the solid surfaces. The inspiration for producing such surfaces comes from nature [1]. Lotus and rice leaves, striders legs, the wings of some insects, rose petals and shark skin are some of the biological species that the researchers have tried to imitate. This is due to the wide range of applications that water-repellent surfaces have in daily life, industry and agriculture. Depending on the type of coating deposited onto such surfaces, pH-, photo-, electro-, chemo- responsiveness can be attained [2,3]. Herein, we focus on surfaces with controlled, switchable wettability in response to one or more external stimuli. Furthermore, the aim is to create surfaces with unidirectional wettability, which may in turn be used as benchtop for novel microfluidic devices such as chemical switches/gates or in lab on chip technologies [4]. Such complex surfaces require advanced design, combining hierarchically structured surfaces with suitable polymeric materials.

Acknowledgements: This research was partially supported by the European Union (European Social Fund, ESF) and Greek national funds through the "ARISTEIA II" Action (SMART_SURF, project No. 3393, 2013SE01380048) of the Operational Programme "Education and Lifelong Learning", NSRF 2007-2013, via the General Secretariat for Research & Technology, Ministry of Education, Greece.

References

- [1] V. Zorba, et al., *Adv. Mater.* **20**, 4049-4054 (2008).
- [2] E. Stratakis, et al., *Chem. Commun.* **46**, 4136-4138 (2010).
- [3] S. H. Anastasiadis, *Langmuir* **29**, 9277-9290 (2013).
- [4] Y. Y. Yan, et al., *Adv. Colloid Interf. Sci.* **169**, 80-105 (2011).

* melina@iesl.forth.gr

Electrical Characterization on PVDF-Graphene samples

S.F. Galata^{*†}, G.T. Malliaros, I. Stavrakas, K. Moutzouris, D. Triantis
*Laboratory of Electrical Characterization of Materials and Electronic Devices,
 Department of Electronic Engineering, Technological Educational Institute of
 Athens, 12210 Athens, Greece*

In recent years there is a great interest on graphene based polymer nanocomposites [1,2]. In this paper permittivity and resistivity measurements on PVDF-Graphene samples are discussed. Six sets of samples were prepared using Polyvinylidene fluoride (PVDF) as host polymeric matrix and Graphene nano-inclusion additives ranging from 0.1 up to 1 wt.%. Permittivity measurements were carried out by means of a high-resolution broadband spectrometer (Novocontrol – Alpha Analyzer) in the frequency range 10^{-2} up to 10^6 Hz [3]. Resistivity was calculated using the slope of the J-E curves obtained through I-V tests in a vacuum chamber using a high resistivity meter (Keithley 6517A) while the applied electric field was varied up to 1kV/cm. The J-E characteristics of the measured samples show ohmic behaviour for applied electric field values up to 1KV/cm. To ensure proper fitting in the sample cell and avoid electrode polarization both sides of the samples were painted with silver conductive paint.

Figure 1 shows the behaviour of resistivity ρ , with respect to the corresponding graphene content. Note that 0 wt.% graphene corresponds to pure PVDF sample without graphene content. A resistivity peak value is found for 0.2 wt.% that is in agreement with the existing literature [2]. This behavior may be attributed to the sample preparation process, since the impact of the preparation technique is recorded as a critical parameter for the electrical characteristics of similar samples [1]. Figure 2 shows the permittivity (real part ϵ') as a function of the wt.% graphene for two representative frequencies, 10 mHz and 10 kHz. Permittivity increases with the increase of wt.% graphene. At lower frequency (10 mHz) permittivity values are higher compared to the ones at higher frequency (10 kHz).

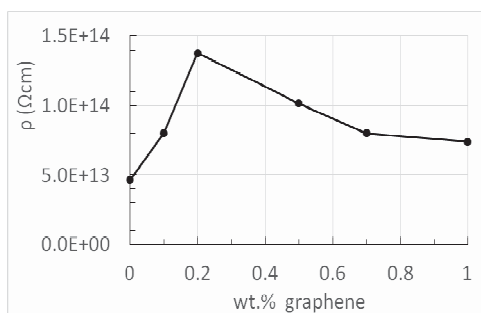


Figure 1: Resistivity ρ (Ωcm) as a function of wt.% graphene for PVDF-Graphene samples.

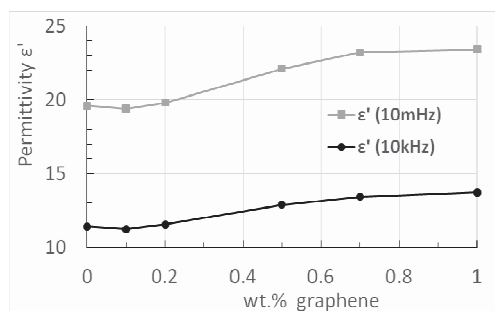


Figure 2: Permittivity (real part ϵ') as a function of wt.% graphene for PVDF-Graphene samples for 10 mHz and 10 kHz.

References

- [1] T. Kuilla, S. Bhadra, D. Yao, N.H. Kim, S. Bose, J.H. Lee, *Prog. Polym. Sci.* **35** 1350 (2010).
- [2] J. Yu, X. Huang, C. Wu and P. Jiang, *IEEETrans. Dielect. Elect. Insulation* **18**, 478 (2011).
- [3] I. Stavrakas, D. Triantis, C. Anastasiadis, *J. Mater. Sci.*, **40**, 4593 (2005).

* sgalata@teiath.gr

3D scaffold micro fabrication via multi photon polymerization of hybrid materials for neural cell cultivations

Iakovos Gavalas^{1,2,*}, Alexandros Selimis¹, Maria Farsari¹

¹*Institute of Electronic Structure and Laser (IESL), Foundation for Research and Technology - Hellas (FORTH)
N. Plastira 100, 70013*

Crete, Greece

²*Department of Materials Science and Technology, University of Crete, Greece*

There is a lot of research in the field of scaffold micro fabrication for cell growth. We present our work into fabrication of 3D scaffolds for neural cell growth using an organic – inorganic hybrid biocompatible material. In order to fabricate our scaffolds, we employ multi-photon polymerization, a direct laser writing technique which allows the selective polymerization of photosensitive material [1,2]. An example of our scaffolds is shown in Figure 1.

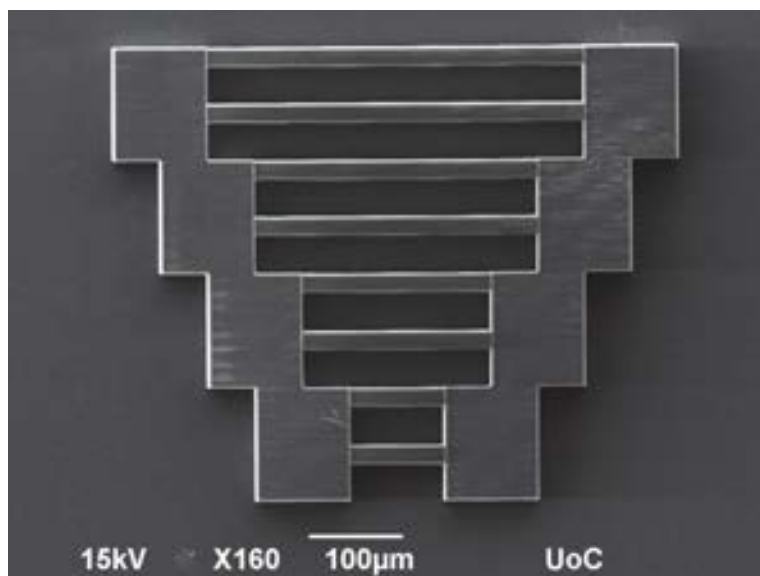


Figure 1: Top view of a 3D scaffold

References

- [1] Melissinaki, V.; Gill, A. A.; Ortega, I.; Vamvakaki, M.; Ranella, A.; Haycock, J. W.; Fotakis, C.; Farsari, M.; Claeysens, F., Direct laser writing of 3D scaffolds for neural tissue engineering applications. *Biofabrication* **2011**, *3*, 045005.
- [2] Farsari, M.; Vamvakaki, M.; Chichkov, B. N., Multiphoton polymerization of hybrid materials. *Journal of Optics* **2010**, *12*, 124001.

*mjacobg@hotmail.com

Enhanced *in vitro* Biological Response of a Chitosan-graft-Poly(e-caprolactone) Copolymer for Bone Repair

A. Georgopoulou*, M.Kaliva, M. Vamvakaki, M. Chatzinikolaidou

Institute of Electronic Structure and Laser, Foundation for Research and Technology-Hellas, Heraklion, Crete, Greece

Department of Materials Science and Technology, University of Crete, Heraklion, Crete, Greece

One of the main challenges of biomaterial's science is the utilization of novel biodegradable and biocompatible scaffolds. Part of this effort focuses on the formation of scaffolds to be used for bone regeneration both *in vitro* and *in vivo*. Scaffolds for osteogenesis should mimic bone morphology, structure and function in order to optimize integration into the surrounding bone. MC3T3-E1 cells are pre-osteoblasts that have the capacity to differentiate into osteoblasts and osteocytes and have been demonstrated to form calcified bone tissue *in vitro* [1]. Based on the above, we synthesized a copolymer comprising poly(e-caprolactone) (PCL) that is chemically modified and grafted onto a chitosan (CS) backbone (CS-g-PCL) [2], and evaluated the biological behavior of MC3T3-E1- cells on this material. First, we showed that CS-g-PCL promotes cell adhesion and proliferation as assessed by cell viability studies. Moreover, by means of scanning electron microscopy we observed that the morphology of MC3T3-E1 cells on CS-g-PCL is identical to that on tissue culture treated polystyrene used as a control sample. In addition, the CS-g-PCL material allowed for cell differentiation assessed by measuring characteristic biological markers for early and late stages of bone morphogenesis, such as collagen type I production, alkaline phosphatase activity, and calcium biomineralization, respectively. Overall, our results suggest that the CS-g-PCL copolymer is an attractive candidate for use in osteoblastic cell growth and differentiation.

References

[1] N. J. Peterson, K. H. Tachiki and D. T. Yamaguchi, Cell proliferation **37**, 325 (2004).

[2] M. Chatzinikolaidou, M. Kaliva, A. Batsali, C. Pontikoglou and M. Vamvakaki, Current Pharmaceutical Design **20**, 2030 (2014).

* anthieg87@yahoo.com

Nanoindentation analysis and biological characteristics of chitosan-*graft*-poly(ϵ -caprolactone) copolymer scaffolds

A. Skarmoutsou, D. Dragatogiannis, C.A. Charitidis*

School of Chemical Engineering, National Technical University of Athens, Greece

M. Kaliva, M. Vamvakaki, M. Chatzinikolaidou

Institute of Electronic Structure and Laser, Foundation for Research and Technology-Hellas, Heraklion, Crete, Greece

Department of Materials Science and Technology, University of Crete, Greece

C. Pontikoglou

School of Medicine, Haematology Laboratory, University of Crete, Greece

Tissue engineering is a promising therapeutic approach in medicine for many diseases and injuries. An amphiphilic graft copolymer, based on two of the most widely used components in bio-applications, chitosan (CS) and poly(ϵ -caprolactone) (PCL), has been developed and investigated for myocardium tissue engineering. This innovative copolymer is biocompatible and biodegradable and displays cationic functional groups that contribute to cell attachment. Moreover, CS can effectively buffer the acidic degradation products of PCL which is advantageous for its application in tissue engineering [1].

In this work, we present the synthesis of a CS-*g*-PCL copolymer, the investigation of its nanomechanical properties during the degradation process, and the examination of its *in vitro* activity for the development of myocardium tissue. Through nanoindentation analysis it was possible to evaluate hardness and Young's modulus values, as well as the time-dependent and viscous behavior of the as prepared samples. Furthermore, we used different mathematical models [2, 3] to correct the elastic modulus values calculated by the Oliver and Pharr model [4].

It was found that the graft copolymer has reduced nanomechanical properties compared to pure CS and PCL. Additional nanoindentation tests and analysis revealed a great effect of the mechanical response of the sample under different loading conditions, suggesting the time-dependent and viscous behavior of the copolymer, as a result of the viscous behavior of the PCL compound. Furthermore, PCL and the graft copolymer were tested after submersion in α -MEM cell culture medium. The nanomechanical properties decreased rapidly with time of immersion due to the hydrolytic degradation of PCL, the porosity and the amorphous regions of the CS-*g*-PCL sample [5]. Despite the large reduction of the nanomechanical properties and the 35% weight loss, the graft copolymer presented sufficient mechanical stability and elastic properties similar to the values reported for soft tissues [6]. Finally, Wharton's jelly mesenchymal stem cells isolated from the inner lining of human umbilical cords were seeded onto the copolymer. Cell proliferation increased after three and seven days in culture. The above results verify that the innovative copolymer possess suitable nanomechanical properties and has thus great potential for soft tissue engineering applications.

References

- [1] Liu L., Li Y., Liu H., Fang Y., Eur. Polym. J. **40**, 2739 (2004).
- [2] Hertz H., J. Reine Angew. Math. **92**, 156 (1881).
- [3] Bembey A.K., Oyen M.L., Bushby A.J., Boyde A., Philosoph. Magaz. **86**, 5691 (2006).
- [4] Oliver W.C. and Pharr G.M., J. Mater. Res. **7**, 1564 (1992).
- [5] Lu L., Biomaterials **21**, 1837 (2000).
- [6] Hiesinger W., et al., J. Thorac. Cardiovasc. Surg. **143**, 962 (2012).

* charitidis@chemeng.ntua.gr

NOVEL POLYMER BRUSHES FOR ANTIFOULING SURFACES

E.I. Koufakis,^{*1,2} Th. Manouras¹ and M.Vamvakaki^{1,2}

¹*Institute of Electronic Structure and Laser, FORTH, 71110 Heraklion, Greece*

²*Department of Materials Science and Technology, University of Crete, 71003 Heraklion, Greece*

Environmentally friendly polymeric materials have attracted significant research interest in scientific areas that require “clean” surfaces and “sterile” conditions such as sensitive sanitary and marine applications. Polymer chains, which are covalently bound onto flat surfaces and bear biocidal species, are particularly advantageous because they remain onto the surface even when it is immersed in water. [1]

In this work, homopolymer brushes based on 2-(dimethylamino)ethyl methacrylate (DMAEMA) were grown on silicon and glass substrates using the “grafting to” or the “grafting from” approach. In the “grafting to” technique, preformed polyDMAEMA chains bearing alkoxy-silane end-functionalities were synthesized via atom transfer radical polymerization (ATRP). The polymer amine groups were quaternized using alkyl halides to form the quaternary ammonium moieties which exhibit a biostatic action and next, the polymer chains were reacted with the hydroxy-silane functionalities on the solid substrates (Figure 1). On the other hand, in the “grafting from” method, ATRP initiator molecules were immobilized onto the solid surfaces to form a self-assembled monolayer (SAM) followed by surface-initiated ATRP of DMAEMA (Figure 1). Quaternization of the tertiary amine groups of the polymer brushes produced a polymer film with biocidal properties. The quaternized polyDMAEMA chains were characterized by ¹HNMR spectroscopy and gel permeation chromatography (GPC) while the morphology and the thickness of the polymer brushes were characterized by atomic force microscopy (AFM), infrared spectroscopy (FTIR) and ellipsometry. [2] The surface wettability was identified by water contact angle measurements.

The polymer grafting density, brush thickness and degree of quaternization was varied and its influence on the biocidal behaviour of the polymer layer is under investigation.

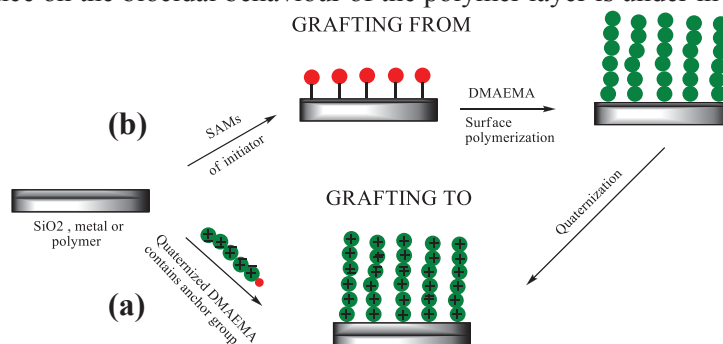


Figure 1: Synthesis of quaternized polyDMAEMA brushes by the “grafting to” (a) and the “grafting from” (b) technique

Acknowledgements:

This research has been co-financed by the European Union (European Social Fund – ESF) and Greek national funds through the Operational Program "Education and Lifelong Learning" of the National Strategic Reference Framework (NSRF) - Research Funding Program: THALES. Investing in knowledge society through the European Social Fund. Project title: “Development of Novel Functional Copolymers and Surfaces with Permanent and/or Controlled released biocidal species” (MIS: 379523).

References

- [1] J. P. Youngblood, L. Andruzzi, C. K. Ober, A. Hexemer, E. J. Kramer, J. A. Callow, J. A. Finlay, M. E. Callow, *Biofouling* **19**, 91 (2003).
 [2] A. Mateescu, J. Ye, R. Narain, M. Vamvakaki, *Soft Matter* **5**, 1621 (2009).

* koufakis@iesl.forth.gr

pH-responsive hollow polymeric capsules

F.K. Krasanakis,^{*1,2} S.H. Anastasiadis,^{1,2} M. Vamvakaki^{1,3}

¹*Institute of Electronic Structure and Laser, Foundation for Research and Technology, 711 10 Heraklion, Crete, Greece*

²*Department of Chemistry, University of Crete, 710 03 Heraklion, Crete Greece*

³*Department of Materials Science and Technology, University of Crete, 710 03 Heraklion, Crete Greece*

Hollow polymer capsules have stimulated increasing scientific and technological interest in the field of materials science and engineering because of their numerous potential applications in drug delivery, catalysis, paints and electronic materials. [1] Their preparation has been reported using different methods such as the layer-by-layer assembly of oppositely charged polyelectrolytes onto inorganic nanoparticles or the use of a polymerization process to form a polymer shell onto organic or inorganic nanoparticles, followed by the selective degradation of the nanoparticle core. [2] The synthesis of hollow capsules that respond to changes of external stimuli, i.e. solution temperature and pH [3], electric or magnetic field, etc, by altering the size and permeability of the capsule wall, is particularly attractive.

In this work, we report the synthesis of ionizable hollow capsules based on a cross-linked polyacid, poly(methacrylic acid) P(MAA), or polybase, poly(2-(diethylamino)ethyl methacrylate) (PDEA), shell, which respond to changes of the solution pH. The preparation of the ionizable hollow capsules involved first the synthesis of polymer microgels particles with a core-shell topology, using a two-step emulsion polymerization process, followed by the selective removal of the microgels' cores. The latter was achieved by either using an acid labile cross-linker in the core or the synthesis of non-cross-linked latex core particles surrounded by a cross-linked shell using a non-degradable cross-linker. [4] After synthesis, the core was removed by washing in a common solvent for the core and the shell of the particles.

Finally, the hollow capsules were characterized by dynamic light scattering, potentiometric titrations and electron microscopy in order to confirm their hollow structure and verify their responsive behaviour.

References

- [1] D. G. Shchukin, G. B. Sukhorukov, H. Mohwald, *Angew. Chem. Int. Ed.*, **42**, 4472 (2003).
- [2] W. Meier, *Chem. Soc. Rev.*, **29**, 295 (2000).
- [3] M. Sauer, D. Streich, W. Meier, *Adv. Mater.*, **13**, 1649 (2001).
- [4] L. Xie, M. Chen, L. Wu, *J. Polym. Sci. A Polym. Chem.*, **47**, 4919 (2009).

* fanisk@iesl.forth.gr

Synthesis and characterization of diblock copolymers containing antifouling and self-polishing groups

T. Manouras,^{1*} E. Koufakis,^{1,2} S. H. Anastasiadis^{1,3} and M. Vamvakaki^{1,2}

¹*Institute of Electronic Structure and Laser, FORTH, 71110 Heraklion, Greece*

²*Department of Materials Science and Technology, University of Crete, 71003 Heraklion, Greece*

³*Department of Chemistry, University of Crete, 71003 Heraklion, Greece*

Surfaces that prevent biofouling from any type of microorganism are known as antifouling surfaces. These are usually developed by the modification of a surface with a hydrophilic polymer coating. Such polymers resist protein adsorption, cell and microorganism adhesion, and thereby minimize unwanted biological responses [1]. Antifouling surfaces are continuously being developed for a plethora of applications spanning from biomedical tools, packaging management, marine technology and navigation.

The main target of this work was to develop new polymeric materials exhibiting controllable antifouling properties in the solid state. These polymeric materials comprise environmental friendly biocidal species and can self-organize into bulk nanostructures to give surfaces with controlled self-polishing and antifouling features. Amphiphilic diblock copolymers (fig. 1) containing hydrophobic and hydrolyzable THPMA (tetrahydropyranyl methacrylate) units and hydrophilic tertiary amine containing DMAEMA ((2-dimethylamino)ethyl methacrylate) moieties were synthesized using group transfer polymerization and were characterized by GPC and ¹H NMR [2]. Symmetric diblock copolymers were designed expected to assemble into lamellae structures in the solid state. Alkyl iodides were used for the quaternization of the DMAEMA units in order to introduce the biocidal groups (fig. 1).

Thin films of the quaternized PDMAEMA-*b*-PThPMA diblock copolymers were spin coated from an ethyl lactate solution onto quartz and silicon wafers and the chemical changes on the polymer as a function of temperature were monitored by UV-vis and FTIR spectroscopies. Furthermore, the thickness and the hydrophilicity of the films were measured by ellipsometry and contact angle measurements.

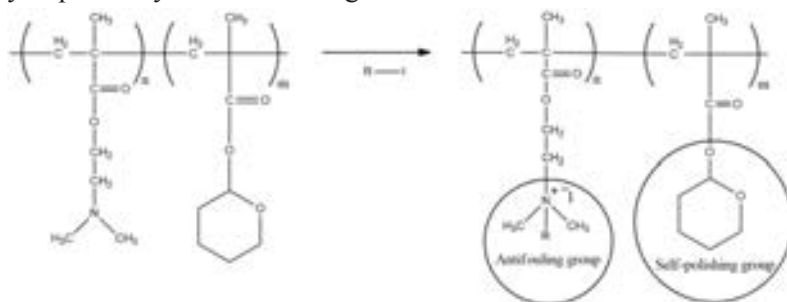


Figure 1: Chemical structure of the PDMAEMA-*b*-PThPMA diblock copolymer and the quaternized analogue

Acknowledgements:

This research has been co-financed by the European Union (European Social Fund – ESF) and Greek national funds through the Operational Program "Education and Lifelong Learning" of the National Strategic Reference Framework (NSRF) - Research Funding Program: THALES. Investing in knowledge society through the European Social Fund. Project title: "Development of Novel Functional Copolymers and Surfaces with Permanent and/or Controlled released biocidal species" (MIS: 379523).

References

- [1] A. B. Lowe, M. Vamvakaki, M. A. Wassall, L. Wong, N. C. Billingham, S. P. Armes, A. W. Lloyd J. Biomed. Mater. Res. **52**, 88 (2000).
 [2] C. S. Patrickios, et al. Macromolecules **27**, 930 (1994).

tman@iesl.forth.gr

Nucleic acid bases and analogues: electronic structure with LCAO.

M. Mantela, C. Simserides*

National and Kapodistrian University of Athens, Faculty of Physics, Department of Solid State Physics, Panepistimiopolis, GR-15784 Zografos, Athens, Greece

We study the electronic structure of nucleic acid bases and analogues with the linear combination of atomic orbitals (LCAO) method taking only p_z atomic orbitals into account, in other words using a type of Hückel model but with the parametrization proposed by Hawke *et al.* [1]. This parametrization can be employed to molecules containing carbon, nitrogen, or oxygen atoms with sp^2 hybridization. For the diagonal matrix elements of the LCAO description, four empirical parameters are used, corresponding to carbon, nitrogen with one or two p_z electrons and oxygen atoms. For the non-diagonal matrix elements between neighbouring atoms the bond-length dependent formula of Harrison is used [3]. The method has already been successfully applied among other molecules to adenine, guanine, cytosine, thymine, and uracil [1] and subsequently used to obtain the tight binding parameters pertinent to charge transfer along DNA [2]. Here we apply it to nucleic acid bases and analogues e.g. purine, 1,4-dioxo pyrazine, 1H-imidazole, 1H-indazole, 1H-benzimidazole, pyrazine, pyrimidine, and so on. We compare our results to experimental ionization energies and HOMO-LUMO gaps.

References

- [1] L.G.D. Hawke, G. Kalosakas, C. Simserides, *Molecular Physics* 107 (2009) 1755.
- [2] L.G.D. Hawke, G. Kalosakas, C. Simserides, *Eur. Phys. J. E* 32 (2010) 291; *ibid.* 34 (2011) 118.
- [3] W.A. Harrison, *Electronic Structure and the Properties of Solids*, 2nd ed. (Dover, New York, 1989); *Elementary Electronic Structure* (World Scientific, River Edge, NJ, 1999).

* csimseri@phys.uoa.gr

Pro-angiogenic features of Wharton's Jelly-derived Mesenchymal stromal cells enhance vascular formation on novel Chitosan-*graft*-Poly (ϵ -Caprolactone) Copolymer

Evdokia Mygdali*^{1,3}, Maria Kaliva^{1,2}, Maria Vamvakaki^{1,2}, Charalampos Pontikoglou⁴,
Maria Chatzinikolaidou^{1,2}

¹University of Crete, Dept. of Materials Science and Technology, 71003 Heraklion, Greece,

²IESL-FORTH, Vasilika Vouton, 71110 Heraklion, Greece,

³University of Crete, Dept. of Biology, 71003 Heraklion, Greece,

⁴University of Crete, Dept. of Haematology, School of Medicine 71003 Heraklion, Greece

INTRODUCTION

Enhanced vascularisation is critical to the treatment of ischemic tissues and the engineering of new tissues and organs [1]. Paracrine factors from Wharton's Jelly-derived Mesenchymal Stromal cells (WJ-MSCs) could act as a stimulant for vascular formation [2,3]. In this study, we report on the strong cell adhesion of Human Umbilical Vein Endothelial Cells (HUVECs) on a novel chitosan-*graft*-poly (ϵ -caprolactone) (Ch-g-PCL) copolymer [2] that can be used as a biodegradable matrix for the formation of angiogenic sprouting induced by WJ-MSCs Conditioned Media (CM) for potential blood vessel regeneration.

MATERIALS AND METHODS

We first synthesize the copolymer by grafting modified PCL-COOH onto a chitosan backbone as recently described [3]. We prepare spin-coated films from the copolymer on glass substrates. Following, we investigate the cellular adhesion of HUVECs by means of Scanning Electron Microscopy and their viability using the alamarBlue® assay. After incubation with CM, we observe the formation of "tip cells" that lead the angiogenic sprouting, by ELISA detection. Furthermore, we examine the gene expression involved in angiogenesis by means of qPCR.

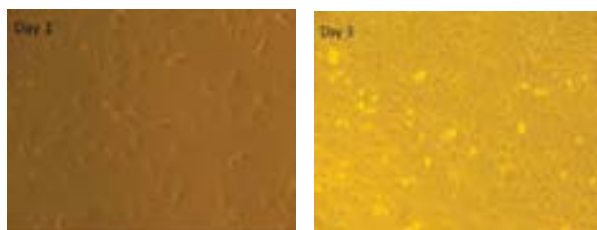


Figure 1: Adhesion and proliferation of HUVECs at passage 3 on Ch-g-PCL matrices supplemented with Endothelial Growth Medium+2% FBS on day 1 and day 3 after seeding.

RESULTS

Our preliminary results demonstrate a strong adhesion of HUVECs on the copolymeric material from the first day in culture, and a proliferation increase after 3 days. Successful seeding of HUVECs on Ch-g-PCL matrices and subsequent treatment with Conditioned Medium from WJ-MSCs led to angiogenic sprouting. This indicates the potential of this system to be used as inductive scaffold for blood vessel regeneration.

REFERENCES

- [1] V. Patel and A. G. Mikos, Journal of Biomaterials Science, Polymer Edition **15**(6) , 701(2004).
- [2] Batsali, A., et al. Cytotherapy **16**(4), S73(2014).
- [3] Chatzinikolaidou, M., et al. Current Pharmaceutical Design **20**(12), 2030 (2014)

* evi.mygdali@gmail.com

Synthesis of PDMAEMA-*b*-PTHPMA copolymers and investigation of their lithographic performance

A. Nika^{3,4,*}, Th. Manouras¹, M. Chatzichristidi^{3,4}, M. Vamvakaki^{1,2} and P. Argitis³

¹Institute of Electronic Structure and Laser, FORTH, 71110 Heraklion, Greece

²Department of Materials Science and Technology, University of Crete, 71003 Heraklion, Greece

³Institute of Nanoscience and Nanotechnology, NCSR 'Demokritos', 15310 Aghia Paraskevi, Greece

⁴Industrial Chemistry Laboratory, Department of Chemistry, University of Athens, Panepistimiopolis Zografou 35, 15771 Athens, Greece

A constant need for smaller, faster and more energy efficient electronic devices has increased demands for higher component density in integrated circuits, and hence smaller component sizes. In addition new device technologies are being proposed in emerging fields including photonic crystals, microsystems and the broad area of bioapplications. Block copolymer lithography is widely considered as a promising patterning technology for miniturized device fabrication, but also for the development of nanofabrication routes facilitating the development of novel devices.

In this work, we present a novel block copolymer system used in top-down lithography for the generation of bottom-up nanoscale patterns. Amphiphilic poly(2-dimethylamino ethyl methacrylate)-*b*-poly(tetrahydropyranyl methacrylate), PDMAEMA-*b*-PTHPMA, copolymers were synthesized by group transfer polymerization and were characterized with ¹H NMR and GPC. Chloromethyl naphthalene was used for the quaternization of the tertiary amine groups of PDMAEMA in order to increase the hydrophilicity and the plasma etch resistance of this block. (Figure 1) The chemical amplified lithographic ability depends on the acid catalysed deprotection of the THPMA blocks. Furthermore, the direct block copolymer lithographic ability depends on the difference in the hydrophilicity of the two blocks following the quaternization of the PDMAEMA block to form the quaternary ammonium salt. Finally, the polymers have been evaluated as components of chemically amplified resist formulations in combination with photoacid generators. Upon exposure to 248 nm, contact printing and 500 nm structures were created.

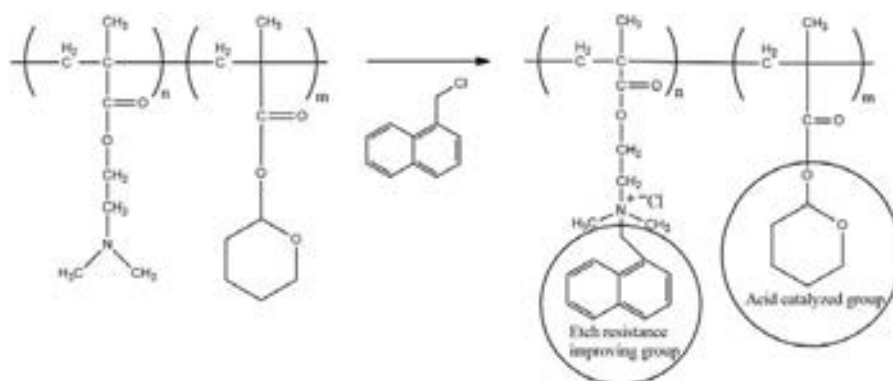


Figure 1: Quaternization reaction of the PDMAEMA-*b*-PTHPMA block copolymer

Controlled synthesis of active metal nanocatalysts within pH-responsive microgel particles

M. Kaliva,^{1,2*} C. Orfanou,³ S.H. Anastasiadis^{1,3} and M. Vamvakaki^{1,2}

¹Institute of Electronic Structure and Laser, Foundation for Research and Technology, 711 10 Heraklion, Crete, Greece

²Department of Materials Science and Technology, University of Crete, 710 03 Heraklion, Crete, Greece

³Department of Chemistry, University of Crete, 710 03 Heraklion Crete, Greece
 Polymer microgel particles can be used as ‘nanoreactors’ for the controlled synthesis of metal nanoparticles (NPs). The use of microgel particles as templates for the in-situ formation of metal nanocatalysts has certain advantages over other polymer matrices, i.e., their facile preparation and functionalization, adjustable size, enhanced colloidal stability over a wide pH range as well as in organic solvents, and their high porosity depending on their cross-link density and the environmental conditions [1]. In this work, electrostatically and sterically stabilized pH-responsive microgel particles based on poly(2-(diethylamino)ethyl methacrylate), (PDEA), poly(acrylic acid), (PAA), and poly(methacrylic acid), (PMAA), were prepared by a free radical emulsion copolymerization process. The pH-sensitive microgels prepared were, then, used as templates for the growth of palladium (Pd), ruthenium (Ru), platinum (Pt) and bimetallic platinum/vanadium (Pt/V) NPs. These metal nanocatalysts were formed within the PDEA, PAA and PMAA microgels following a two-step process (Figure 1a). First metal precursors capable to interact with the polymer functional groups (tertiary amine and carboxylic acid for PDEA and PAA/PMAA, respectively) were incorporated within the microgel particles. In the second step, the metal species were reduced to produce the catalytically active metal NPs within the microgels [2]. The microgel-based nanocatalysts were characterized by dynamic light scattering, thermogravimetric analysis, transmission electron microscopy (TEM), X-ray diffraction and X-Ray photoelectron spectroscopy. Representative, TEM images show the homogeneous distribution of Ru and Pt/V NPs within the PDEA microgels and verify the controlled synthesis of monodisperse metal nanoparticles (Figure 1b).

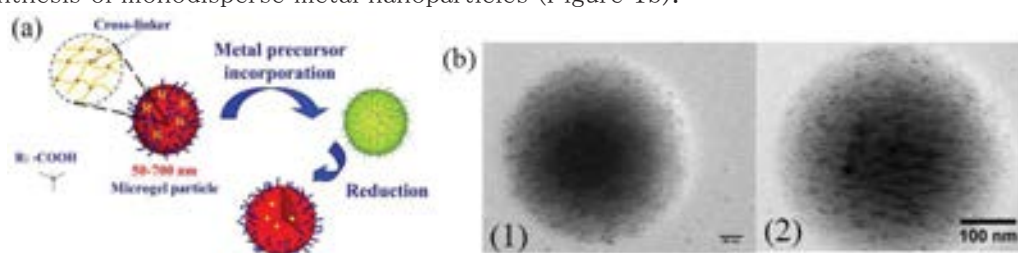


Figure 1: (a) Schematic representation of the synthesis of metal nanoparticles within the microgel particles (b) TEM images of Ru (1) and Pt/V (2) NPs within the PDEA microgels.

References

- [1] N. Welsch, M. Ballauff and Y. Lu, *Adv. Polym. Sci.* **234**, 129-163 (2010)
 [2] Kaliva, M. A. Frysalis, C. Flouraki, L. Papoutsakis, M. Vamvakaki and S.H. Anastasiadis, *Macromol. Symp.* **331-332**, 17-25 (2013)

* kalivm@iesl.forth.gr

Synthesis and Characterization of Biodegradable Copolymers for Tissue Engineering

A. Papadopoulos,^{1,*} M. Kaliva,^{1,2} G. Kaklamani,² M. Vamvakaki^{1,2}

¹Department of Materials Science and Technology, University of Crete, 710 03
Heraklion, Crete, Greece

²Institute of Electronic Structure and Laser, Foundation for Research and Technology, 711 10
Heraklion, Crete, Greece

Polymers have been extensively used to fabricate scaffolds for tissue regeneration in order to repair or reconstruct damaged tissues *in vitro* or *in vivo* [1]. Chitosan (CS) and polycaprolactone (PCL) are among the most widely studied polymers. Chitosan (CS), a natural polysaccharide, is a biocompatible, biodegradable and non-toxic polymer, however, it exhibits low mechanical strength and also, due to its hydrophilicity, it can be slightly dissolved in an aqueous culture medium [2]. On the other hand, PCL is a biocompatible, biodegradable and nontoxic synthetic polymer, with excellent mechanical properties [3]. In this work CS-graft-PCL copolymers were prepared by grafting hydrophobic PCL polymer chains on the CS backbone to alter the solubility of CS and improve its mechanical properties. First, PCL functionalized with one carboxylic acid terminal group (PCL-COOH) was prepared by ring opening polymerization of ϵ -caprolactone, using glycolic acid as the initiator and tin octanoate as the catalyst. Polymers of different molecular weights were obtained and were characterized by gel permeation chromatography and proton nuclear resonance (¹H NMR) spectroscopy. Next, the PCL-COOH chains were chemically grafted onto the CS backbone via the hydroxyl groups of CS (Fig. 1a) [4]. The purified products as well as the intermediates of the reaction were characterized by attenuated total reflectance Fourier transform infrared and ¹H NMR spectroscopies. Next, thin films of the CS-g-PCL samples were produced using the drop casting method and cellular compatibility of the materials was examined. The 2D scaffolds were seeded with NRK cells for 7 days and the viability of the cells was tested using live-dead staining (Fig. 1b) and MTT assay. The topographical characteristics of the cells attached on the polymer surface were visualized using SEM. After a week study the cellular behavior was enhanced showing an increased cell number, very good cell attachment and proliferation.

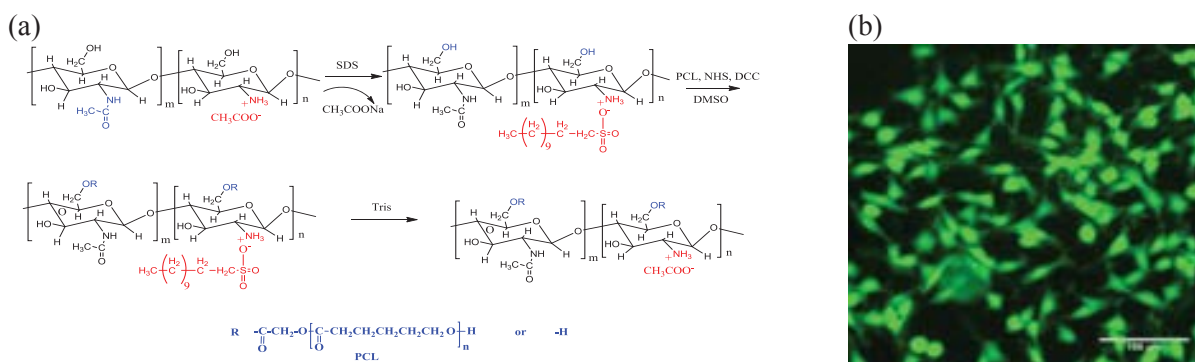


Figure 1: a) Synthetic procedure followed for the preparation of the CS-g-PCL copolymers and b) Cellular viability on a CS-g-PCL film on Day 3 of cell culture.

References

- [1] J.A. Hubbell, Nature Biotechnology **13**, 565 (1995).
- [2] S.V. Madihally, H.W.T. Matthew, Biomaterials **20**, 1133 (2009).
- [3] M.R. Wilson, A.G.A. Coombes, Biomaterials **25**, 459 (2004).
- [4] M. Chatzinikolaidou, M. Kaliva, A. Batsali, C. Pontikoglou, M. Vamvakaki, Current Pharmaceutical Design **20**, 12 (2014).

* mst597@edu.materials.uoc.gr

Electrospun, pH-responsive microfibrinous membranes as adsorbents for bacteria removal from contaminated aqueous solutions

Petri Ch. Papaphilippou¹, Ioannis Virydes², Theodora Krasia-Christoforou¹

¹ *Department of Mechanical and Manufacturing Engineering, University of Cyprus, Nicosia, Cyprus*

² *Department of Environmental Science and Technology, Cyprus University of Technology, Limassol, Cyprus*

Water is one of the most essential elements in human life. Through many decades, humanity is facing a major problem of water contamination with subsequent high risks in human health and quality of life. During the last years there is an increased interest on the protection and purification of urban wastewater contaminated by pathogens [1]. Several techniques currently used to treat wastewater rely on direct chemical processes, (i.e. Chlorination and Advanced Oxidation Processes (AOPs)), which however, lead to the generation of harmful byproducts. Membrane filtration technologies are often employed for the decontamination and purification of water supplies including Microfiltration (MF), Ultrafiltration (UF), Nanofiltration (NF) and Reverse Osmosis (RO). Such technologies have been proved to be energy-efficient and in addition they do not require the use of chemicals [2].

Herein, novel materials in the form of microfibrinous membranes have been generated by means of the electrospinning technique and further evaluated as adsorbents for selected bacteria microorganisms. Electrospinning is a low-cost method that is used for the production of fibrous materials with fiber diameters ranging between a few nanometers up to a few micrometers [3]. Consequently, such materials are characterized by high surface-to-volume ratios rendering them appropriate in various applications including water remediation through filtration [4]. Random copolymers consisting of the hydrophobic methyl methacrylate (MMA) and the hydrophilic/pH-responsive 2-diethylamino ethyl methacrylate (DEAEMA) (pKa ~ 7.3) synthesized by conventional free radical polymerization have been electrospun under specific electrospinning conditions to yield cylindrical, beaded-free microfibrinous polymer membranes. The morphology and the thermal stability of the membranes were determined by scanning electron microscopy (SEM) and thermal gravimetric analysis (TGA), respectively. The aforementioned materials were assessed against the gram-negative bacteria of *Pseudomonas aeruginosa* and *Advenella species* in order to determine their performance as wastewater filtration systems. The bacteria removal by the microfibrinous membranes was studied by measuring the optical density (OD) of the microorganisms by UV-Vis spectrophotometry.

Acknowledgements

This work has been funded by the University of Cyprus and the University of Cyprus Grant "New Researchers".

References

- [1] Joao P.S. Cabral, "Water Microbiology. Bacterial Pathogens and Water", *Int. J. Environ. Res. Public Health*, 2010, 7, 3657-3703. [2] B. Van der Bruggen, C. Vandecasteele, "Distillation vs. membrane filtration: overview of process evolutions in seawater desalination", *Desalination*, 2002, 143(3), 207-218. [3] Z.-M. Huang, Y.-Z. Zhang, M. Kotakic, S. Ramakrishna, "A review on polymer nanofibers by electrospinning and their applications in nanocomposites", *Compos. Sci. Technol.*, 2003, 63, 2223-2253. [4] R. Gopal, S. Kaur, Z.W. Ma, C. Chan, S. Ramakrishna, T. Matsuura, "Electrospun nanofibrous filtration membrane", *J. Membr. Sci.*, 2006, 281(1-2), 581-586.

The effect of nano graphene platelets addition on the mechanical performance of epoxy resin

Z. Paragkamian*, N.D. Alexopoulos

Department of Financial Engineering, University of the Aegean, Chios, Greece

P. Poulin

Université de Bordeaux, Centre de Recherché Paul Pascal – CNRS, Pessac, France

The present work investigates the effect of the addition of different nanographene platelets (NGP) of various concentrations in epoxy resin. NGPs of various geometrical dimensions (thickness of the layers) were exploited as reinforcement to improve the mechanical properties of the matrix. The required amount of NGPs was dispersed in a solvent by ultrasonication for 1 h. Then the required amount of epoxy resin was introduced into the above dispersion and mixed under vigorous mechanical stirring followed by ultrasonication for 30 min. The mixture was then degassed for about 20 min under vacuum until it was completely bubble free [1]. Afterwards, the hardener was added into the mixture, and the mixture was cast on metal mould (Figure 1a) and dried under vacuum in desiccators for overnight at room temperature. Then, they were allowed to cure at 120°C for further study. Tensile (Figure 1b) and fracture toughness specimens were produced with varying types of NGPs and NGPs concentration in the resin according to ASTM D638 and D5045 designations, respectively.



Figure 1: Photographs of the (a) metallic mould that tensile specimens were produced and (b) demoulded tensile specimens.

Tensile and fracture toughness tests were performed in an MTS-Insight 10 kN loading frame and according to their corresponding standard test methods. During the tests, time, force, extensometer, crack opening displacement and crosshead displacement were continuously monitored and recorded. It was found that the addition of NGPs essentially increased the tensile modulus of elasticity; the mechanical tensile test results will be explicitly discussed.

References

- [1] Vairis, Alexopoulos, Favvas, Nitodas and Stefopoulos, Proceedings of the ASME 2013 International Mechanical Engineering Congress & Exposition ASME 2013 November 15-21, 2013, San Diego, California, USA

* Zafeiroula Paragkamian, email: fme08082@fme.aegean.gr

Influence of the cohesion between polymer chains on the structure and the electrical properties of polyaniline and polypyrrole nanocomposites with zeolite and ZnO

S. Sakkopoulos*, E. Vitoratos, Ch. Anestis

Department of Physics, University of Patras, GR-26500 Patras, Greece

E. Dalas, P. Mougoyannis

Department of Chemistry, University of Patras, GR-26500 Patras, Greece

The intercalation of conductive polyaniline (PANI) and polypyrrole (PPy) chains in zeolite galleries, a few nanometers wide, allows obtaining composite materials with significantly improved mechanical properties, thermal and chemical stability [1]. These nanocomposites can find application in hydrogen storage, solid electrolyte cells, chemical gas or pH sensors, membranes, fabrication of molecular wires, etc. Moreover, PANI and PPy combined with ZnO can make composite polymer/insulating materials suitable for solar cells [1–3].

In PANI there is a strong very short ≈ 2.45 Å hydrogen bond between neighboring chains, making PANI semicrystalline, though in PPy weak van der Waals forces hold together the aromatic groups at a distance of ≈ 3.42 Å making the polymer amorphous [4].

In the PANI/zeolite composites the conductivity and thermal stability remain practically unchanged with increasing zeolite content. On the contrary, in PPy/zeolite composites these properties improve with increasing zeolite concentration. Moreover, SEM images and XRD patterns of PANI/ZnO composites reveal that a number of the ZnO particles are expelled from the matrix, although in PPy/ZnO composites ZnO is completely encapsulated into the polymer. These differences are attributed to the stronger bond between PANI chains which justify the formation of crystalline conductive grains in it in contrast to the much weaker packing of polymer chains in amorphous PPy.

The difficulty of monomer diffusion, the much slower polymerization and the powerful mutual attachment of the PANI chains minimize the growth of them into the zeolite galleries. On the other hand, the more loosely attached PPy chains penetrate more easily the nanopores of the zeolite. So, a greater number of the former disorderly arranged PPy chains become aligned increasing the electrical conductivity and making the composites more resistant to aging.

In the case of the PANI/ZnO composites the strong attachment of the polymer chains, expels a number of the zeolite particles from the composite matrix. On the contrary, PPy with the weaker bonds between the chains can encapsulate a much greater number of ZnO particles inside it.

References

- [1] Shakoor, Rizvi and Hina, *J. Appl. Polym. Sci.* 124, 3434 (2012).
- [2] Dalas, Vitoratos, Sakkopoulos and Malkaj, *J. Power Sources* 128, 319 (2004).
- [3] Vitoratos, Sakkopoulos, Dalas, Malkaj and Anestis, *Curr. Appl. Phys.* 7, 578 (2007).
- [4] Colomban, Gruger, Novak and Régis, *J. Mol. Struct.* 317, 261 (1994).

* sakkop@physics.upatras.gr

Photodegradable polyacetal-based cross-linkers

D. Terzakis,^{2,*} A. Tsintsifa,² Th. Manouras¹ and M. Vamvakaki^{1,2}

¹*Institute of Electronic Structure and Laser, FORTH, 71110 Heraklion, Greece*

²*Department of Materials Science and Technology, University of Crete, 71003 Heraklion, Greece*

Photodegradable polymers constitute an emerging class of materials that finds numerous applications in biotechnology, biomedicine, and nanoscience [1]. Photodegradable polymers in the form of hydrogels are of particular interest, because of their excellent adaptation in cell cultures allowing also the spatiotemporal control of their gelation behavior by an external stimulus such as light irradiation.

In this work, we have synthesized photodegradable cross-linkers based on a photodegradable acetal oligomer decorated with methacrylate terminal groups. The photodegradable methacrylate terminated oligomers were synthesized via a two-step process. In the first step, 2-nitroresorcinol was reacted with an excess of cyclohexanol divinyl ether in mildly acidic conditions to obtain a photocleavable acetal oligomer with vinyl ether terminal groups. For the second step, 2-hydroxyethyl methacrylate was added in the reaction to convert the vinyl ether terminal groups of the oligomer into methacrylate functionalities (figure 1). The progress of the reaction was monitored by gel permeation chromatography and proton nuclear magnetic resonance spectroscopy.

Our novel photocleavable cross-linker is a potentially versatile and convenient material used for the development of photodegradable hydrogels for biomedical applications. Their degradation upon visible light irradiation at very low dosages is envisaged [2].

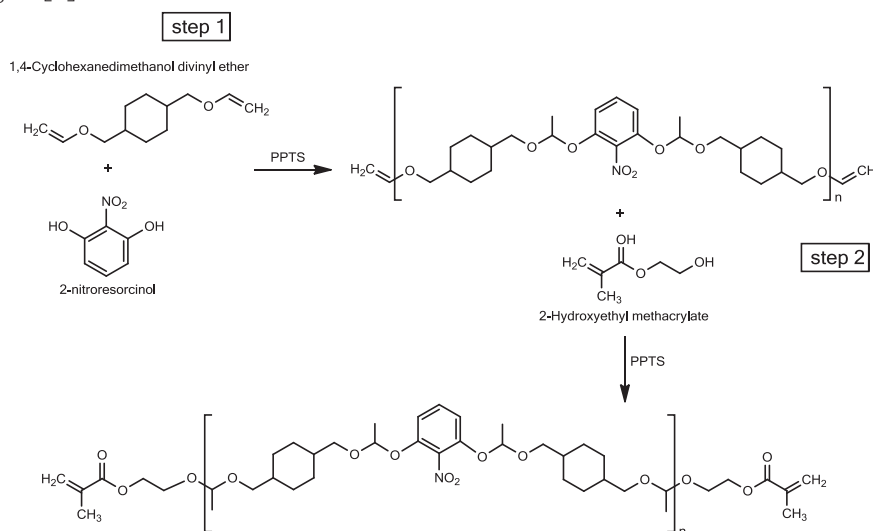


Figure 1: Synthesis of a photodegradable cross-linker

References

- [1] G. Pasparakis, T. Manouras, A. Selimis, M. Vamvakaki and P. Argitis, *Angewandte Chemie International Edition* 50, 4142–4145 (2011).
 [2] G. Pasparakis, T. Manouras, M. Vamvakaki, P. Argitis, *Nature Comm.*, 5, 3623 (2014).

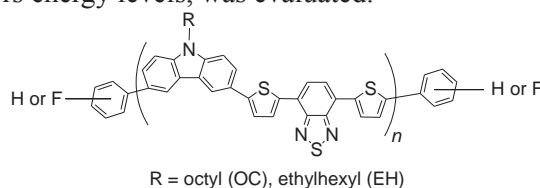
Electrochemical characterization of polymer electron donors for organic solar cells

K. Theodosiou^{*1}, S. Kakogianni², A. Andreopoulou², G. Leftheriotis¹, J. Kallitsis²
¹Renewable Energy and Environment Laboratory, Physics Department,

²Advanced Polymers & Hybrid Nanomaterials Research Laboratory, Department of Chemistry.

University of Patras, 26500 Patras, Greece

Development of novel polymer compounds is essential to the fabrication of efficient and durable organic photovoltaics (OPVs). Suitable materials can be developed, tailoring the HOMO and LUMO levels of the compounds. In this report, cyclic voltammetry was used for the determination of HOMO and LUMO levels of two highly promising materials belonging to the PCDTBT class of alternating donor-acceptor polymers. The structures of the examined polymers are given in Scheme 1. The effect of the end-groups employed to cap the macromolecular chains (either phenyl or perfluorophenyl) and of their molecular weight on the polymers energy levels, was evaluated.



P3,6C^RDTBT-(Ph or 5F)

Scheme 1: Chemical structures of the two polymers studied.

The experiments were carried out with use of an Autolab electrochemical analyzer. A three electrode cell was used, consisting of a platinum wire counter electrode, an Ag/AgCl reference electrode and an ITO/Glass working electrode versus ferrocene. The polymers were drop-casted from solution on the ITO conductive side. The HOMO and LUMO levels were calculated by the following empirical relations with use of the Fc level of -4.8 eV [1,2]:

$$E_{HOMO} = -e(E_{onset}^{ox} - E_{1/2}^{Fc}) - 4.8 [eV], \quad E_{LUMO} = -e(E_{onset}^{red} - E_{1/2}^{Fc}) - 4.8 [eV]$$

The estimated redox potentials and the HOMO, LUMO energy levels are summarized in Table 1. It follows that both compounds exhibit energy levels suitable for use in OPVs. The higher E_g of P3.6C-DTBT-5F (TOL) and of P3.6C-DTBT-Ph (TOL) is caused by its lower molecular weight.

Compound/Solvent	E_{ons}^{red} (V)	E_{ons}^{ox} (V)	E_g (eV)	Homo (eV)	Lumo (eV)
P3.6C-DTBT-Ph (TCE)	-0.94	+0.95	1.89	-5.2	-3.3
P3.6C-DTBT-Ph (TOL)	-1.04	+1.16	2.20	-5.4	-3.2
P3.6C-DTBT-5F (CB)	-1.08	+1.10	2.18	-5.4	-3.2
P3.6C-DTBT-5F (TOL)	-1.16	+1.17	2.33	-5.4	-3.1

Table 1: HOMO/LUMO levels obtained from cyclic voltammetry

Acknowledgments. Financial support by the “ARISTEIA” Action of the “Operational Programme Education and Lifelong Learning” co-funded by the European Social Fund (ESF-EU) and National Resources (Greece), through the project "Design and Development of New Electron Acceptor Polymeric and Hybrid Materials and their Application in Organic Photovoltaics" – DENE A 2780, is gratefully acknowledged.

References

- [1] Al Ibrahim M. et. al. Organic Electronics **6**, 65 (2005).
 [2] Ruby M. et. al. J. Photochem. & Photobiol. A: Chemistry **52**, 247 (2012).

* krtheodosiou@upatras.gr

Modelling of application related effects for flexible capacitive strain sensors

V. Tsouti* □ S. Chatzandroulis

*Institute of Nanoscience and Nanotechnology, Department of Microelectronics,
NCSR “Demokritos”, Athens, Agia Paraskevi, Greece*

The wide range of applications of strain sensors leads to an increased interest on flexible, cost effective and low power devices for strain and bending measurements [1–2]. A simply structured sensor that meets these requirements is studied using finite element analysis (FEA). The device is depicted in Fig.1 and is essentially composed of 5 thin flexible layers: three layers of pure Polydimethylsiloxane (PDMS) separated by two conducting PDMS layers that can be made by dispersing nanoparticles e.g. carbon black, in the PDMS matrix (CB/PDMS). The operation principle of the sensor is based on the capacitance change between the two flexible conductive plates. The sensor modelling focuses on the sensor performance variations for different applications and takes into account the fabrication process that can be used for elastomeric sensors. The FE simulations were used in order to study factors that influence the strain sensor response in different possible applications. For this purpose, two models have been developed. The first one considers elongations of the sensor and two different boundary conditions were applied reflecting different sensor mountings. The second model places the sensor on the surface of a cantilever beam that is deflected vertically combining small strain with bending. Differences in the sensor response are observed depending on the mounting conditions and the model studied.

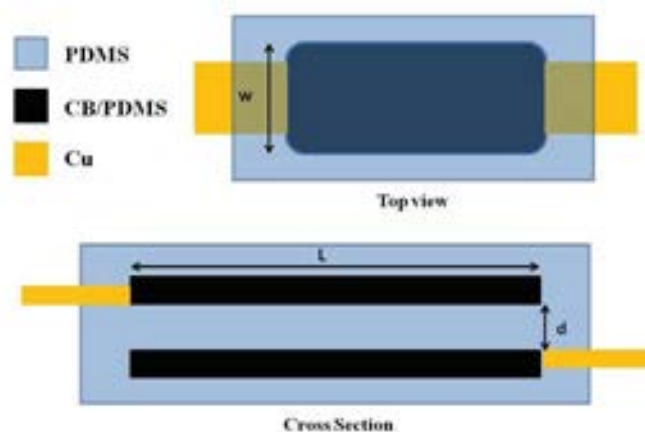


Figure 1: Schematic representation of the strain sensor.

Acknowledgment: Financial support from “IKT fellowships of excellence for postgraduate studies in Greece–Siemens program” is gratefully acknowledged.

References

- [1] D.J. Cohen, D. Mitra, K. Peterson, M.M. Maharbiz, *NanoLett.* **12**, 1821 (2012)
- [2] S-H Bae, Y. Lee, B. K. Sharma, H-J Lee, J-H Kim, J-H Ahn, *Carbon*, **51**, 236 (2013)

* vasso@imel.demokritos.gr

Collapse transitions in thermosensitive multi-block copolymers: A Monte Carlo study

A. N. Rissanou¹, D.S. Tzeli^{*2}, S.H Anastasiadis^{3,4}, and I.A. Bitsanis⁴

¹ *Department of Mathematics and Applied Mathematics, University of Crete.*

² *Department of Material Science and Technology, University of Crete.*

³ *Department of Chemistry, University of Crete.*

⁴ *Foundation for Research and Technology-Hellas, Institute of Electronic Structure and Laser, Heraklion, Greece.*

The focus of the present study is to investigate the self-assembly behavior of a single linear multiblock copolymer chain of various lengths (N), via Monte Carlo simulations.[1] More specifically, the chain is of type $(A_n B_n)_m$ and consists of alternating A and B blocks, where A are solvophilic (i.e., extended conformations are preferred) and B are solvophobic (i.e., condensed conformations are preferred “globules”) and $N = 2nm$. We explore the conformational transitions of the chain and their dependence of the chain length and the number of blocks. In order to achieve this we classify the chain transitions in five cases based on the globules formed by the solvophobic B -blocks (Figure 1). We study systems with relatively high molecular weights i.e., N in the range of [500 – 5000] units. Energy parameters have values which correspond to good - almost athermal solvent for A -blocks and very poor solvent for B -blocks. A rich phase behavior is observed as a result of the alternating architecture of the multiblock copolymer chain. Furthermore the combination of all parameters of the phase space plays a key role in the preferred conformations. We trust that thermodynamic equilibrium has been reached for chains of N up to 2000 units, while the results for longer chains indicate kinetic issues. Finally, we compare the globules formed by the copolymer chains with their homopolymer analogs.[2] This comparison underlines the substantial influence of solvophilic B -blocks on the chain configurations.

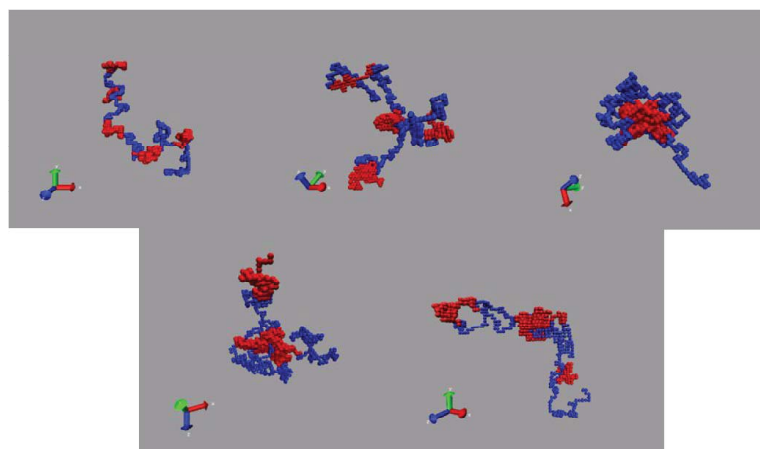


Figure 1: Snapshots of configurations of a single multiblock copolymer chain.

References

- [1] A. N. Rissanou, D.S. Tzeli, S.H Anastasiadis, and I.A. Bitsanis “Collapse transitions in thermosensitive multi - block copolymers: A Monte Carlo study”, *Journal of Chemical Physics* **140**, 204904 (2014).
- [2] A. N. Rissanou, S.H Anastasiadis, and I.A. Bitsanis “A Monte Carlo Study of the Coil-to-Globule Transition of a Model Polymeric System”, *Journal of Polymer Science: Part B: Polym. Phys.* **44**, 3651-3666 (2006).

* tzeli@materials.uoc.gr

Mechanical and Dielectric Properties versus Structure: Study of epoxy resin /barium titanate nanocomposites

I.A. Asimakopoulos^{1*}, G.C. Psarras² and L. Zoumpoulakis¹

¹*National Technical University of Athens, School of Chemical Engineering, Departement III "Materials Science and Engineering", Laboratory Unit "Advanced and Composite Materials", 9-Heroon Polytechniou street, Zografou Campus, Athens 157 73, Greece*

²*Department of Materials Science, School of Natural Sciences, University of Patras, Patras 26504, Greece*

The development of microelectronic devices targets on reducing both their dimensions and weight. New high dielectric constant and low loss materials are needed to replace the current wire insulators of silicon dioxide, thereby reducing the signal delays and electrical power loss in the new generations of large scale integrated circuits [1–4]. Nano-inclusions can be considered as a distributed network of nanocapacitors, which can be charged and discharged defining an energy storing process, at the nanoscale level [5-8]. Epoxy resins are presently important organic matrices in composite industry. They are frequently used in demanding applications due to their excellent mechanical properties, thermal stability and chemical resistance. Furthermore, they also have good resistance to moisture, solvents and chemical attacks [9- 11]. Inorganic additives, such as silica and alumina have been used to increase the toughness of epoxies without sacrificing their basic properties, but the presence of numerous inorganic particles increase the viscosity leading to poor dispersion and processing difficulty [11–14]. The aim of this study is the investigation of composites combining epoxy resin with embedded nano-barium titanate particles studied as far as their structure (SEM, DSC, FTIR, XRD etc.) and their mechanical (shear strength) and dielectric properties are concerned.

References

- [1] Homma T., *Materials Science and Engineering R: Reports* **23**, 243–285 (1998).
- [2] Geng Z., Lu Y., Zhang S., Jiang X., Huo P., Luan J., Wang G., *Polymer International*, (in press).
- [3] Cho E-B., Mandal M., Jaroniec M., *Chemistry of Materials*, **23**, 1971–1976 (2011).
- [4] Wang C., Wang T. M., Wang Q. H., *Express Polymer Letters*, **7**, 667-672 (2013).
- [5] Psarras G. C., *Express Polymer Letters*, **2**, 460 (2008).
- [6] Tantis I., Psarras G. C., Tasis D., *Express Polymer Letters*, **6**, 283–292 (2012).
- [7] Asimakopoulos I., Zoumpoulakis L., Psarras G. C., *Journal of Applied Polymer Science*, **125**, 3737-3744 (2012).
- [8] Asimakopoulos I.A., Psarras G. C., Zoumpoulakis L., *Express Polymer Letters* (in press).
- [9] Kim J., Yim B-S., Kim J-M., Kim J., *Microelectronics Reliability*, **52**, 595–602 (2012).
- [10] Jiao J., Sun X., Pinnavaia T. J., *Polymer*, **50**, 983–989 (2009).
- [11] Qi B., Lu S. R., Xiao X. E., Pan L. L., Tan F. Z., Yu J. H., *Express Polymer Letters*, **8**, 467-479 (2014).
- [12] Tang L.C., Zhang H., Sprenger S., Ye L., Zhang Z., *Composites Science and Technology*, **72**, 558–565 (2012).
- [13] Lu S-R., Jiang Y-M., Wei C., *Journal of Materials Science*, **44**, 4047–4055 (2009).
- [14] Johnsen B. B., Kinloch A. J., Mohammed R. D., Taylor A. C., Sprenger S., *Polymer*, **48**, 530–541 (2007).

Effect of carbon nanotubes reinforcement on mechanical and electrical properties of mortar for restoration of monuments of cultural heritage

S. Boutsoukou*, N.D. Alexopoulos

Department of Financial Engineering, University of the Aegean, Chios, Greece

F. Giannakopoulou

Glontech S.A. TE.S.P.A "Lefkippos" Ag. Paraskevi, Attica, Greece

S.K. Kourkoulis

Laboratory of Testing and Materials, National Technical University of Athens, Athens, Greece

The effect of multi-wall carbon nanotubes addition as a reinforcement in mortar that is currently used in applications such as restoration of monuments of cultural heritage was investigated. The incorporation of the nano-reinforcements in different concentrations is expected to increase the mortar's mechanical properties [1, 2]. Furthermore, the addition of the nano-structures at concentrations above the percolation threshold might enhance its monitoring ability via the electrical resistance change method. Traditional approaches for structural health monitoring of Historical Monument components currently focuses on strain gauges that can be applied on the outer material's surface and therefore cannot detect any strain changes or induced damage inside the material/structure. The incorporation of electrically conductive carbon nanotubes, is expected to improve the mechanical performance of mortars and supply them with improved electrical properties.



Figure 1: (a) Experimental three-point bending test set-up of 0.2% MWCNTs mortar and (b) macro-photograph of the electrical resistance testing of the prismatic samples.

The present work primarily investigates the efficient dispersion of multi-wall carbon nanotubes (MWCNTs) in the cementitious material using several different types of surfactants at various concentrations. The MWCNTs/surfactant solutions were sonicated using a titanium probe. The mortars were mixed using a standard mixer, following the ASTM specifications. Compression and three-point bending tests were performed on intact and notched specimens, respectively. During the tests, time, force and displacement were continuously monitored and recorded. Preliminary results indicate that sodium dodecyl benzene sulfonate (SDBS), a surfactant typically used for the dispersion of MWCNTs in polymers [3], is not suitable for use in cementitious materials. The use of a chemical admixture, compatible with the cement, is proposed.

Acknowledgements

The authors acknowledge the financial support of the EU (European Social Fund – ESF) and Greek national funds through the Program "Support newly established firms in their research and development activities", Research Funding Program: "Monitoring of the structural integrity of restored structural parts in ancient monuments of cultural heritage by employing hybrid materials reinforced with CNTs".

References

- [1] Metaxa, Seo, Konsta-Gdoutos, Hersam and Shah, *Cement and Concrete Composites* **34**, 612 (2012).
- [2] Konsta-Gdoutos, Metaxa and Shah, *Cement and Concrete Composites* **32**, 110 (2010).
- [3] Tang, Shafiq, Chan, Wong and Cheung, *Journal of Nanoscience and Nanotechnology* **10**, 4967 (2010).

* Boutsoukou Spyridoula. Email: irida.bou@gmail.com

EFFECT OF IRON SLAG AS MINERAL ADMIXTURE ON DURABILITY OF CONCRETE

N. Chousidis, E. Rakanta, G. Batis

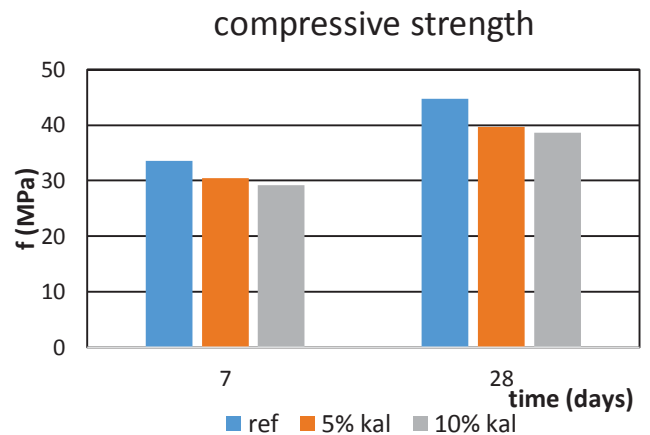
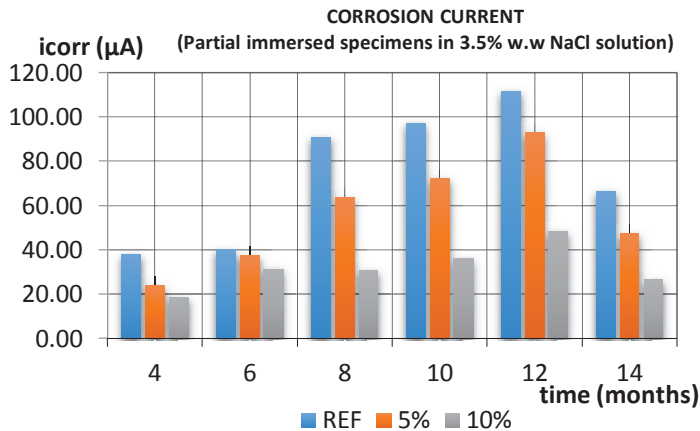
School of Chemical Engineering, National Technical University of Athens, Athens, Greece

Keywords: *pitting corrosion, carbonation, mineral additives, Calamine, XRD.*

The present study investigated the durability of concrete by partial replacement of cement with iron slag known as calamine (95%w.w Iron Oxide). Specifically, the replacement of cement by the additive became in percentages 5% w.w and 10% w.w. cylindrical reinforcement mortar specimens with diameter 50mm and height 100mm were prepared. Steel rebars type B500C Tempcore were used with diameter 10mm (D10) and 100mm length.

Reinforced mortar specimens were partially immersed in 3.5%w.w NaCl solution and exposed in atmosphere for 15 months. The purpose of replacement, is the protection of steel rebars from corrosion by chlorine ions, and concrete from carbonation. Also, due to reduction of cement are reduced CO₂ emissions and reduce the cost of cement.

For the assessment of the concrete resistance, were measured the corrosion potential E_{corr} , corrosion current i_{corr} , the mass loss of reinforcement steel, the carbonation depth of cement mortars, the concentration of total Chloride ions, the compressive strength at 7 & 28 days, the slump of fresh concrete, and the density of fresh and hardened concrete.



Based on the up-to-now results of this study, the specimens with addition 10% of MnO₂ appear smaller corrosion currents and mass loss of steel than reference specimens. Also, the compressive strength with 5% & 10% addition is appeared to be slightly smaller from the reference specimens at 28 days.

It is concluded that calamine is suitable for the production of composite cements, having beneficial effect on reinforcement corrosion in the above corrosive environments.

Microwave Synthesis and Characterization of The Series $\text{Co}_{1-x}\text{Fe}_x\text{Sb}_3$ High Temperature Thermoelectric Materials

A. A. Ioannidou^{1*}, M. Rull², M. Martin-Gonzalez², A. Moure⁴, A. Jacquot³, D. Niarchos¹

1. I.A.M.P.P.N.M. NCSR "Demokritos", 15341, Aghia Paraskevi, Athens, Greece
2. Thermoelectric Research group, Instituto de Microelectronica de Madrid, IMM-CSIC, c/ Issac Newton, 8 PTM, Tres Cantos 28760 Madrid, Spain
3. IPM, Fraunhofer, 79110 Freiburg, Germany
4. Instituto de Cerámica y Vidrio, ICV-CSIC, C/Kelsen 5. Campus de Cantoblanco. 28049 Madrid.

The use of microwave energy for materials processing has a major potential and real advantages over conventional heating such as a) time and energy savings, b) rapid heating rates (volumetric heating vs. conduction), c) considerably reduced processing time and temperature, d) fine microstructures and hence improved mechanical properties and better product performance and e) finally lower environmental impact. In this study we investigated the use of microwave-assisted synthesis, to synthesize the series of $\text{Co}_{1-x}\text{Fe}_x\text{Sb}_3$ using this novel approach, which gave high quality materials with little or no impurity in a fraction of time compared to the conventional synthesis. X-ray diffraction analysis was used to examine the structure and the lattice parameters of the samples while SEM with EDX analysis was used to study the morphology of the compounds. The samples were sintered by SPS and the highest $zT \sim 0.33$ was obtained for $x=0.2$ at 700 K.

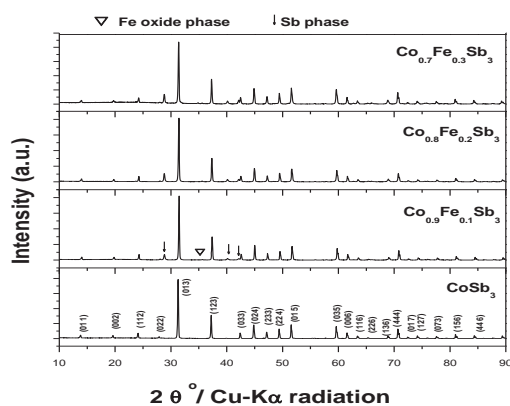


Figure 1: X-ray diffraction analysis of Fe-doped samples after microwave synthesis.

Mechanical behavior of MWCNT reinforced GFRP composites under fatigue constant amplitude loadings with the presence of artificial notches

I. Lazaridou*, N.D. Alexopoulos

Department of Financial Engineering, University of the Aegean, Chios, Greece

A. Vairis, M. Petoussis

Department of Mechanical Engineering, Crete Institute of Technology, Heraklion, Greece

The present work investigates the effect of artificial surface notches on glass fiber reinforced polymers (GFRP) under constant amplitude fatigue loadings and for various nano-reinforced matrices. Different concentrations of Multi-Wall Carbon Nanotubes (MWCNTs) were added to the resin before the vacuum assisted resin infusion (VARI) of the composites [1]. Three different MWCNT nanocomposites were manufactured that had concentrations namely 0.5, 0.75 and 3.0 % MWCNTs [2]. Typical tensile coupons according to ASTM D3039 were machined from the composite plates that had 10 plies of unidirectional S-glass fabric. The artificial surface notches were introduced by a precise saw cut and the notch depth was measured with image analysis (Figure 1a). Two regions of the specimen were monitored by the electrical resistance change method; the so-called “healthy” region and the “notched” region that had the presence of the artificial notch. On the opposite flat surface of the coupon, strain gauges were attached and the readings of strain gauges and electrical resistance were continuously recorded during the progressive fatigue cycles.

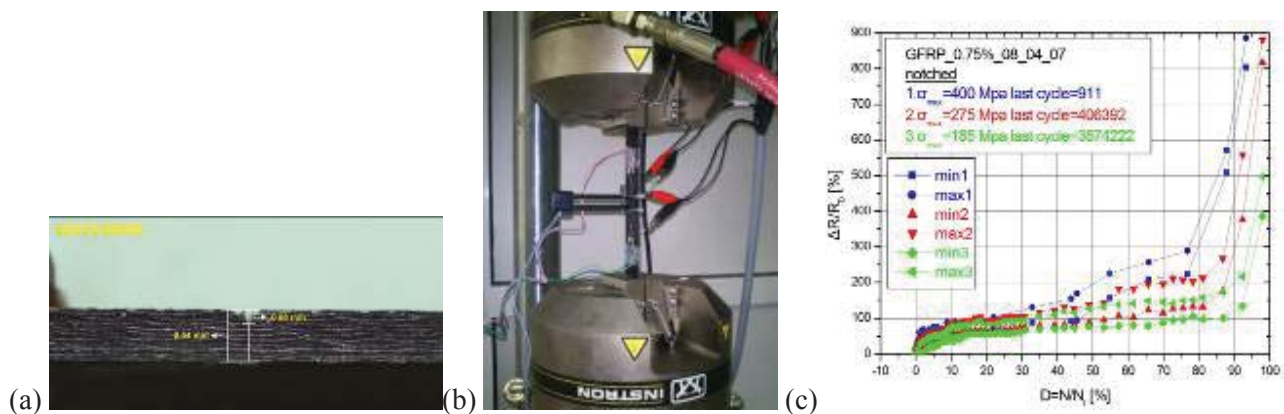


Figure 1: (a) Photograph of the composite’s cross section along with the artificial surface notch, (b) testing set-up with electrical resistance and strain gauges and (c) electrical resistance results of 0.75%wp MWCNTs composite over fatigue life.

Fatigue tests were performed in an MTS 100 kN loading frame with constant stress ratio of $R = 0.1$. Three different fatigue maximum stress levels were selected so as to address all fatigue regimes. It was found (Figure 1c) that a sudden increase takes place on the transition of stage III of the fatigue mechanism. This sudden increase point in the resistance change was applied maximum stress as well as MWCNT concentration (different material) dependant.

Acknowledgements

The present work is a result in the framework of NSRF. The “NANOSTRENGTH” Project (Archimedes Framework) of the Crete Institute of Technology is co-financed by Greece and the European Union in the frame of operational program “Education and lifelong learning investing in knowledge society”. Ministry of Education and religious affairs, culture and sports. NSRF 2007-2013.

References

- [1] Tapeinos, Miaris, Mitschang and Alexopoulos, *Composites Science and Technology* **72**, 774-787 (2012).
- [2] Vairis, Alexopoulos, Favvas, Nitodas and Stefopoulos, *Proceedings of the ASME 2013 International Mechanical Engineering Congress & Exposition ASME 2013 November 15-21, 2013, San Diego, California, USA.*

* Ilona Lazaridou, email: lazaridou.ilona@gmail.com

Intelligent Thermochromic Coatings Grown by Chemical Vapor Deposition at Atmospheric Pressure

D. Louloudakis^{1,2*}, D. Vernardou¹, E. Spanakis³, N. Katsarakis^{1,4,5}, E. Koudoumas^{1,4} and G. Kiriakidis^{2,5}

¹Center of Materials Technology & Photonics, Technological Educational Institute of Crete, 710 04 Heraklion, Crete, Greece

²Department of Physics, University of Crete 711 00 Heraklion, Crete, Greece

³Department of Materials Science & Technology, University of Crete 711 00 Heraklion, Crete, Greece

⁴ Department of Electrical Engineering, School of Applied Technology, Technological Educational Institute of Crete, 710 04 Heraklion, Crete, Greece

⁵ Institute of Electronic Structure & Laser, Foundation for Research & Technology-Hellas, P.O. Box 1527, Vassilika Vouton, 711 10 Heraklion, Crete, Greece

**corresponding author, e-mail dimitr17@yahoo.gr*

Thermochromic materials, such as vanadium dioxide, have the ability to change from a semi-conductive to a metal state when their temperature reaches a specific value, which is called transition temperature (T_c). For the deposition of a thermochromic layer, many methods have been used such as magnetron sputtering, pulsed laser deposition, atomic layer deposition, sol-gel, spin coating etc. Nevertheless, a low cost method using non-toxic precursors and easily transferred to large scale is needed.

In this work, vanadium dioxide films were fabricated using a chemical vapor deposition at atmospheric pressure (APCVD) on fluorine doped tin dioxide pre-coated glass substrates using vanadyl (IV) acetylacetonate as vanadium precursor at 500 °C. The samples were characterized by X-ray diffraction, Raman spectroscopy, Scanning Electron Microscopy (SEM), UV-Vis-NIR spectroscopy measurements at temperatures below and above T_c as well as transmittance measurements as a function of temperature at an incident radiation of 1500 nm. The effect of oxygen flow rate through the reactor on the properties and the subsequent thermochromic characteristics of the samples is discussed.

Acknowledgements: This project is implemented through the Operational Program "Education and Lifelong Learning" action Archimedes III and is co-financed by the European Union (European Social Fund) and Greek national funds (National Strategic Reference Framework 2007 - 2013).

Assessment diagnostics of the functionality of composite insulators operating in the 150kV power network of Crete

N. Mavrikakis^{*1,2}, K. Siderakis² and E. Koudoumas³

¹High Voltage Laboratory, School of Electrical & Computer Engineering, Faculty of Engineering, Aristotle University of Thessaloniki, Greece

²High Voltage Laboratory, Electrical Engineering Department, Technological Educational Institute of Crete, Greece

³Center of Materials Technology and Photonics and Electrical Engineering Department, Technological Educational Institute of Crete, Greece

The performance of high voltage insulators utilized in overhead transmission and distribution lines is a key factor for the reliability of power delivery. Ceramic insulators are replaced by composite insulators, made nowadays by Silicone Rubber with the later providing considerably improved pollution performance in comparison to the ceramic counterparts. The feature that enables composite insulators to perform better than ceramic is their surface behaviour, which is hydrophobic and thus suspends the possibility of surface wetting by dew or fog, which is recognized as a phenomenon critical component. Furthermore in the case of silicone rubber, a more advanced hydrophobicity performance has been developed, capable of recovering the surface behaviour even if hydrophilic contaminants are deposited on the material surface. However, surface hydrophobicity, as a material oriented property, is strongly affected by the ageing mechanisms present in service conditions [1]. Actually, the efficiency of the recovery feature, experienced in the case of SIR is related to the housing material condition and the existing stress conditions. In order to reduce the failure probability, combined diagnostic techniques are required for the assessment of the functionality of composite insulators [2], their results being essential in deciding the maintenance or the replacement of the installed material.

In Crete, more than 50% of the currently installed insulators are made of SIR. In addition, a considerable amount of room temperature vulcanized SIR coatings has been implemented in high voltage substations. In both applications, an average service period of 16 years has been experienced and no flashovers or other insulator failures in the have been recorded. Nevertheless, despite this encouraging fact, according to the international literature and the experience of other utilities, exceeding the age of 15 years in service must be a concern. In this direction the operational condition of composite insulators is under investigation, aiming to evaluate their efficiency and the level of stress that the ageing mechanisms present have applied. In this study, an inspection procedure is presented and analyzed, implemented to field aged composite insulators of the 150kV power network of Crete, incorporating electrical, structural and morphological characterization (Fig. 1) is employed in order to evaluate the condition of field composite insulators of the 150kV power network of Crete.

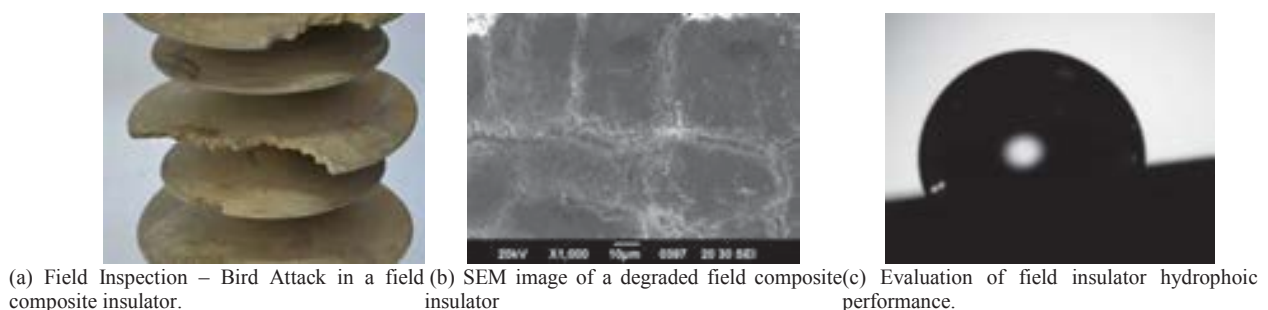


Figure 1: Diagnostic Techniques for evaluating the condition of field composite insulators

References

[1] IEEE Guide for Ageing Mechanisms and Diagnostic Procedures in Evaluating Electrical Insulation Systems, ANSI/IEEE Std 943 1986.

[2] CIGRE Technical Brochure No 545, Assessment of in-service Composite Insulators by using Diagnostic Tools, WG B2.21, 2013.

* mavrikakisnikos@gmail.com

Development, Characterization, and Energy Storage in Barium Titanate Nano- and/or Micro- Polymer Composites

A. C. Patsidis^{*1}, A. Kanapitsas², C. Tsonos², G. C. Psarras¹

¹*Department of Materials Science, School of Natural Sciences, University of Patras, Patras, 26504, Greece.*

²*Department of Electronics, Technological Educational Institute of Stereas Ellados, Lamia, Greece.*

Recently there is an increasing interest upon polymer matrix/ferroelectric ceramic particles composites, due to the technological demands for flexible, high dielectric permittivity and high dielectric breakdown strength materials. Possible applications of these composite systems include integrated capacitors, by-passing, filtering, self-current regulators and timing capacitors [1,2]. The electrical response of these micro- or nano-composites can be suitably adjusted by controlling the type and the amount of the ferroelectric inclusions [3-5]. Ferroelectric particles are considered as active dielectrics, since they undergo a structural transition from the polar ferroelectric phase to the non-polar paraelectric phase, at a critical temperature. The resulting variable polarization provides functional behaviour to the composites.

In this study micro- or nano-BaTiO₃/epoxy composites, as well as hybrid micro- and nano-BaTiO₃/epoxy composites were prepared and studied, varying the amount of the filler. Morphology, thermal properties and dielectric response of the prepared systems were investigated by means of Scanning Electron Microscopy (SEM), X-ray diffraction (XRD), Differential Scanning Calorimetry (DSC) and Broadband Dielectric Spectroscopy (BDS) respectively. Functional behaviour, and energy storage efficiency were examined with parameters the type and the amount of the employed filler, temperature, and frequency.

Acknowledgements:

This research has been partially co-financed by the European Union (European Social Fund - ESF) and Greek national funds through the Operational Program "Education and Lifelong Learning" of the National Strategic Reference Framework (NSRF) - Research Funding Program: THALES. Investing in knowledge society through the European Social Fund.

References

- [1] V. Toner, G. Polizos, E. Manias, C.A. Randall, *J. Appl. Phys.* **108**, 074116 (2010).
 - [2] L. Ramajo, M.M. Reboredo, M.S. Castro, *Int. J. Appl. Ceram. Technol.* **7**, 444 (2010).
 - [3] A. Patsidis, G.C. Psarras, *Express Polym. Lett.* **2**, 718 (2008).
 - [4] A. C. Patsidis, K. Kalaitzidou, G.C. Psarras, *Mater. Chem. Phys.*, **135**, 798 (2012).
 - [5] A. C. Patsidis, G. C. Psarras, *Smart Materials and Structures*, **22**, 115006 (2013).
- Watson and Crick, *Nature* **171**, 737 (1953).

* patsidis@gmail.com

Development, Characterization, and Energy Storage of Polar Oxides/Polymer Matrix Nanodielectrics

G. N. Tomara¹,

¹*Department of Physics, University of Patras, 26504, Patras, Greece,*

C. Tsonos², A. Kanapitsas²,

²*Department of Electronics, TEI of Stereas Ellados, Lamia, Greece,*

G. C. Psarras^{3*}

³*Department of Materials Science, University of Patras, Patras, 26504, Greece*

Polymer matrix composites incorporating ceramic nanoinclusions receive enhanced scientific and technological interest, because of their advanced performance, which includes high dielectric permittivity, and dielectric strength, in tandem with light weight, flexibility, corrosive resistant, good mechanical behaviour and ease processing [1–3]. This type of materials, which is also referred as nanodielectrics, appears to be able to replace conventional insulating materials in numerous applications. Furthermore, current emerging technologies such as stationary power systems, cellular phones, wireless personal digital assistants and hybrid electric vehicles require materials' systems where energy could be stored and harvested.

Nanodielectrics consisted of a polymer matrix and polar oxides nanoparticles exhibit tunable polarization. The latter is related to the piezoelectric and/or ferroelectric behaviour of the employed ceramic particles [3–5]. In this study various ceramic polar oxides are as used reinforcing phase in a commercially available epoxy resin. The employed fillers are BaTiO₃, ZnTiO₃, ZnO, TiO₂ nanoparticles. For each type of nanofiller a series of nanocomposites is prepared varying the ceramic content. Morphology, thermal properties, and dielectric response are investigated by means of scanning electron microscopy, differential scanning calorimetry, and broadband dielectric spectroscopy, respectively. Data analysis is focused in realizing the optimum type and amount of reinforcing phase with respect to dielectric behaviour, functionality and energy storage efficiency.

Acknowledgements:

This research has been partially co-financed by the European Union (European Social Fund - ESF) and Greek national funds through the Operational Program "Education and Lifelong Learning" of the National Strategic Reference Framework (NSRF) - Research Funding Program: THALES. Investing in knowledge society through the European Social Fund.

References

- [1] V. Toner, G. Polizos, E. Manias, C.A. Randall, J. Appl. Phys. 108, 074116 (2010).
- [2] L. Ramajo, M.M. Reboredo, M.S. Castro, Int. J. Appl. Ceram. Technol. 7, 444 (2010).
- [3] A. Patsidis, G.C. Psarras, Express Polym. Lett. 2, 718 (2008).
- [4] A. C. Patsidis, K. Kalaitzidou, G.C. Psarras, Mater. Chem. Phys., 135, 798 (2012).
- [5] A. C. Patsidis, G. C. Psarras, Smart Materials and Structures, 22, 115006 (2013).

*G. C. Psarras@upatras. gr

Broadband dielectric spectroscopy of muscovite and biotite micas at elevated temperatures

V. Saltas*, I. Fitis, F. Vallianatos

Laboratory of Geophysics and Seismology, Department of Environmental and Natural Resources Engineering, Technological Educational Institute of Crete, Greece

D. Pentari

Department of Mineral Resources Engineering, Technical University of Crete, Greece

The unique physico-chemical, electrical, mechanical and thermal properties of micas make them suitable for a wide range of industrial applications and thus the scientific interest for this kind of hydrous aluminosilicate minerals is still persistent [1]. In the present work, broadband dielectric spectroscopy measurements over a broad frequency range (10MHz - 1MHz) and at elevated temperatures (423K - 1373K) were carried out in muscovite and biotite micas, perpendicular to their cleavage planes. Different formalisms of data representation were used (Cole-Cole plots of complex impedance, complex electrical conductivity and electric modulus) to analyze the electrical behavior of micas and its correlation with the dehydroxylation process (Fig. 1). The electrical conductivity is strongly affected by the different concentrations of Fe and Ti and low estimated activation energies suggest proton and/or polaron conduction due to bound water and different oxidation states of Fe, respectively.

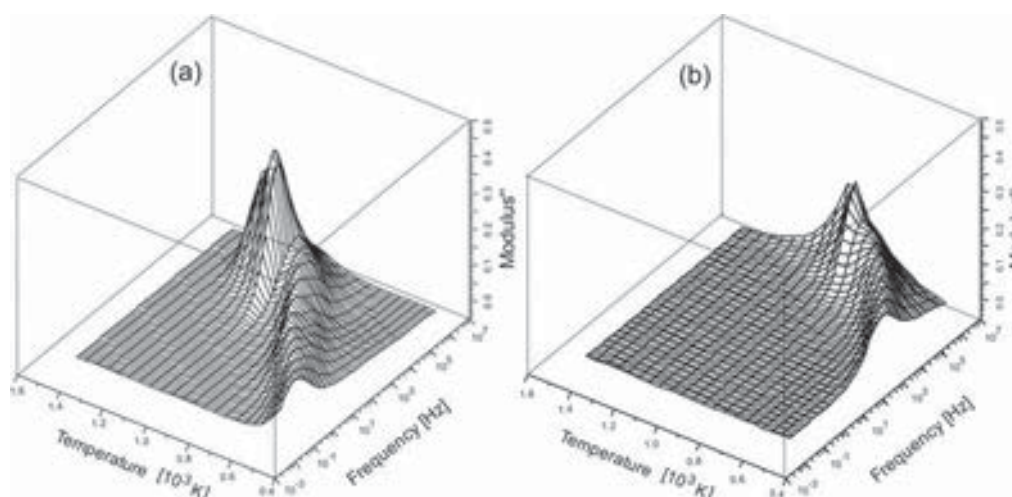


Figure 1: 3D-plane plots of imaginary part of electric modulus (M'') as a function of frequency and temperature up to 1373K for (a) muscovite and (b) biotite mica.

References

- [1] Fleet, Rock-Forming Minerals: micas, Vol. **3A**, 2nd ed. (2002).

* vsaltas@chania.teicrete.gr

Boron Carbide polymer composites: dielectric properties and energy storage.

E.C.Senis, A.C.Patsidis, G.C.Psarras

Department of Materials Science, University of Patras, 26504 Rion, Greece

In the last few decades polymer matrix composite materials filled with inorganic ceramic inclusions have been in the centre of the scientific and industrial interest. In the present study composite systems of epoxy resin and ceramic B₄C (Boron carbide) particles with mean diameter less than 10 microns, have been prepared varying the volume fraction of the inclusions [1,2,4]. The dielectric response of the composites was studied in a wide frequency and temperature range. Broadband Dielectric Spectroscopy (BDS) has been proved to be a powerful tool for the investigation of molecular mobility, phase changes, conductivity mechanisms and interfacial effects in polymers and complex systems. The dielectric response of composites was examined by means of Broadband Dielectric Spectroscopy (BDS) in the frequency range 10⁻¹-10⁷ Hz and temperature interval from 30°C to 160°C. Experimental results include relaxation phenomena arising from both the polymeric matrix and the filler [3]. Three distinct relaxation modes were recorded in the spectra of all systems. They were attributed to interfacial polarization, glass transition (α -relaxation) and motion of small polar side groups (β -relaxation) of the polymer matrix. The energy density was also calculated in order to determine the amount of stored energy.

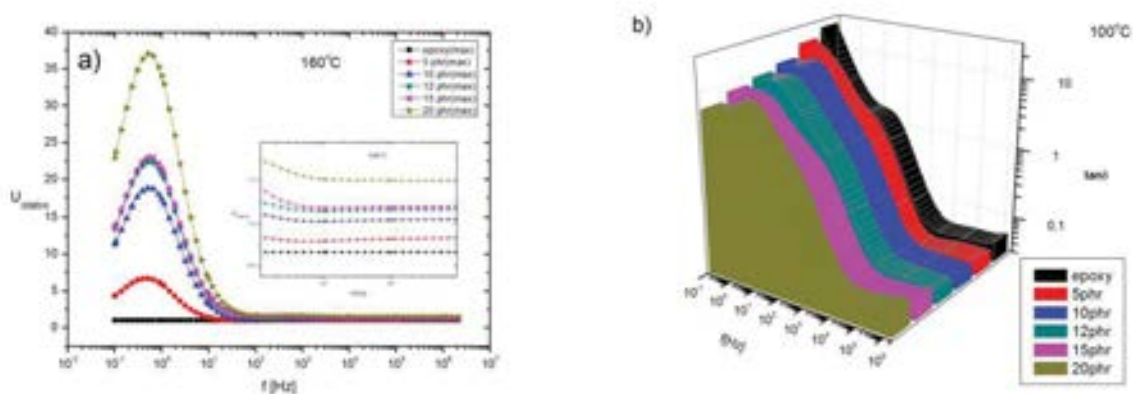


Figure 1: **a)** $U_{relative}$ plot for all specimens at 160°C, **b)** comparative plot for the loss tangent for all specimens at 100°C.

References

- [1] Patsidis A., Psarras G.C., *Exp. Pol. Lett.* 4, 234 (2008).
- [2] Ioannou G., Patsidis A., Psarras G.C., *Comp. A.* 42, 104 (2011).
- [3] Patsidis A.C., Kalaitzidou K., Psarras G.C., *Materials Chemistry and Physics, Volume 135, issue 2-3 (August 15, 2012), p. 798-805.*
- [4] Vladislav Domnich, Sara Reynaud, Richard A. Haber, and Manish Chhowalla, *J. Am. Ceram. Soc.*, 94 [11] 3605-3628 (2011)

* ecsenis@upatras.gr, G.C.Psarras@upatras.gr

EFFECTIVE DISPERSION OF NANO GRAPHENE PLATELETS

A. Talarou¹, N.D. Alexopoulos

Department of Financial Engineering, University of the Aegean, Chios, Greece

E.P. Favvas

Division of Physical Chemistry, NCSR “Demokritos”, Ag. Paraskevi, Attica, Greece

The objective of this study is the development of a cementitious multifunctional material that itself can be simultaneously used as a construction material and a strain/damage sensor of structural components. To achieve this, the implementation of nano graphene platelets (NGPs) was studied. Initially, a method to effectively disperse the graphene nanoplatelets in the cementitious matrix was developed. Typically, NGPs tends to form agglomerates due to Van der Waals forces and their efficient dispersion is not a straightforward procedure. To this end, it is important for NGPs to be uniformly dispersed within the matrix so as to achieve effective reinforcement and improve the properties of the cementitious material. Use of ultrasonic processing and treatment with a 3rd generation superplasticizer was employed to homogeneously disperse NGPs in the mixing water. The latter was exploited as it is commonly used to improve the workability of cement based materials and is typically used within the matrix. The effect of the superplasticizer concentration was studied first, as several studies have indicated that the dispersing agent’s concentration significantly affects the nanomaterials’ dispersion. For homogeneous dispersion, a superplasticizer concentration close to 0.7% by weight of cement was found to be most efficient. To further improve the dispersion method, the effect of ultrasonic energy was investigated. Finally, the effect of different concentrations of the NGPs was studied. The electrical properties of the nanocomposites and specifically the electrical resistivity were evaluated using the 4-wire Ohms method. Three-point bending tests were performed at the 20×20×80 mm beam specimens at the age of 28 days, as shown in Figure 1. The mechanical properties of the NGPs-cementitious materials were evaluated using notched specimens. Fourier Transform Infrared (FTIR), X-ray diffraction (XRD), Scanning Electron Microscopy (SEM) and nitrogen porosimetry (N₂ adsorption) have been used in order to evaluate the structural characteristics of the pure graphene additive materials.

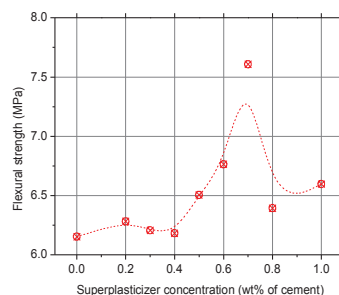


Figure 1: LEFT: Three-point bending test set up. RIGHT: Effect of superplasticizer concentration on the flexural strength of cementitious nanocomposites.

Acknowledgements

The authors would like to acknowledge the financial support of the John S. Latsis Public Benefit Foundation under the “Scientific Projects 2014”, project entitled “Self sensing graphene/cement based nanocomposites for structural integrity monitoring”.

References

- [1] Metaxa, Seo, Konsta-Gdoutos, Hersam and Shah, *Cement and Concrete Composites* **34**, 612 (2012).
- [2] Konsta-Gdoutos, Metaxa and Shah, *Cement and Concrete Research* **32**, 110 (2010).
- [3] Tang, Shafiq, Chan, Wong and Cheung, *Journal of Nanoscience and Nanotechnology* **10**, 4967 (2010).

¹ angel-niki.talarou@gmail.com

Dielectric characterisation of low content PVDF/CNTs and PVDF/Graphene nanocomposites

G.N. Tomara*, P. K. Karahaliou, S. N. Georga, C.A. Krontiras
Department of Physics, University of Patras, 26504, Patras, Greece

G.C. Psarras

Department of Materials Science, University of Patras, 26504, Patras, Greece

E. Siores

Institute of materials research and Innovation, University of Bolton, Deane Road, Bolton BL3 5AB, United Kingdom

Polyvinylidene fluoride (PVDF) is a polymeric material with a variety of technological applications mostly due to its piezoelectric character [1]. On the other hand allotropic forms of carbon such as carbon nanotubes (CNTs) or graphene layers are newly fabricated materials and attract scientific attention due to their outstanding electrical and mechanical properties.

The purpose of this work is to investigate the molecular dynamics of PVDF polymer chains and the way these dynamics are influenced by the presence of the filler. A powerful technique to study the molecular dynamics for composite systems is Broadband Dielectric Spectroscopy (BDS). PVDF/CNTs and PVDF/Graphene nanocomposites were prepared in three different concentrations 0.1%, 0.5% and 1%. Pure PVDF samples were also prepared and investigated as reference. Isothermal scans over a wide frequency range from 10^{-1} Hz to 10^6 Hz were conducted from -100°C to 150°C in steps of 10°C .

3D indicative graphs (figure 1a and 1b) of the imaginary part of dielectric modulus (M'') as a function of frequency and temperature for the composites with 1% PVDF / CNTs and PVDF / Graphene are presented respectively. The first recorded relaxation is the α_a -mode observed at low temperatures, also referred to as the primary relaxation, attributed to the glass to rubber transition of the polymer matrix. Around 0°C the α_c -mode is observed and it is attributed to molecular motions of the polymer crystalline region arising from the imperfections of the crystal remaining present till the upper measured temperature. Finally, around 100°C another mode is observed, namely Interfacial Polarisation (IP), arising from the morphological differences of the crystalline and amorphous phase [2, 3].

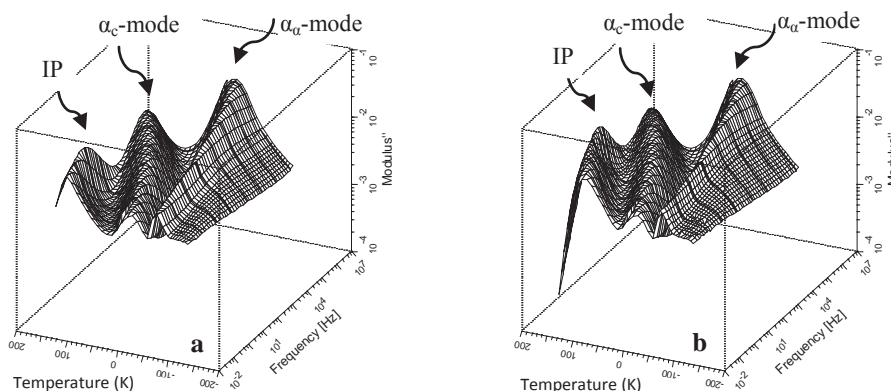


Figure 1: Imaginary part of dielectric Modulus (M'') as a function of frequency and temperature for the composites with 1% PVDF / CNTs (a) and PVDF / Graphene (b).

References

- [1] I. Patel, E. Siores, T. Shah, *Sensors and Actuators A* **159**, (2010)
- [2] Huda Rekik et al, *Composites: Part B* **45**, (2013)
- [3] V. Kochervinskii et al, *Journal of Non-Crystalline Solids* **353**, 47 (2007)

This research has been co-financed by the European Union (European Social Fund – ESF) and Greek national funds through the Operational Program "Education and Lifelong Learning" of the National Strategic Reference Framework (NSRF) - Research Funding Program: THALES (MIS 379346). Investing in knowledge society through the European Social Fund.

Microstructural investigation and mechanical performance of hybrid thermal protection systems for aerospace applications

K. Triantou^{1*}, K. Mergia¹, A. Marinou¹, G. Vekinis¹, W. Fischer², G. Pinaud³
and J. Barcena⁴

¹National Centre for Scientific Research “Demokritos”, Athens, Greece

²Airbus Defence and Space, Germany

³Airbus Defence and Space, France

⁴TECNALIA Research and Innovation, San Sebastian, Spain

The development of new concepts for Thermal Protection Systems (TPS) is critical for space applications where resistance to extreme oxidative environments and high temperatures are required. In the current study a hybrid thermal protection solution for atmospheric earth re-entry based on low density ablator on top of a thermo-structural ceramic composite is investigated.

The joints of Ceramic Matrix Composite (CMC) material (carbon fibers embedded in silicon carbide matrix C_f/SiC, SICARBONTM) to ablative material (carbon fibers and phenolic resin, ASTERMTM) using commercial high temperature inorganic adhesives are microstructurally and mechanically studied. Three types of adhesives were used based on Al₂O₃, ZrO₂-ZrSiO₄ and graphite. The cross section of the joints was analysed using Scanning Electron Microscopy with Energy Dispersive Analysis. Mechanical tests were performed at ambient and cryogenic conditions in order to assess the shear strength of the joints. All the joints exhibit good bonding with both base materials with similar shear strength at ambient conditions. Joints with ZrO₂-ZrSiO₄ and graphite based adhesives have the highest ultimate shear strain. At liquid nitrogen the shear strength compared to that at ambient conditions increases from 30 up to 100%. This is attributed to the increase of stiffness of the ablative material. The fracture takes place inside the ablative material and the shear strength is similar (for the tests performed at the same conditions), reflecting the shear strength of the ablative material.

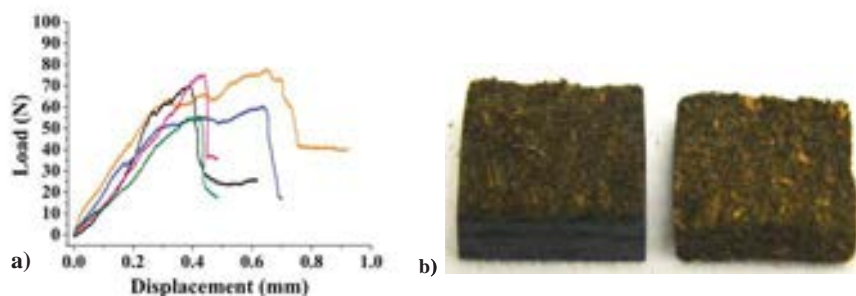


Figure: a) Curves of shear tests at ambient conditions of the SICARBON/ASTERM joints using ZrO₂-ZrSiO₄ based adhesive and b) Fracture surfaces of a joint using graphite adhesive.

Acknowledgments: This work has been performed as a part of the FP7 European Project “HYDRA” (n.283797), which is funded from the European Union.

* ktriantou@ipta.demokritos.gr

Vitrification of incinerated tannery sludge

S. Varitis*, P. Kavouras, G. Kaimakamis, E. Pavlidou, G. Vourlias, K. Chrissafis,
G. P. Dimitrakopoulos, Th. Karakostas, Ph. Komninou
*Department of Physics, Aristotle University of Thessaloniki, Thessaloniki 54124,
Greece*

Stabilization of tannery waste is of great importance due to its high organic and chromium content. This issue can be dealt with by applying vitrification, which is a promising method for the fabrication of glass and glass ceramic products with potential use for structural and decorative applications.

The chromium containing tannery sludge was first incinerated for 1.5 h at 500°C in anoxic conditions and the resulting ash was vitrified using SiO₂, CaO and Na₂O powders in various relative proportions. This work aimed to the synthesis of (a) vitrified products using the chromium containing ash and (b) glass ceramics products for various applications.

Three different batch compositions were examined containing from 10wt% to 20wt% chromium containing ash and the vitrifying agents mentioned above. All batch mixtures were heated at 1400°C for 2h in order to achieve a homogeneous melt and subsequently rapidly cooled down. The resulting vitrified products were studied by X-Ray Diffraction (XRD), Differential Thermal Analysis (DTA), Scanning Electron Microscopy (SEM), Transmission Electron Microscopy (TEM) and microindentation.

Thermal treatment of the vitrified products was conducted for 30 min for each sample, with temperature decided from the DTA results. Devitrification occurred by surface crystallization of Devitrite (Na₂Ca₃Si₆O₁₆) or by surface and bulk crystallization of Combeite (Na₄Ca₄Si₆O₁₈) (Figure 1b). Crystallization mechanisms in the case of Combeite depended on the thermal treatment temperature.

Microindentation was conducted in order to study microhardness and crack propagation in vitrified and glass ceramic products, as a function of batch composition and microstructure. Microhardness was increased after crystallization, while crack propagation depended on the morphology of the separated crystallites.

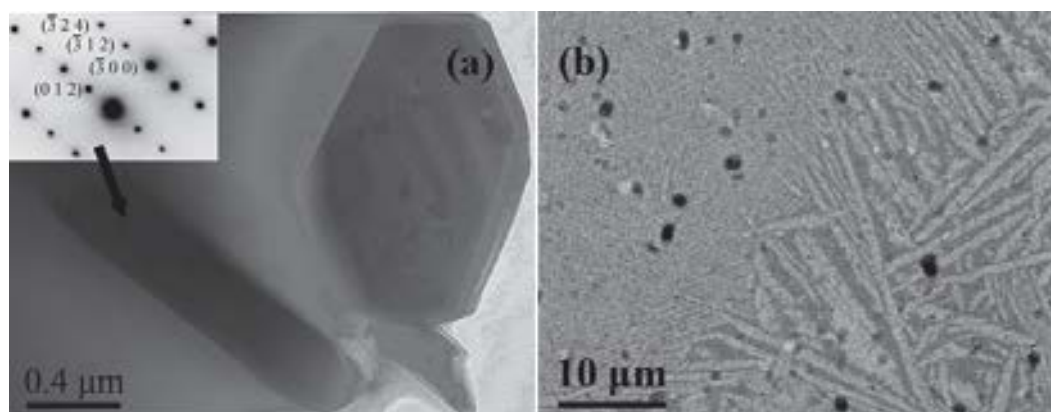


Figure 1: (a) TEM image obtained from GL1-850 devitrified product. A Cr₂O₃ crystal is denoted by the arrow and the corresponding diffraction pattern along [06-3] zone axis. (b) SEM micrograph from GL3-880°C glass ceramic product.

Acknowledgement: This research has been co-financed by the European Union (European Social Fund - ESF) and Greek national funds through the Operational Program "Education and Lifelong Learning" of the National Strategic Reference Framework (NSRF) - Research Funding Program: THALES: Reinforcement of the interdisciplinary and/or inter-institutional research and innovation.

* svaritis@physics.auth.gr

Dielectric Behaviour of Epoxy Resin – BaSrTiO₃ Nanocomposites

O. Vrionis*, G. C. Psarras

Department of Materials Science, University of Patras, Patras 26504, Greece

Ceramic-polymer composites incorporating ferroelectric and piezoelectric nanoparticles, homogeneously dispersed within an amorphous matrix represent a novel class of materials. Ceramic nanoparticles embedded into a polymer provide composites exhibiting synergy between the flexibility, and high dielectric breakdown strength of polymers with the high permittivity values of the ceramics. These type of material systems can be used in numerous applications such as integrated decoupling capacitors, acoustic emission sensors, angular acceleration accelerometers, smart skins and leakage current controllers, as well as in military equipment and transport applications [1-5]. In the present study, nanocomposites of epoxy resin and ceramic BaSrTiO₃, were prepared and studied varying the filler concentration. Dielectric properties and related relaxation phenomena were investigated by means of Broadband Dielectric Spectroscopy in the temperature range from 30 to 160 °C and in the frequency range from 10⁻¹ to 10⁻⁷ Hz.

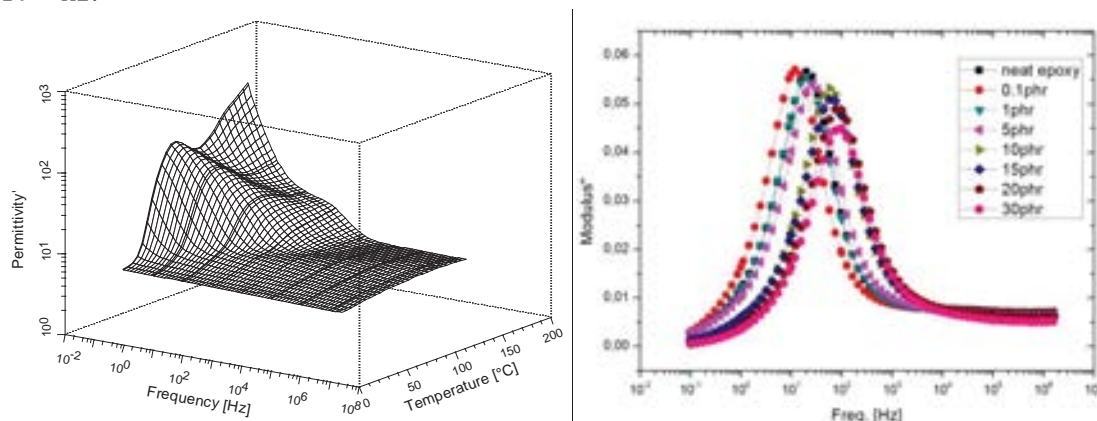


Figure 1. Real part of dielectric permittivity of the nanocomposite with 1 phr BaSrTiO₃ as a function of frequency and temperature (left). Imaginary part of electric modulus for all specimen, as a function of frequency at 80°C (right).

References

- [1] Patsidis A., Psarras G.C., *Exp. Pol. Lett.* **4**, 234 (2008).
- [2] Tan, D., Irwin P. "Polymer Based Nanodielectric Composites." in *Advances in Ceramics - Electric and Magnetic Ceramics, Bioceramics, Ceramics and Environment*, Ed. Sikalidis C., **InTech**, 115 (2011)
- [3] Ioannou G., Patsidis A., Psarras G.C., *Comp Part A*, **42**, 104 (2011).
- [4] Patsidis A.C., Kalaitzidou K., Psarras G.C., *Mater Chem Phys*, **135**, 798 (2012).

* ovrionis@upatras.gr, G.C.Psarras@upatras.gr

SERS in a broad range of analytical applications - membranes

J. Anastasopoulos^{1,2*}, A. Soto Beobide¹, G. A. Voyiatzis¹

¹FORTH/ICE-HT, P.O. Box 1414, GR-265 04, Rio-Patras, Greece

²Dept. of Chem. Engineering, University of Patras, GR-265 00, Patras, Greece

In an effort to establish surface enhanced Raman scattering (SERS) as an extremely simple and practical analytical method for a broad range of analytical applications, we apply this technique in membrane technology. In the waste water treatment, it is anticipated to overcome the immanent limitation of counterbalance between flux and selectivity by the infiltration of CNTs into a porous polymeric membrane. A basic principle of the CNT incorporated membranes is the efficient binding of CNTs in the membranes to minimize probable health risk associated with chances of product water getting contaminated with CNTs. SERS was very recently used for the quantification of MWCNTs in water suspensions at quite low concentration range, after being released from CNT-embedded membranes [1]. The functionalization of the MWCNTs with pyridine groups seems to favor the surface enhancement of the relevant Raman signal and this study constituted the first step of a work in progress for the characterization of CNTs by SERS in any water suspension.

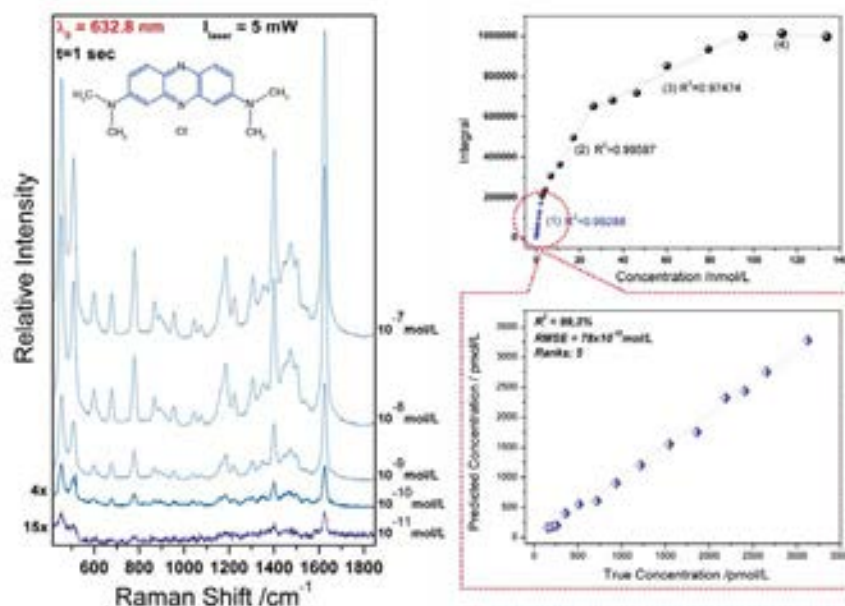


Figure 1: Representative SERS spectra of Methylene Blue in Ag nano-colloids (Right).

Calibration curve in a large concentration range (Left-top).

Predicted versus known concentrations at very low concentration range (Left-bottom).

Moreover, given that extremely small amounts of foulants can be detected and further quantified via SERS in large volume samples, SERS was applied in the investigation of waste water effluents. More precisely, we present SERS measurements of aqueous solutions containing pg levels of methylene blue, a heterocyclic aromatic dye used in the textile industry that causes severe central nervous system toxicity at plasma concentrations over 1.33 mol/L.

Acknowledgements: The research has received funding from the European Union's Seventh Framework Programme (FP7/2007-2013) under the grant agreement n°246039.

References

[1] J.A. Anastasopoulos, A. Soto Beobide, L. Sygellou, S.N. Yannopoulos, G.A. Voyiatzis, *J Raman Spectrosc* 45 (2014) 424.

* j.anast@iceht.forth.gr

Combustion synthesis of Li–Mn spinel nanostructures as cathode materials for lithium–ion batteries

Pinelopi Angelopoulou and George Avgouropoulos*

Department of Materials Science, University of Patras, GR-26504 Rio, Greece

In recent years, lithium–ion batteries have been considered as the most promising power sources of consumer’s electronic devices such as mobile phones and laptop computers. Common commercial cathode materials used in lithium–batteries are the compounds of transition metal oxides: LiCoO_2 (layered), LiMn_2O_4 (spinel), LiNiO_2 (layered) and LiFePO_4 (olivine). LiMn_2O_4 spinel nanostructure is of great interest as positive electrode, due to its low cost, simple preparation, environmental friendliness and good safety. However, this cathode material suffers from some limitations such as capacity fading during charge/discharge cycling. To overcome this problem, many researchers have tried to modify the material structure either by tuning the synthesis parameters or/and substituting a small amount of Mn ions by various ions of Co, Ni, Al, Mo, Cr etc. Recently, Kebede *et. al.* [1] synthesized pristine LiMn_2O_4 and Al-doped LiMn_2O_4 ($\text{LiAl}_x\text{Mn}_{2-x}\text{O}_4$) spinel cathode materials using a solution combustion method. The samples $\text{LiAl}_{0.05}\text{Mn}_{1.95}\text{O}_4$ and $\text{LiAl}_{0.1}\text{Mn}_{1.9}\text{O}_4$ exhibited higher discharge capacity for the first two cycles compared to the first cycle discharge capacity of pristine LiMn_2O_4 .

The combustion method involves the autoignition of an aqueous solution containing an oxidizer (the corresponding metal nitrates) and an organic fuel, such as urea. The resulting material characteristics, such as surface area and crystallite size, are strongly dependent on the fuel/oxidant ratio [2]. The combustion reaction is most vigorous and reaches high temperatures, when the fuel/nitrate molar ratio is close to its stoichiometric value, leading to large particles or agglomerates. Rapid evolution of a large volume of gases during the process cools immediately the product, limits the occurrence of agglomeration, thus leading to nanocrystalline powders.

In this work, we report on the physicochemical and electrochemical properties of LiMn_2O_4 spinel nanostructures prepared via the combustion method. Parameter of this study was the urea/nitrate ratio. $\text{Li}(\text{NO}_3)$ and $\text{Mn}(\text{NO}_3)_2$ were used as starting materials (oxidizing agents) and urea [$\text{CO}(\text{NH}_2)_2$] as fuel (reducing agent). $\text{Cu}(\text{NO}_3)_3$ was also employed as a precursor in the case of doped nanostructure. The materials were characterized by N_2 adsorption, X-ray powder diffraction (XRD), scanning electron microscopy (SEM) and X-ray photoelectron spectroscopy (XPS), while electrochemical measurements (charge–discharge, cyclic voltammetry) were performed at ambient temperature by two–electrode cells including a positive electrode (LiMn_2O_4) as the working electrode and a Li foil as reference electrode and counter electrode (electrolyte: 1M LiPF_6 in EC/DMC). For comparison reasons, a commercial LiMn_2O_4 positive electrode was also employed.

References

- [1] M.A. Kebede, M.J. Phasha, N. Kunjuzwa, L.J.le Roux, D.Mkhonto, K.I. Ozoemena, M.K. Mathe, *Sustainable Energy Technologies and Assessments* **5**, 44 (2014).
- [2] G. Avgouropoulos and T. Ioannides, *Applied Catalysis A* **244**, 155 (2003).

* geoavg@upatras.gr

Effect of hydrothermal conditions on the physicochemical properties of Cu–Ce oxide nanostructures

George Avgouropoulos*

Department of Materials Science, University of Patras, GR-26504 Rio, Greece

Joan Papavasiliou

FORTH/ICE-HT, GR-26504 Platani, Patras, Greece

The development of efficient and low-cost nanomaterials for fuel cell energy systems has attracted huge research attention during the last decade [1–7]. Polymer Electrolyte Membrane Fuel Cells (PEMFCs) which operate with pure H₂ appear to be an ideal energy solution for portable and mobile energy applications. In order to avoid several technical and safety limitations concerning the use of pure H₂, the utilization a H₂-rich gas mixture is favored. This gas mixture can be produced from hydrocarbons or alcohols (natural gas, gasoline, methanol) as a H₂ carrier, through a catalytic fuel processor. The starting fuel is converted in a H₂-rich gas through a catalytic processor. However, the produced reformat gas contains a significant concentration of carbon monoxide (ca. 1% CO), thus needing further purification, since this amount of CO poisons the anode electrocatalysts of low temperature PEM fuel cell. Preferential catalytic CO oxidation (PROX reaction) is a simple and cost-effective method for removing CO to less than 20 ppm from reformed fuels. Cu–Ce mixed oxides have been prepared with different methods (impregnation, co-precipitation, sol-gel, combustion) and proposed for the title process [3]. Recent years, the research community employs new chemical synthesis methods, aiming to the preparation of nanostructured catalysts with high selectivity, extremely high activity, low energy demands and long life time [4]. These can be achieved only by controlling the size, the shape, the particle size distribution, the composition and the electronic structure of the surface, the thermal and chemical stability of the specific nanocomponents.

In this work hydrothermal method was employed, using citric acid as chelating agent, sodium hydroxide as precipitating agent and copper nitrate and cerium nitrate as copper and cerium precursors, respectively. Synthesis parameters of CuCeOx catalysts were temperature and duration of hydrothermal process, and sodium hydroxide concentration. Choosing proper combination of these parameters, different nanostructures (rods, cubes, polyhedra, spheres) can be obtained, with attractive physicochemical characteristics. Activity and selectivity of nanostructured catalysts were tested for CO preferential oxidation in the presence of excess H₂.

References

- [1] M. Kipnis, *Appl. Catal. B* **152–153**, 38 (2014).
- [2] K. Liu, A. Wang, T. Zhang, *ACS Catalysis* **2**, 1165 (2012).
- [3] G. Avgouropoulos, T. Ioannides, *Chem. Eng. J.* **176–177**, 14 (2011).
- [4] R. Si, M. Flytzani-Stephanopoulos, *Angew. Chem. Int. Ed.* **47**, 2884 (2008).

* geoavg@upatras.gr

Nuclear Resonant Scattering

D. Bessas*, D. G. Merkel, A. Chumakov, R. Rüffer
European Synchrotron Radiation Facility, F-38043 Grenoble, France

Nuclear resonant scattering is an experimental technique which is directly related to interdisciplinary applications such as magnetism and lattice dynamics. It is comprised into the excitation of nuclei by synchrotron radiation from the nuclear ground state into a nuclear excited state. The finite energy width of the excited state corresponds to a finite lifetime. Hence, the resonantly scattered photons are delayed with respect to the non-resonantly scattered (prompt) photons. The delayed events are separated from the prompt pulse using fast electronics. Both coherently [1], Nuclear Forward Scattering and incoherently [2], Nuclear Inelastic Scattering, scattered radiation are observed simultaneously and are recorded by two sets of avalanche photo diodes.

On one hand, the Nuclear Forward Scattering of synchrotron radiation [3, 4] provides information similar to Mössbauer spectroscopy [5] (energy domain), *i.e.*, isomer shift, electric field gradient and hyperfine magnetic field, in time domain. This technique is particularly useful when preparation of the radioactive source for Mössbauer spectroscopy is difficult, when the lifetime of the radioactive source is short, or when the experimental setup requires a collimated or a small-size beam. The typical lifetime of the excited states ranges between 0.2 and 200 ns and matches the bunch structure of the current synchrotron radiation facilities. Hence, the Nuclear Forward Scattering can, in principle, be measured for any of the Mössbauer isotopes.

On the other hand, the Nuclear Inelastic Scattering [6, 7] of synchrotron radiation is an inelastic X-ray scattering technique resonant in nature. The resonant nuclei, which might/or not be included in the studied system, act as an energy analyser and the scattered radiation is purely incoherent. Thus, the measured energy distribution of the nuclear inelastic absorption is integrated over the momentum transfer and the *true* density of phonon states is extracted. This technique is particularly useful when the *true* partial or total density of phonon states, the element specific inter-atomic mean force constant, and the speed of sound, is of interest, or when sub-meV resolution along the spectrum is required.

In this poster, the experimental setup of nuclear resonant scattering will be explained, state of the art results obtained at ID18/ESRF [8] will be presented, and hints on future studies and collaborations will be given.

References

- [1] A. Q. Baron, A. Chumakov, H. F. Grünsteudel, L. Niesen, R. Rüffer, Phys. Rev. Lett. 77, 4808 (1997).
- [2] V. G. Kohn and A. Chumakov, J. Phys.: Condens. Matter 14, 11875 (2002).
- [3] J. B. Hastings, D. P. Siddons, U. van Bürck, R. Hollatz, and U. Bergmann, Phys. Rev. Lett. 66, 770 (1991).
- [4] U. van Bürck, D. P. Siddons, J. B. Hastings, U. Bergmann, and R. Hollatz, Phys. Rev. B 46, 6207 (1992).
- [5] P. Gülich, E. Bill, and A. X. Trautwein, “Mössbauer spectroscopy and Transition Metal Chemistry: Fundamentals and Applications” (Springer, 2011).
- [6] M. Seto, Y. Yoda, S. Kikuta, X. W. Zhang and M. Ando, Phys. Rev. Lett. 74, 3828 (1995).
- [7] W. Sturhan, T. S. Tollner, E. E. Alp, X. W. Zhang, M. Ando, Y. Yoda, S. Kikuta, M. Seto, C. W. Kimball, B. Dabrowski, Phys. Rev. Lett. 74, 3832 (1995).
- [8] R. Rüffer, A. Chumakov, Hyperfine Interact. 97/98, 589 (1996).

* bessas@esrf.fr

Synthesis of Iron oxide Nanoparticles for 3D Nanostructure Fabrication

A. N. Giakoumaki^{1,2*}, A. Selimis¹, M. Vamvakaki^{1,3}, M. Farsari¹

1. IESL-FORTH, N. Plastira 100, 70013, Heraklion, Crete, Greece

2. Department of Chemistry, University of Crete, Heraklion, Crete, Greece

3. Department of Materials Science and Technology, University of Crete, Heraklion, Crete, Greece

We demonstrate the fabrication of 3D nanostructures by multiphoton polymerization using a material that contains magnetic Iron Oxide Nanoparticles .

Direct fs laser writing by multiphoton polymerization is a technique that allows the fabrication of 3D structures with sub-100 nm resolution. It has been implemented using a variety of purely organic or hybrid materials, for applications in photonics, metamaterials and biomedicine[1-3].

We report here the fabrication of high quality, 3D structures employing a photosensitive material containing Iron oxide Nanoparticles synthesized by thermal decomposition and by laser ablation of a bulk Fe target.

By incorporating the magnetic nanoparticles in a polymer structure we aim to enable their remote manipulation by a magnetic field.

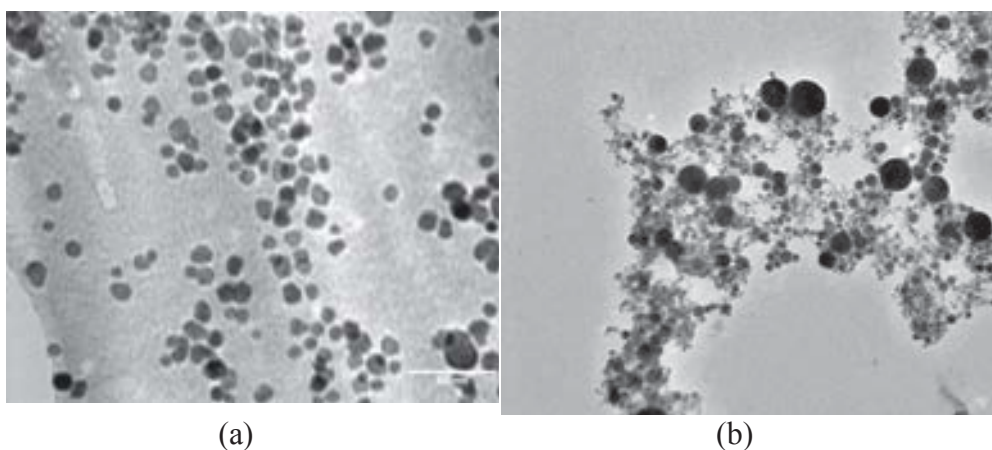


Figure 1 TEM images of iron oxide nanoparticles synthesized (a) chemically by thermal decomposition and (b) laser ablation of a Fe target.

References

[1] I. Sakellari, E. Kabouraki, D. Gray, V. Purlys, C. Fotakis, A. Pikulin, N. Biturin, M. Vamvakaki, M. Farsari, "Diffusion-Assisted High Resolution Direct Femtosecond Laser Writing", ACS Nano, 6 2302 (2012).

[2] N. Vasilantonakis, K. Terzaki, I. Sakellari, V. Purlys, D. Gray, C.M. Soukoulis, M. Vamvakaki, M. Kafesaki, M. Farsari, "Three-Dimensional Metallic Photonic Crystals with Optical Bandgaps", Advanced Materials, 24 1101(2012).

[3] V. Melissinaki, A.A. Gill, I. Ortega, M. Vamvakaki, A. Ranella, J.W. Haycock, C. Fotakis, M. Farsari, F. Claeysens, "Direct laser writing of 3D scaffolds for neural tissue engineering applications", Biofabrication, 3 045005 (2011).

* argyrogia@gmail.com

Surface Enhanced Raman Spectroscopy substrates based on silver nanoparticles and thin films

L. Patsiouras*, M. Panagopoulou, S. Stathopoulos, Y. S. Raptis, D. Tsoukalas
School of Appl. Math. & Phys. Sciences, NTUA, GR157- 80, Athens, Greece

The exploration of new techniques for precise, reproducible and rapid detection of chemical substances has concerned the scientific community the last years. Surface Enhanced Raman Spectroscopy (SERS) is a novel, well established method of chemical sensing [1]. This technique is based on an effect in which metallic nanostructured surfaces enhance the scattered Raman signal by molecules which are attached to these surfaces [2]. The plasma resonance of the free electrons of the metal surface is responsible for the enhancement of the local EM field scattered by the molecules which are close to the surface.

In this work we compare the SERS signal obtained from various substrates that we particularly prepare to optimize amplification using a prototype molecule for detection such as Rhodamine. Our first approach makes use of periodic structures decorated with silver nanoparticles. Nanoparticles of average diameter 5 nm observed by Transmission Electron Microscopy** were fabricated by a physical deposition method based on DC sputtering and gas condensation. Thus periodic structures were fabricated on silicon through the fracture induced structuring technique (FIS) [3] and electron beam lithography and they were coated with silver nanoparticles. The alignment of nanoparticles across the sharp peaks on resist and their aggregation in bigger clusters produce pure SERS signal up to 100 times stronger than the normal signal gained from a surface without nanoparticles. An another category of SERS substrates which was developed, is making use of thin silver films deposited by sputtering on a pre-strain PDMS sample [4] with thickness of 8 to 12nm. By this way the semi-continuous metal film causes the signal enhancement which strongly depends by the film thickness. The SERS signals obtained from the above approaches will be compared and discussed.

References

- [1] X., Y., Zhang, M., A., Young, O., Lynardes, R., V., Duyne, J. Am. Chem. Soc., **127**, 4484, 2005.
- [2] P., Hildebrandt, M. Stockburger, J. Phys. Chem., 88 (24), 5935-5944, 1984.
- [3] L., Pease, P., Deshpande, Y., Wang, W., B., Russel, S., Y., Chou, Nature Nano., 2, 545-548, 2007.
- [4] P., C., Lin, S., Yang, Appl. Phys. Lett., **90**, 241903, 2007.

* lampros.p88@gmail.com

** the TEM study was carried out in the "Centre for Electron Microscopy, Microanalysis and Structural Characterization of Materials" of the School of Mining and Metallurgical Engineering- NTUA

Pt/TiO₂ and Pt/CeO₂ nanostructured materials for fuel cell applications

Alexandra Paxinou^{1,2}, Joan Papavasiliou² and George Avgouropoulos*^{1,2}

¹ Department of Materials Science, University of Patras, GR-26504 Rio, Greece

² FORTH/ICE-HT, GR-26504 Platani, Patras, Greece

Methanol may offer much higher energy densities than either batteries or fuel cells operating on stored H₂, making it an attractive source for advanced portable power. A challenge for fuel processing with respect to the operation level of high temperature PEM fuel cells (200–220°C) is the development of highly active and selective catalysts for methanol reforming to H₂ [1]. Commercially available CuZnAlO_x catalysts have been widely used for generating H₂ from methanol. Even though these catalysts are widely used in H₂ plants, several drawbacks limit their application in small stationary or mobile systems. Especially, their pyrophoric behaviour has to be controlled when reduced Cu is abruptly exposed to air after turning off the feed of reactants, since major local temperature spikes can occur due to fast copper oxidation, which may lead to sintering/deactivation of Cu particles. Noble metal-based catalysts have been also proposed as an alternative solution [2]. In this work hydrothermal method was employed for the preparation of titania nanotubes and ceria nanorods as catalyst supports. Platinum nanoparticles were dispersed on the oxide nanostructures (Fig. 1) following three different methods: (a) impregnation, (b) deposition-precipitation and (c) combustion. The catalytic performance of Pt/TiO₂ and Pt/CeO₂ nanostructures has been investigated for the steam reforming of methanol (Table 1) and discussed on the basis of the physicochemical characterization.

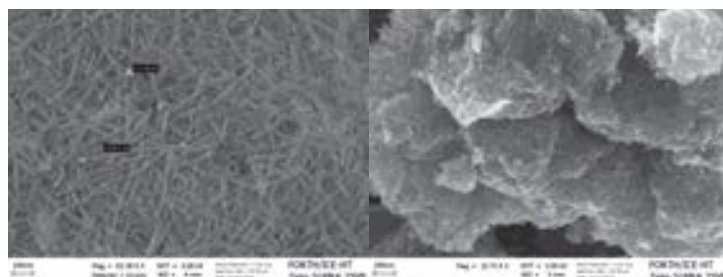


Figure 1: SEM images of Pt/ceria nanorods (left) and Pt/titania nanotubes (right)

Table 1: Catalytic properties of various Pt-based catalysts

	3wt.%Pt/CeO ₂ (combustion method)	5wt.%Pt/TNTs (impregnation)	30wt.%Pt/TNTs (impregnation)	30wt.%Pt/C (commercial)
MeOH conversion, %	81	90	99	<5
H ₂ selectivity, (%)	85	77	86	67
H ₂ yield, %	70	69	85	1.5
R _{H₂} , cc/min/g _{Pt}	810	484	99	2

References

- [1] G. Avgouropoulos, T. Ioannides, J.K. Kallitsis, S. Neophytides, Chem. Eng. J. **176–177**, 95 (2011).
- [2] G. Avgouropoulos, J. Papavasiliou, T. Ioannides, Chem. Eng. J. **154**, 274 (2009).

* geoavg@upatras.gr

Correlation of complex electrical conductivity and acoustic emissions time-series during uniaxial compression of limestone samples

V. Saltas*, I. Ftilis, F. Vallianatos

Laboratory of Geophysics and Seismology, Department of Environmental and Natural Resources Engineering, Technological Educational Institute of Crete, Greece

In the present work, time-series measurements of complex electrical conductivity were carried out in conjunction with acoustic emission (AE) monitoring in limestone samples subjected to different types of uniaxial compressive stress, up to ultimate failure. During linear loading, ac-conductivity obeys the same general self-similar law for critical phenomena that has been reported for the energy release before materials fracture [1]. In all types of uniaxial loading (linear, stepped and sawtooth) ac-conductivity exhibits a strong correlation with AE activity (Fig. 1) due to charge transfer caused by microcracks generation and propagation in limestone. These fracture-induced phenomena are of great importance in searching precursory signals in mechanical damage and in earthquakes prediction [2].

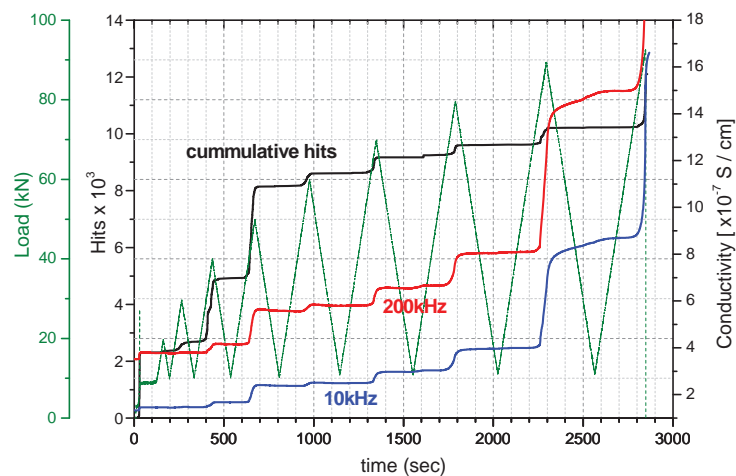


Figure 1: Time-series of ac-conductivity at two selected frequencies (10kHz, 200kHz) and the corresponding AE activity (cumulative hits) during sawtooth uniaxial compression of limestone.

This research has been funded by the European Union and Greek national resources under the framework of the “THALES Program: SEISMO FEAR HELLARC (MIS 380208)” project of the “Education & Lifelong Learning” Operational Programme.

References

- [1] Moura et al., J. Mech. Phys. Solids **54**, 2544 (2006).
- [2] Lavrov, Strain **41**, 135 (2005).

* vsaltas@chania.teicrete.gr

Silica coated magnetic iron oxide nanoparticles doped with Thioflavin-T for beta-amyloid targeting

A. Tsolakis, G. Litsardakis*

Dept. of Electrical and Computer Engineering, AUTH, Greece

L. Chalevas, A. Salifoglou

Dept. of Chemical Engineering, AUTH, Greece

N. Vouroutzis

Dept. of Physics, AUTH, Greece

One of the key factors influencing the onset of Alzheimer's disease, the most common age related human neurodegenerative disorder, is believed to be the accumulation of beta-amyloid (A β) peptide aggregates, which lead to the development of brain amyloid plaques [1]. The aggregated peptides constitute a potential target for early diagnosis and/or therapy of the disease. Various approaches, based on the design and engineering of nanoparticulate entities with multiple modalities present new possibilities in imaging, delineation of protein binding and interactions [2][3][4], collectively potentiating an early detection and better understanding of the disease process. To that end, magnetic iron oxide nanoparticles (MIONs) were synthesized using a modification of the iron salt co-precipitation method proposed by Kobayashi et al. [5].

Following production of MIONs, silica was overlaid in order to create core-shell magnetic nanoparticles [6]. During the encapsulation process of the magnetic core, Thioflavin-T (ThT), a fluorescent protein-marker was also added, for co-encapsulation and staining of the core-shell MIONs [7]. Ultimately, ThT doped silica coated magnetic nanoparticles were prepared, with well-established magnetic properties, detectable by both confocal and MRI imaging. The samples were characterised during the preparation phases by XRD, VSM, FTIR, Confocal Microscopy, Fluorescence Spectroscopy, and TEM.

The results at hand indicate that ThT has been successfully encapsulated in the silica core-shell MIONs, thus providing a valuable bimodal tool a) for targeting *in vitro/in vivo* A β aggregates, and b) in an effort to develop diagnostic/therapeutic technology in AD.



Figure 1: TEM – Silica coated MIONPs

References

- [1] Findeis M.A., *Pharmac & Therap.* **116**(2), 266-286 (2007).
- [2] Gobbi M., Re F., Canovi M., Beeg M., Gregori M., Sesana S., Sonnino S., Brogioli D., Musicanti C., Gasco P., Salmona M., Masserini M.E., *Biomaterials* **31**, 6519-6529 (2010).
- [3] Skaat H. and Margel S., *Biochem. Biophys. Research Com.* **386**, 645-649 (2009).
- [4] Mahmoudi M., Quinlan-Pluck F., Monopoli M., Sheibani S., Vali H., Dawson K., Lynch I., *ACS Chem. Neuroscience* **4**, 475-485 (2012)
- [5] Kobayashi H. and Matsunaga T., *J. Colloid Interf. Sci.* **141**(2), 505-511 (1990)
- [6] Andrade A.L., Souza D.M., Pereira M.C., Fabris J.D., Domingues R.Z., *Cerâmica* **55**, 420-424 (2009)
- [7] Du X. and He J., *J. Colloid Interf. Sci.* **345**, 269-277, (2010)

* Lits@eng.auth.gr

Nanostructured coatings for electromagnetic shielding in the GHz frequency band

G. Tzagkarakis^{1,2}, M. Sucheai^{1,3}, I. V. Tudose^{1,3}, G. Kenanakis^{1,4}, M. Katharakis¹, E. Drakakis², E. Koudoumas^{1,2}

¹Center of Materials Technology and Photonics, Technological Educational Institute of Crete, 710 04 Heraklion, Crete, Greece

²Electrical Engineering Department, School of Applied Technology, Technological Educational Institute of Crete, 710 04 Heraklion, Crete, Greece

³"Al.I.Cuza" University of Iasi, 11 Bulevardul Carol I, Iasi, 700506, Romania, Romania

⁴Institute of Electronic Structure & Laser (IESL), Foundation for Research and Technology (FORTH) Hellas, P.O. Box 1385, Heraklion 70013, Crete, Greece

The last few years, a strong need of innovative materials for efficient electromagnetic shielding appeared, since the applications of wireless communication systems have increased vastly. These new materials should combine excellent shielding effect (SE) in particular GHz frequency bands, ease of production, low weight and minimal cost. It is well established in literature that allotropic forms of carbon exhibit all of the above criteria and have been considered as a very promising group of materials for electromagnetic shielding.

Towards this direction, we investigated the potential use in electromagnetic shielding applications of carbon allotropes and especially of graphene in polymer matrices. Coatings of various concentrations and thicknesses were prepared on foam board, consisting primarily of graphene platelets, PEDOT:PSS and polyaniline (PANI). Transmission measurements were performed in free space, using a Hewlett-Packard 8722 ES vector network analyzer and four sets of microwave standard-gain horn antennas covering the range 3-24GHz. Both the total transmission (S_{21}) and reflection (S_{11}) were measured in decibels (dB) and the results were used to determine the mechanisms behind the samples' SE. The results were compared with those of commercial products, which in general are required to have a SE of at least 20 dB. Prior to every measurement, an absorbing chamber was created using typical microwave absorbers (ECCOSORB AN-77) over all surfaces except the top, and each sample was placed in the middle of each set of horn antennas.

The results up to now are very promising, since in most of the cases, a SE of about 30 dB was obtained. The measurements indicated a strong dependence of the shielding effect on the relative concentration of the materials, the thickness of the coating as well as its conductivity.

Acknowledgements: This project is implemented through the Operational Program "Education and Lifelong Learning" action Archimedes III and is co-financed by the European Union (European Social Fund) and Greek national funds (National Strategic Reference Framework 2007 - 2013).

Mesoporous Au-TiO₂ nanoparticle assemblies as efficient catalysts for the chemoselective reduction of nitro compounds

Ioannis Tamiolakis¹, Ioannis N. Lykakis² and Gerasimos S. Armatas¹

¹*Department of Materials Science and Technology, University of Crete, Heraklion 71003, Greece.*

²*Department of Chemistry, Aristotle University of Thessaloniki, Thessaloniki 54124, Greece*

Synthesis of aromatic amines by selective hydrogenation of aromatic nitro compounds has emerged as one of the most important and, synchronously, challenging task in synthetic organic chemistry. Amines are highly valuable intermediate chemicals particularly used in the manufacture of pharmaceuticals, polymers, dyes and cosmetics. Although various noble metal nanoparticles (NPs) supported on a metal oxide, such as Au/CeO₂, Pt/Al₂O₃ and Au/Fe₂O₃, have been successfully used to reduce nitroaromatic compounds, these catalysts require harsh reaction conditions and are characterized by poor selectivity [1]. The selective hydrogenation of nitro into amine groups is not trivial because of the unavoidable formation of azo- and azoxy-derivatives during the reaction process. Therefore, exploring new catalytic systems offering high chemoselective production of aromatic amino-compounds is an ongoing research.

Gold supported on TiO₂ is the most promising catalyst for hydrogenation or oxidation of alkene, carbonyl and nitro compounds. In this work, we demonstrate novel mesoporous Au-sensitized TiO₂ as high-effective catalysts for the selective transformation of nitroaromatics into the corresponding amines. Namely, we utilized deposition-precipitation of gold hydroxides within the pores of mesoporous TiO₂ nanoparticle ensembles (MTA) [2]. The obtained materials (Au-MTA) possess a continuous network of interconnected gold and anatase TiO₂ (ca. 9 nm) nanoparticles with controllable gold particle size (i.e. ranging from 3 to 10 nm) and exhibit large and accessible pore surface area (ca. 100–160 m²/g), as evidenced by SAXS, XRD, TEM and N₂ physisorption measurements [3]. Interestingly, Au-MTA show outstanding performance for the selective reduction of nitro into amine groups using sodium borohydride as reducing agent. We also addressed the role of supported gold particles on the chemoselective response of Au-MTA, showing that the yield and product composition are highly related to the Au loading and particle size. As a result the 2% Au-MTA catalyst associated with 5-nm-sized Au nanoparticles has found to be a prominent catalyst for the reduction of nitroaromatics, not only giving exceptionally high selectivity (>96%) and conversion yield (>92%) to the corresponding amines, but also allowing the efficient synthesis of aromatic amino-compounds at ambient conditions.

References

- [1] X. Ke, X. Zhang, J. Zhao, S. Sarina, J. Barry, H. Zhu, *Green. Chem.* **15**, 236 (2013).
- [2] I. Tamiolakis, I. N. Lykakis, A. P. Katsoulidis, G. S. Armatas, *Chem. Commun.*, **48**, 6687 (2012).
- [3] I. Tamiolakis, S. Fountoulaki, N. Vordos, I. N. Lykakis, G. S. Armatas, *J. Mater. Chem. A*, **1**, 14311 (2013).

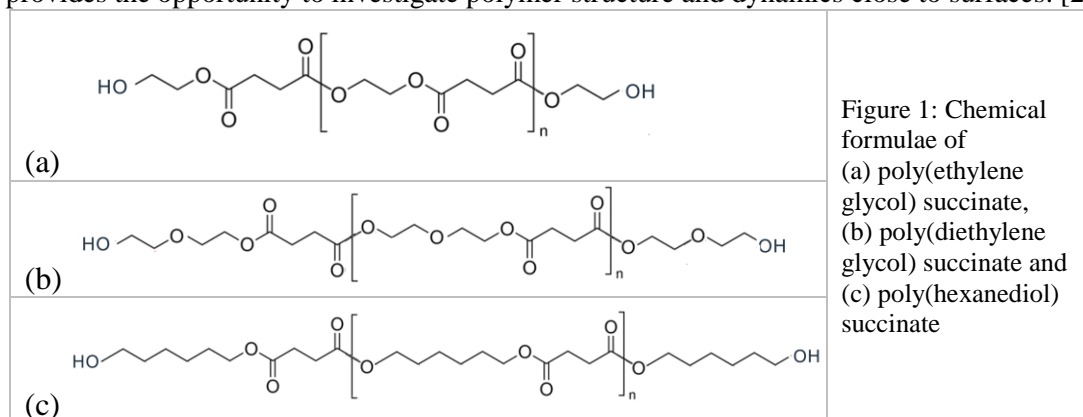
Structure and Dynamics of Polyester Polyols in the Bulk and Under Severe Confinement

K. Androulaki,^{1,2*} K. Chrissopoulou,¹ S. H. Anastasiadis^{1,2}

¹ *Institute of Electronic Structure and Laser, Foundation for Research and Technology-Hellas, Heraklion Crete, Greece*

² *Department of Chemistry, University of Crete, Heraklion Crete, Greece*

In recent years, there is a great need for the development of improved waterborne systems for coating applications that follow the strict European legislative framework on chemicals. The main properties of such a coating should be the ability for good film formation, an efficient stain, scratch, imprint and block resistance, improvable wetting properties, etc. Good candidates can be novel water-based PURs produced by polyols and polyisocyanates with the polyol structure being the key factor to obtain a waterborne coating with the desired properties. [1] On the other hand, nanocomposites consisting of polymers and layered silicates are considered as a new generation of composite materials due to their unique properties, which render them candidates for numerous applications; especially intercalated nanohybrids, where polymer chains form a 1-2nm film within the inorganic galleries provides the opportunity to investigate polymer structure and dynamics close to surfaces. [2]



In this work, the structure and dynamics of three different linear polyester polyols are investigated in the bulk and under severe confinement when mixed with a hydrophilic layered silicate. The polymers are poly(diethylene glycol) succinate, poly(hexanediol) succinate, and poly(ethylene glycol) succinate (Figure 1), whereas the inorganic material is Na⁺-MMT. The polymers molecular characterization with Nuclear Magnetic Resonance (NMR) and Infrared Spectroscopy was followed by the investigation of their solubility in different solvents. Their thermal behavior was investigated with Differential Scanning Calorimetry (DSC) and their thermal stability with Thermogravimetric Analysis (TGA). X-ray diffraction (XRD) was utilized to verify the intercalated structure of the hybrids whereas Dielectric Spectroscopy was utilized to investigate the dynamics, for temperatures covering the regimes of both sub-T_g local processes and segmental (alpha-) relaxation. Similarities and differences were found between the three systems depending on the polymer structure whereas the structure and the dynamics of both the bulk and the confined systems were compared with respective results obtained from non-linear hyperbranched polyesters. [3]

References

- [1]. M. J. van Ginkel, "Facts in Formulating Water Based Industrial Wood Coatings", Neoresins (2002).
 [2] T. J. Pinnavaia, G.W. Beall, Polymer-Clay Nanocomposites; John Wiley & Sons, West Sussex (2000)
 [3] K. Androulaki, K. Chrissopoulou, D. Prevosto, M. Labardi and S. H. Anastasiadis *ACS Appl. Mater. Int.* **7**, 12387 (2015).

This research has been co-financed by the European Union and Greek General Secretariat for Research and Technology through the Programme for the Development of Industrial Research and Technology, IIABET2013 (782-BET-2013).

* krysand@iesl.forth.gr